Developing novel therapeutic strategies for targeting the p53 pathway in renal cell carcinoma

Thesis presented in accordance with the University of Liverpool for the degree of Doctor in Philosophy (Ph.D.)

By

Amro Ahmed-Ebbiary

Abstract

Renal cell carcinoma (RCC) is a notoriously difficult cancer to treat. RCC has an unpredictable course, is radio- and chemo-resistant and survival in response to treatment with current therapies for the metastatic disease is generally very poor. This underscores the necessity for novel therapeutics for this condition. The tumour suppressor p53 is rarely mutated in RCC and up-regulation of p53 and its negative regulator, MDM2, has recently been shown to be an independent prognostic indicator for patients with poor outcome. The function of p53 in RCC cells in culture appears to be partially intact and is regulated by MDM2. Rescue of p53 from the inhibitory effects of MDM2 using inhibitors of the p53-MDM2 interaction results in cell cycle arrest or senescence, not apoptosis, three cell fates that p53 can induce depending on the tissue or tumour type. Because of the potentially deleterious effects of senescent cells on the tissue microenvironment, it was decided that apoptosis would be the preferable cell fate for the therapeutic reactivation of p53 in RCC cells. To that end, the MDM2 inhibitor Nutlin-3 was combined with the Bcl-2 family inhibitor ABT-737. This combination of drugs synergistically inhibited the proliferation of RCC cells harbouring wild type p53 but not in cells harbouring mutant p53. This synergistic inhibition of proliferation was shown to be p53-dependent and was confirmed to be inducing apoptosis, but only in RCC cells that had high levels of p53 protein. The synergistic inhibition of proliferation was not recapitulated when an inhibitor of MDM2 ubiquitin ligase activity was combined with ABT-737. The combination of Nutlin-3 and ABT-737 induced pro-apoptotic Puma and Noxa in RCC cells and the apoptosis was shown to be substantially Bax-dependent. This study suggests that the combination of Nutlin-3 and ABT-737

should be considered as a candidate for pre-clinical development in the treatment of RCC.

Acknowledgements

In the name of God, Most Gracious, Most Merciful. I wish to thank God, first and foremost. Thank you to my family and my wife Nadia whose unwavering support has helped me tremendously. You never gave up on me. Mum, Dad, Alyaa, Anan, Omar, Ola and Abla thanks for appreciating how important this was for me. My good friends Phil, Ty, Umar and Saif, thanks for all of your help.

I would like to thank Professor Mark Boyd and Dr Nikolina Vlatković for giving me the amazing opportunity of doing a PhD in their lab. It has been an awesome experience and I wouldn't trade it for anything. Thank you to Dr Carlos Rubbi who has helped me a great deal both professionally and personally. Thank you to all of the members of the p53/MDM2 Research Team. Special mention goes to Radek Polanski, Kerryanne Crawford, Shie Hong Chang, Afeef Aslam, Arpita Ray Sinha, Nav Upile, Anna Behrendt, Mike Thornton and Andy Lau.

Declaration of originality

I declare that all of the work in this thesis is my own, with the exception of two cell lines generated by Dr Radoslaw Polanski (see Section 3.2.2) and is not being presented for any other degree or qualification. All work described was performed by me unless otherwise indicated.

Amro Ahmed-Ebbiary

January 2014

Contents

Abstract I
Acknowledgements III
Declaration of originality IV
Contents V
List of tables IX
List of figures X
List of abbreviations XIV

Chapter 1: Introduction 1
1.1 Introduction to renal cell carcinoma 1
1.1.1 Introduction to kidney cancer 1
1.1.2 RCC 2
1.1.3 Risk factors 2
1.1.4 Prognostication of RCC tumours 3
1.1.5 Genetic abnormalities in RCC 5
1.1.5.1 MET 5
1.1.5.2 FLCN 6
1.1.5.3 VHL 7
1.1.6 Molecular biology of RCC 7
1.1.6.1 VHL and HIF 8
1.1.6.2 p53 and MDM2 in RCC 9
1.1.7 Treatment of RCC 12
1.2 p53 14
1.2.1 Introduction to p53 14
1.2.2 p53: overview of structure and function 15
1.2.3 Cell cycle arrest 19
1.2.4 The role of p53 in cell cycle arrest 20
1.2.5 Senescence 22
1.2.6 The role of p53 in senescence 23
1.2.7 Apoptosis 24
1.2.7.1 The Extrinsic Apoptosis pathway 27

1.2.7.2 The Intrinsic Apoptosis pathway 28
1.2.7.3 The Granzyme B pathway 29
1.2.7.4 Interactions between the Bcl-2 family members and models of apoptosis 29
1.2.7.5 BH3 mimetics 32
1.2.8 The role of p53 in apoptosis 33
1.3 MDM2 and regulation of p53 34
1.3.1 Introduction to MDM2 34
1.3.2 Regulation of p53 by MDM2 and other proteins 37
1.3.3 Pharmacological restoration of p53 function in cancer 39
1.4 Use of drug combinations in cancer therapy 40
1.4.1 Bliss independence 42
1.4.2 Lowe additivity 43
1.5 Aims 45

Chapter 2: Materials and Methods 46
2.1 List of reagents 46
2.1.1 General list of reagents 46
2.1.2 Tissue culture reagents 47
2.1.3 Drugs 48
2.1.4 Antibodies for Western Blotting 48
2.1.4.1 Primary Antibodies for Western Blotting 48
2.1.4.2 Secondary antibodies used for western blot 53
2.2 Cell lines 53
2.2.1 Cell lines used in this study 53
2.2.2 Cell culture medium 53
2.2.3 Sub-culture of cell lines 55
2.2.4 Preparation of cryopreserved cells 56
2.2.5 Transfection of cells with siRNA using Lipofectamine-2000 56
2.3 Cell proliferation and viability assays 57
2.3.1 MTT Assay 57

2.3.1.1 Seeding of cells for MTT assay 59
2.3.1.2 Treatment with MTT and absorbance reading 59
2.3.2 Detection of apoptotic cells by flow cytometry using Annexin V and Propidium iodide 60
2.3.2.1 Reagents used for detection of apoptotic cells by flow cytometry using Annexin V and propidium iodide 55
2.3.2.2 Harvesting of cells and detection of apoptotic cells by Annexin V/PI staining and flow cytometry 60
2.4 Western Blotting 62
2.4.1 Reagents for western blotting 62
2.4.2 Sample preparation for western blotting 64
2.4.3 Gel electrophoresis and protein detection for western blotting 64
2.5 Crude preparation of mitochondria from tissue culture cells 66
2.5.1 Reagents for crude preparation of mitochondria 66
2.5.2 Protocol for crude preparation of mitochondria 67
2.6 Isolation of mitochondria by sucrose density centrifugation 68
2.6.1 Reagents for isolation of mitochondria by sucrose density gradient centrifugation 68
2.6.2 Protocol for isolation of mitochondria by sucrose density centrifugation 68
2.7 Live cell imaging 69
2.8 Immunoprecipitation 70
2.8.1 Reagents for immunoprecipitation 70
2.8.2 Procedure for immunoprecipitation 70

Chapter 3: A study of the effects of the combination of Nutlin-3 and ABT-737 on the proliferation and survival of renal cell carcinoma cell lines 73

3.1 Introduction 73
3.2 Results 74
3.2.1 The Combination of Nutlin-3 and ABT-737 synergistically inhibits proliferation of renal cell carcinoma cells harbouring wild type p53 74
3.2.2 Synergy between Nutlin-3 and ABT-737 is p53-dependent 83

3.2.3 The combination of Nutlin-3 and ABT-737 promotes apoptosis in renal cell carcinoma cells harbouring wild type p53 91
3.2.4 An inhibitor of the ubiquitin-ligase activity of MDM2 does not synergise with ABT-737 in RCC cells that harbour wild type p53 110
3.3 Summary 117

Chapter 4: A study into the mechanism underlying the p53-dependent apoptosis observed in response to the combination of Nutlin-3 and ABT-737 in renal carcinoma cells harbouring wild type p53 119
4.1 Introduction 119
4.2.1 Relative protein levels of Bcl-2 family members in RCC cells 125
4.2.2 The combination of Nutlin-3 and ABT-737 enhances apoptotic signalling in RCC cell lines harbouring wild type p53 121
4.2.3 The combination of Nutlin-3 and ABT-737 promotes Bax oligomerization at mitochondria 143
4.2.4 Apoptosis in response to the combination of Nutlin-3 and ABT-737 is Bax-dependent 167
4.2.5 A study of pro-apoptotic proteins at the mitochondria in response to the combination of Nutlin-3 and ABT-737 175
4.2.6 A study into the possible role of Puma in promoting Bax activation in response to the combination of Nutlin-3 and ABT-737 190
4.3 Summary 201

Chapter 5: Discussion 203
References 214
Appendices 237

List of tables

Table 1.1 Staging of kidney tumours using TNM classification 4

Table 1.4 Description and symbols of synergism or antagonism in drug combination studies analysed by the combination index 44

Table 2.1.4.1. Primary antibodies used for western blotting in this study 49

Table 2.1.4.2. Secondary antibodies used for western blotting in this study 52

Table 2.2.1 Cell lines used in this study 54

Table 2.3.1.1 Seeding densities of cells used in MTT assay 58

Table 2.4.3.1 Composition of SDS PAGE gels 65

Table 2.8.1 Antibodies used in immunoprecipitation 72

Table 3.2.1.1 Summary of IC_{50} and IC_{70} values of cells treated with Nutlin-3 or ABT-737 76

Table 3.2.1.2 Combination indices at IC_{50} and IC_{70} for RCC cells treated with Nutiln-3 and ABT-737 81

Table 3.2.2.1 Summary of IC_{50} and IC_{70} values of ACHN scrambled shRNA and ACHN p53 shRNA-expressing cells treated with Nutlin-3 or ABT-737 88

Table 3.2.2.2 Combination indices at IC_{50} and IC_{70} for ACHN scrambled shRNA and ACHN p53 shRNA-expressing cells treated with Nutiln-3 and ABT-737 89

Table 3.2.4.1 Summary of IC_{50} and IC_{70} values of cells treated with HLI373 or ABT-737 111

Table 3.2.4.2 Combination indices at IC_{50} and IC_{70} for RCC cells treated with HLI373 and ABT-737 114

Table 4.2.1.1 Summary of relative protein level of Bcl-2 family members in renal cell lines used in this study 122

List of figures

Figure 1.2.1 Functional domains of p53 17
Figure 1.2.2 Structural arrangement of p53 18
Figure 1.2.3 The cell cycle 21
Figure 1.2.4 The Bcl-2 family of proteins 25
Figure 1.2.5 Specificity of the BH3-only proteins for anti-apoptotic Bcl-2 family members 30
Figure 1.3.1 Functional domains of MDM2 and MDM4 36
Figure 2.3.2.1 Schematic summarizing populations of cells after Annexin V/PI staining 61
Figure 3.2.1.1 p53 and MDM2 protein level in the cell lines used in this study 75
Figure 3.2.1.2 Survival curves of cells treated with Nutlin-3 and/or ABT-737 77
Figure 3.2.1.3 Analysis of Nutlin-3 and ABT-737 drug interaction in RCC cells 80
Figure 3.2.2.1 Analysis of expression levels of p53 and MDM2 in ACHN cells expressing shRNAs 84
Figure 3.2.2.2 Survival curves of ACHN scrambled shRNA and ACHN p53 shRNA-expressing cells treated with Nutlin-3 and/or ABT-737 85
Figure 3.2.2.3 Analysis of Nutlin-3 and ABT-737 drug interaction in ACHN scrambled shRNA and ACHN p53 shRNA-expressing cells treated with Nutlin-3 and ABT-737 86
Figure 3.2.3.1 Images obtained from live cell imaging of ACHN cells (I) 93
Figure 3.2.3.2 Images obtained from live cell imaging of ACHN cells (II) 94
Figure 3.2.3.3 Single cell time-lapse study of ACHN cell dying in response to the combination of Nutlin-3 and ABT-737 95
Figure 3.2.3.4 Images obtained from live cell imaging of 111 cells (I) 98

Figure 3.2.3.5 Images obtained from live cell imaging of 111 cells (II) 99
Figure 3.2.3.6 Survival curves for ACHN and 111 cells treated with Nutlin-3 and/or ABT-737 100
Figure 3.2.3.7 Analysis of apoptosis and cell death in cells treated with Nutlin-3 and/or ABT-737 (I) 103
Figure 3.2.3.8 Analysis of apoptosis and cell death in cells treated with Nutlin-3 and/or ABT-737 (II) 106
Figure 3.2.3.9 Analysis of Annexin V positive cells treated with Nutlin-3 and/or ABT-737 107
Figure 3.2.4.1 Survival curves of RCC cells treated with HLI373 and/or ABT-737 112
Figure 3.2.4.2 Analysis of HLI373 and ABT-737 drug interaction in RCC cells 113
Figure 4.2.1.1 Analysis of relative levels of Bcl-2 family proteins 117
Figure 4.2.2.1 Steady state level of p53, MDM2 and proteins associated with apoptosis in ACHN, Caki2 and 117 cell lines 126
Figure 4.2.2.2 Steady state level of p53, MDM2 and proteins associated with apoptosis in A498 and 115 cell lines 127
Figure 4.2.2.3 Steady state level of p53, MDM2 and proteins associated with apoptosis in 111 and 154 cell lines 128
Figure 4.2.2.4 Steady state level of p53, MDM2 and proteins associated with apoptosis in H1299 and U2OS cell lines 129
Figure 4.2.2.5 Steady state level of p53, MDM2 and proteins associated with apoptosis in scACHN and sh-p53ACHN cell lines 137
Figure 4.2.3.1 Schematic illustrating stabilization of Bax oligomer with BMH 145
Figure 4.2.3.2 Optimization of homogenization of ACHN cells 147
Figure 4.2.3.3 Subcellular fractionation of ACHN cells 149
Figure 4.2.3.4 Western blot of mitochondrial lysates treated with BMH or DMSO 150

Figure 4.2.3.5 Western blot of mitochondrial lysates treated with BMH or DMSO 151
Figure 4.2.3.6 Subcellular fractionation of ACHN cells following treatment of homogenate with BMH or DMSO 153
Figure 4.2.3.7 Western blot of mitochondria from ACHN cells treated with DMSO or BMH in homogenate 154
Figure 4.2.3.8 Subcellular fractionation of ACHN cells following treatment of homogenate with BMH or DMSO 156
Figure 4.2.3.9 Western blot of mitochondria from ACHN cells treated with DMSO or BMH in homogenate 158
Figure 4.2.3.10 Western blot of mitochondria from ACHN cells treated with DMSO or BMH in homogenate 159
Figure 4.2.3.11 Subcellular fractionation of 111 cells following treatment of homogenate with BMH or DMSO 161
Figure 4.2.3.12 Western blot of mitochondria from 111 cells treated with DMSO or BMH in homogenate 162
Figure 4.2.3.13 Western blot of mitochondria from 111 cells treated with DMSO or BMH in homogenate 163
Figure 4.2.3.14 Summary of approaches taken to co-purify Bax and/or Bak oligomers with mitochondria 164
Figure 4.2.4.1 Optimization of Bax knockdown in ACHN cells using siRNA 168
Figure 4.2.4.2 Knockdown of Bax in ACHN cells transfected with siRNAs 3 and 4 169
Figure 4.2.4.3 Analysis of apoptosis and cell death in ACHN cells treated with Nutlin-3 and/or ABT-737 upon down-regulation of Bax (I) 172
Figure 4.2.4.4 Analysis of apoptosis and cell death in ACHN cells treated with Nutlin-3 and/or ABT-737 upon down-regulation of Bax (II) 173
Figure 4.2.5.1 Centrifuge tube prepared for purification of mitochondria from crude homogenate before and after ultra-centrifugation 177
Figure 4.2.5.2 Analysis of subcellular fractions following fractionation

of ACHN cells by sucrose density gradient centrifugation....178
Figure 4.2.5.3 Analysis of subcellular fractions following fractionation of 111 cells by sucrose density gradient centrifugation....179
Figure 4.2.5.4 Enrichment of mitochondria from ACHN cells....180
Figure 4.2.5.5 Enrichment of mitochondria from 111 cells....181
Figure 4.2.5.6 Pro-apoptotic proteins at the mitochondrial fractions from fractionated ACHN and 111 cells....184
Figure 4.2.5.7 Comparison of Puma protein in whole cell lysates and mitochondrial fractions of ACHN cells....185
Figure 4.2.6.1 Optimization of Bax 6A7 immunoprecipitation....192
Figure 4.2.6.2 N-terminal exposure of Bax....194
Figure 4.2.6.3 Optimization of Puma knockdown using siRNA....196
Figure 4.2.6.4 Steady state level of Puma upon transfection with siRNAs to Puma 1 and 4....198
Figure 4.2.6.5 Bax N-terminal exposure of ACHN cells upon down-regulation of Puma and treatment with Nutlin-3 and ABT-737....199

List of abbreviations

Apaf-1	apoptotic protease activating factor 1
Arf	Alternative reading frame
ATM	Ataxia telangiectasia mutated
ATR	Ataxia telangiectasia and Rad3-related
AV	Annexin V
BH	Bcl-2 homology
Bad	Bcl-2 associated death promoter
Bax	Bcl-2 associated X protein
Bcl-B	Bcl-2 family protein resembling Boo
Bcl-2	B cell lymphoma 2
Bcl-xL	B cell lymphoma extra large
Bid	BH3-interacting domain death agonist
Bik	Bcl-2 interacting killer
Bim	Bcl-2-interacting mediator of cell death
Bmf	Bcl-2-modifying factor
BMH	Bismaleimidohexane
BSA	Bovine serum albumin
CARD	Caspase recruitment domain
CDK	Cyclin-dependent kinase
CI	Combination index
COX4	Cytochrome C oxidase IV
CTL	Cytotoxic T lymphocytes
DBD	DNA binding domain
DD	Death domain
DISC	Death induced signalling complex
DMSO	Dimethyl sulphoxide
DR	Death receptor
FACS	Fluorescence activated cell sorting
FADD	Fas-associated protein with death domain
FasR	Fas receptor
FBS	fetal bovine serum

FITC	fluorescein isothiocyanate
GLUT1	glucose transporter 1
GTF	general transcription factor
HIF	hypoxia inducible factor
HLI	Hdm2 ubiquitin ligase inhibitor
HRE	hypoxia response elements
HRP	horseradish peroxidase
IFNα	interferon α
IL-2	interleukin 2
IMS	intermembrane space
IP	immunoprecipitation
IR	ionizing radiation
Mcl-1	induced myeloid leukemia cell differentiation protein
MDM2	mouse double minute 2
MEFs	mouse embryonic fibroblasts
MOM	mitochondrial outer membrane
MOMP	mitochondrial outer membrane permeablization
MT	mutant
mTOR	mechanistic target of rapamycin
MTT	3-(4,5-dimethylthiazol-2-yl)-2,5-diphenyl tetrasodium bromide
NES	nuclear export sequence
NoLS	nucleolar localization sequence
ODD	oxygen-dependent degradation domain
PARP	poly ADP ribose polymerase
PBS	phosphate buffered saline
PHD	prolyl hydroxylase
PI	propidium iodide
PIDD	p53-induced protein with death domain
PDGF	platelet derived growth factor
RCC	renal cell carcinoma
RS	replicative senescence
SF	serum free
siRNA	small interfering RNA
SUMO	small ubiquitin-like modifier

TAD	transactivation domain
TNF-R	tumour necrosis factor receptor
tBid	truncated BH3-interacting domain death agonist
TBP	TATA-binding protein
TM	transmembrane
VEGF	vascular endothelial growth factor
VHL	Von Hippel Lindau
WT	wild type

Chapter 1: Introduction

The aim of this thesis was to explore the possibility of the therapeutic restoration of wild type p53 apoptotic function in renal cell carcinoma (RCC) using a combinatorial approach. The purpose of this section therefore is to lead the reader through the background and concepts pertinent to this study. Section 1.1 introduces RCC and discusses the incidence, risk factors, epidemiology, the molecular biology of the disease and current strategies used in the treatment of RCC and how the underlying molecular biology of the disease is targeted in its treatment. Section 1.2 addresses the tumour suppressor p53 in greater depth and includes an overview of three important effects of p53 activation: cell cycle arrest, senescence and apoptosis. Section 1.3 addresses MDM2, the main negative regulator of p53 and how p53 is regulated by both MDM2 and other factors. Section 1.4 is a brief discussion about the theoretical basis underlying combination treatment of cancer. Section 1.5 summarizes the aims of this thesis.

1.1 Introduction to renal cell carcinoma

This section will address the epidemiology, incidence and risk factors associated with RCC including a discussion regarding commonly mutated genes in RCC and the underlying molecular biology of the disease. A discussion on the treatment of RCC is at the end of this section so that the relevant grounding in the molecular biology of RCC is provided before a detailed discussion of targeted therapy.

1.1.1 Introduction to kidney cancer

Cancer of the kidney represents 4% of all diagnosed cancer cases in men and over 2% of cancer cases in women in the UK (Cancer Research UK Statistics, 2010).

Over 102,000 patients die from this disease annually worldwide, and the number is rising by approximately 2-3% per decade (Gupta et al., 2008). Overall, the incidence of the disease has doubled over the past thirty years. In the UK, the incidence of the disease has increased from 4.9 cases per 100,000 of the population in 1975 to 11.8 per 100,000 in 2010 (Cancer Research UK Statistics). Approximately 200,000 new cases of kidney cancer are diagnosed every year internationally. The incidence of kidney cancer varies between different populations in different regions (Chow et al., 2010). Clear cell renal cell carcinoma, which is cancer derived from the renal epithelium, is the most common type of kidney cancer, representing over 75% of cases.

1.1.2 RCC

RCC is believed to originate from the tubular structures of the kidney (Lubensky et al, 1996) and is a heterogeneous disease, comprising a number of different subtypes. Approximately 4 % of RCC cases are hereditary and the remaining 96 % are sporadic. RCC has been classified into four major histological subtypes: clear cell RCC (ccRCC) is the most frequently encountered, representing 75-80% of all RCC. Other types are papillary (10-15%), chromaphobe (5%) and collecting duct (1%) (Lopez-Beltran et al., 2006; Pavlovich et al., 2004; Zbar et al., 2003).

1.1.3 Risk factors

A number of risk factors are believed to be associated with increased susceptibility to RCC. Age is the most important risk factor for RCC and age-standardized incidence rates of RCC have generally been observed to be higher among men than women, a pattern repeated consistently throughout the world (Cancer Research UK Statistics,

2010). Tobacco smoking has been identified as a risk factor for RCC by a number of studies. A meta-analysis of 24 studies showed that there was an increased risk associated with smoking and this was estimated to be 54% in men and 22% in women. A clear dose-response relationship was shown, with heavier smoking associated with increased risk (Hunt et al., 2005; Theis et al., 2008). Excess body weight has been associated with increased risk of RCC in several studies. In a meta-analysis and systematic review of studies into body mass index (BMI) and incidence of cancer, an association between risk of RCC and a $5kg/m^2$ increase in BMI was proposed (relative risk = 1.24 $p < 0.0001$) (Renehan et al., 2008).

1.1.4 Prognostication of RCC tumours

RCC tumours can be classified based on a number of criteria. Staging systems categorize different tumours according to their anatomical features, thereby classifying patients into groups that represent different risks of disease progression and death. This provides useful information for the planning of appropriate treatment strategies. The TNM (tumour node metastasis) staging system is used in patients with RCC (table 1.1). The five year disease specific survival for stages I, II, II and IV has been observed to be 89.6 %, 82.7 %, 57.7 % and 18.3 % respectively (Elmore et al., 2003). Another system commonly used in the prognostication of RCC is Fuhrman grading, which is used for classification of RCC by evaluating nuclear morphology. Grade 1 cells possess nuclei that less than 10μm in size with a round nuclear shape and have inconspicuous nucleoli. Grade 4 cells, which are of the highest grade on the Fuhrman scale, possess nuclei that are greater than 20μm in size, have a multilobate nuclear shape and possess enlarged nucleoli (Fuhrman et al., 1982). Fuhrman grade has been shown to significantly correlate with tumour size,

Table 1.1 Staging of kidney tumours using TNM classification. Taken from Rini et al., 2009.

TNM stage of cancer, venous system invasion, lymph node involvement and distant metastases. Further, the Fuhrman grade of a RCC tumour can serve as an independent prognostic indicator for survival in RCC cases (Medeiros et al., 1988; Bretheau et al., 1995; Ficarra et al., 2001; Zhang et al., 2012).

1.1.5 Genetic abnormalities in RCC

Cancer is a disease that results from de-regulated growth and survival signals that promotes the unrestrained proliferation of cells resulting in tumour formation. The step-wise accumulation of mutations in genes that are involved in processes such as proliferation, growth, survival and angiogenesis (amongst other processes) can confer a survival advantage to cells that have undergone this mutation process and these cells can proceed to proliferate and form tumours (Hanahan and Weinberg, 2000). The study of hereditary kidney cancer syndromes has led to the identification of genes involved in the pathogenesis of RCC. Commonly mutated genes in RCC are MET, VHL and FLCN and a discussion of these genes is in the remainder of this section. As the tumour suppressor p53 is rarely mutated in RCC (reviewed in Noon et al., 2010) but is of particular relevance to this thesis, a discussion regarding this gene in RCC is reserved for section 1.1.6.2.

1.1.5.1 MET

Individuals with hereditary papillary renal cell carcinoma (HPRCC), which is an inherited form of RCC, develop multiple, bilateral RCC with papillary histology (Zbar et al., 1994). Mutation of the tyrosine kinase domain of *MET* was identified by genetic linkage analysis in families with this inherited cancer syndrome (Schmidt et al., 1997). In a study by Schmidt and colleagues, mutation of MET was observed in

17 out of 129 (13%) sporadic cases of HPRCC (Schmidt et al., 1999). Of these 17 cases of HPRCC that were apparently sporadic, 8 were germline mutations. The *MET* proto-oncogene encodes a cell surface tyrosine kinase receptor for hepatocyte growth factor (HGF), which is important for proliferation, cell migration, morphogenesis and differentiation (Perruzi and Bottaro, 2006). Most of the *MET* mutations associated with HPRCC lie in the Met activation loop or in the ATP binding pocket, which causes constitutive Met activation, independent of any ligand binding (Jeffers et al., 1997).

1.1.5.2 FLCN

Birt-Hogg-Dubé syndrome is a genetic disorder that can promote susceptibility to renal carcinoma, renal and pulmonary cysts and non-cancerous tumours of the hair follicles refered to as fibrofolliculomas. The condition is caused by mutation in the *FLCN* gene, which encodes a protein called folliculin (Menko et al., 2009). *FLCN* mutations have been observed in ~90% of families afflicted with this disease (Nickerson et al., 2002). In sporadic RCC, the *FLCN* gene can be inactivated by loss of heterozygosity or promoter methylation. Mutation in this gene was observed in 2.6% of cases of sporadic RCC tested (Khoo et al., 2003). Most germline mutations of *FLCN* are predicted to truncate the protein product of the gene, folliculin. The function of folliculin is unclear however, the protein has been observed to form a complex with folliculin interacting protein 1 and 2 (FNIP1 and FNIP2). This complex can bind AMPK, a nutrient sensor that can regulate mTOR. The importance of mTOR in RCC will be discussed in section 1.1.6.1 (Baba et al., 2006; Hasumi et al., 2008).

1.1.5.3 VHL

The most commonly observed genetic abnormality in RCC is inactivation of the Von Hippel Lindau (VHL) tumour suppressor gene. Von Hippel Lindau disease is a hereditary cancer syndrome; individuals affected by the disease have an increased risk for the development of tumours in a number of organs, including the kidneys. Positional cloning was used to identify the *VHL* gene locus on the short arm of chromosome 3 in patients with Von Hippel Lindau disease (Seizinger et al. 1988). Consistent with the Knudson two-hit hypothesis (Knudson 1971), *VHL* was subsequently identified as a tumour suppressor gene based on the observation that the gene was mutated at both alleles in hereditary Von Hippel Lindau disease and sporadic RCC (Latif et al., 1993). This hypothesis was further strengthened by the observation that the ability of the *VHL* null RCC cell line 786-O to form tumours in nude mice was severely perturbed upon stable transfection of *VHL* into these cells (Iliopoulos et al. 1995). Further work showed that somatic mutation of *VHL* were present in 57% of RCC cases and that 97% of these exhibited loss of the second *VHL* allele (Gnarra et al. 1994). Herman et al. showed that a further 10-20% of renal cell carcinomas exhibit hypermethylation of typically unmethylated CpG islands near the 5' region of the *VHL*, resulting in the loss of *VHL* gene expression (Herman et al., 1994). Hence, inactivation of the *VHL* tumour suppressor gene, whether by mutation or methylation, is a common occurrence in RCC.

1.1.6 Molecular biology of RCC

As mentioned briefly in section 1.1.5, mutation of certain genes in cells permits their unrestrained replication, which can result in cancer. The significance of VHL mutation will be discussed in the section 1.1.6.1, as this is one of the most commonly

mutated genes in RCC and mutation of this gene is important to the development of RCC. A discussion of p53 and MDM2 in RCC follows section 1.1.6.2 and this is to give the reader grounding in the significance of this pathway in RCC, as it is central to this thesis.

1.1.6.1 VHL and HIF

The following is a description of pVHL function, the protein product of the *VHL* gene, as it relates to RCC. Hypoxia inducible factors (HIFs) are a family of oxygen sensitive, heterodimeric transcription factors that are involved in regulating oxygen delivery and cellular adaptation to oxygen deprivation. HIF-α can bind the constitutively expressed HIF-β subunit and promote the transcription of genes that regulate energy metabolism, angiogenesis and other functions required in the adaptation to hypoxia by binding hypoxia response elements (HREs) in the relevant gene promoters (Semenza, 2010a). For example, HIFs can promote the transcription of vascular endothelial growth factor (VEGF) to promote angiogenesis and glucose transporter 1 (GLUT1) to promote glucose uptake (Semenza, 2010b). pVHL forms part of a ubiquitin ligase complex that also includes cullin2, elongin B, elongin C and Rbx1 which is responsible for targeting HIFs for degradation (Kamura et al., 1999; Shen and Kaelin, 2013). During normoxia, HIF-α is hydroxylated on a critical proline residue within the oxygen-dependent degradation (ODD) domain of the protein by HIF prolyl hyrdroxylase (PHD) (Cockman et al., 2000). This reaction is dependent on the presence of oxygen. This modification of HIF-α permits binding to pVHL and the subsequent ubiquitination of HIF-α resulting in its degradation by the proteasome (Maxwell et al., 1999). During hypoxia, PHD no longer hydroxylates HIF-α and the pVHL-cullin2-elongin B-elongin C-Rbx1 complex does not associate

with HIF-α. This results in the accumulation of HIF-α (Semenza, 2009). Mutations of the pVHL protein due to mutation in *VHL* perturb the ability of pVHL to associate with HIF-α, resulting in the accumulation of HIF-α and subsequent up-regulation of the transcriptional targets of HIF (Stebbins et al., 1999; Ohh et al, 2000). The up-regulation of the transcriptional targets of HIF is the driver of the angiogenic and invasive phenotype of RCC tumours (Baldewijns et al., 2010). The translation of HIF-α can also be regulated by the mammalian target of rapamycin (mTOR), part of the mTORC1 complex (Zhong et al., 2000; Hudson et al., 2002). mTORC1 is a protein complex that functions as an energy sensor and can control protein synthesis (Laplante and Sabatini, 2012). Thomas et al. showed that the proliferation of RCC cells that possessed up-regulated HIF-1α as a result of *VHL* knockdown was inhibited upon treatment with mTOR inhibitors (Thomas et al., 2006). This provided the rationale for the use of mTOR inhibitors in a clinical setting. The importance of the biology of pVHL and HIF in the treatment of RCC will be discussed in section 1.1.7.

1.1.6.2 p53 and MDM2 in RCC

p53 is commonly described as the "guardian of the genome" and plays a vital role in tumour suppression, primarily through functioning as a transcription factor for genes whose protein products are involved in tumour suppression (Lane, 1992). Upon up-regulation and activation, p53 can promote, amongst other responses, cell cycle arrest, senescence or apoptosis. The potentially lethal effect of unrestrained p53 function is countered by MDM2, the main essential regulator of p53 (Iwakuma and Lozano, 2003) and a transcriptional target of p53 (Wu et al., 1993). MDM2 regulates p53 by acting as an E3 ubiquitin ligase for p53, targeting p53 for

degradation by the proteasome, or through direct binding to p53, masking the ability of p53 to function as a transcription factor (Honda et al., 1997; Oliner et al., 1993). A more detailed discussion of p53 and MDM2 function are found in sections 1.2 and 1.3, however for the purposes of this section, the role of p53 and MDM2 in RCC will be discussed. p53 is mutated in roughly 50% of cancers, highlighting the importance of this gene in tumour suppression (Hainaut et al., 1997). Several studies have examined mutational status of p53 in RCC and levels of p53 and MDM2 in tissue samples in RCC (reviewed in Noon et al., 2010) to determine the prognostic value of the expression of both of these proteins. Owing to the differences in tumour grade, antibodies used in IHC studies and techniques used to analyse p53 mutation status in samples, it has been difficult to assess the significance of p53 mutation status and levels of p53 and MDM2 in the progression of RCC when referring to the literature (Noon et al., 2010). Some of the literature regarding p53 and MDM2 expression in RCC is summarized below. Chemeris et al., performed IHC on 88 renal tumours and showed that the level of p53 was elevated in renal tumours and using single strand conformation polymorphism, it was shown that p53 was always wild type in the samples tested (Chemeris et al., 1995). The authors of this study concluded that mutation of p53 was unlikely to contribute to the development of RCC and that the elevation of p53 was independent of any mutation in p53. Moch and colleagues showed that elevated p53 was associated with poor prognosis and that p53 positivity was strongly associated with MDM2 positivity but positivity for both proteins was not associated with reduced survival (Moch et al., 1997). Using 194 tumour samples, of a variety of stages and histological grades, in combination with clinical outcome data, Haitel et al. showed that elevated p53 and MDM2 was an independent prognostic indicator and that patients with tumours that were positive for both

proteins performed worse overall (Haitel et al., 2000). The apparent contradiction between Moch et al. and Haitel et al. regarding the association of p53 and MDM2 up-regulation and patient outcome may have been due to differences in the staging of the tumours between both sets of data and different cut-off points used in each study. Noon et al. showed that in a cohort of patients treated by radial nephrectomy, up-regulation of both p53 and MDM2 was significantly associated with reduced disease specific survival and that p53 in these tumours was rarely mutated (Noon et al., 2011).

The dearth of observed p53 mutations in cases of RCC is consistent with the behaviour of p53 in renal epithelial cells, as discussed in Vlatkovic et al., 2011: in response to stress, p53 in cells of the renal epithelium is up-regulated but apoptosis does not take place (MacCallum et al., 1996; reviewed in Vlatkovic et al., 2011). The p53-dependent transcription of Bax, an important effector of apoptosis commonly up-regulated by p53 in response to ionizing radiation in a number of tissues (Miyashita et al., 1994), did not take place in renal epithelium tissue, whereas transcription of p21, an important mediator of cell cycle arrest (El-Deiry et al., 1993), was up-regulated in these cells (Bouvard et al., 2000). Taken together, these observations suggest that p53 is incapable of mediating a pro-apoptotic response in renal epithelial cells in response to stress. Hence, there is little requirement for mutation of p53 in these cells for subsequent development of cancer in this tissue. The behaviour of p53 in renal tissue is reflected in the behaviour of p53 in RCC cells *in vitro*. p53 in cultured RCC cells that possess wild type p53 is at least partially able to function as a transcription factor, insofar as p53 can promote the transcription of p21 in response to UV radiation and down-regulation MDM2 by siRNA resulted

in increase p53 and and p21 protein level (Warburton et al., 2005). Further, RCC cells cultured *in vitro* can spontaneously increase p53 and MDM2 expression and this increase in expression of both proteins results in increased motility (Polanski et al., 2010). Increased motility and by extension, increased metastasis, as a result of up-regulation of p53 and MDM2 may be a possible explanation for the poor outcome of patients with p53/MDM2 positive RCC tumours, however this remains to be elucidated (Noon et al., 2011). Having addressed the relevant molecular and cell biology of RCC in this section, the next section will address treatment strategies for RCC. A more detailed general discussion about p53 and MDM2 structure and function will follow the next section.

1.1.7 Treatment of RCC

RCC is both radio-resistant and chemo-resistant; hence these treatment modalities are not used as treatment options in RCC patients. Surgical resection of the primary tumour is the most favoured therapeutic option if the tumour is sufficiently localized (Rini et al., 2009). Partial nephrectomy, which is surgical resection of the tumour whilst leaving the remainder of the kidney intact, is becoming a preferred method for dealing with renal masses. Comparisons of radical nephrectomy, which is complete removal of the kidney, with partial nephrectomy have shown that there is no significant difference between both approaches in relationship to patient outcome (Uzzo and Novick, 2001; Kopp et al., 2013). Spontaneous regression of metastatic RCC lesions in response to nephrectomy is a rare but recognized occurrence. Spontaneous regression has been observed to take place in <1% of patients that have undergone nephrectomy (Snow and Schellhammer, 1982) however, this phenomenon has also been observed in the absence of surgery and spontaneous regression may not

necessarily be associated with nephrectomy (De Riese et al., 1991; Lekanidi et al., 2007). A possible explanation for spontaneous regression in response to nephrectomy is that removal of the primary tumour removes a source of immunosuppressive factors. Alternatively, nephrectomy may remove an important source of pro-angiogenic and growth factors (Biswas and Eisen, 2009). These observations led to an increased interest in immunotherapy in the treatment of RCC. Before the advent of targeted therapy for the treatment of RCC, interferon-α (IFNα) and high dose interleukin-2 (IL-2) were treatments used in patients that suffered from the metastatic disease (Fyfe et al., 1995; Jonasch and Haluska, 2001). High dose IL-2 is the only treatment for metastatic RCC that has been shown to mediate a complete response although this has been typically in less than 5% of patients (Fyfe et al., 1995; McDermott et al., 2005). An increased understanding of the underlying molecular biology of RCC has driven the use of targeted therapy for the treatment of the metastatic disease. All of the current targeted therapies for the treatment of metastatic RCC are directed towards inhibition of downstream effects of *VHL* mutation. Sorafenib, Sunitinib, Axitinib and Pazopanib are all multikinase inhibitors that can inhibit isoforms of the VEGF receptor, c-kit and PDGF receptor. Bevacizumab is a monoclonal antibody that can target VEGF-A and Temsirolimus and Everolimus both target mTOR, the inhibition of which can lower HIF-1α production (Linehan et al., 2010). The use of targeted therapy has been met with limited success in the clinic, with targeted therapies increasing median progression free survival and overall survival by only a few months over placebo or other controls (Hutson, 2011). In a recent trial of patients that had failed first line therapy of either Sunitinib, Bevacizumab in combination with IFN-α, Temsirolimus or cytokine therapy, patients were treated with Axitinib, a second generation

multikinase inhibitor, or Sorafenib (Rini et al., 2011). There was a statistically significant increase in progression free survival (PFS) in the group treated with Axitinib when compared to the Sorafenib-treated group and the median PFS was 6.7 months vs 4.7 months and both drugs had a similar safety profile. Axitinib may therefore become the future second line therapy for metastatic RCC. Overall, targeted therapy has increased median overall survival from roughly 12 months in patients treated with immunotherapy (McDermott et al., 2005), to over 24 months (Hutson, 2011). However, survival data from all of the current therapeutic regimes leave much to be desired in terms of improved treatments for the metastatic condition.

1.2 p53

1.2.1 Introduction to p53

The tumour suppressor p53 is widely regarded as the "guardian of the genome" (Lane, 1992) because of the central position of the protein in connecting multiple pathways that maintain the integrity of genetic information upon exposure to different types of stress (Fridman and Lowe, 2003). p53 primarily functions as a transcription factor, promoting the transcription of genes whose protein products can determine a number of cell fates, however, transcription-independent functions of p53 have been described (Speidel, 2010).

p53 was first discovered as a protein that co-precipitated with large T antigen in SV40 virus-infected cells by three independent groups (Kress et al., 1979; Lane and Crawford, 1979; Linzer and Levine, 1979). Early studies on p53 suggested a role for the protein in promoting cell proliferation. An increase in the level of p53 mRNA

and p53 protein synthesis was observed in growth arrested mouse fibroblasts stimulated by the addition of serum, and this peaked at the G1/S boundary (a more detailed description of the cell cycle is presented in section 1.2.3), before initiation of DNA replication (Reich and Levine, 1984). Similar observations in normal resting lymphocytes (Milner and McCormick, 1980) and normal diploid fibroblasts (Mercer et al., 1984) suggested that p53 expression always accompanied cell growth. The observation that co-transfection of what was believed to be wild type p53 complementary DNA (cDNA) with co-introduced activated Ras oncogene could cause transformation of rat embryonic fibroblasts (Eliyahu et al., 1984) led researchers to believe that p53 could function as an oncogene. It was later demonstrated that p53 studied in cancer cells was mutated and that wild type p53 lacked transforming ability *in vitro* (Hinds et al., 1989). Further experiments showed that co-transfection of a plasmid coding for wild type p53 reduced the transformation potential of plasmids encoding an activated Ha-Ras gene (Eliyahu et al., 1989). The role of p53 as a tumour suppressor was finally confirmed when it was observed that the p53 gene was absent or mutated in colorectal carcinoma (Baker et al., 1989). p53 activity is important in inducing a number of cell fates in response to stress. These include, but are not limited to: cell cycle arrest, senescence and apoptosis. The following is a summary of each of these cell fates and a description of the contribution made by p53 in determining each of these outcomes.

1.2.2 p53: overview of structure and function

p53 is a 393 amino acid-long protein consisting of a number of functional domains. These include an amino-terminus transactivation domain (TAD), a proline-rich regulatory domain, a DNA-binding domain (DBD), an oligomerization domain and a

carboxy-terminus regulatory domain (Okorokov and Orlova, 2009). The organization of domains of the p53 polypeptide is shown on figure 1.2.1. Nuclear export signals can be found within the TAD and oligomerization domain of p53 and three nuclear import signals can be found at the carboxy-terminus regulatory domain of the protein (Vousden and Lu, 2002). What follows is a discussion of the contribution made by each domain to the function of the p53 protein. The TAD, encompassing amino acids 1-43, plays a role in the recruitment of the basal transcription machinery upon binding of p53 to DNA. The TAD can be further sub-divided into two separate transactivation domains, TAD1 and TAD2 (Chang et al., 1995). Recent work has suggested that the response of p53 to acute DNA damage is dependent upon TAD1 but the response to oncogenic signalling is dependent on both TADs (Brady et al., 2011). General transcription factors (GTFs) are required for transcription in eukaryotes (Thomas and Chiang, 2006). The TAD of p53 has been shown to be important in the binding of the TATA binding protein (TBP) subunit of TFIID and can promote the recruitment of TFIID (Chen et al., 1993; Liu et al., 1993). Mutation of amino acids 22 and 23 of p53 disrupt the interaction between p53 and TAFII31, abrogating the ability of p53 function as a transcription factor (Lu and Levine, 1995).

As mentioned earlier, p53 is a sequence specific transcription factor which can bind DNA via its DBD to a consensus sequence composed of two copies of the following DNA bases: 5'-PuPuPuC(A/T)(T/A)GPyPyPy-3' (where Pu represents a purine and Py represents a pyrimidine) separated by 0-13 base pairs (El Deiry et al., 1992). The importance of the DBD to the function of p53 is highlighted by the observation that the overwhelming majority of mutations in p53 that are observed in cancer occur in

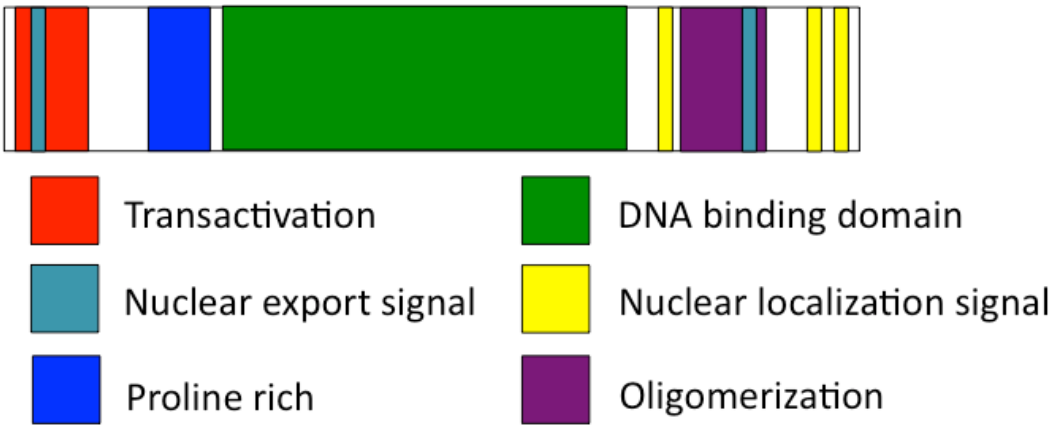

Figure 1.2.1 Functional domains of p53. Adapted from Vousden and Lu, 2002.

Figure 1.2.2 Structural arrangement of p53. L1, 2 and 3 indicate loops and LSH indicates loop-sheet-helix motif. Amino acids that tetrahedrally co-ordinate Zinc and that make contact with DNA are also indicated. Reproduced from Soussi and Beroud, 2001.

this domain (Hollstein et al., 1991; Petitjean et al., 2007). Structural studies have demonstrated that the DBD folds into an anti-parallel ß-sandwich that co-ordinates two loops to permit interaction with DNA. These loops are stabilised by a Zn^{2+} ion to form a loop-sheet-helix motif (figure 1.2.2). The DBD interacts with the DNA minor groove and makes contact with the phosphate backbone at the centre of the consensus sequence. Structural studies of the p53-DNA binding complex suggest that the amino acid residues most frequently altered in mutant p53 are the residues that make direct contact with DNA (Cho et al., 1994).

The carboxy-terminus of p53 harbours an oligomerization domain and nuclear import/export sequences. The carboxy-terminus domain is comprised of a α-helix and a ß-strand. This motif joins three other carboxy-terminus domains, interacting via hydrophobic interactions, through an anti-parallel helix–helix interface to form a tetramer (Clore et al., 1994; Okorokov and Orlova, 2009).

Upon activation, p53 can promote a number of responses that can contribute to the role of p53 as a tumour suppressor, including cell cycle arrest, senescence and apoptosis. The following is a description of each response and how p53 is involved in promoting these cell fates.

1.2.3 Cell cycle arrest

The cell cycle comprises a coordinated series of events where the outcome is the duplication of all cell components and division to produce two cells, a mother and a daughter cell, each containing the complete cell contents required for further growth and division. A combination of checkpoints and controls within the cell cycle permit

the smooth transition between each stage. Whereas cell growth is continuous, DNA synthesis and mitosis are divided into phases: S (DNA synthesis), G2 (post-synthetic gap), M (mitosis) and G1 (pre-synthetic gap) (Norbury and Nurse, 1992). The cell cycle is summarised in figure 1.2.3. Progression through the cell cycle is directed by an orchestrated series of regulatory events, chief among them, the sequential activation and de-activation of hetero-dimeric cyclin-dependent kinases (CDKs)-cyclin complexes. Progression through G1 is dependent on CDKs binding to cyclins D and E. S and M phase progression, however is dependent upon CDKs binding to cyclins A and B (Diaz-Moralli et al., 2013). Sensor mechanisms, called checkpoints, maintain an accurate sequence of events by ensuring a new phase of the cell cycle is not initiated until the completion of the current phase. A driving force for the development and subsequent progression of cancer is DNA damage (Hanahan and Weinberg, 2000). One mechanism that has evolved to permit repair of damaged DNA before continuation through the cell cycle is cell cycle arrest. Cell cycle arrest is a temporary pause in the cell cycle that allows damaged DNA to be repaired before allowing the cell to continue replication of the DNA or subsequent division.

1.2.4 The role of p53 in cell cycle arrest

p53 can promote the transcription of a number of genes whose protein products are involved in inducing cell cycle arrest. p53 can promote arrest of the cell cycle at two stages: G1 and G2. p53 can promote the expression of p21 (also known as WAF1/Cip1) (El Deiry et al., 1993) which can bind to and inhibit CDK4/6-cyclin D, CDK1-cyclin B and CDK1/2-cyclin A. This results in a block to cell cycle progression (Xiong et al., 1993; El Deiry et al., 1994). p21 can also interact with PCNA, a DNA replication processivity factor. Binding of p21 to PCNA perturbs the

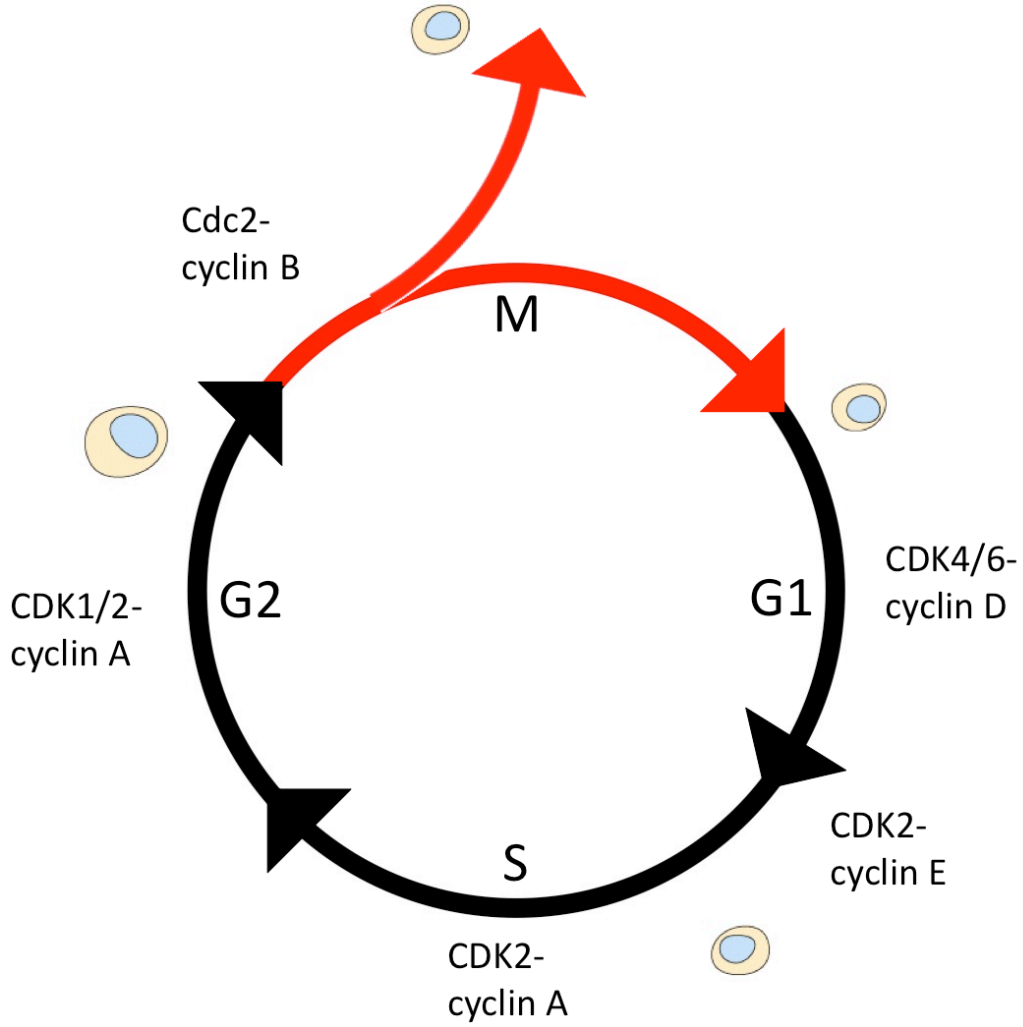

Figure 1.2.3 The cell cycle. In response to mitogens, a resting cell in G0 can enter the cell cycle. Cyclin D-dependent CDKs accumulate and initiate the phosphorylation of Retinoblastoma, a process that is completed by CDK2-cyclin E. The restriction point is the stage at which the cell is committed to continuation of the cell cycle. At S-phase entry, cyclin E is degraded and cyclin A associates with CDK2. This allows continuation of the process to M phase, when a cell undergoes mitosis and divides into two daughter cells. Adapted from Lodish et al., 2000.

ability of PCNA to function as a processivity factor for DNA polymerase in DNA replication, hence causing cell cycle arrest (Waga et al., 1994). p53 can promote the transcription of GADD45 (Kastan et al., 1992). Gadd45 has been shown to perturb the interaction between Cdc2-cyclin B1, resulting in G2 arrest (Zhan et al., 1999).

p53 can also promote the transcription of 14-3-3σ, a protein which can halt G2-M phase progression (Hermeking et al., 1997). 14-3-3σ can sequester CDK1-cyclinB in the cytoplasm preventing the entry of this protein into the nucleus. This inhibits progression of the G2 phase of the cell cycle (Katayama et al., 2005). Reprimo is a p53-inducible protein that can inhibit G2/M phase. The exact mechanism underlying Reprimo function has yet to be thoroughly elucidated however, it is believed that Reprimo may inhibit nuclear import of the Cdc2-cyclinB complex (Ohki et al., 2001).

1.2.5 Senescence

Senescence is defined as irreversible exit from the cell cycle; when a cell remains metabolically active but can no longer divide and proliferate. Most somatic cells possess a limited replicative lifespan. Each cell division is accompanied by erosion of telomeres, the repetitive DNA sequence at the end of chromosomes. Irreversible exit from the cell cycle as a result of telomere shortening is described as replicative senescence (Acosta and Gil, 2012). Senescent cells in culture have a large, flattened morphology and are associated with increased β-galactosidase activity, also termed senescence associated β-galactosidase activity (SA-βgal). The senescent state can also be induced by the action of oncogenes, in a process termed oncogene induced senescence. This was first illustrated in primary human fibroblasts when a

constitutively active Ras allele, H-*ras*V12 was introduced into cells by retroviral transduction. This resulted in accumulation of p53 and the CDK inhibitor p16, which was accompanied by senescence (Serrano et al., 1997). Senescence has since been shown to be an important tumour suppressive response at least in some scenarios, for example, a p53-dependent senescence program led to the clearance of tumours in a mouse model for liver carcinoma (Xue et al., 2007). p53-dependent senescence has also been shown to be important in promoting regression of lymphoma in an *Eμ-myc* model in response to the chemotherapeutic agent cyclophosphamide (Schmitt et al., 2002).

Contrary to the important role played by senescence in tumour suppression, it has been suggested that senescent cells can have a deleterious affect on surrounding, non-senescent cells (Krtolica et al., 2001). Senescent cells can stimulate the proliferation, movement and differentiation of surrounding cells via the secretion of several different molecules in what is described as the senescence-associated secretory phenotype (SASP) (Coppé et al., 2010). Secretion of pro-inflammatory cytokines and proteases that permit remodelling of the extra-cellular matrix by senescent cells provides an environment that favours proliferation and motility of surrounding cells (Davalos et al., 2010). Hence, activation of senescence may not be the most desirable outcome of cancer therapy.

1.2.6 The role of p53 in senescence

In response to DNA damage induced by ionizing radiation (IR), ataxia telangiectasia mutated (ATM) kinase and checkpoint kinase 2 (CHK2) can phosphorylate and activate p53 (Gire et al., 2004; Larsson, 2011). p53 can subsequently promote the

transcription of p21, which can inhibit cell cycle regulators to induce senescence (Brown et al., 1997). Senescence can also take place independently of both p53 and p21 as neither protein is essential for senescence to take place (Medcalf et al., 1996).

1.2.7 Apoptosis

Apoptosis, also commonly described as programmed cell death, is a programme that is essential for the healthy development of multi-cellular organisms that, when activated, culminates in destruction of the cell. Apoptosis can take place as part of normal development and as a homeostatic mechanism in the maintenance of healthy cell populations in tissues. Cells undergoing apoptosis are conspicuous by a number of morphological features that occur in a step-wise manner. Shrinkage of the cell is followed by chromosome condensation. This is accompanied by fragmentation of the nucleus. The cell membrane blebs and apoptotic bodies form, which can subsequently be engulfed by phagocytes (Kerr et al., 1972). Asymmetry of membrane phospholipids upon apoptosis permits detection of apoptotic bodies by phagocytes (Fadok et al., 1992). There are currently three known pathways that result in initiation of the apoptosis cascade, the extrinsic apoptosis pathway, the intrinsic apoptosis pathway and the granzyme B pathway. The extrinsic and granzyme B pathways are initiated by extracellular signals and the intrinsic pathway is initiated by intracellular signals, however, all three pathways converge at the mitochondrial outer membrane (MOM), where members of the Bcl-2 family interact to control the release of cytochrome C from the mitochondria (Elmore, 2007) after which, the caspase cleavage cascade ensues, resulting in the destruction of structures within the cell. Details of the steps in each of the pathways that result in cytochrome

Figure 1.2.4 The Bcl-2 family of proteins. The Bcl-2 family of proteins regulate apoptosis and can be divided into three subfamilies: anti-apoptotic, pro-apoptotic multi-BH domain and pro-apoptotic BH3-only proteins. BH – Bcl-2 homology. TM – trans-membrane. α represents a α helix in the secondary structure of the protein. Figure taken from Cory and Adams, 2002.

C release and hypothetical models of apoptosis will be discussed after a discussion of the Bcl-2 protein family members involved in this process.

The Bcl-2 family of proteins can broadly be divided into 3 main groups based sequence homology and function: the anti-apoptotic Bcl-2 family proteins comprise Bcl-2, Bcl-w, Bcl-xL, Mcl-1, Bfl-1/A1 and Bcl-B which suppress apoptosis and contain Bcl-2-homology (BH) domains 1-4. The pro-apoptotic multi-BH domain Bcl-2 family effectors, which contain BH1-3 domain comprise of the proteins Bax, Bak and Bok. The pro-apoptotic BH3-only domain proteins only possess the BH3 domain and comprises of Bid, Bim, Puma, Hrk, Noxa, Bad, Bmf and Bik. Figure 1.2.4 summarizes the sequence homology and classification of this family of proteins. In response to a death-inducing signal, the pro-apoptotic effector proteins Bax and Bak can be activated to oligomerize at the MOM and allow the efflux of cytochrome C and other pro-apoptotic proteins such as SMAC/Diablo and Omi/Htra from the intermembrane space (IMS) between the MOM and mitochondrial inner membrane (Westphal et al., 2013). Interaction of cytochrome C with Apaf-1 (apoptosis protease activating factor-1) results in the assembly of the apoptosome. The apoptosome is a multi-protein complex that is responsible for the cleavage of pro-caspase 9 (Bratton and Salvesen, 2010). Caspase 9 proceeds to cleave caspase 7 and caspase 3 and this sets in motion the cleavage of further caspases that are involved in demolition of the cell (Elmore, 2007). Whilst the mechanism regarding inhibition of Bax and Bak oligomerization by members of the anti-apoptotic Bcl-2 family such as Bcl-2, Mcl-2, Bcl-2 and Bcl-xL remains controversial (and will be discussed in further detail shortly) it is believed that the anti-apoptotic Bcl-2 family members prevent oligomerziation of Bax and Bak by i) directly sequestering Bax and

Bak at the MOM, which can be impeded by displacement of both of these proteins from the anti-apoptotic family members by the BH3-only family; or ii) by abrogating the interaction between the 'direct activator' BH3-only family members, tBid, Bim and Puma and Bax or Bak, preventing the conformational changes necessary in Bax or Bak that permit both proteins to oligomerize (Bender and Martinou, 2013).

1.2.7.1 The Extrinsic Apoptosis pathway

Cellular trans-membrane receptor and ligand interactions are involved in the initiation of the extrinsic apoptosis pathway. This process involves death receptors of the tumour necrosis factor receptor (TNF-R) family and Fas receptor (FasR). Members of the death receptor family are characterised by the presence of a death domain (DD), a 80–100 amino-acid long motif involved in the transduction of the apoptotic signal (Tartaglia et al., 1993). Apoptosis via FasR will be used to illustrate the mechanism underlying this pathway. Upon binding of Fas ligand to FasR, the DD of FasR recruits and activates FADD (Fas associated death domain protein). FADD subsequently associates with pro-caspase 8 through interaction of the DDs from each protein. At this point, the death induced signalling complex (DISC) is formed. Pro-caspase 8 is activated at the DISC by autocatalysis. Caspase 8 can then cleave caspase 3, at which point the caspase cascade that leads to apoptosis ensues (Lavrik and Krammer, 2012). Caspase 8 can also cleave the BH3-only domain protein Bid into the active form of the protein, tBid. tBid localises to and inserts into the MOM where it can either directly activate Bax or Bak or inhibit the anti-apoptotic Bcl-2 family members to perturb their interaction with Bax and Bak. This promotes efflux of cytochorome C from the IMS, promoting further caspase cleavage and an enhancement of the apoptosis cascade (Danial and Korsmeyer, 2004).

1.2.7.2 The Intrinsic Apoptosis pathway

The intrinsic apoptosis pathway is initiated from signals from within the cell itself and the initiation of this pathway is independent of extracellular signalling. A number of different stimuli can initiate the intrinsic apoptosis pathway and these stimuli include, but are not limited to, growth factor deprivation, DNA damage, cytokine deprivation and hypoxia. Intrinsic apoptosis is mediated by members of the BH3-only family of pro-apoptotic proteins such as Bid, Puma, Noxa, Hrk and Bad and members of this family are modified by post-translational mechanisms or up-regulated in response to pro-apoptotic stimuli, before they can contribute to apoptosis. For example, Noxa and Puma are up-regulated by increased transcription, Bid is cleaved into its active form, tBid and Bad requires de-phosphorylation for the protein to be activated (Happo et al., 2012). A description of Puma up-regulation will be used to illustrate the intrinsic apoptosis pathway. Puma, also known as Bbc3, is a potent pro-apoptotic BH3-only family member that can promote Bax and Bak activation through either direct allosteric activation of Bax and Bak or by engaging anti-apoptotic Bcl-2 family members such as Bcl-2 and Bcl-xL (Hikisz and Kiliańska, 2012). As stated previously, intrinsic apoptosis can be initiated in response to DNA damage or growth factor deprivation. Puma can be up-regulated by p53 in response to DNA damage (Han et al., 2001) or by FOXO3a in response to growth factor deprivation (You et al., 2006). Puma can then localize to the mitochondria to promote the efflux of apoptotogenic factors from the IMS and the caspase cascade ensues.

1.2.7.3 The Granzyme B pathway

Cytotoxic T lymphocytes (CTL) can eliminate cells infected with a virus or tumour cells via apoptosis using the granzyme B pathway. CTL cells secrete a pore forming protein into the membrane of the affected cell called perforin. This permits the entry of granzyme B, which subsequently cleaves caspase 3 and Bid. Caspase 3 cleavage results in the cleavage of downstream caspases and resulting cellular destruction. Cleavage of Bid to tBid by granzyme B, promotes the efflux of cytochrome C from the mitochondria, which ultimately allows cleavage of caspases upstream from caspase 9, thus enhancing downstream caspase signalling and enhancement of the apoptotic effect (Elmore et al., 2007; Rousalova and Krepela, 2010).

1.2.7.4 Interactions between the Bcl-2 family members and models of apoptosis

A complex network of interactions between anti-apoptotic and pro-apoptotic proteins determine whether cytochrome C is released from the IMS or maintained in the mitochondria. What follows is a discussion regarding structure function relationships of the Bcl-2 family members, regulation of members of the Bcl-2 family and current models of Bax/Bak-mediated apoptosis.

Pro-apoptotic effectors Bax and Bak and the anti-apoptotic Bcl-2 family proteins have a similar tertiary structure. They are small globular proteins that exhibit a characteristic arrangement of 7-8 amphipathic α-helices surrounding the central hydrophobic helix 5 (Chipuk et al., 2010). This α-helical bundle folds to form a conserved hydrophobic surface groove. Several structural and biochemical studies have shown that the interaction between members of the anti-apoptotic Bcl-2 family and the pro-apoptotic proteins of the Bcl-2 family occurs between this groove on the

Figure 1.2.5 Specificity of BH3-only proteins for anti-apoptotic Bcl-2 family members. Cartoon depicting the specificity of each member of the BH3-only family for members of the anti-apoptotic Bcl-2 family. Figure taken from Chipuk et al., 2010.

anti-apoptotic proteins and the ~26 amino acid-long, alpha helical BH3 domain of the pro-apoptotic proteins (Sattler et al., 1997). Subtle differences in the BH3-alpha helix-groove interaction confers specificity of interaction between the pro-apoptotic BH3-only proteins and anti-apoptotic Bcl-2 family members. Bim, Puma and tBid will bind to any of the anti-apoptotic Bcl-2 family member, others are more specific in their interactions. For example, the Noxa BH3-only protein is a potent interacting partner and thus inhibitor, of the anti-apoptotic protein Mcl-1. However, Noxa has poor affinity for Bcl-2, Bcl-w and Bcl-xL. Conversely, Bad has a high affinity for Bcl-2, Bcl-w and Bcl-xL but not to Mcl-1 (Chen et al., 2005; Certo et al., 2006; Deng et al., 2007). The different specificties of the BH3 family and the anti-apopototic Bcl-2 family are summarized in figure 1.2.5.

Bak and/or Bax are essential for the efflux of cytochrome C from the mitochondrial IMS that leads to apoptosis (Wei et al., 2001). Bak is constitutively localized to the outer membrane of the mitochondria and Bax is predominantly cytosolic until pro-apoptotic signalling promotes Bax translocation to the mitochondria. The events leading up to the Bax/Bak pore formation at the mitochondrial OM have been the subject of debate for several years. The "de-repressor" model postulates that the anti -apoptotic Bcl-2 family members sequester Bax and Bak at MOM. Interaction of the BH3-only proteins with the anti-apoptotic Bcl-2 proteins results in the displacement of the anti-apoptotic family members from Bax and Bak. Liberation of Bax and Bak from the anti-apoptotic proteins permits auto-activation and subsequent oligomerization, which results in apoptosis (Chen et al., 2005; Willis et al., 2007; Uren et al., 2007).

The "direct activation" model, on the other hand, posits that "activator" BH3-only proteins tBid, Bim and possibly Puma transiently interact with Bax or Bak, promoting a conformational change that results in the activation of Bax or Bak, allowing oligomerization of Bax and Bak. In this model, the remaining BH3-only proteins act as "sensitizers" that displace the activators from anti-apoptotic Bcl-2 family members, permitting the interaction between the activators and Bax and Bak (Bender and Martinou, 2013; Westphal et al., 2013).

1.2.7.5 BH3 mimetics

Irrespective of how apoptosis is promoted at the MOM by Bax and Bak, the Bcl-2 family of anti-apoptotic proteins are an attractive target for therapeutic intervention. Evasion of apoptosis is considered to be one of the hallmarks of cancer (Hanahan and Weinberg, 2000). Because of the important role played by the anti-apoptotic Bcl-2 family in preventing the initiation of apoptosis, the design of small molecule inhibitors of this group of proteins has been an area of intense research for several years. The hydrophobic groove formed by the BH1, BH2 and BH3 domains within proteins that are members of the anti-apoptotic Bcl-2 family lends itself to the design of small molecule mimetics, because of the importance of the groove in acting as the interface for the interaction between the anti-apoptotic Bcl-2 family members and the pro-apoptotic Bcl-2 family members (Letai, 2003). Abbot Laboratories developed a BH3 mimetic in 2005 (Oltersdorf et al., 2005) by linking two separate small molecules that bound the hydrophobic groove of Bcl-xL at two proximal sites in the groove. Further iterative manipulations of the lead molecule resulted in the development of ABT-737, a small molecule inhibitor of Bcl-2, Bcl-w and Bcl-xL that has a $K_i < 1nM$. Because of the affinity of ABT-737 to these anti-apoptotic

proteins, the compound has been described as a mimetic for the pro-apoptotic protein Bad (figure 1.2.5; Van Delft et al., 2007). Of the putative BH3 mimetics tested by the study of Van Delft et al., only ABT-737 was capable of promoting cell death via Bax and Bak activity, suggesting that ABT-737 was the first BH3 mimetic discovered that genuinely promoted the intrinsic apoptosis pathway. Further, it was shown that levels of Mcl-1 could modulate resistance to ABT-737-mediated apoptosis. Because Noxa is a potent Mcl-1 inhibitor, resistance to ABT-737 could be reversed by either reducing Mcl-1 protein levels or increasing Noxa protein levels (Van Delft et al., 2007). Intriguingly, treatment of a number of cell lines from a variety of different tissue backgrounds with ABT-737 or its derivatives has resulted in the increased *de novo* synthesis of Noxa protein (Hauck et al., 2009; Sale and Cook, 2013). This has since been shown to be dependent on transcriptional up-regulation of Noxa by E2F1/pRb (Bertin-Ciftci et al., 2013).

1.2.8 The role of p53 in apoptosis

As described previously, p53 functions predominantly as a transcription factor hence one of the major functions of p53 in apoptosis is to promote the transcription of genes whose protein products are involved in apoptosis. The p53-mediated transcription of several genes preceding apoptosis is highly dependent on the nature of pro-apoptotic stimulus and the tissue type (reviewed in Vlatković et al., 2011). p53 can promote the transcription of a mitochondrial effector of apoptosis Bax (Miyashita and Reed, 1995). p53 can also promote the transcription of BH3-only family members Noxa (Oda et al., 2000) and Puma (Nakano et al., 2001; Yu et al., 2001), both of which can be important in promoting apoptosis at the mitochondria. p53 can repress the transcription of the anti-apoptotic protein Bcl-2, due to the

presence of p53 negative response elements in the promoter of the *BCL-2* gene, though the precise mechanism of how this takes place is not fully understood (Miyashita et al., 1994). p53 can also promote the up-regulation of proteins involved in the extrinsic apoptosis pathway. p53 can promote the transcription of Fas/APO-1 (Owen-Schaub et al., 1995), LRDD (also known as PIDD, Lin et al., 2000) and DR5 (Wu et al., 1997). A role for the direct involvement of cytosolic p53 at the mitochondria has been described (Chipuk et al., 2003, 2005). It is thought that during apoptosis, cytosolic p53 can translocate to the mitochondria where p53 can directly activate Bax or interact with anti-apoptotic Bcl-2 family members to promote apoptosis.

1.3 MDM2 and regulation of p53

1.3.1 Introduction to MDM2

MDM2 is one of two essential regulators of p53. MDM4, also known as MDMX, is the second essential regulator of p53. The importance of MDM2 and MDM4 as regulators of p53 is best illustrated by knockout mouse models. Mice that lack Mdm2 or Mdm4 are embryonic lethal. Knockout of p53 concomitant with Mdm2 or Mdm4 knockout rescues the lethal phenotype, highlighting the deleterious effect of unrestrained p53 activity and the importance of both MDM2 and MDM4 in regulating p53 (Jones et al., 1995; Parant et al., 2001). A comparison of the functional domains in both MDM2 and MDM4 is shown in figure 1.3.1. A brief discussion regarding the interaction of MDM4 with MDM2 and the role of MDM4 in the regulation of p53 will follow shortly however the remainder of this section will be devoted to MDM2.

MDM2 is the main negative regulator of p53 (Iwakuma and Lozano, 2003). Interaction of MDM2 with p53 is mediated by the p53-binding domain located at the N-terminal of MDM2 (figure 1.3.1) (Chen et al. 1993). MDM2 also possesses a nuclear import and nuclear export sequence that allows shuttling of the protein from the cytoplasm to the nucleus (Roth et al., 1998). Arguably the most important functional domain on the MDM2 protein is the RING finger domain, which mediates ubiquitination of p53 and MDM2 itself. This ultimately targets p53 for degradation at the proteasome (Honda et al., 1997; Fang et al., 2000). Within the RING finger domain of MDM2, there is a nucleolar localization sequence, which is involved in the localization of the p14Arf-MDM2 complex to the nucleolus (Lohrum et al., 2001; Weber et al., 2000), the importance of which will be discussed shortly.

Because of the potentially deleterious effects of unfettered p53 activity, as illustrated by the embryonic lethal phenotype observed in mice lacking the *Mdm2* gene, one mechanism that has evolved to regulate p53 levels in the cell is the transcriptional induction of MDM2 by p53 (Wu et al., 1993). Transcription of the *MDM2* gene can occur from two promoters, P1 and P2 (Perry et al., 1993). A basal level of MDM2 protein in the cell is dependent upon transcription from the P1 promoter of the *MDM2* gene. In unstressed cells, p53 is maintained at low levels by MDM2. In response to stress signals, the interaction between p53 and MDM2 is typically abrogated by post-translational modification of both proteins, one of a number of steps (the remainder will be discussed in section 1.3.2), which results in increased p53 levels. p53 can subsequently promote the transcription of MDM2 from the P2 promoter, elevating levels of MDM2 protein, which can lower p53 protein back to basal levels observed before the stress response was initiated. Hence, p53 and

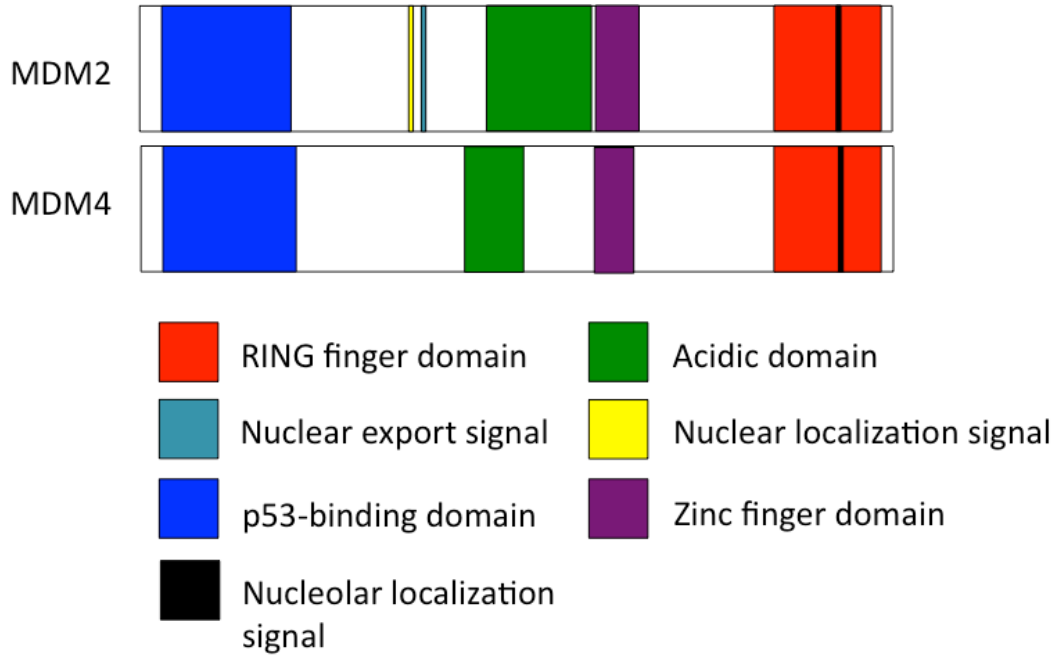

Figure 1.3.1 Functional domains of MDM2 and MDM4. Comparison of the functional domains present in MDM2 and MDM4. Adapted from Marine et al., 2007.

MDM2 are engaged in an auto-regulatory feedback loop (Saucedo et al., 1999; Mendrysa and Perry, 2000; Vousden and Lu, 2002; Wu et al 1993).

MDM2 can also regulate p53 by controlling the sub-cellular localization of p53. Mono-ubiquitination of p53 by MDM2 can promote the exposure of the carboxy-terminus nuclear export sequence within the oliogomerization domain of p53. This allows p53 to be exported from the nucleus to the cytoplasm (Stommel et al., 1999; O'Keefe et al., 2003). MDM4 is a homologue of MDM2 that can associate with p53 but lacks the ubiquitin ligase function that MDM2 possesses. MDM4 can heterodimerize with MDM2 and this interaction takes place via the RING finger domain of each protein (Tanimura et al., 1999). MDM4 is thought to stimulate the ability of MDM2 to ubiquitinate p53 (Linares et al., 2003)

1.3.2 Regulation of p53 by MDM2 and other proteins

As discussed earlier, p53 is maintained at low levels in an unstressed cell by MDM2. When a cell is exposed to stress, it is important that p53 levels increase rapidly to mount a swift response to this. Rescue of p53 from its main negative regulator, MDM2, allows rapid accumulation of the protein when compared to *de novo* synthesis of p53, hence one of the main mechanisms for the up-regulation of p53 is the post-translational modification of both p53 and MDM2 such that the interaction between both proteins is abrogated until a time when a p53-mediated stress response is no longer required (Prives and Hall, 1994). For example, in response to IR, p53 is phosphorylated on Serine 15 by ATM kinase (Banin et al., 1998; Canman et al., 1998) whereas in response to UV radiation, p53 is phosphorylated on Serines 15 and 37 by the ATM-related (ATR) kinase (Tibbetts et al., 1999). MDM2 can also be

phophorylated by ATM kinase in response to ionising radiation (Khosravi et al., 1999). These post-translational modifications of both p53 and MDM2 disrupt the interaction between both of these proteins, resulting in the rescue of p53 from negative regulation by MDM2 and subsequent stabilization of p53.

Alternatively, the p53-MDM2 interaction can be abrogated by interaction of MDM2 with p14Arf. p14Arf is an alternative reading frame product of the CDKN2A locus and is activated in response to oncogene activation (Quelle et al., 1995; Sherr and Lowe, 2003). The interaction between p14Arf and MDM2 can sequester MDM2 at the nucleolus and prevent ubiquitination of p53 by MDM2 (Tao and Levine, 1999).

p53 activity can also be regulated by other post-translational modifications, such as acetylation, NEDDylation and SUMOylation but the precise details of how all of these modifications affect p53 function are in need of further elucidation (Kruse and Gu, 2009). p53 can be acetylated by the histone acetyl transferase, p300 (Gu and Roeder, 1997). Acetylation of p53 at Lysine residues clustered around the C-terminal of the protein is a post-translational modification that can compete with ubiquitination of the same Lysine residues by MDM2. This is thought to exert an effect on the stability of p53 and increased acetylation of p53 correlates with a p53-mediated stress response (Sakaguchi et al., 1998; Luo et al., 2000). Within the DBD of p53, acetylation at Lysine 120 has been shown to be important in the transcription of pro-apoptotic *PUMA* and *BAX* and abrogation of this post-translational modification by substituting Arginine for Lysine reduces p53-dependent apoptosis (Sykes et al., 2006; Tang et al., 2006)

1.3.3 Pharmacological restoration of p53 function in cancer

Because of the central role of p53 in tumour suppression and the fact that p53 is mutated in roughly 50% of cancers, much interest has been focused on the development of compounds that can restore wild type conformation to mutant p53. An example of one such compound is PRIMA-1, which can promote restoration of wild type conformation to mutant p53, promoting p53-dependent transcription and ultimately senescence or apoptosis (Bykov et al., 2002). Because these compounds have been reviewed elsewhere (Bykov et al., 2009), and the focus of this thesis is on RCC, where the overwhelming majority of cases harbour wild type p53, this class of compounds will not be discussed here. In the remaining 50% of cancers that maintain wild type p53, one strategy to restore wild type p53 function is to inhibit the interaction between MDM2 and p53. The crystal structure of the amino terminal of MDM2 bound by a peptide of the transactivation domain of p53 was resolved in 1996 (Kussie et al., 1996). MDM2 contains a deep hydrophobic pocket in its amino terminal, residues 25-109, where the transactivation domain of p53 binds MDM2. Eighteen years subsequent to this discovery, a small molecule compound, Nutlin-3, was identified that could fit into this binding pocket and inhibit the interaction between MDM2 and p53 (Vassilev et al., 2004). The cis-imadazoline analogue Nutlin-3 has since been shown to be a potent inhibitor of the MDM2-p53 interaction and treatment of cells harbouring wild type p53 from a variety of tumour types with this compound has resulted in p53-mediated cell cycle arrest, senescence and apoptosis (Vassilev et al., 2004; Tovar et al., 2006; Van Maerken et al., 2006). Since the discovery of Nutlin-3, a number of other compounds have been discovered that can displace p53 from the same p53-binding pocket of MDM2, including the MI series of compounds (Ding et al., 2005), AM-8553 (Rew et al., 2012) and

isoindolinone-based MDM2 inhibitors (Hardcastle et al., 2005). An alternative strategy to liberating p53 from the inhibitory effects of MDM2 in cancer cells is the development of inhibitors of the E3 ligase domain of MDM2. This family of compounds, such as HLI373 (Kitagaki et al., 2008) and Sempervine (Sasiela et al., 2008) have been shown to induce p53-dependent cell cycle arrest or apoptosis in a variety of cell lines.

An alternative approach to the restoration of p53 function in cancer has been the introduction of adenoviral vectors expressing wild type p53 directly into the tumours of cancer patients (reviewed in Tazawa et al., 2013). This approach is currently in clinical trials for patients suffering from non-small cell lung cancer, head and neck squamous cell carcinoma and ovarian cancer, amongst other conditions.

1.4 Use of drug combinations in cancer therapy

Over the past decade, with an increased knowledge of the underlying molecular biology of several malignancies, a major focus of cancer research has been the development of therapeutic agents that can target specific signalling pathways that are dysregulated in cancer. This approach has been successful in a few cancers, such as treatment of chronic myeloid leukaemia with imatinib, which has resulted in durable responses in a high number of cases (Druker et al., 2006). The use of a single targeted therapy has proven less successful in RCC and several other cancers (see section 1.1.7). Pathways that regulate proliferation and survival in cancer cells consist of multiple feedback loops and compensatory mechanisms that are highly adaptive to selective pressures exerted upon them (Hanahan and Weinberg, 2000). Indeed, in a model used to determine resistance mechanisms to the anti-angiogenesis

agent, Sunitinib, hypoxic cancer cells activated pathways to increase invasion of surrounding tissue, to permit access to normal tissue vasculature (Azzam et al., 2010; Ebos et al., 2009). An approach to dealing with adaptation to therapeutic intervention is the use of rational drug combinations (Kummar et al., 2010). The concept of combining drugs for the treatment of cancer is not new (DeVita et al., 1975) and can offer a number of advantages over single agent therapy for example, increasing the effectiveness of the therapeutic effect, slowing down drug resistance and decreasing dosage of one of the agents to avoid toxicity (Chou, 2006). The targeting of one or more pathways with a combination of agents is an attractive concept in cancer therapy because it may address the issue of adaptation of cancer cells to a single agent. Hypothetically, if cancer cells respond to targeted inhibition of pathway A by up-regulating or activating pathway B, which can compensate for inhibition of pathway A, then inhibition of pathway A alone would be fruitless. However, if both pathways A and B are inhibited, and both pathways regulate a process that is essential to cell survival and there are no other compensatory mechanisms, death would be the only outcome to this hypothetical scenario. This is a very simplified description of the underlying theoretical basis of how combining of agents can result in cell death (Yeh and Kishony, 2007; Chan and Giaccia, 2011).

The interaction of two or more drugs in a biological system can broadly be categorized into an additive interaction between the drugs used, a synergistic interaction or an antagonistic interaction. When two or more compounds act without interaction and the total effect does not differ from what can be expected from the dose-effect relations of the individual agents, this is described as an additive effect (Goldoni and Johansson, 2007). When there is a greater than additive effect, this is

termed synergy. Conversely, when one drug reduces the effectiveness of another drug in a combination, this is termed antagonism. What follows is a brief discussion of two commonly used methods to measure drug interactions in biological systems, Bliss independence and Loewe additivity.

1.4.1 Bliss independence

The central assumption underlying the Bliss independence model is that the toxic agents applied act independently of each other (Bliss, 1939). For two compounds, A and B, the expected inhibition by the combination of compounds, f(AB) is:

$$f(AB) = f(A) + f(B) - f(A) \times f(B)$$

Where f(A) and f(B) are the individual levels of inhibition for compounds A and B. If the observed level of inhibition is greater than the expected inhibition, the interaction is synergistic. Conversely, if the observed level of inhibition is less than the expected level of inhibition, the interaction is antagonistic. Otherwise, there is no interaction and the combination is additive. The Bliss model, whilst very simple, suffers from a number of limitations. In many experimental situations, two drugs may be acting on targets that are not completely independent of each other. The Bliss model does not take into account the shape or the slope of those dose response curve for each drug used; in extreme examples where the dose response curve for a drug is particularly steep, a single compound can be shown to be synergistic with itself.

1.4.2 Loewe additivity

The basic assumption of the Loewe additivity model is the opposite of the Bliss model: all toxicants in the mixture act on the same biological site by the same mechanisms of action and differ only in their potency (Loewe, 1953). The combination index (CI) for a combination of drugs A and B at a given level of inhibition is calculated using the following equation:

$$[A]_{comb.}/[A]_{alone} + [B]_{comb.}/[B]_{alone}$$

where $[A]_{comb.}$ represents the concentration of A used in the combination treatment and $[A]_{alone}$ represents the concentration of A used alone. $CI < 1$ is considered to be a synergistic interaction and $CI > 1$ is considered to be an antagonistic interaction. $CI = 1$ suggests no net effect and is considered to be an additive interaction. Table 1.4 summarizes different degrees of synergism and antagonism that are observed upon analysis of drug interaction using the combination index (Chou, 2006). Combination indices can also be expressed graphically using isobolograms. This is discussed further in section 3.2.1. One limitation of the Loewe model is that the individual dose response curves for both drugs need to have similar shapes and slopes. Further, from a practical point of view, more data points are required than the Bliss model for calculation of the drug interaction (Goldoni and Johansson, 2007).

Table 1.4 Description and symbols of synergism or antagonism in drug combination studies analysed by the combination index. Table reproduced from Chou, 2006.

Range of combination indices	Description	Graded symbols
<0.1	Very strong synergism	+ + + + +
0.1-0.3	Strong synergism	+ + + +
0.3-0.7	Synergism	+ + +
0.7-0.85	Moderate synergism	+ +
0.85-0.90	Slight synergism	+
0.90-1.10	Nearly additive	±
1.10-1.20	Slight antagonism	-
1.20-1.45	Moderate antagonism	- -
1.45-3.3	Antagonism	- - -

1.5 Aims

RCC is a notoriously difficult cancer to treat. Current therapies for the metastatic disease do not prolong life beyond 20 months on average; therefore there is a need for novel therapeutic strategies to deal with this (Section 1.1.7). p53, a potent tumour suppressor, is typically wild type in RCC and is expressed at high levels, with MDM2, the negative regulator of p53, in patients that have the worst prognosis (Section 1.1.5.3). Rescue of wild type p53 from the inhibitory effects of MDM2 in RCC cells in culture using inhibitors of the p53-MDM2 interaction has resulted in cell cycle arrest or senescence, not apoptosis (Tsao and Corn, 2010; Polanski et al., submitted). This response may be related to the nature of the behaviour of p53 in renal epithelial cells, the tissue from which RCC is derived (Section 1.1.5.3). Because of the potentially deleterious effects of senescent cells in the tumour microenvironment (Section 1.2.5), we intend to restore p53 function in RCC cells harbouring wild type p53 to commit the cell fate decision to apoptosis rather than senescence. Because an important aspect of cancer cell survival is the de-regulation of multiple signalling pathways that control growth, survival and resistance to death signals, this thesis describes experiments aimed at investigating a combinatorial approach that targets more than one molecular entity in the cell to restore wild type pro-apoptotic p53 function in RCC cells.

Chapter 2: MATERIALS AND METHODS

2.1 List of reagents

2.1.1 General list of reagents

REAGENT/PRODUCT	SUPPLIER
Acrylogel 40% solution (acrylamide:bis-acrylamide, 37.5:1)	VWR
Ammonium persulfate (APS)	Sigma
Aprotinin	Roche
Albumin from bovine serum (BSA), 96%	Sigma
Blotting grade blocker, non-fat dry milk	Bio-rad
Bromophenol blue	Sigma
CHAPS	Calbiochem
Dimethyl Sulphoxide (DMSO)	Sigma
Dithiothreitol (DTT)	Sigma
ECL Prime	GE Healthcare
ECL Select	GE Healthcare
Ethanol, absolute	Sigma
Ethylene diamine tetra-acetic acid disodium salt	Sigma
Glycerol	Sigma
Glycine	Fisher-Scientific
HEPES free acid, molecular biology grade	Calbiochem
Hybond^{TM} Nitrocellulose membrane	GE Healthcare
Leupeptin	Roche
Magnesium chloride	Sigma
Mannitol	Sigma

Methanol, analytical grade	Fisher Scientific
Pepstatin	Roche
Phenylmethylsulphonyl fluoride (PMSF)	Sigma
Ponceau S	Sigma
Pre-stained protein marker, broad range, 7-175 kDa	NEB
Protein assay dye reagent	Bio-rad
Sodium chloride	VWR
Sodium dodecyl suphate	Fisher Scientific
Sodium dihydrogen phosphate dihydrate ($NaH_2PO4{\cdot}2H_20$)	Sigma
Sodium phosphate dibasic dihydrate ($Na_2HPO_4{\cdot}2H_20$)	Sigma
Sucrose	Sigma
N, N, N', N'-tetramethylenediamine (TEMED)	BDH
Tris base	Calbiochem
Triton X-100	Amersham Biosciences
Trypsin inhibitor from soybean (STI)	Roche
Tween-20	Sigma

All H_2O used was ultra-pure >18 MΩ cm H_2O produced in a MilliQ water purifier.

2.1.2 Tissue culture reagents

REAGENT/PRODUCT	**SUPPLIER**
Dulbecco's Phosphate buffered saline	Sigma
Eagle's Minium Essential Medium (M5650)	Sigma
Fetal Bovine Serum	Sigma

McCoy's 5a Medium (M8403)	Sigma
Non-essential amino acids (100x)	Sigma
RPMI-1640 Medium (R8758)	Sigma
Sodium bicarbonate solution (7.5%)	Sigma
Sodium pyruvate solution (100mM)	Sigma
Trypsin-EDTA solution (1x)	Sigma

2.1.3 Drugs

ABT-737. Stock solution prepared by dissolving to 30mM in DMSO. Supplied by Selleck Chemicals. Long-term storage was at -80°C.

Nutlin-3. Stock solution prepared by dissolving to 30mM in DMSO. Supplied by Selleck Chemicals. Long-term storage was at -80°C.

Staurosporine. Stock solution prepared by dissolving to 1mM in DMSO. Supplied by LC Laboratories. Long-term storage was at 4°C.

2.1.4 Antibodies for Western Blotting

2.1.4.1 Primary Antibodies for Western Blotting

For western blotting, antibodies from stock were diluted in 5% blotting grade milk-PBS-Tween solution. Table 2.1.4.1 lists primary antibodies used for western blotting in this study.

Table 2.1.4.1. Primary antibodies used for western blotting in this study.

Antibody	Supplier	Catalogue number	Epitope	Working dilution
Actin (C2), mouse monoclonal	Santa Cruz Biotechnology	sc-8432	Epitope between amino acid 350-375 of human actin	3µg/ml
Bak (G-23), rabbit polyclonal	Santa Cruz Biotechnology	sc-832	Internal region of human Bax	3µg/ml
Bax (N-20), rabbit polyclonal	Santa Cruz Biotechnology	sc-493	Antibody raised against peptide mapped to N-terminus of human Bax	3µg/ml
Bcl-2 (50E3), rabbit monoclonal	Cell Signalling Technology	#2870	Antibody raised against peptide mapped to carboxy terminus of human Bcl-2	1:2000
Bcl-w (G-21), rabbit polyclonal	Santa Cruz Biotechnology	sc-130701	Antibody raised against peptide mapped to N-terminus of human Bcl-w	3µg/ml
Bcl-xL (54H6), rabbit polyclonal		#2764	Antibody raised against peptide corresponding to residues surrounding Asp61 on human Bcl-xL	1:2000

Antibody	**Supplier**	**Catalogue number**	**Epitope**	**Working dilution**
COX4 (D-20), goat polyclonal	Santa Cruz Biotechnology	sc-69359	Antibody raised against peptide mapped to N-terminus of human COX4	3µg/ml
Histone H3, rabbit polyclonal	Abcam	ab1791	Antibody raised against peptide corresponding to amino acids 100 to the C terminus of Histone H3	1µg/ml
Mcl-1 (D35A5), rabbit monoclonal	Cell Signalling Technology	#5453	Antibody raised against peptide corresponding to residues surrounding Leu210 on human Mcl-1	1:2000
MDM2 (IF-2), mouse monoclonal	Calbiochem	OP46	Within amino acids 26-169 of human MDM2	3µg/ml
PARP (42/PARP), mouse monoclonal	BD Transduction Laboratories	P76420	Within amino acids 22-219 of human PARP	3µg/ml

Antibody	**Supplier**	**Catalogue number**	**Epitope**	**Working dilution**
p53 (DO-1), mouse monoclonal	Calbiochem	OP43	Amino acids 21-25 of human p53	3µg/ml
Noxa (114C307), mouse monoclonal	Calbiochem	OP180	Data not available	3µg/ml
Puma, rabbit polyclonal	Cell Signalling Technology	#4976	Antibody raised against peptide corresponding to carboxy-terminal region of human Puma	1:2000
Tubulin (DM1A), mouse monoclonal	Sigma	T6199	Amino acid 426-430 on human tubulin	1:2000

Table 2.1.4.2. Secondary antibodies used for western blotting in this study.

Antibody	Manufacturer	Catalogue number	Working dilution
Sheep anti-mouse	GE Healthcare	RPN4201	1:2 500
Donkey anti-rabbit	GE Healthcare	NA934	1:5 000
Rabbit anti-goat	Jackson ImmunoResearch Laboratories	305-036-003	1:20 000

2.1.4.2 Secondary antibodies used for western blot

Secondary antibodies used in this study were conjugated to horseradish peroxidase for detection by chemiluminescence. Antibodies from stock were diluted in 5% blotting grade milk-PBS-Tween solution. Secondary antibodies used are summarised in table 2.1.4.2.

2.2 Cell lines

2.2.1 Cell lines used in this study

A498, ACHN and Caki2 renal cell carcinoma lines were obtained from the American Type Culture Collection (ATCC). Renal cell carcinoma lines 111, 117 and 154 were a kindly provided by Professor W M Linehan. HL-60 cells were a gift from the Haematology Department, University of Liverpool.

2.2.2 Cell culture medium

All tissue culture was performed in a class II safety cabinet. Cells were grown in Nunclon flasks (Nunc, Thermo Fisher Scientific) in 5 % CO_2 in air at 37 °C. Culture medium for each cell line is described below.

A498, ACHN, U2OS, 117 (and derivatives of these cell lines): Eagle's minimum essential medium supplemented with 2mM L-glutamine, 1.5 g/L sodium bicarbonate, 0.1 mM non-essential amino acids, 1 mM sodium pyruvate and 10% fetal bovine serum (FBS).

Table 2.2.1 Cell lines used in this study

Cell line	p53 status	Site of origin	Histology
ACHN	WT[1]	Renal cell adenocarcinoma derived from metastatic site (pleural effusion)	Clear cell
A498	WT[1]	Renal carcinoma, primary site	Clear cell
115	WT[2]	Renal carcinoma, primary site	Clear cell
Caki2	WT[1]	Renal carcinoma, primary site	Clear cell
117	WT[2]	Renal carcinoma, primary site	Clear cell
111	MT[2]; Codon 173, Val to Gly	Renal carcinoma, primary site	Clear cell
154	MT[2]; Codon 248, Arg to Gln	Renal carcinoma, primary site	Clear cell
U2OS	WT[3]	Osteosarcoma	N/A
H1299	Null[4]	Non-small cell lung carcinoma, derived from metastatic site (lymph node)	N/A
HL-60	Null[5]	Acute promyelocytic leukaemia	N/A
HEK293	WT[6]	Human embryonic embryonic kidney	N/A

1 – See Tomita et al., 1996; 2 – See Reiter et al., 1993; 3 – See Florenes et al., 1994; 4 – See Mitsudomi et al., 1992; 5 – See Wolf et al., 1985; 6 – See Lehman et al., 1993. WT – wild type. MT – mutant. N/A – not available.

111 and 154: Eagle's minimum essential medium supplemented with 2mM L-glutamine, 1.5g/L sodium bicarbonate, 0.1mM non-essential amino acids, 1mM sodium pyruvate and 15% FBS.

Caki2: McCoy's 5a medium with 1.5mM L-glutamine and 2.2g/L sodium bicarbonate supplemented with 1% streptomycin and penicillin and 10% FBS.

H1299 and HL-60 cells: RPMI-1640 medium supplemented with 10% FBS.

2.2.3 Sub-culture of cell lines

Cell lines used in this study grow as an adherent monolayer on cell culture treated surfaces, with the exception of HL-60 cells, which grew in suspension. Once cells reach maximum confluence in culture, cell death can occur from overcrowding and its ensuing stress. Thus sub-culture, or passage, of cells was performed to maintain cells at optimum health. Upon reaching of maximum confluence, passaging was carried out as follows: media was aspirated and the cell monolayer was washed in PBS (Sigma-Aldrich), typically 5 ml per 175 cm^2 of culture. PBS was aspirated then 3-5 ml of trypsin-EDTA (Sigma-Aldrich) was added to the monolayer and the culture vessel was then incubated at 37 °C. The culture vessel was agitated as appropriate to aid in the detachment of cells from the substrate. Neutralization of trypsin-EDTA was achieved by adding an equal amount of medium to the culture vessel. Cells were then re-suspended to create a single cell suspension and the relevant volume of cells in culture medium was aspirated from the vessel. Media was added to the vessel, typically 20-35 ml per 175 cm^2 of substrate.

2.2.4 Preparation of cryopreserved cells

For the cryopreservation of cells, cells were harvested by trypsinization as described above and centrifuged at 300 x g for 5 min. The cell pellet was re-suspended in freezing media (10% DMSO in FBS) and the cell suspension was transferred to cryovials. The cryovials were then transferred to a pre-cooled stryofoam rack and stored at -80°C to permit slow freezing of the cells. Upon freezing, cryovials would be transferred to liquid nitrogen for long-term storage. Typically, no more than 24 - 48 h would elapse between freezing at -80°C and transfer to liquid nitrogen.

To recover cells from stocks stored in liquid nitrogen, cryovials were thawed at 37°C and re-suspended in 0.5 ml of media at the same temperature. This suspension was transferred to a tissue flask containing at least 25 ml of media that was pre-warmed to 37°C.

2.2.5 Transfection of cells with siRNA using Lipofectamine-2000

Cells were seeded into 6-well multi-well plates (Nunc) for transfection with siRNA using Lipofectamine-2000 (Invitrogen). Cells were seeded 24h before transfection such that the cells were 30-50% confluent on the day of transfection. Serum-free (SF) Opti-MEM media and Lipofectamine-2000 were equilibrated to room temperature before transfection. siRNA was thawed before transfection. Cells were transfected with siRNA to a final concentration of 32nM. For one well of a 6-well plate, 80pmol of siRNA were diluted in 250 µl of SF media and 4 µl of Lipofectamine-2000 were diluted in an equal amount of SF media. Both mixtures were incubated at room temperature for 5 min. Following incubation, both mixtures were combined and left to incubate at room temperature for a further 20 min. The

combined transfection mixture was added drop-wise to cells that were bathed in 2 ml of complete growth medium. The plate was then rocked gently to ensure even distribution of siRNA-liposome complexes in the growth media. Following 6h incubation in at 37°C in a tissue culture incubator, the media was aspirated and replaced with complete growth media.

The following siRNAs were used:

Scrambled (5'-GGA CGC AUC CUU CUU AAU-3')

p53 (5'-GCA UGA ACC GGA GGC CCA-3')

Bax siRNA 3 (5'-ACA UGU UUU CUG ACG GCA A-3')

siRNA 4 (5'-CAU UGG ACU UCC UCC GGG A-3')

Puma siRNA 1 (5'-GGC GGA GAC AAG AGG AGC A-3')

siRNA 4 (5'-CGG ACG ACC UCA ACG CACA-3')

2.3 Cell proliferation and viability assays

2.3.1 MTT Assay

The 3-(4,5-dimethylthiazol-2-yl)-2,5-diphenyl tetrazolium bromide (MTT) assay was used to measure cell viability, (Mosmann 1983). The MTT assay is a rapid colorimetric assay that relies on mitochondrial function as a surrogate indicator of cell viability. Mitochondrial dehyrodgenase enzymes in living cells are capable of cleaving the tetrazolium ring in MTT, reducing yellow MTT into a purple formazan precipitate, which can be dissolved with DMSO. Hence, absorbance at 595 nm can be used as a surrogate indicator of how metabolically active and hence how viable cells treated with MTT are.

Table 2.3.1.1 Seeding densities of cells used in MTT assay.

Cell line	Cells per well
117	1,000
ACHN	5,000
A498	2,000
Caki2	5,000
115	2,000
111	5,000
154	5,000

2.3.1.1 Seeding of cells for MTT assay

Cells were trypsinized as described above and following three independent counts from a Coulter counter (Beckmann Coulter, California, USA) a mean was taken. Serial dilutions were performed on the cells in culture medium, ensuring cells were thoroughly mixed before each dilution, to give the desired concentration of cells/ml. Cells were seeded to 96-well plates (Nunc) using a multichannel pipette (Costar, Corning Incorporated). Cells in culture medium were agitated regularly to ensure even uptake of cells into the pipettor. Seeding densities for each cell line are shown in table 2.3.1.1. Media was replenished every 48 hours.

2.3.1.2 Treatment with MTT and absorbance reading

The MTT assay was performed by adding 20 µl of 5 mg/mL MTT (Molekula, UK) to each well. The 96-well plate was subsequently incubated at 37 °C for 3.5 h. Following incubation, all of the liquid was aspirated from each well and 100 µl of DMSO added to dissolve the purple formazan precipitate. After further incubation at 37 °C for 30 min, optical absorbance at 590 nm was measured using a Multiskan EX plate reader (Thermo Fisher Scientific, Massachusetts, USA).

2.3.2 Detection of apoptotic cells by flow cytometry using Annexin V and Propidium iodide

Phosphatidylserine (PS) is the only known phospholipid to be completely sequestered away from the outer monolayer of a cell membrane in mammalian cells (reviewed in Schlegel and Williamson, 2001). During apoptosis, membrane asymmetry is lost and subsequently PS is exposed. Annexin V (AV) is a protein that can bind to PS in a calcium-dependent manner (Andree et al., 1990). Conjugating

fluorescent dyes to AV, such as fluoroscein isothiocyanate (FITC) allows the detection of apopototic cells (Koopman et al., 1994) by detecting fluorescence emission after stimulation with lasers. Healthy, living cells that have an intact plasma membrane can exclude the fluorescent DNA intercalating agent, propidium iodide (PI). Dead cells, or cells with a perturbed plasma membrane, permit the influx of PI into the cell (reviewed in Steensma et al., 2003). Hence, by staining cells with both FITC-conjugated AV and PI and measuring the emission of fluorescence from the fluorophores using a flow cytometer, it is possible to identify four distinct populations of cells: living cells, cells in the early stages of apoptosis, dead cells that have undergone apoptosis and necrotic cells (figure 2.3.2.1). These populations can be distinguished, or gated, based on the fluorescence emitted.

2.3.2.1 Reagents used for detection of apoptotic cells by flow cytometry using Annexin V and propidium iodide

FITC-conjugated Annexin V solution (Cambridge Biosciences)

PI solution – 100μg/ml propidium iodide (Sigma) in 10 mM potassium phosphate (pH 7.4), 150mM NaCl.

10 X Annexin binding buffer: 0.1 M HEPES/NaOH (pH 7.4), 1.4 M NaCl, 25 mM $CaCl_2$.

2.3.2.2 Harvesting of cells and detection of apoptotic cells by AV/PI staining and flow cytometry

After treatment with drug or drug vehicle, cells were treated with trypsin as described in section 2.2.3 and centrifuged at 150 x g for 5 min in a pre-cooled centrifuge to harvest cells. Cells floating in the media and cells present in the PBS

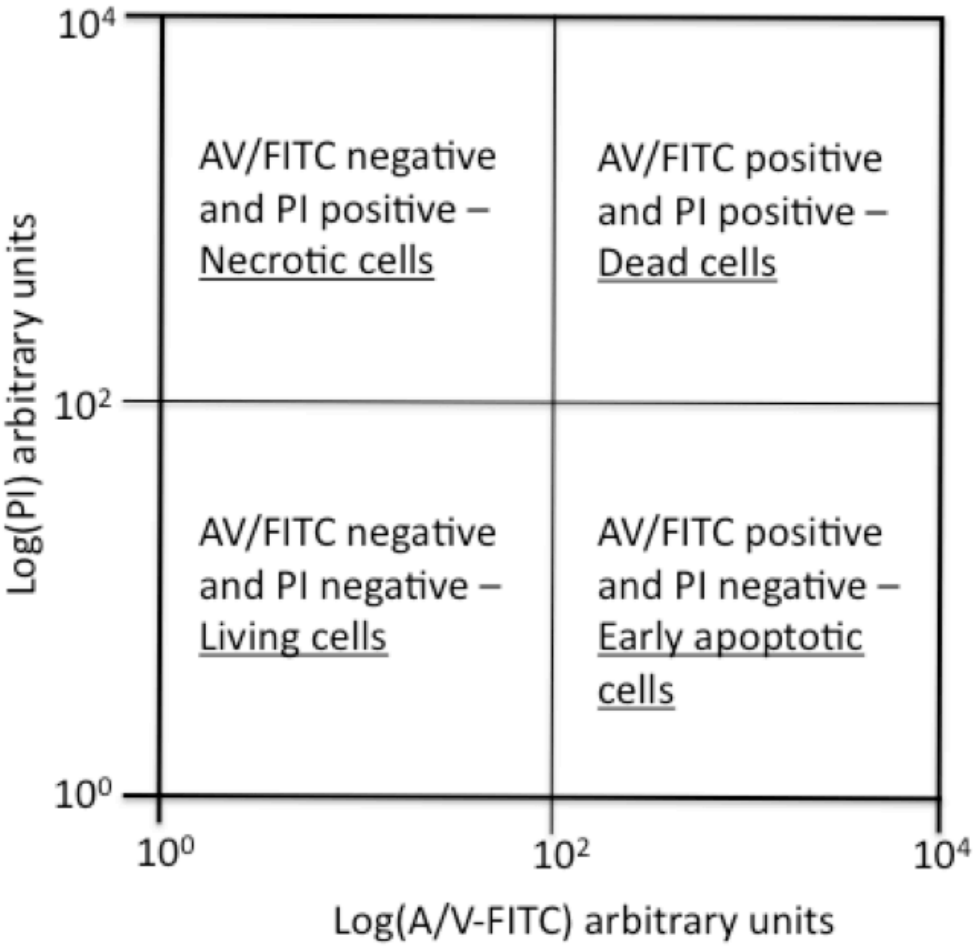

Figure 2.3.2.1 Schematic summarizing populations of cells after Annexin V/propidium iodide staining. Diagram summarizing positions of cell populations on a dot plot after treatment with FITC-conjugated Annexin V (A/V-FITC) and propidium iodide (PI) and analysis by flow cytometry.

washing step were included harvested with the adherent cells. Samples were kept on ice throughout the protocol. The cell pellet was gently re-suspended in 2 ml FBS to disaggregate the cell pellet without damaging cells. This suspension was then centrifuged at 150 x g for 5 min and the pellet re-suspended in 5 ml of ice cold PBS. Cells were counted using a Coulter Counter and density was adjusted to 1 million cells per sample. This suspension was centrifuged at 150 x g and washed in PBS as described above. Following a final centrifugation at 150 x g, the cell pellet was re-suspended in 1 x annexin binding buffer. 5 µl of FITC-conjugated AV was added to 385 µl of cell suspension and this was incubated in the dark on ice for 10 min. The sample was then treated with 10 µl PI solution before being passed into the flow cytometer for analysis. A BD FACSCalibur flow cytometer was used to detect fluorescence from AV and PI. The data was analysed on CellQuest Pro Software.

2.4 Western Blotting

2.4.1 Reagents for western blotting

CHAPS-modified SLIP Buffer (100 ml)

50mM HEPES pH 7.5

10% glycerol

1% CHAPS

150mM NaCl

0.5mg/ml BSA

Solution made up to 100ml with H_2O.

PBS/Tween (4 litres)

44.8g $Na_2HPO_4.2H_2O$

9.67g $NaH_2PO_4.2H_2O$

17.52g NaCl

4ml of Tween-20

Solution made up to 4 litres with H_2O.

Tris-Glycine Electrophoresis Running Buffer

25mM Tris

250mM glycine

0.1% (w/v) SDS

Tris-Glycine Transfer Buffer

25 mM Tris

192 mM glycine

20% (v/v) methanol

4 X Sample buffer (10ml)

0.25 M Tris (pH 6.8)

8% (w/v) SDS

40% (v/v) glycerol

4mg/ml bromophenol blue

600 mM DTT

Made up to 10 ml with H_2O. Diluted with H_2O to make 2X and 1X samples. Stored at -20°C.

2.4.2 Sample preparation for western blotting

Western blotting (protein immunoblotting) is a technique used to separate proteins of different mass by gel electrophoresis. Proteins for analysis were extracted from cells typically harvested from 10 cm tissue culture dishes by trypsinization and subsequent centrifugation at 300 x g. Supernatant was aspirated from the centrifuge tube and the pellet was typically frozen at -80°C. Cell pellets were lysed by re-suspension in CHAPS-modified SLIP buffer supplemented with the following protease inhibitors: aprotinin (2 μg/ml), leupeptin (0.5 μg/ml), pepstatin A (1 μg/ml), trypsin inhibitor from soybean (100 μg/ml) and PMSF (1mM in ethanol). Upon incubation on ice for 10 minutes, lysates were centrifuged for 16,100 x g at 4°C and the supernatant from this centrifugation was transferred to a clean 1.5 ml Eppendorf tube. Concentration of protein in a sample was determined by comparison to protein standards in a Bradford assay (Bradford 1976). Typically, 20μg of the protein was mixed with 2X or 1X sample buffer to obtain a final concentration of 1X sample buffer and 20 μg of protein in the sample.

2.4.3 Gel electrophoresis and protein detection for western blotting

A SDS polyacrylamide gel was used to separate proteins by gel electrophoresis. The separating gel was prepared as described in table 2.4.3.1. The percentage of acrylamide used corresponded to the size of the protein to be resolved. A higher percentage acrylamide gel permitted the resolution of low molecular weight proteins; conversely, a lower percentage polyacrylamide gel permitted the resolution of higher molecular weight proteins. Protein was transferred from the gel to a nitrocellulose membrane (Amersham). The membrane was blocked in PBS/Tween-20 (0.1% w/v) containing 5% w/v non-fat milk for 30 minutes. The membranes were subsequently

Table 2.4.3.1 Composition of SDS PAGE gels.

Reagent	Separating gel		Stacking gel
	10%	15%	
Water	4.8ml	3.55ml	7.225ml
40% acrylamide mix	2.5ml	3.75ml	1.275ml
1.5M Tris (pH 8.8)	2.5ml	2.5ml	_____
1.0M Tris (pH 8.8)	_____	_____	1.25ml
10% SDS	100µl	100µl	100µl
10% APS	100µl	100µl	100µl
TEMED	8µl	8µl	10µl

incubated with primary antibody for 1 hour at room temperature, washed six times for 5 min in PBS/Tween-20 before incubation with secondary antibody for 1 hour at room temperature. After washing in PBS/Tween-20 as described previously, either ECL Select or ECL Prime reagents were applied for 5 min., depending on the sensitivity required. Signal was detected by chemiluminescence and recorded on a Kodak IM4000 image station using Kodak Molecular Imaging software.

2.5 Crude preparation of mitochondria from tissue culture cells

2.5.1 Reagents for crude preparation of mitochondria

RSB buffer

10mM NaCl

1.5mM $MgCl_2$

10mM Tris-HCl, pH 7.5

Supplemented with the following protease inhibitors: aprotinin (2 μg/ml), leupeptin (0.5 μg/ml), pepstatin A (1 μg/ml), trypsin inhibitor from soybean (100 μg/ml) and PMSF.

2 x MS buffer

420mM mannitol

140mM sucrose

10mM Tris-HCl, pH 7.5

2mM EDTA, pH 7.5

Supplemented with the same protease inhibitors as RSB buffer.

2.5.2 Protocol for crude preparation of mitochondria

Cells were harvested as described in section 2.4.2. The supernatant was aspirated and the cell pellet was re-suspended in 10 ml ice cold PBS and centrifuged again at 300 x g for 5 min. All centrifugation was carried out at 4 °C. This was repeated a further two times and the supernatant was aspirated. The pellet was re-suspended in ice cold RSB buffer, and swelling of cells was monitored using a phase contrast microscope. The volume of RSB buffer added was typically 5 x the packed cell volume. After 10-15 min, the cell suspension was transferred to an ice-cold Potter-Elvejhem homogenizer and cells were homogenized until ~90% of cells were broken which was typically after 30-70 strokes. Disruption of cell membranes was visually monitored every 10-20 strokes using a phase contrast microscope. A volume of 2 x MS buffer equal to the homogenate was added to the broken cells in the Potter homogenizer and this suspension was transferred to a centrifuge tube. The homogenate was spun at 1,300 x g for 5 min to remove unbroken cells, large membrane fragments and nuclei. The supernatant from this centrifugation was transferred to a clean centrifuge tube and the 1,300 x g centrifugation was repeated. Transferring the supernatant into a clean centrifuge tube followed by a centrifugation at 1 300 x g was repeated until no pellet was observed at the bottom of the centrifuge tube. The supernatant was then transferred into clean centrifuge tubes and centrifuged at 17 000 x g for 15 minutes to pellet mitochondria and other organelles. The pellet was re-suspended in 500µl MS buffer and centrifuged at 17 000 x g for 15 min. The supernatant was discarded and the pellet was again re-suspended in MS buffer and centrifuged at 17 000 x g for 15 min. This pellet was lysed using CHAPS-modified SLIP buffer and was analysed for protein as described in the section 2.4.2.

2.6 Isolation of mitochondria by sucrose density centrifugation

2.6.1 Reagents for isolation of mitochondria by sucrose density gradient centrifugation

Sucrose solutions

1.0M sucrose	**1.5M sucrose**
10mM Tris-HCl, pH 7.5	10mM Tris-HCl, pH 7.5
1mM EDTA, pH 7.5	1mM EDTA, pH 7.5

Both solutions supplemented with the following protease inhibitors: aprotinin (2 µg/ml), leupeptin (0.5 µg/ml), pepstatin A (1 µg/ml), trypsin inhibitor from soybean (100 µg/ml) and PMSF.

2.6.2 Protocol for isolation of mitochondria by sucrose density centrifugation

Harvesting and homogenization of cells was exactly as described in section 2.5.2. The homogenate was centrifuged at 1,300 x g for 5 min at 4°C until no visible pellet formed. A two-step discontinuous sucrose gradient was formed by layering 1.5 ml 1.0M sucrose solution over 1.5ml 1.5M sucrose solution in a 5 ml thin wall polyallomer centrifuge tube (Beckman, code 326819). The homogenate was carefully pipetted on top of the gradient. To prevent collapse of the centrifuge tube from centrifugal forces during the ultracentrifugation, tubes were filled to within 3 mm of the top of the tube. If the amount of sample was insufficient to fill a tube to this level, the remaining volume was made up with 1 x MS buffer. Tubes that were centrifuged opposite each other were balanced to within 0.1 g and centrifuged in a MLS-50 rotor at 85,000 x g for 60 min at 4 °C in a Beckman Coulter Optima MAX preparative ultracentrifuge. The slowest acceleration setting was used (setting 9) and

the centrifuge was set to stop by coasting from 85,000 x g without braking. Following centrifugation, the mitochondria were removed from the interphase of the sucrose gradient by lateral suction with a syringe. This suspension was carefully pippetted into a 12 ml polypropylene copolymer centrifuge tube (Beckman, code 3110-0120). This mitochondrial suspension was made up to 10 ml 1 x MS buffer. To avoid osmotic shock of the mitochondria, 1 x MS buffer was added dropwise to the mitochondrial suspension and mixed gently using the lowest setting on a Vortex Genie 2 (Scientific Industries Inc.). Mitochondria in 1 x MS were then centrifuged at 17 000 x g for 20 min at 4 °C in a SS-43 rotor in a Sorvall RC 5C Plus centrifuge. Supernatant was discarded and the pellet was re-suspended in 1 ml of 1 x MS buffer before centrifuging at 17 000 x g for 20 min at 4 °C in a bench top centrifuge to wash mitochondria. The pellet was washed a second time and mitochondria were re-suspended in 1 x MS buffer for subsequent preparation of samples for western blotting.

2.7 Live cell imaging

Live cell imaging is a technique that can be used to visually observe the behaviour of cells over a period of time. A Nikon TE300 microscope was used. During an experiment, a 6-well plate (Corning) was maintained in a humidified atmosphere permeated with CO_2 and maintained at a temperature of 37°C. A thermocouple was inserted into water placed at the centre of the 6-well plate to monitor the temperature inside the microscope chamber. Each well represented a different treatment condition, for example drug and drug vehicle. Two positions were selected per well and positions in each well were imaged with a time lapse of 5 minutes for roughly 24

hours. ImageJ software (National Institute of Health, USA) was used to convert collected images into movies.

2.8 Immunoprecipitation

Immunoprecipitation (IP) is the small-scale affinity purification of antigen using a specific antibody. IP is a commonly used method for detection of protein-protein interactions or changes in protein conformation using conformation-specific antibodies. IP was used in this study to detect exposure of the Bax N-terminus using the conformation-specific Bax 6A7 antibody.

2.8.1 Reagents for immunoprecipitation

Bax N-terminal capture (BNTC) buffer

142.5mM KCl

2.0mM $CaCl_2$

20.0mM Tris-HCl pH 7.4

Buffer supplemented with the following protease inhibitors: aprotinin (2µg/ml), leupeptin (0.5µg/ml), pepstatin A (1µg/ml), trypsin inhibitor from soybean (100µg/ml) and PMSF. Buffer was made up to 1.0% CHAPS or 0.1% Triton X-100 depending on requirements.

2.8.2 Procedure for immunoprecipitation

Cells were harvested as described in section 2.4. The cell pellet was lysed with BNTC buffer and protein was extracted and quantified as described in section 2.4.2. Typically, 500µg of protein were used for IP and this was made up to 500µl using BNTC buffer. All samples were kept on ice during the procedure. 100µl of Protein

G Sepharose beads (Sigma) were washed three times by centrifugation at 16,000 x g at 4°C for 1 min and washing with BNTC buffer. After the final wash, the beads were re-suspended in BNTC buffer to obtain a 50% slurry. 50µl of the Protein G beads were added to each 500µl sample of protein and incubated at 4°C for 1 h on a nutator to remove protein that bound non-specifically to the beads. Following incubation, samples were centrifuged at 16,000 x g at 4°C for 30 sec and the supernatant was transferred to a fresh tube. 2µg of Bax 6A7 antibody, or the relevant isotype control (table 2.8.1), was added to the sample and the sample was incubated overnight on a nutator at 4 °C. 50 µl of Protein G Sepharose beads slurry was added to each sample after the overnight incubation step and samples were further incubated for 2 h at 4 °C to capture antibody-antigen complexes on the beads. Beads were then collected by centrifugation at 16,000 x g for 30 sec. The supernatant was discarded and the beads were washed three times using 500 µl of BNTC buffer. All of the remaining BNTC buffer was aspirated after the last wash and the beads were typically re-suspended in 100µl 1X sample buffer. For analysis by SDS-PAGE, samples were boiled at 100°C for 10 min and 20µl before loading into a SDS-PAGE gel.

Table 2.8.1 Antibodies used in immunoprecipitation

Antibody	Manufacturer	Catalogue number
Bax 6A7, mouse monoclonal	Trevigen	AMSBIO 2281-MC-100
CD20, mouse monoclonal	Becton Dickinson	347201

Chapter 3: A study of the effects of the combination of Nutlin-3 and ABT-737 on the proliferation and survival of renal cell carcinoma cell lines

3.1 Introduction

As discussed in Section 1.1.1, the incidence of RCC is increasing and novel treatments are required for the treatment of this disease. The tumour suppressor p53 is rarely mutated in renal cell carcinoma (RCC) (reviewed in Noon et al., 2010) and co-up-regulation of both p53 and MDM2 is associated with poor survival in RCC (Noon et al., 2011). RCC cells in culture that harbour wild type p53 exhibit intact p53 function: upon treatment with UV radiation, p53 is up-regulated and this results in the induction of cell cycle inhibitor p21. Furthermore, p53 is regulated by MDM2 in these cells (Warburton et al., 2005). Taken together, wild type p53 function in RCC may represent a therapeutic target for pharmacological restoration.

Attempts to restore wild type p53 function in RCC cells using Nutlin-3, an inhibitor of the p53-MDM2 interaction (Tsao and Corn, 2010; Polanski et al., submitted), have resulted only in cell cycle arrest and senescence, not apoptosis. A possible explanation for this phenotype is that the apoptotic pathway is defective downstream of p53 activation in cells of the renal epithelium, from which RCC cells derive (Vlatković et al., 2011). A marginal increase in the transcription of the pro-apoptotic genes *Bax*, *Puma* and *Noxa* has been observed upon treatment of a number of RCC cell lines with Nutlin-3, but this was insufficient to commit the cells to apoptosis (Tsao and Corn, 2010). Based on the observation that Nutlin-3 treatment alone is inadequate in inducing apoptosis in RCC cells harbouring wild type p53, we considered the possibility of combining Nutlin-3 with a pro-apoptotic drug. ABT-

737 is a small molecule mimetic of the pro-apoptotic BH3-only family of proteins that can inhibit the anti-apoptotic Bcl-2 family members Bcl-2, Bcl-xL and Bcl-w (Oltersdorf et al., 2005).

3.2 Results

3.2.1 The Combination of Nutlin-3 and ABT-737 synergistically inhibits proliferation of renal cell carcinoma cells harbouring wild type p53

A panel of RCC cells harbouring either wild type or mutant p53, and non-tumorigenic HEK293 cells were treated with either Nutlin-3 alone, ABT-737 alone or a combination of both agents. After 72h treatment, a MTT assay was performed (as described in Section 2.3). Absorbance at 595nm relative to vehicle-treated cells was used as a surrogate measurement to indicate inhibition of cell proliferation for each treatment.

Figure 3.2.1.1 shows a western blot that shows the levels of p53 and MDM2 in the cell lines used in this study. Figure 3.2.1.2 shows the survival curves for the treated cell lines and Table 3.2.1.1 summarizes the p53 and MDM2 status of each cell line together with the IC_{50} and IC_{70} data. Overall, RCC cells harbouring wild type p53 appear to be more sensitive to the inhibitory effects of Nutlin-3 at both 50% and 70% levels of inhibition when compared to the mutant p53 cells (as expected from previous work in our laboratory, Polanski et al, submitted). However, it would have been expected that difference in sensitivity to Nutlin-3 alone would have been greater overall between the wild type p53 RCC cells and the mutant p53 RCC cells. This may be attributed to off-target effects of Nutlin-3: there may be other proteins that can be inhibited by Nutlin-3 other than MDM2. Or alternatively, Nutlin-3 may

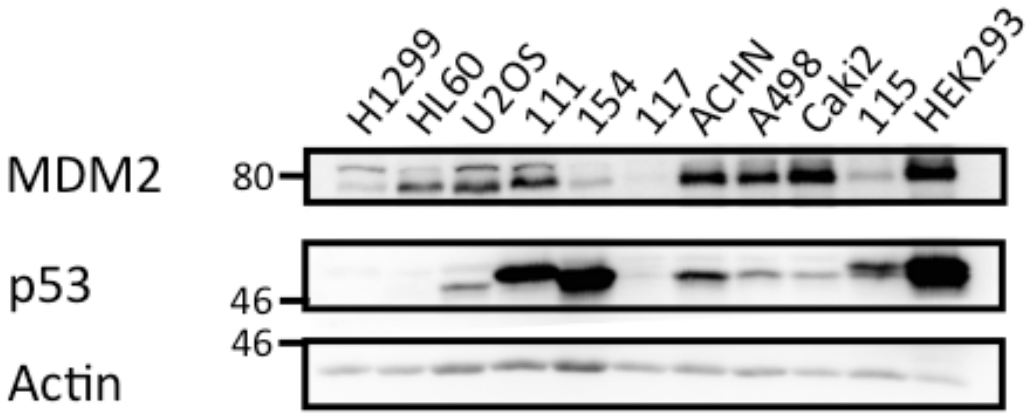

Figure 3.2.1.1 p53 and MDM2 protein level in the cell lines used in this study. Cells from sub-confluent cultures of the indicated cell lines were harvested and lysed and the concentration of protein was quantified as described in Section 2.4. Relative protein level was analysed by western blot as described in Section 2.4. 10µg of protein was analysed in each lane and antibodies used for detection are described in table 2.1.

Table 3.2.1.1 Summary of IC_{50} and IC_{70} values of cells treated with Nutlin-3 or ABT-737

Cell line	p53 status	**Relative levels of p53/MDM2 protein**	**Nutlin-3 (μM)**		**ABT-737 (μM)**	
			IC_{50}	**IC_{70}**	**IC_{50}**	**IC_{70}**
ACHN	WT[1]	**High p53, high MDM2**	6	15	10	18
A498	WT[1]	**Moderate p53, high MDM2**	3.3	20	14	23
115	WT[2]	**High p53, moderate MDM2**	7	28	17	28
Caki2	WT[1]	**Moderate p53, high MDM2**	10	30	1.3	2.2
117	WT[2]	**Low p53, low MDM2**	2.5	7	10	22
111	MT[2]	**Very high p53, high MDM2**	18	28	18	23
154	MT[2]	**Very high p53, moderate MDM2**	12	23	20	28

1 – See Tomita et al., 1996; 2 – See Reiter et al., 1993. IC_{50} – concentration at which 50% inhibition of proliferation occurs. WT – wild type; MT – mutant.

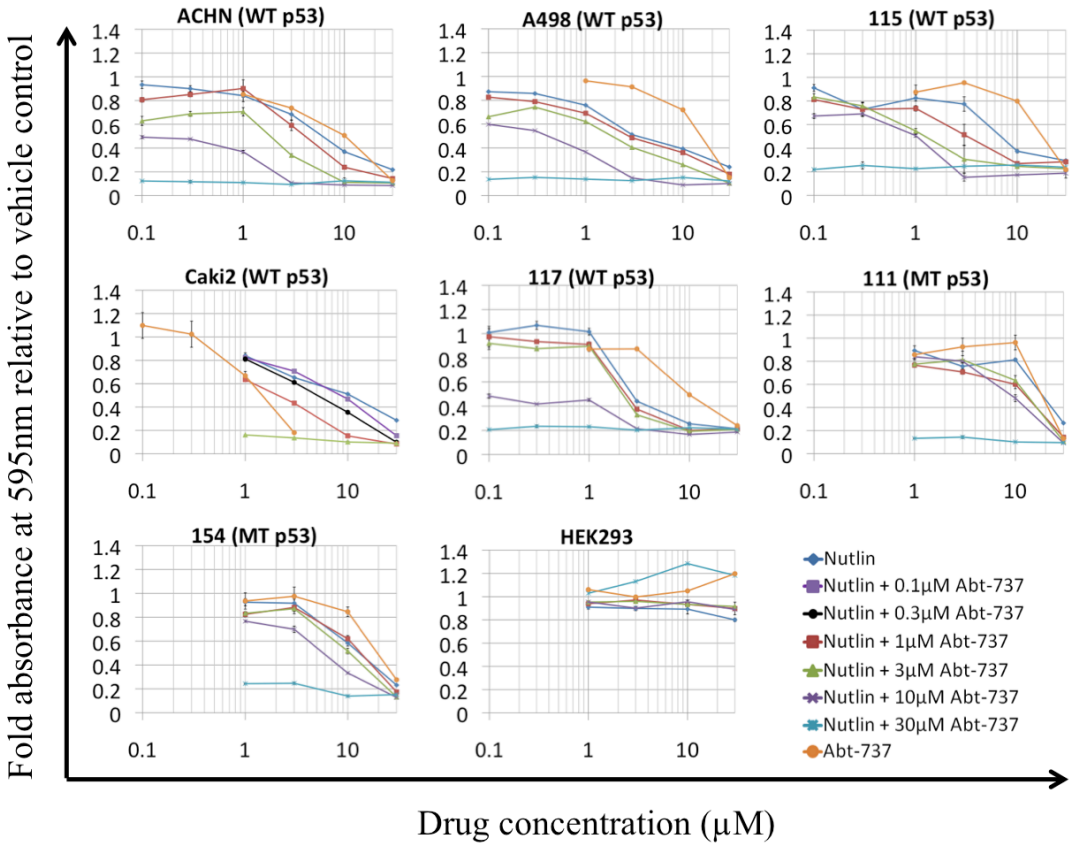

Figure 3.2.1.2 Survival curves of cells treated with Nutlin-3 and/or ABT-737. Cells were seeded as described in section 2.3.1.1 and treated with the indicated drugs for 72h. Cells were then treated with MTT as described in section 2.3.1.2. After treatment with MTT, absorbance at an optical density of 595nm was measured. As a measure of proliferation, absorbance of drug-treated cells at 595nm was divided by absorbance of vehicle treated cells to give proliferation relative to drug-vehicle treated cells. WT – wild type. MT – mutant. Figures representative of at least 2 repeats.

inhibit the interaction of MDM2 with other proteins that may be involved in survival and/or proliferation (Nicholson et al., 2012). With respect to ABT-737, cell lines harbouring both wild type and MT p53 displayed similar sensitivity, the exception being the Caki2 cell line, which was 10-fold more sensitive to the inhibitory effects of ABT-737. To illustrate, the IC_{50} for ABT-737 of Caki2 cells was 1.3 μM whereas ACHN and 117 cell lines, the two most sensitive cell lines after Caki2 cells both had IC_{50} values of 10 μM (table 3.2.1.1).

The Loewe additivity model (discussed in section 1.4.2) was selected to analyse drug interactions shown in figure 3.2.1.2. p53 and its transcriptional targets, such as Noxa, Puma and Bax interact closely with members of the anti-apoptotic Bcl-2 family proteins (see section 1.2.8). Considering that Nutlin-3 promotes the rescue of p53 from degradation by MDM2 and potentially the induction of pro-apoptotic proteins that interact with the anti-apoptotic Bcl-2 family of proteins, and ABT-737 is an inhibitor of anti-apoptotic Bcl-2 family proteins Bcl-2, Bcl-xL and Bcl-w, the possibility that each compound acted independently of the other could not be excluded. This consideration meant that the Bliss model could not be used to analyse drug interactions in these experiments, hence the Loewe model was selected. Synergy, additivity and antagonism can be analysed graphically using isobolograms (figure 3.2.1.3), which are a graphical representation of the combination index, discussed in section 1.4.2. The concentration of each drug is plotted on one of the axes and for a specified level of inhibition, a line connecting the vertical and horizontal axis, the isobole, is drawn. Drug combination points for the same level of inhibition are plotted on the isobologram. Drug combination points that fall on the isobole suggest an additive effect. Drug combination points that fall below the

isobole suggest a synergistic effect. Drug combination points that fall above the isobole suggest an antagonistic effect. The further a drug combination point deviates from the isobole, the greater the synergy or antagonism. At 50% inhibition, the synergy between Nutlin-3 and ABT-737 can be observed in all of the RCC cells harbouring wild type p53 with the exception of the 117 and A498 cell lines (figure 3.2.1.3, red isoboles). The for synergy is lower in the mutant p53 RCC cell lines at 50% inhibition as indicated by the decreased deviation of the combination points below the red isobole. At 70% inhibition (figure 3.2.1.3, black isoboles), the synergy is much greater in all of the RCC cell lines harbouring wild type p53 when compared to the cell lines harbouring mutant p53. This suggests that the synergy between Nutlin-3 and ABT-737 may be dependent upon the presence of wild type p53. Considering that Nutlin-3 has been shown to be effective in cells that harbour wild type p53 but not mutant p53 (Vassilev et al., 2004), this was to be expected.

Combination indices were calculated as described in section 1.4.2. Table 3.2.1.2 summarises the combination indices obtained at both IC_{50} and IC_{70} from the data shown in figure 3.2.1.2 and the corresponding graded symbols denoting the degree of synergy (as described in table 1.4) have been included. Corresponding with the isobolgram data above, the synergy between Nutlin-3 and ABT-737 observed at IC_{50} is greater in all of the cell lines harbouring wild type p53 with the exception of both the 117 and A498 cell lines. The CI values range from 0.49-1.14 (slight antagonism to synergism, as described on table 1.4) in the RCC cells harbouring wild type p53 at IC_{50}. At IC_{70}, treatment of all of the RCC cells harbouring wild type p53 with the combination of Nutlin-3 and ABT-737, with the exception of 117 cells resulted in combination indices that ranged from 0.20 (strong synergism) to 0.69 (synergism).

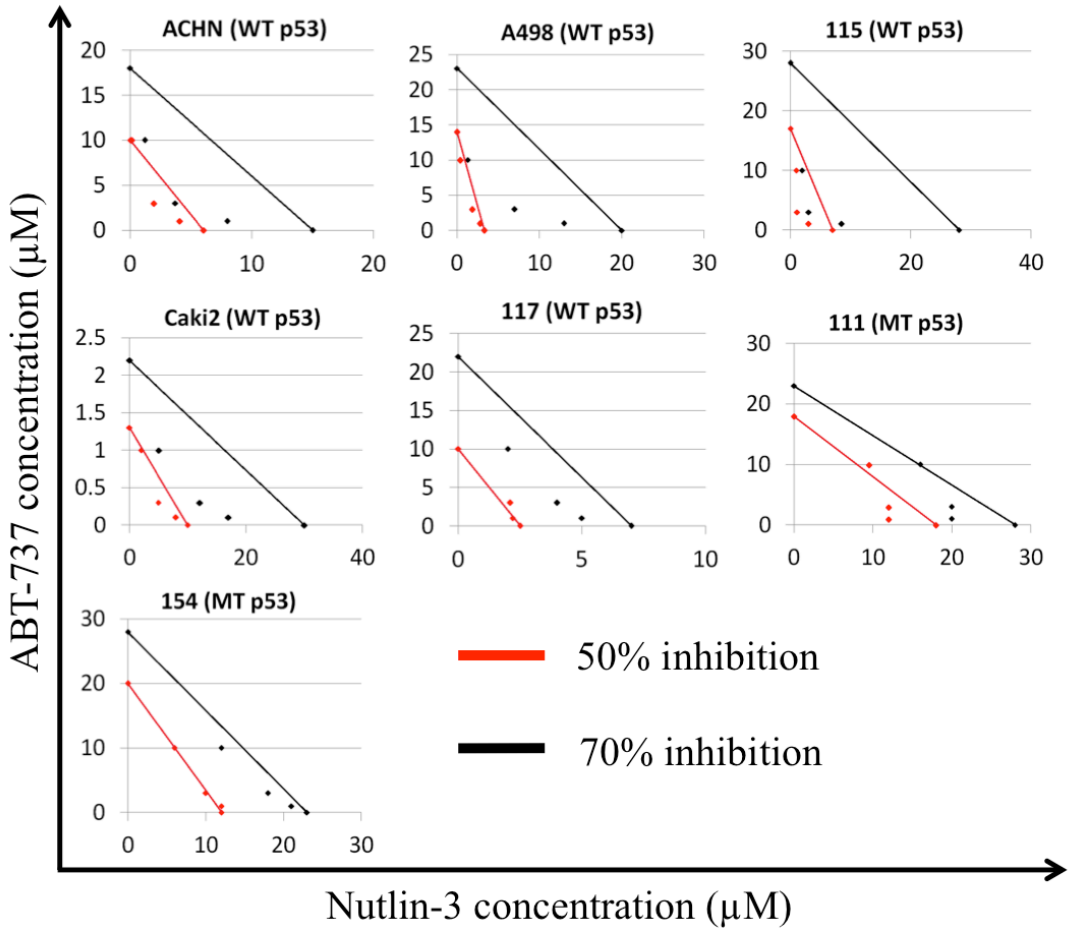

Figure 3.2.1.3 Analysis of Nutlin-3 and ABT-737 drug interaction in RCC cells. Isobolograms produced from data shown in figure 3.2.1.2. IC_{50} and IC_{70} values were plotted onto the vertical and horizontal axes for ABT-737 and Nutlin-3 respectively to give isoboles. Drug combination points were then expressed on the isobolograms to assess the synergy between both drugs.

Table 3.2.1.2 Combination indices at IC_{50} and IC_{70} for RCC cells treated with Nutiln-3 and ABT-737.

Cell line	p53 status	IC_{50}*				IC_{70}*		
		ABT-737 (μM)	Nutlin-3 (μM)	Combination index#		ABT-737 (μM)	Nutlin-3 (μM)	Combination index#
ACHN	WT	1	4	0.60 + + +		1	8	0.59 + + +
		3	1.8	0.77 + +		3	3.3	0.39 + + +
						10	1.3	0.64 + + +
A498	WT	1	2.8	0.92 ±		1	13	0.69 + + +
		3	1.8	0.76 + +		3	7	0.48 + + +
		10	0.4	0.84 + +		10	1.3	0.50 + + +
115	WT	1	3	0.49 + + +		1	8.5	0.31 + + +
		3	1.2	0.35 + + +		3	3	0.20 + + + +
		10	1	0.73 + +		10	1.9	0.41 + + +
Caki2	WT	0.1	8.5	0.93 ±		0.1	18	0.61 + + +
		0.3	5	0.73 + +		0.3	12	0.54 + + +
		1	2	0.97 ±		1	5	0.62 + + +
117	WT	1	2.3	1.02 ±		1	5	0.76 + +
		3	2.1	1.14 -		3	4	0.71 + +
						10	2	0.74 ++
111	MT	1	13	0.78 + +		1	20	0.76 + +
		3	13	0.89 +		3	20	0.84 ++
		10	9	1.06 ±		10	17	1.04 ±
154	MT	1	12	1.05 ±		1	21	0.95 ±
		3	10	0.98 ±		3	18	0.88 +
		10	6	1.00 ±		10	12	0.88 +

* - IC_{50} and IC_{70} were the levels of inhibition of proliferation selected to perform analysis of drug interaction by combination index.

- Combination index calculated using the following equation $D1_{comb.}/D1_{alone} + D2_{comb.}/D2_{alone.}$

The weaker synergism associated with the combination treatment of 117 cells (0.71-0.76; moderate synergism) when compared to the remaining RCC cells harbouring wild type p53 may be attributed to the relatively lower levels of wild type p53 in 117 cells when compared to the other wild type RCC cells (figure 3.2.1.1). At IC_{70} there is less evidence of synergy in the mutant p53 cell lines, 111 and 154 with CI values in the range 0.76 to 1.04 (moderate synergism to nearly additive). Analysis of cell proliferation data using both isobolograms and the corresponding combination index suggest that both Nutlin-3 and ABT-737 synergise to inhibit proliferation in RCC cells harbouring wild type p53 but not in cells harbouring mutant p53.

Consistent with previous studies, we have shown that the proliferation of RCC cells that harbour wild type p53 is inhibited by treatment with Nutlin-3 and to some degree, mutant p53 cells also respond to Nutlin-3. Further, we have shown that combining the pro-apoptotic drug ABT-737 with Nutlin-3 results in a synergistic inhibition of proliferation which is more pronounced in the RCC cell lines that harbour wild type p53 over the cell lines that harbour mutant p53. To summarize, although inhibition of proliferation of RCC cells by Nutlin-3 appears to be p53-dependent, synergy between Nutlin-3 and ABT-737 appears to depend upon p53. In the following section, we discuss the role of p53 in the synergistic inhibition of proliferation in these cells.

3.2.2 Synergy between Nutlin-3 and ABT-737 is p53-dependent

Results presented in the previous section showed that Nutlin-3 and ABT-737 synergise to inhibit the proliferation of RCC cells and the degree of synergy observed was greater in the cell lines harbouring wild type p53 when compared to those harbouring mutant p53. Since Nutlin-3 acts to inhibit the interaction between MDM2 and p53 and treatment of tumour cell lines that harbour wild type p53 with this compound results in the liberation of p53 subsequent activation of p53, this result was expected. If it could be shown that this synergy was indeed p53-dependent, then we would have succeeded in pharmacologically rescuing p53 function to inhibit proliferation. To determine whether reducing p53 expression altered the previously observed synergy between Nutlin-3 and ABT-737 in ACHN cells (section 3.2.1), we used ACHN cells stably expressing shRNA to p53 and cells of the same cell line expressing the scrambled control shRNA that were generated by a former lab member (Dr Radoslaw Polanski; Polanski et al., submitted). Figure 3.2.2.1 shows the western blot of lysates from the parental ACHN cell line, the ACHN cell line harbouring scrambled shRNA (here after referred to as sc-ACHN cells) and the ACHN cell line harbouring p53-specific shRNA (hereafter referred to as sh-p53-ACHN cells). As expected, the level of p53 protein is reduced in the clone harbouring the shp53ACHN cells relative to scACHN cells. The reduced level of MDM2 protein in the sh-p53ACHN cells is also expected because MDM2 is a transcriptional target for p53 (Wu et al., 1993).

Cells were treated with Nutlin-3 or ABT-737 either singly or in combination as described in Section 3.2 and a MTT assay as performed 72h post-treatment to

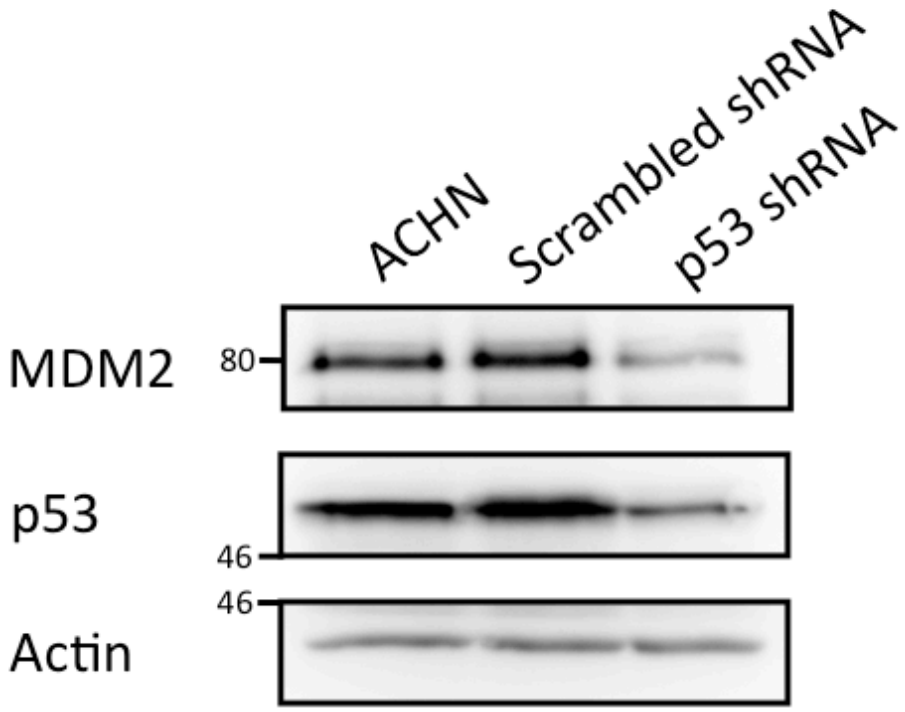

Figure 3.2.2.1 Analysis of expression levels of p53 and MDM2 in ACHN cells expressing shRNAs. Subconfluent cultures of ACHN cells and ACHN cells modified to express scrambled shRNA or p53-specific shRNAwere harvested and lysed and the concentration of protein was quantified as described in Section 2.4. Relative protein level was analysed by western blot as described in Section 2.4. 20μg of protein was analysed in each lane and antibodies used for detection are described in table 2.1.

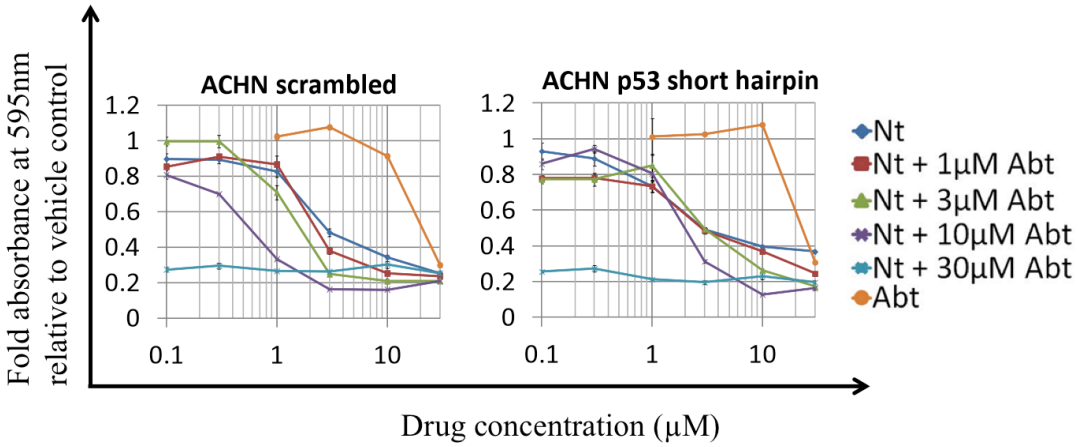

Figure 3.2.2.2 Survival curves of ACHN scrambled shRNA and ACHN p53 shRNA-expressing cells treated with Nutlin-3 and/or ABT-737. Cells were seeded as described in section 2.3.1.1 and treated with the indicated drugs for 72h. Cells were then treated with MTT as described in section 2.3.1.2. After treatment with MTT, absorbance at an optical density of 595nm was measured. As a measure of proliferation, absorbance of drug-treated cells at 595nm was divided by absorbance of vehicle treated cells to give proliferation relative to drug-vehicle treated cells. Representative data from at least 2 repeats.

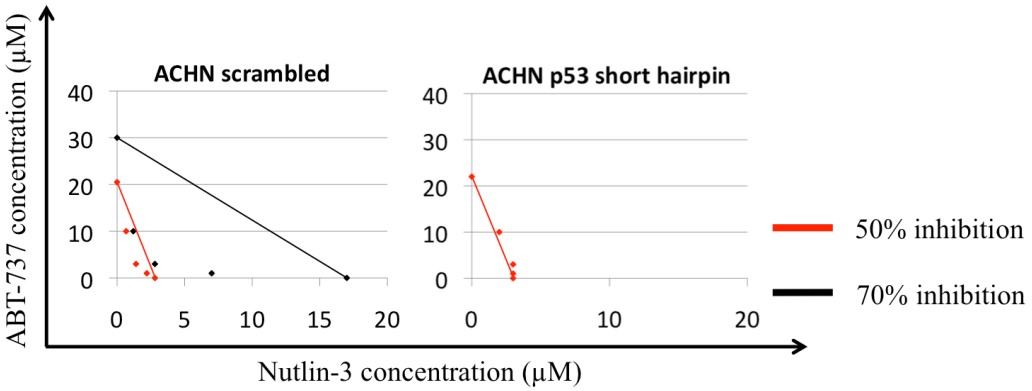

Figure 3.2.2.3 Analysis of Nutlin-3 and ABT-737 drug interaction in ACHN scrambled shRNA and ACHN p53 shRNA-expressing cells treated with Nutlin-3 and ABT-737. Isobolograms produced from data shown in figure 3.2.2.2. IC_{50} and IC_{70} values were plotted onto the vertical and horizontal axes for ABT-737 and Nutlin-3 respectively to give isoboles. Drug combination points were then expressed on the isobolograms to assess the for synergy between both drugs.

analyse the interaction between Nutlin-3 and ABT-737 in these cell lines. Survival curves for both cell lines summarizing the responses to solo and combination treatments are shown in figure 3.2.2.2. Isobolograms derived from figure 3.2.2.2 are shown in figure 3.2.2.3 and the combination indices for the combination treatments are summarized on table 3.2.2.2. A simple analysis of figure 3.2.2.2 shows that the curves representing Nutlin-3 plus 3 μM ABT-737 and Nutlin-3 plus 10 μM ABT-737 are shifted further to the left when compared to Nutlin-3 alone on the graph for the scACHN cells line but not for the sh-p53ACHN cells. Synergy is observed in response to the combination treatment at both IC_{50} and IC_{70} in the scACHN cell line, which can be observed on the isobologram in figure 3.2.2.3 showing combination points fall below the isoboles. The combination of 1 μM ABT-737 and Nutlin-3, 3 μM ABT-737 with Nutlin-3 and 10 μM ABT-737 have combination indices of 0.87, 0.64 and 0.73 respectively at IC_{50} (Table 3.2.2.2). At IC_{70}, the combination indices for these treatments are 0.56, 0.26 and 0.41. At IC_{50} there is no evidence of synergy in the sh-p53ACHN cells, indeed the combination indices for the combinations tested in this cell line are >1. This was expected as these cells harbour less p53 protein than their scrambled control counterparts (figure 3.2.2.1) and they were previously shown to be less sensitive to treatment with Nutlin-3 (Polanski et al., submitted). An IC_{70} value for Nutlin-3 alone in this cell line was not achieved, most likely due to the relatively low level of p53 in these cells; meaning combination indices could not be calculated at this level of inhibition. This lack of synergy in response to the combination treatment in the sh-p53ACHN cells was due to the insensitivity of these cells to Nutlin-3 (table 3.2.2.1). If sensitivity to Nutlin-3 alone was determined by the presence of wild type p53 (Vassilev et al., 2004) then it would follow that

Table 3.2.2.1 Summary of IC_{50} and IC_{70} values of ACHN scrambled shRNA and ACHN p53 shRNA-expressing cells treated with Nutlin-3 or ABT-737.

Cell line	Nutlin-3 (μM)		ABT-737 (μM)	
	IC_{50}	IC_{70}	IC_{50}	IC_{70}
ACHN scrambled shRNA	2.8	17	20.5	30
ACHN p53 shRNA	3	N/A	22	30

N/A – not available.

Table 3.2.2.2 Combination indices at IC_{50} and IC_{70} for ACHN scrambled shRNA and ACHN p53 shRNA-expressing cells treated with Nutiln-3 and ABT-737.

Cell line	IC_{50}*				IC_{70}*		
	ABT-737 (μM)	Nutlin-3 (μM)	Combination index#		ABT-737 (μM)	Nutlin-3 (μM)	Combination index#
ACHN scrambled shRNA	1	2.30	0.87 +		1	9.00	0.56 + + +
	3	1.40	0.64 + + +		3	2.80	0.26 + + + +
	10	0.67	0.73 + +		10	1.20	0.41 + + +
ACHN p53 shRNA	1	3.00	1.12 -				
	3	3.00	1.13 -				
	10	2.00	1.04 ±				

* - IC_{50} and IC_{70} were the levels of inhibition of proliferation selected to perform analysis of drug interaction by combination index.

- Combination index calculated using the following equation $D1_{comb.}/D1_{alone} + D2_{comb.}/D2_{alone.}$

reduction in the expression of p53 would confer some resistance to the inhibitory effects of Nutlin-3. By extension, if this combination treatment was p53-dependent, then reduction in p53 levels would decrease the synergy observed as a result of this treatment. This is indeed what was observed. To summarise, the synergy observed in response to the combination of Nutlin-3 and ABT-737 in RCC cells harbouring wild type p53 is p53-dependent.

3.2.3 The combination of Nutlin-3 and ABT-737 promotes apoptosis in renal cell carcinoma cells harbouring wild type p53

The data presented in section 3.2.1 of this chapter showed that the combination of Nutlin-3 and ABT-737 synergistically inhibited the proliferation of RCC cells harbouring wild type p53 and that this inhibition of proliferation is p53-dependent (section 3.2.2). The next issue to address was determining the mechanism by which this combination of drugs inhibited proliferation of RCC cells.

As discussed in the Section 3.1, Nutlin-3 treatment alone induces cell cycle arrest and senescence in RCC cells that harbour wild type p53 (Tsao and Corn, 2010; Polanski et al., submitted). ABT-737 has been shown to promote apoptotic cell death in ACHN and A498 cell lines (Song et al., 2008) and two other studies showed that ABT-737 was capable of inducing apoptosis in a variety of RCC cell lines that were not used in our present study (Zall et al., 2010; Zhu et al., 2013). Considering ABT-737 was observed to inhibit proliferation, albeit at high does, in the RCC cell lines used in this study (figure 3.2.1.2), and this inhibition of proliferation was most likely due to the induction of apoptosis (Song et al., 2008) and that Nutlin-3 did not promote the death of RCC cells harbouring wild type p53 but acted synergistically with ABT-737 in RCC cells harbouring wild type p53 but not mutant p53, we envisaged a scenario whereby Nutlin-3 enhanced the pro-apoptotic effect of ABT-737. As Nutlin-3 did not promote apoptosis in these cell lines (Tsao and Corn, 2010), and it was likely that ABT-737 did, it was hypothesised that there was some latent pro-apoptotic function to p53 rescued by Nutlin-3 treatment in these cells that was insufficient to promote apoptosis alone but could contribute towards ABT-737-mediated apoptosis. Indeed a recent study showed that cell lines that possessed wild

type p53 that did not respond to Nutlin-3 treatment by undergoing apoptosis could be induced to undergo apoptosis upon combination of Nutlin-3 with ABT-263 (Kracikova et al., 2013), a derivative of ABT-737 that targets the same anti-apoptotic proteins as ABT-737, with doses of ABT-263 that did not promote apoptosis alone. The authors proposed a threshold model for p53-dependent cell fate decisions whereby the threshold for p53-mediated apoptosis could be lowered by combination of a Bcl-2 family inhibitor with an inhibitor of the MDM2-p53 interaction (Kracikova et al., 2013). Considering our own observations, that Nutlin-3 did not promote apoptosis alone but synergised with ABT-737 to inhibit the proliferation of RCC cells in a p53-dependent manner, the next question to address was whether apoptosis was taking place in our panel of cell lines in response to the combination treatment.

The approach employed initially was to visually observe the response of the cells treated with the compounds. As described in Section 1.7.7, apoptotic cells are conspicuous by a number of changes to the cell, some of which can be observed visually by phase contrast microscopy, such as cell shrinkage and apoptotic body formation. ACHN wild type p53 cells and 111 mutant p53 cells were used in this experiment. Cells were seeded into six well plates at a density of 100 000 cells per well. Preliminary observations by phase contrast microscopy suggested that none of the changes associated with apoptosis could be observed visually in response to any of the compounds until ~24 h post-treatment, hence live cell imaging commenced 18 h after treatment with drug vehicle, 3μM Nutlin-3, 10μM ABT-737 or a combination of both treatments and images were acquired at 5 min intervals for 24.5h. A more

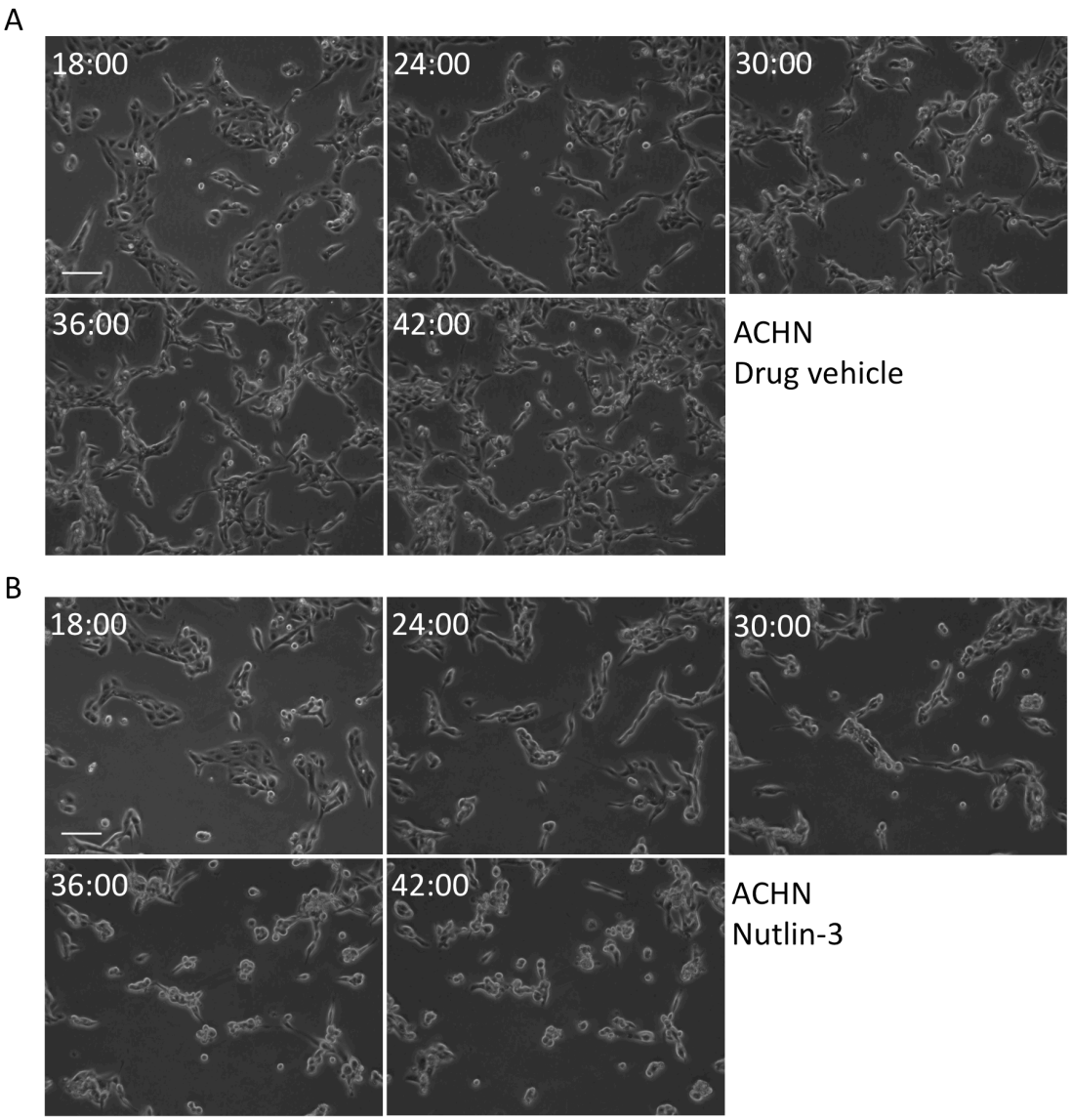

Figure 3.2.3.1 Images obtained from live cell imaging of ACHN cells (I). ACHN cells were seeded at a density of 100,000 cells per well. 24h after seeding, cells were treated with either drug vehicle (A) or 3μM Nutlin-3 (B) and live cell imaging commenced 18h after drug treatment. Live cell imaging was performed as described in section 2.7. Time is in hours and minutes. Scale bar = 160μm.

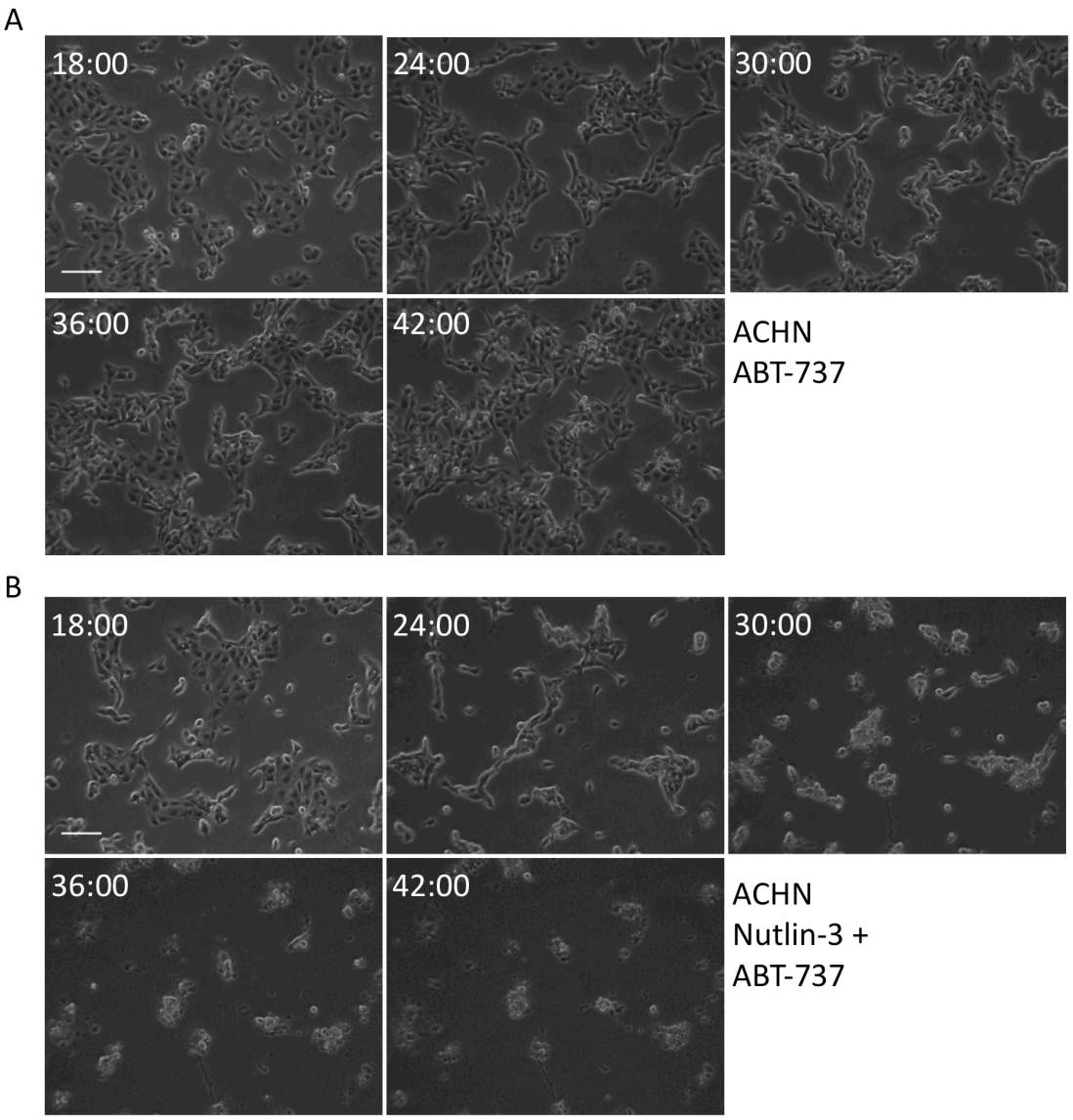

Figure 3.2.3.2 Images obtained from live cell imaging of ACHN cells (II). ACHN cells were seeded at a density of 100,000 cells per well. 24h after seeding, cells were treated with either 10 μM ABT-737 (A) or a combination of 3μM Nutlin-3 and 10μM ABT-737 (B) and live cell imaging commenced 18h after drug treatment. Live cell imaging was performed as described in section 2.7. Time is in hours and minutes. Scale bar = 160μm.

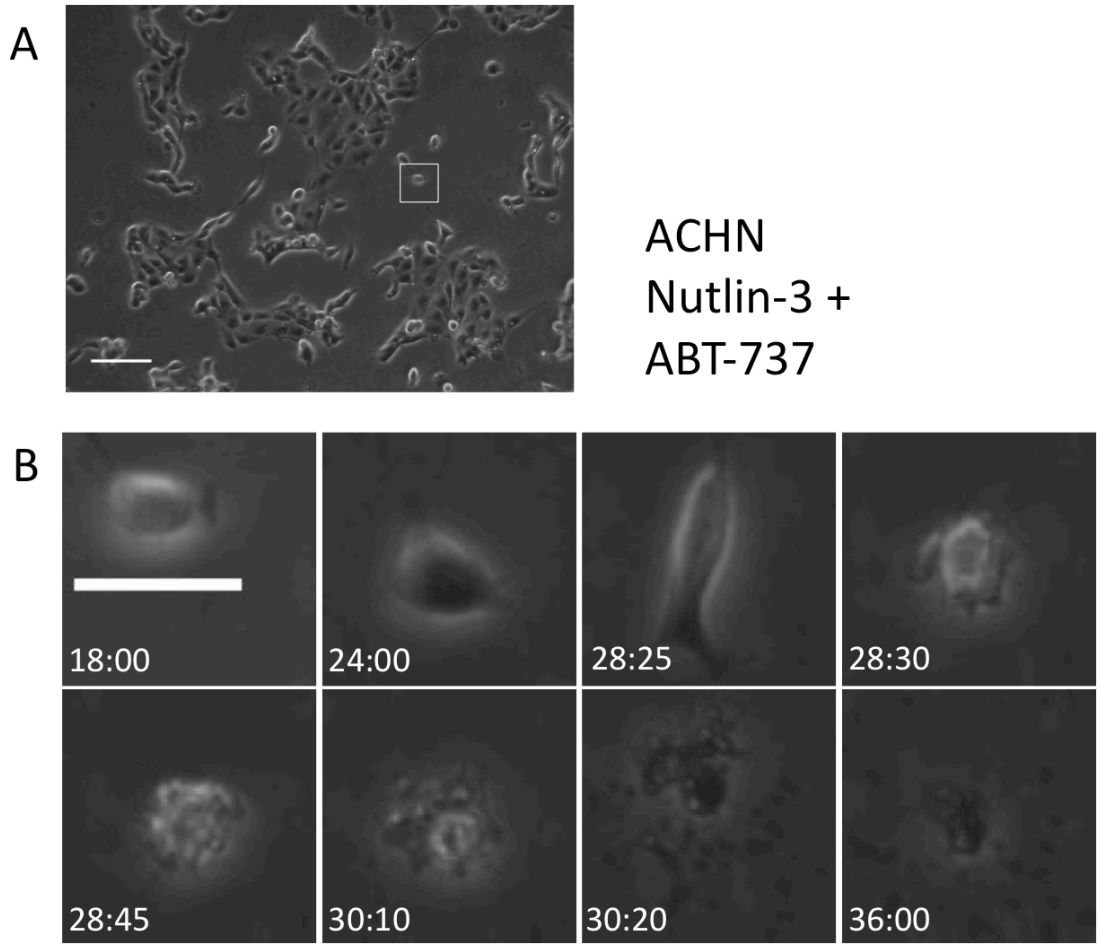

Figure 3.2.3.3 Single cell time-lapse study of ACHN cell dying in response to the combination of Nutlin-3 and ABT-737. The experimental conditions were as described in the legend of figure 3.2.3.2. A. ACHN cells treated with 3μM Nutlin-3 and 10μM ABT-737 at 18 h post-treatment, reproduced from figure 3.2.3.2B. Scale bar = 160μm. B. Time lapse images of single cell from white box in figure 3.2.3.3A. Scale bar = 56μm.

detailed description of the protocol for live cell imaging is shown in section 2.7. Representative movies that were made from the images collected are included on the attached DVD (Appendix 1).

Figure 3.2.3.1 and 3.2.3.2 show images acquired at six-hour intervals from the initial image acquired 18 h after drug treatment. In response to drug vehicle, ACHN cells continued to proliferate and divide and appeared healthy (figure 3.2.3.1A and supplementary movie 1, Appendix 1) as time progressed. In response to treatment of ACHN cells with Nutlin-3, little death appeared to take place, however at roughly 18h, cells appeared to form highly motile inclusions that oscillated for the remainder of the movie. Single cells that were not part of these inclusions appeared to be motile, but did not divide. Cells did not appear to proliferate and divide for the duration of the movie. ACHN cells treated with ABT-737 overall appeared to proliferate and divide as normal. Some cells appeared to die towards the end of the experiment, however, this appeared to have little affect on overall cell number because the remaining cells appeared to proliferate in a manner similar to drug vehicle treated cells. At 18 h, the density ACHN cells treated with the combination of Nutlin-3 and ABT-737 was comparable to that observed in the other three treatments (figure 3.2.3.2B). Cell death could be observed taking place immediately after the 18h time point. At 30h, all of the cells appear to be dying and this continued for the duration of the movie until no healthy cells were observed. Figure 3.2.3.4B is a representative single cell analysis summarizing the key points of the cell death taking place in response to the combination of Nutlin-3 and ABT-737. At 18:00 until 28:25, the cell appeared healthy. At 28:25, the cell elongated then at 28:30, the cell took on a more circular appearance. At 28:45, the cell appeared to

undergo membrane blebbing that is characteristic of cells undergoing apoptosis, resulting in the formation of apoptotic bodies. Dissociation of the apoptotic bodies from the main body of the cell appeared to be taking place at 30:10. This process continued, until the remainder of the cell was surrounded by apoptotic bodies that had dissociated from the main body of the cell (30:20 and 36:00, figure 3.2.3.4B).

111 cells appeared to proliferate and appeared healthy in response to treatment with drug vehicle (figure 3.2.3.5A and Appendix 1, movie 5). A similar observation was made in when 111 cells were treated with Nutlin-3 (figure 3.2.3.5A and Appendix 1, movie 6), and the cells appeared to proliferate as normal. Some cell death could be observed in response to ABT-737 alone (figure 3.2.3.5B and Appendix 1, movie 7) but overall, cells continued to proliferate. Dying cells appeared undergo blebbing followed by death that was observed in the ACHN cells in figure 3.2.3.4B. 111 cells treated with the combination of Nutlin-3 and ABT-737 proliferated in a similar manner to the 111 cells treated with ABT-737 alone and some cell death took place but overall, combination treated 111 cells were not dissimilar to ABT-737-treated 111 cells in that the cells continued to proliferate in response to the treatments and cell death was minimal. Interestingly, the dramatic cell death that was observed in the ACHN cells in response to the combination treatment was not observed in the 111 cells, emphasizing the importance of wild type p53 in the response to this treatment (compare figure 3.2.3.3B and 3.2.3.6B at 42:00).

To summarise, Nutlin-3 appeared to inhibit the proliferation of ACHN cells but did not appear to promote cell death. ABT-737 treatment induced some cell death in ACHN cells but proliferation did not appear hindered. The combination of both

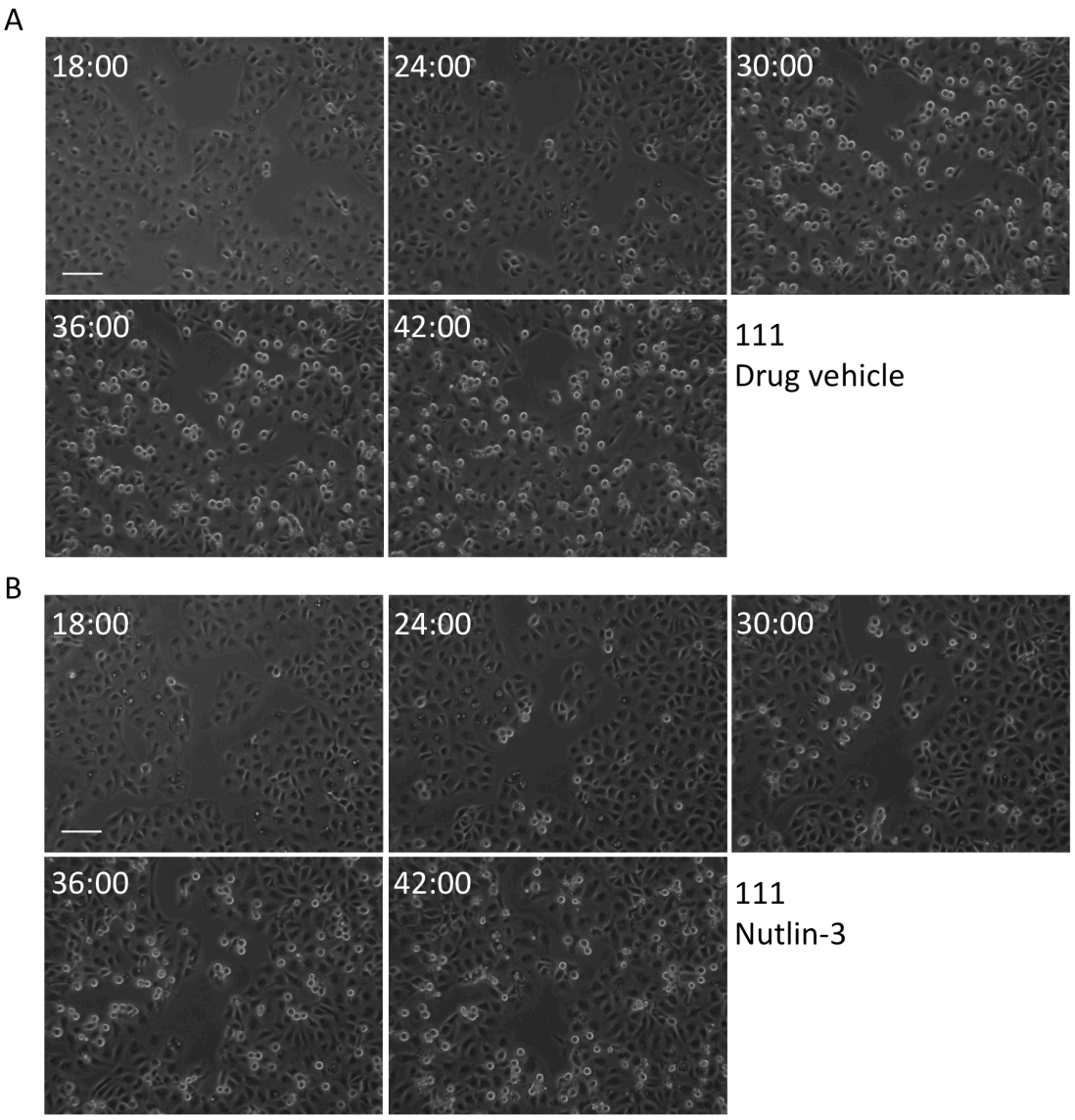

Figure 3.2.3.4 Images obtained from live cell imaging of 111 cells (I). 111 cells were seeded at a density of 100,000 cells per well. 24h after seeding, cells were treated with either drug vehicle (A) or 3μM Nutlin-3 (B) and live cell imaging commenced 18h after drug treatment. Live cell imaging was performed as described in section 2.7. Time is in hours and minutes. Scale bar = 160μm.

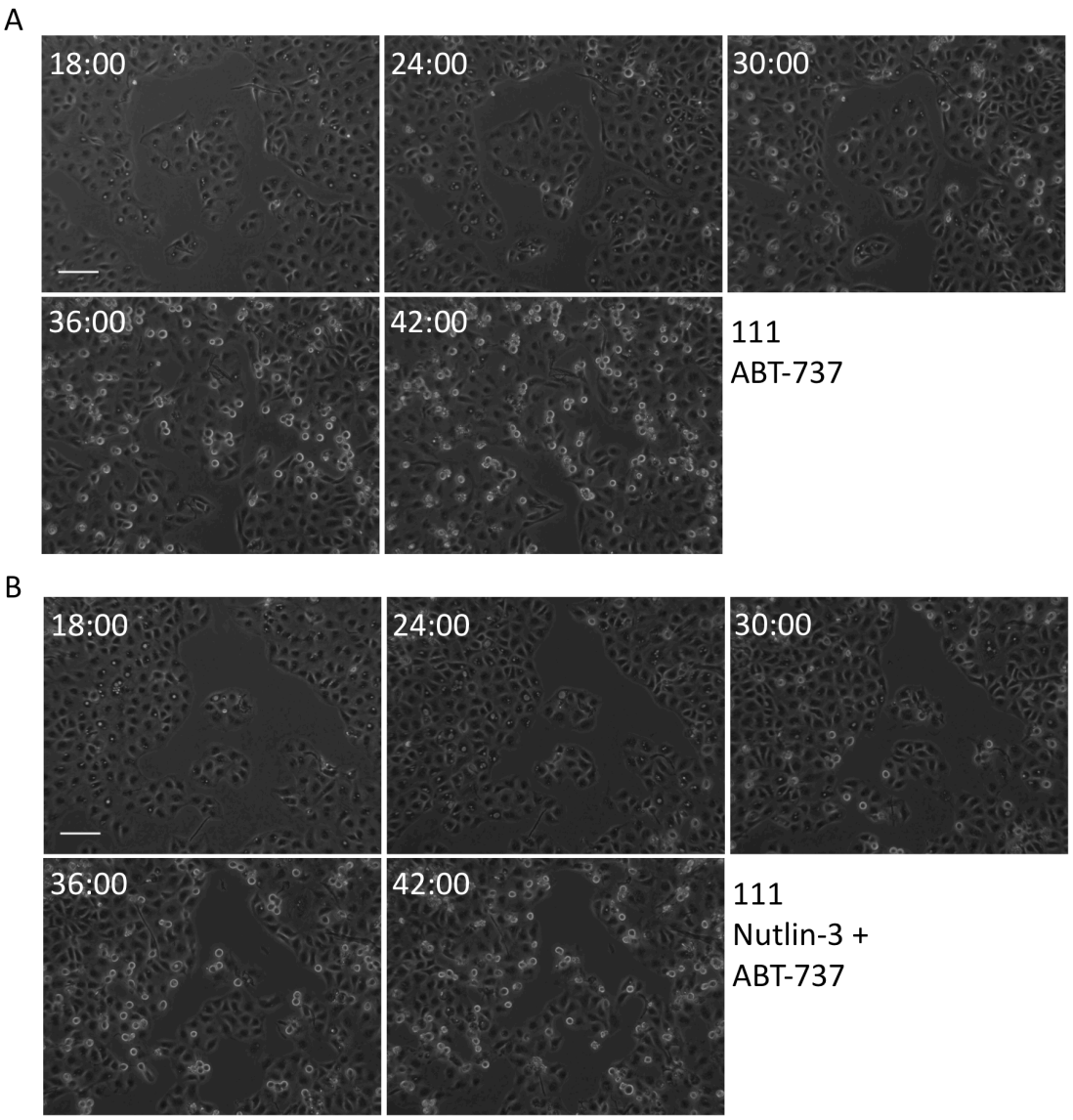

Figure 3.2.3.5 Images obtained from live cell imaging of 111 cells (II). 111 cells were seeded at a density of 100,000 cells per well. 24h after seeding, cells were treated with either 10μM ABT-737 (A) or a combination of 3μM Nutlin-3 and 10μM ABT-737 (B) and live cell imaging commenced 18h after drug treatment. Live cell imaging was performed as described in section 2.7. Time is in hours and minutes. Scale bar = 160μm.

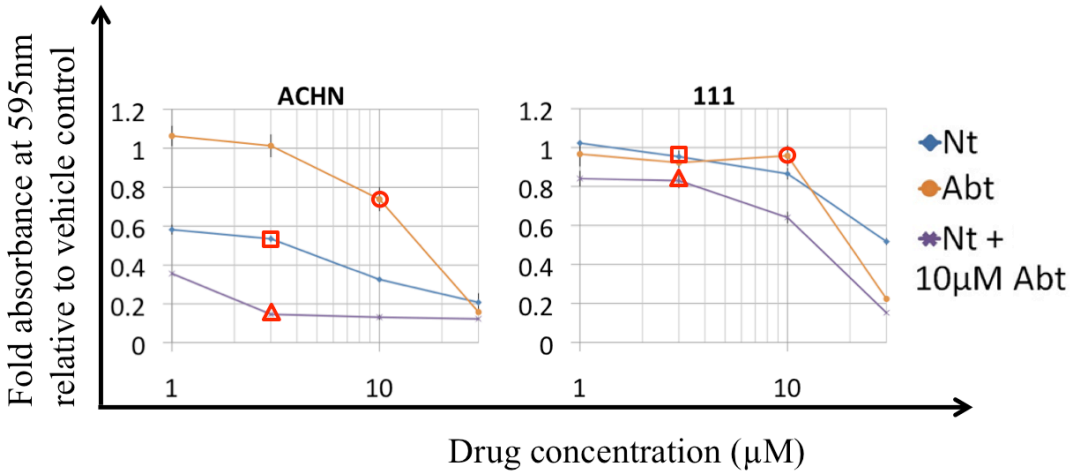

Figure 3.2.3.6 Survival curves for ACHN and 111 cells treated with Nutlin-3 and/or ABT-737. Cells were seeded as described in section 2.3.1.1 and treated with the indicated drugs for 42.5h. Cells were then treated with MTT as described in section 2.3.1.2. After treatment with MTT, absorbance at an optical density of 595nm was measured. As a measure of proliferation, absorbance of drug-treated cells at 595nm was divided by absorbance of vehicle treated cells to give proliferation relative to drug-vehicle treated cells. Red square – 3μM Nutlin-3. Red circle – 10μM ABT-737. Red triangle – combination of 3μM Nutlin-3 and 10μM ABT-737.

treatments induced dramatic cell death in ACHN cells. This is consistent with the data presented in section 3.2.1. Nutlin-3 appeared to have no affect on 111 cells.

ABT-737 and combination treatment both had similar affects on 111 cells, such that proliferation was not perturbed and little cell death was induced. This was consistent with the finding presented in section 3.2.2, that inhibition of proliferation of RCC cells in response to this combination treatment is p53-dependent. Survival curves for ACHN and 111 cells that were treated with Nutlin-3 and ABT-737 for the corresponding length of time as the experiment described in this section are shown in figure 3.2.3.6 (42.5 h). The treatments used in the above experiment are highlighted on both of the survival curves in figure 3.2.3.6 by red shapes. Data from these survival curves is consistent with the observations from the live cell imaging: proliferation of ACHN cells is inhibited by Nutlin-3 treatment, without the promotion of cell death, as has been previously established (Tsao and Corn, 2010; Polanski et al., submitted). Nutlin-3 treatment had no effect on the proliferation of 111 cells, consistent with the absence of wild type p53. ABT-737 promoted some cell death in ACHN cells but proliferation was not hindered; a similar observation could be made about 111 cells, although this cell line was slightly more resistant to the cell death promoting affect of ABT-737 (figure 3.2.3.5, table 3.2.1.1 and compare figures 3.2.3.2A and 3.2.3.5A).

The combination of Nutlin-3 and ABT-737 promoted dramatic cell death in ACHN cells (figure 3.2.3.2B) and this is consistent with the data shown in figure 3.2.3.6 (red triangle). 111 cells were largely resistant to the cell death promoting affects of the combination of Nutlin-3 and ABT-737 and this was reflected in the survival data. In

conclusion, the inhibition of proliferation observed upon treatment of RCC cells harbouring wild type p53 with the combination of Nutlin-3 and ABT-737 appeared to be due to cell death rather than inhibition of cell proliferation.

In this section, the term apoptosis has not yet been used to describe the nature of the cell death observed in response to ABT-737 and the combination treatment, although this is the most likely cell fate that is being promoted in response to these treatments, considering that the pro-apoptotic effects of ABT-737 are well documented and also the nature of cell death observed in figure 3.2.3.3. To verify whether apoptosis was indeed taking place in response to these treatments in this panel of cell lines, FITC-conjugated Annexin V (AV) and propidium iodide (PI) staining of cells was used, followed by quantification of cells expressing the different fluorophores using flow cytometry, as described in Section 2.3.2. Cells were treated with 3μM Nutlin-3, 10μM ABT-737 or a combination of both treatments for 36h before staining with AV and PI and subsequent quantification using a flow cytometer. Caki2 cells were treated with only 1μM ABT-737 because of the increased sensitivity of this cell line to ABT-737 (table 3.2.1.1). Figure 3.2.3.7 and 3.2.3.8 show the dot plots from the flow cytometry quantification of cells treated with the single drug or the combination and figure 3.2.3.8 summarises the percentages of AV positive cells in each treatment. A cursory inspection of all of the dot plots showed that cells treated with drug vehicle had low percentages of cells that were positive for AV alone or both AV and PI (Figures 3.2.3.7 and 3.2.3.8). The highest percentage of AV positivity in response to drug vehicle was observed in HEK293 cells (14.4%, figure 3.2.3.9). Considering that AV positivity was an indicator that a cell was undergoing apoptosis (discussed in Section 2.3.2) and the PI positivity was an indicator of cell death, and that AV and

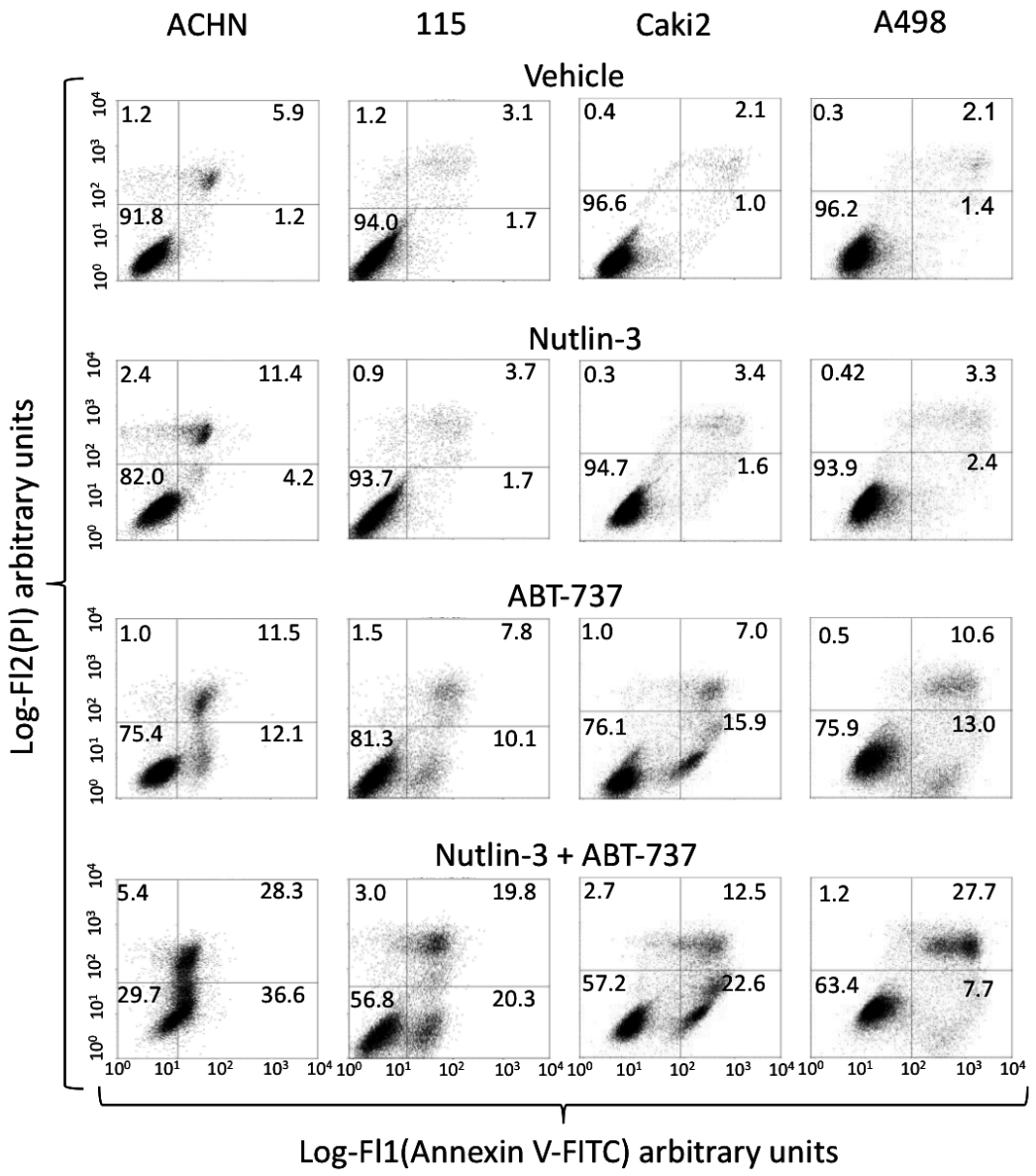

Figure 3.2.3.7 Analysis of apoptosis and cell death in cells treated with Nutlin-3 and/or ABT-737 (I). Cells were treated with drug-vehicle, 3μM Nutlin-3, 10μM ABT-737 or a combination of both treatments for 36h and passed through a flow cytometer as described in section 2.3.2. Caki2 cells were treated with 1μM ABT-737 due to the greater sensitivity of this cell line to the compound. 20,000 events were counted by the flow cytometer and values in each quadrant indicate the percentage of cells in that quadrant relative to the total number of counted cells. Representative data from at least 3 repeats.

PI positivity was observed at the same time as cells that were positive for AV alone, we therefore surmised that most of the AV and PI positive cells (dead cells) were cells that had undergone apoptosis earlier than cells that were only AV positive. Hence, the cells that were AV (lower right quadrant on the dot plot) positive were categorized as apoptotic and AV and PI positive (upper right quadrant) cells were categorized as dead cells that had undergone apoptosis.

Nutlin-3 treatment alone had little effect in terms of promoting apoptosis in these cell lines (figures 3.2.3.7, 3.2.3.8 and 3.2.3.9). There was no greater than an 8.6% increase in the proportion of apoptotic and dead cell in response to treatment with Nutlin-3 over drug-vehicle treated cells across all of the cell lines tested (figure 3.2.3.9), suggesting that Nutlin-3 treatment alone was ineffective in promoting apoptosis in these cells. This was consistent with previous observations RCC cells that harboured wild type p53 (Tsao and Corn, 2010).

When compared to drug-vehicle treated cells, treatment with ABT-737 resulted in an increase in apoptosis and cell death due to apoptosis, which was generally greater than that observed in response to treatment with Nutlin-3, with the single exception of 111 cells (figures 3.2.3.7, 3.2.3.8 and 3.2.3.9). 111 cells exhibited a 1.1% increase in apoptosis and cell death in response to Nutlin-3 over that observed in response to ABT-737 (figures 3.2.3.8 and 3.2.3.9). This minor increase was likely due to handling of the cells during preparation of the sample rather than any real biological effect. Further, the sensitivity of 111 cells to both Nutlin-3 and ABT-737 is identical (IC_{50} =18 μM, table 3.2.1) therefore it is unlikely that this minor difference in percentage of apoptotic cells in response to Nutlin-3 or ABT-737 was a direct effect

of either of treatment. The Caki2 and A498 cell lines were the most sensitive to ABT-737, with the percentage of apoptotic and dead cells totalling 19.8 and 20.1% relative to their respective drug-vehicle treated controls (figures 3.2.3.7 and 3.2.3.9). There was a more modest increase in the proportion of apoptotic and dead cells upon ABT-737 treatment in the ACHN, 115 and 154 cell lines with 16.5, 13.2 and 10.5 % apoptotic and dead cells relative to respective drug vehicle treated control of each cell line (figures 3.2.3.7, 3.2.3.8 and 3.2.3.9). Overall, the RCC cells harbouring wild type p53 appeared to be more sensitive to ABT-737 when compared to their mutant counterparts in this assay (figure 3.2.3.9). This is unsurprising, considering that in several tissue and tumour backgrounds, p53 can promote the transcription of proteins such as Puma and Noxa, that can interact with anti-apoptotic Bcl-2 family members to promote apoptosis (see section 1.2.8).

Treatment with the combination of Nutlin-3 and ABT-737 resulted in an increase in the number of apoptotic and dead cells in all of the RCC cells harbouring wild type p53 with the exception of the 117 cell line, when compared to both drug-vehicle or each of the solo-agents (figures 3.2.3.7, 3.2.3.8 and 3.2.3.9). The wild type p53 cell lines: ACHN, 115, Caki2 and A498 exhibited an increase in apoptosis of 57.8, 35.4, 37.0 and 31.9% relative to their respective drug-vehicle-treated controls. The mutant p53 cell lines: 111 and 154 also displayed an increase in apoptosis of 5.5 and 11.4% relative to their respective drug-vehicle-treated controls in response to the combination of Nutlin-3 and ABT-737 (figures 3.2.3.8 and 3.2.3.9), but this is considerably less than is observed in the p53 wild type cell lines. Relative to their respective ABT-737 single treatments, the increases in the number of apoptotic cells observed in the 111 and 154 cell lines are only 4.1 and 1.0%, suggesting that the

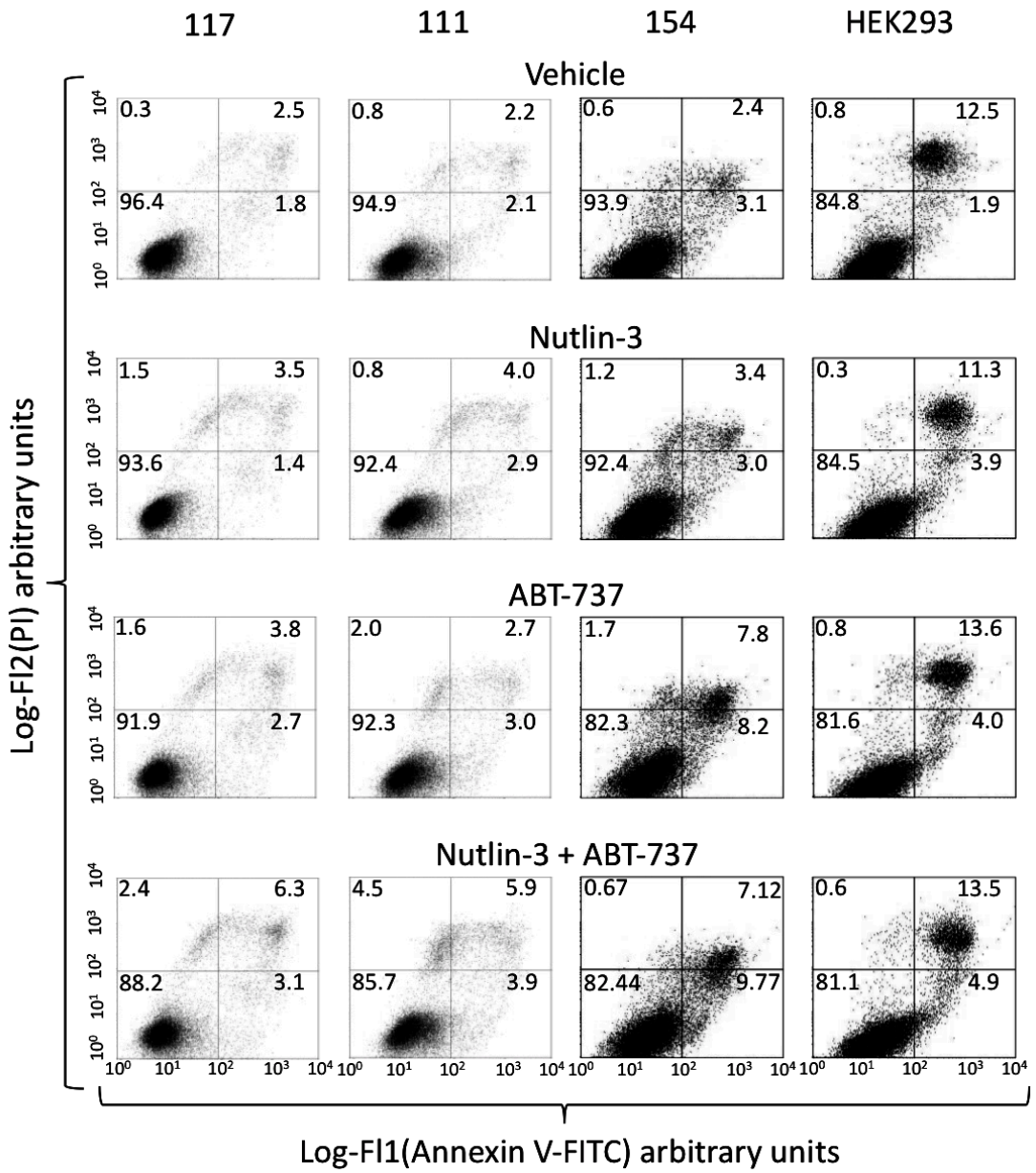

Figure 3.2.3.8 Analysis of apoptosis and cell death in cells treated with Nutlin-3 and/or ABT-737 (II). Cells were treated with drug-vehicle, 3μM Nutlin-3, 10μM ABT-737 or a combination of both treatments for 36h and passed through a flow cytometer as described in Section 2.3.2. 20,000 events were counted by the flow cytometer and values in each quadrant indicate the percentage of cells in that quadrant relative to the total number of counted cells. Representative data from at least 3 repeats.

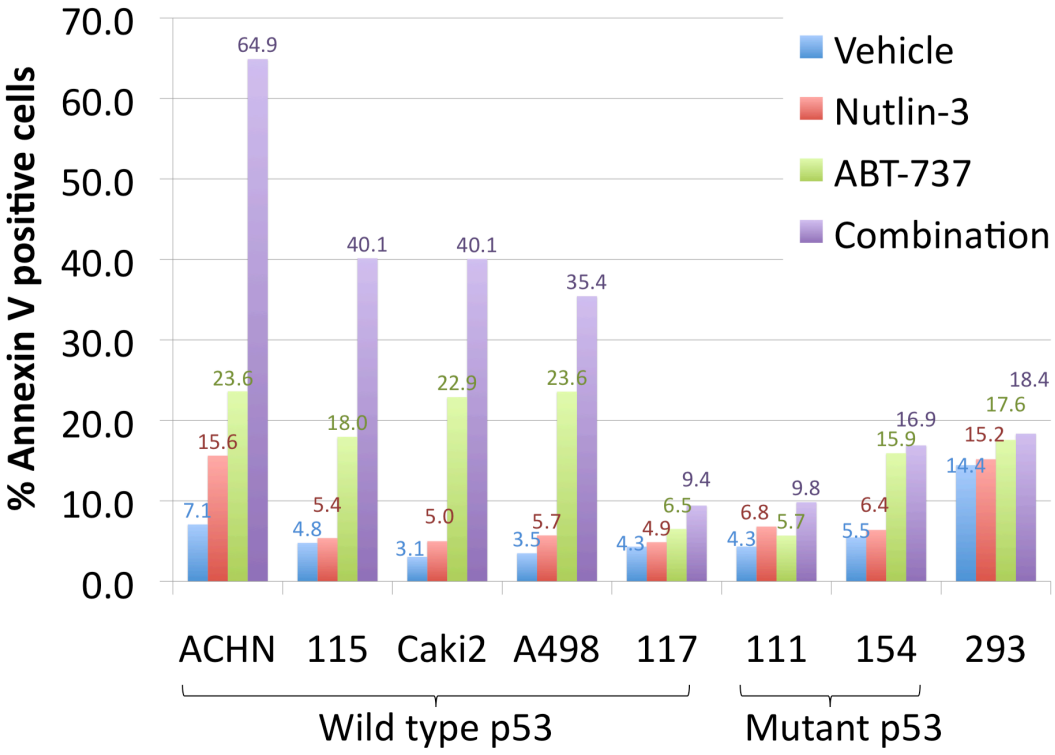

Figure 3.2.3.9 Analysis of Annexin V positive cells treated with Nutlin-3 and/or ABT-737. Summary of flow cytometric analysis of renal cells after 36h treatment with drug-vehicle, 3μM Nutlin-3, 10μM ABT-737 or a combination of both treatments (Caki2 cells were treated with only 1μM ABT-737, see legend of figure 3.2.3.7). Histogram bars represent sum of lower right quadrant events (apoptotic cells) and upper right quadrant events (cells that had died as result of apoptosis).

presence of Nutlin-3 in the combination treatment did very little to contribute to the increased apoptosis observed in both of these cell lines relative to their drug-vehicle-treated controls. The obvious difference in the responses of the RCC cells that harbour wild type p53 ACHN, 115, A498 and Caki2 to the RCC cells that harbour mutant p53 in response to the combination treatment underscored the importance of wild type p53 to the apoptotic response of these cells to the combination treatment. This is consistent with the data presented in section 3.2.2, that the inhibitory response to the combination of Nutlin-3 and ABT-737 is p53-dependent. The 117 wild type p53 RCC cell line responded to the combination treatment in similar manner to the mutant p53 cell lines in that combining Nutlin-3 with ABT-737 did not particularly increase apoptosis over the ABT-737 single treatment. This was consistent with the data presented in section 3.2.1 showing that synergy between Nutlin-3 and ABT-737 was less apparent in the 117 cell line when compared to the other RCC cell lines that harboured wild type p53 (figure 3.2.1.3 and table 3.2.1.2). This less dramatic response to the combination Nutlin-3 and ABT-737 when compared to the other wild type p53 RCC cell lines maybe because the 117 cell line possesses an almost undetectable level of p53 protein when compared to the other wild type p53 RCC cell lines tested (lane 6, figure 3.2.1.1). It is possible that relatively higher levels of wild type p53 are required for this combination of drugs to promote apoptosis in RCC cells. This is an intriguing possibility, since higher levels of wild type p53 and MDM2 has been shown to be an independent prognostic indicator for worse outcome in patients with RCC (Noon et al., 2011; section 1.1.5.3), this data suggests that this drug combination may be p53-level-specific and hence biomarker specific.

Interestingly, there was comparatively little apoptosis observed in response to either single agents or the combination of agents in the HEK293 cell line. This is consistent with the data presented in section 3.2.1. The proportion of apoptotic and dead cells increased by only 3.9% in response to the combination treatment. This might be evidence that tumorigenicity is a pre-requisite for the effectiveness of this combination and may be the basis for a therapeutic index however this is highly speculative and xenograft models would be required to begin to address this issue.

To conclude this section, the combination of Nutlin-3 and ABT-737 inhibits the proliferation of RCC cells harbouring wild type p53 by promoting apoptosis. ABT-737 treatment alone promoted apoptosis in these cell lines, however, combining Nutlin-3 with ABT-737 increased the degree to which this apoptosis took place. This is consistent with the hypothesis outlined at the beginning of this section suggesting that Nutlin-3 enhanced the pro-apoptotic effects of ABT-737. The p53-dependent nature of this combination treatment in the RCC cell lines harbouring wild type p53 was further supported by the observations made using live cell imaging and the decreased apoptotic response observed in the RCC cells harbouring mutant p53.

3.2.4 An inhibitor of the ubiquitin-ligase activity of MDM2 does not synergise with ABT-737 in RCC cells that harbour wild type p53

In Section 3.2.1, it was shown that the combination of Nutlin-3 and ABT-737 synergistically inhibited the proliferation of RCC cells harbouring wild type p53. In the Section 3.2.2, ACHN cells expressing scrambled control shRNA that expressed the same level of p53 as parental ACHN cells, and ACHN cells expressing p53-specific shRNA that possessed a relatively lower level of p53 protein compared to the scrambled control were used, to show that this synergistic effect was indeed dependent on p53. In Section 3.2.3, it was shown that this inhibition of proliferation described in the first section was actually apoptosis taking place in response to the combination treatment. Nutlin-3 is an inhibitor of the MDM2-p53 interaction (Section 1.3.3; Vassilev et al., 2004) and as discussed in the Section 1.3.1, MDM2 can regulate p53 activity by targeting p53 for degradation at the proteasome upon ubiquitination of p53 by MDM2 or to a lesser extent, by directly binding to p53 (Section 1.3.1; Oliner et al., 1993; Honda et al, 1997; Kubbutat et al., 1997). Considering that Nutlin-3 is an inhibitor of the MDM2-p53 interaction, and combining this compound with the pro-apoptotic drug ABT-737 synergistically promoted apoptosis in the RCC cells harbouring wild type p53, it would have been interesting to observe whether the same synergistic effect was observed in upon combining ABT-737 with an inhibitor of the ubiquitin ligase activity of MDM2. HLI98 is an inhibitor of the E3 ubiqutin ligase activity of MDM2 (Yang et al., 2005) and HLI373 (Kitagaki et al., 2008) is a more potent, water-soluble derivative of HLI98 (See Section 1.3.3). Both of these compounds have been shown to promote p53-dependent cell cycle arrest or apoptosis in a cell lines derived from different

Table 3.2.4.1 Summary of IC_{50} and IC_{70} values of cells treated with HLI373 or ABT-737.

Cell line	HLI373 (μM)		ABT-737 (μM)	
	IC_{50}	IC_{70}	IC_{50}	IC_{70}
ACHN	1.3	2.3	13.0	20.0
A498	2.3	4.4	7.0	13.0
Caki2	3.0	8.0	1.9	4.0
115	6.0	13.0	19.0	23.0
117	2.2	3.0	11.0	19.0

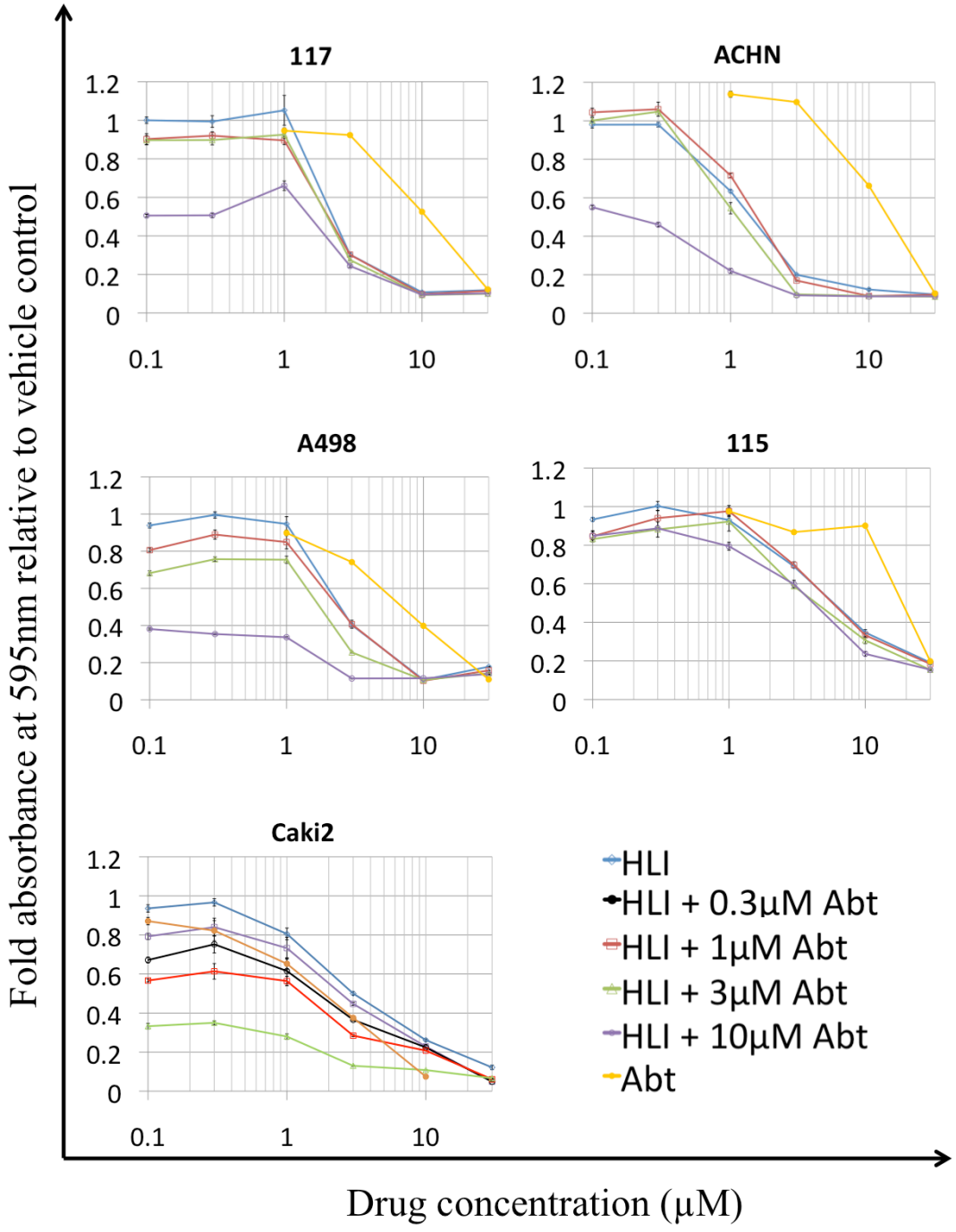

Figure 3.2.4.1 Survival curves of RCC cells treated with HLI373 and/or ABT-737. Cells were seeded as described in section 2.3.1.1 and treated with the indicated drugs for 72h. Cells were then treated with MTT as described in section 2.3.1.2. After treatment with MTT, absorbance at an optical density of 595nm was measured. As a measure of proliferation, absorbance of drug-treated cells at 595nm was divided by absorbance of vehicle treated cells to give proliferation relative to drug-vehicle treated cells. Representative data from at least 2 repeats.

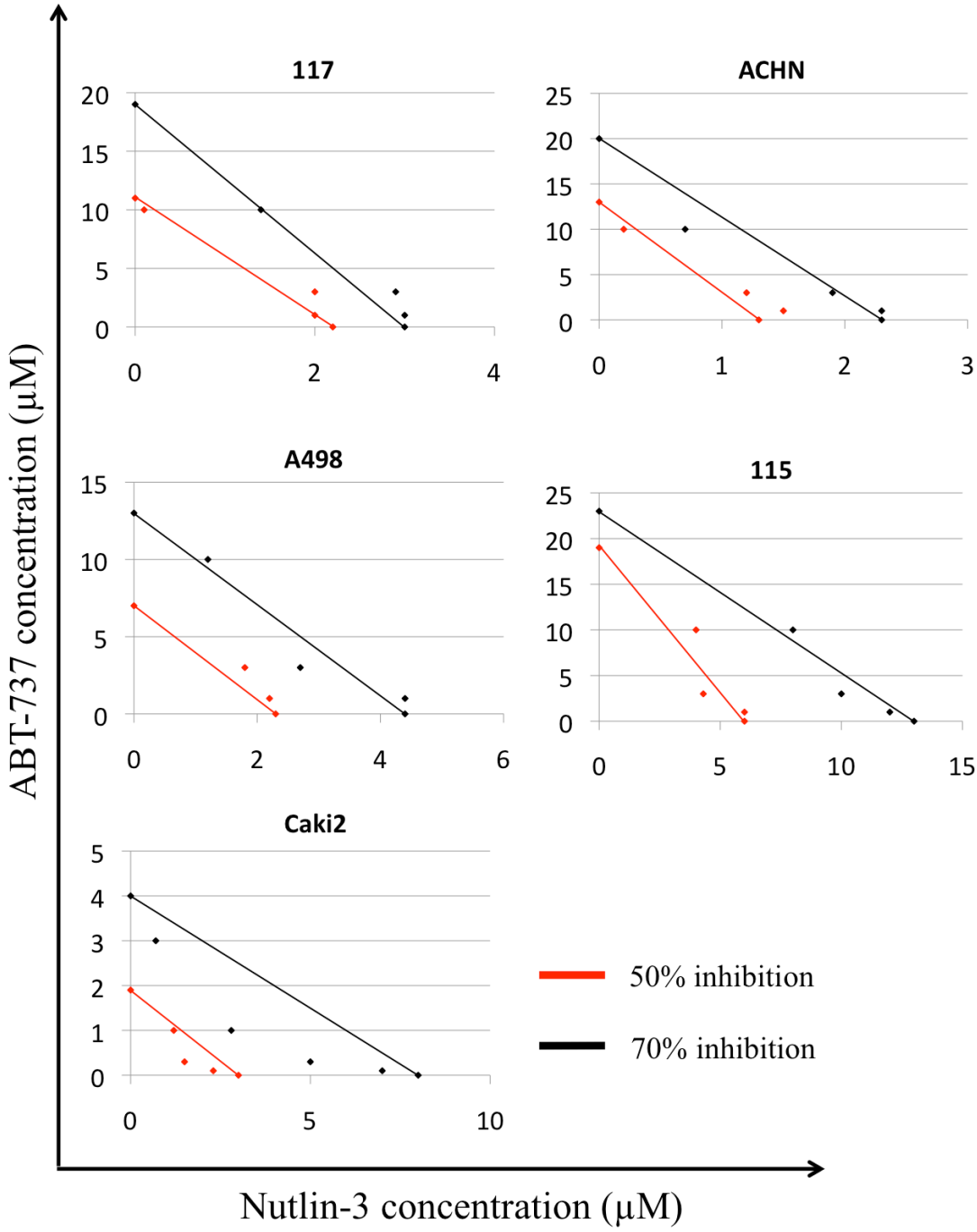

Figure 3.2.4.2 Analysis of HLI373 and ABT-737 drug interaction in RCC cells. Isobolograms produced from data shown in figure 3.2.4.1. IC_{50} and IC_{70} values were plotted onto the vertical and horizontal axes for HLI373 and ABT-737 respectively to give isoboles. Drug combination points were then expressed on the isobolograms to assess the for synergy between both drugs.

Table 3.2.4.2 Combination indices at IC_{50} and IC_{70} for RCC cells treated with HLI373 and ABT-737.

Cell line	p53 status	IC_{50}*			IC_{70}*		
		ABT-737 (μM)	HLI373 (μM)	Combination index#	ABT-737 (μM)	HLI373 (μM)	Combination index#
ACHN	WT	1	1.5	1.23 - -	1	2.3	1.05 ±
		3	1.2	1.15 -	3	1.9	0.98 ±
		10	0.2	0.92 ±	10	0.7	0.80 + +
A498	WT	1	2.2	1.10 -	1	4.4	1.10 -
		3	1.8	1.21 - -	3	2.7	0.84 + +
					10	1.2	1.04 ±
Caki2	WT	0.1	2.3	0.81 + +	0.1	7.0	0.90 ±
		0.3	1.5	0.66 + + +	0.3	5.0	0.70 + +
		1	1.2	0.93 ±	1	2.8	0.60 + + +
115	WT	1	6.0	1.05 ±	1	12.0	0.97 ±
		3	4.3	0.87 +	3	10.0	0.90 ±
		10	4.0	1.19 -	10	8.0	1.05 ±
117	WT	1	2.0	1.00 ±	1	3.0	1.05 ±
		3	2.0	1.18 -	3	2.9	1.12 -
		10	0.1	0.95 ±	10	1.4	1.00 ±

* - IC_{50} and IC_{70} were the levels of inhibition of proliferation selected to perform analysis of drug interaction by combination index.

- Combination index calculated using the following equation $D1_{comb.}/D1_{alone} + D2_{comb.}/D2_{alone.}$

WT – wild type.

tumours. It was hypothesized that combining a MDM2 ubiquitin ligase inhibitor with ABT-737 would have resulted in the synergistic inhibition of proliferation of RCC cells harbouring wild type p53 in a manner similar to that observed upon treatment with the combination of Nutlin-3 and ABT-737 simply because both Nutlin-3 and HLI compounds both liberate p53 from inhibitory regulation by MDM2. To test this, a similar approach was taken as that described in section 3.2.1. A panel of RCC cells harbouring wild type p53 were treated with HLI373, ABT-737 or a combination of both treatments for 72 h and a MTT assay was performed as described in section 2.3. Absorbance at 595nm from each drug treatment was divided by absorbance at 595 nm from the drug vehicle treatment to give a surrogate indicator of viability in response to drug treatment, as performed previously. Figure 3.2.4.1 summarises the survival curves for the cell lines treated with HLI373 and ABT-737 and table 3.2.4.1 summarises the IC_{50} and IC_{70} values for both treatments. The IC_{50} of HLI373 for the RCC cell lines tested ranged between 1.3 and 6.0μM, suggesting that the cell lines tested exhibited similar sensitivities to HLI373. At IC_{70} there was roughly a 5-fold difference in the sensitivity to HLI373 between the most resistant cell line (115, 13.0μM) and the most sensitive (ACHN 2.3μM). Sensitivity to ABT-737 alone (table 3.2.4.1) was comparable to that observed in the experiment described in section 3.2.1 (table 3.2.1). To understand the nature of the drug interaction between HLI373 and ABT-737 in these cells, isobolograms were plotted from the data shown in figure 3.2.4.1 (figure 3.2.4.2). As can be seen from the isobolograms, the only cell line in which HLI373 and ABT-737 appear to act synergistically is the Caki2 cell line. The interaction between both compounds in the remaining cell lines appears additive, with combination points clustering close to the isobole at both IC_{50} and IC_{70}. Combination indices at IC_{50} and IC_{70} are summarized

on table 3.2.4.2. Excluding Caki2 cells, the combination indices at IC_{50} and IC_{70} range from 0.87 to 1.23 and 0.80 to 1.12 respectively. This underscored the lack of synergism between both of these compounds in the RCC cell lines tested with the exception of Caki2 cells. Some synergy was observed in Caki2 cells at both IC_{50} and IC_{70}, the lowest combination indices at these levels of inhibition being 0.66 and 0.60 respectively; this was comparable to the synergy observed in response to the combination of Nutlin-3 and ABT-737.

Two questions arose from these data: 1) why was there no synergy observed between the MDM2 ubiquitin ligase inhibitor and ABT-737 in most of the RCC cell lines harbouring wild type p53? 2) Why was synergy observed in Caki2 cells but not in the other cell lines? As discussed in the Section 1.3.1, MDM2 can regulate p53 activity by functioning as an ubiquitin ligase for p53, targeting p53 for proteolytic degradation or masking the transactivation domain of p53, inhibiting the function of p53 as a transcription factor. p53 in RCC cells is subject to regulation by MDM2 (Warburton et al., 2005) and knockdown of MDM2 using siRNA results in increased p53 protein level in RCC cells (Warburton et al., 2005; Polanski et al., 2010). Binding of MDM2 to p53 is a prerequisite for MDM2 to function as an ubiquitin ligase to p53. To our knowledge, there is no evidence to suggest that HLI373 inhibits binding of MDM2 to p53. It could therefore be speculated, since Nutlin-3 synergises with ABT-737 but HLI737 does not synergise with ABT-737, that inhibition of the ubiquitin ligase activity of MDM2 is less important to the rescue of p53 than inhibition of MDM2 binding to p53. Caki2 was more sensitive to HLI373 at IC_{70} than the remaining cell lines tested (table 3.2.4.1). The synergy observed in the Caki2 cell line may be an extension of this increased sensitivity.

3.3 Summary

To restore wild type p53 function in RCC cells that harbour wild type p53, we rationally selected the combination of Nutlin-3 and ABT-737, the former for its ability to inhibit the MDM2-p53 interaction and the latter for its documented ability to promote apoptosis in cells from a variety of tumour backgrounds. We have demonstrated that the combination of both of these agents synergistically inhibits the proliferation of RCC cells that harbour wild type p53 but does not have this synergistic effect on RCC cells that harbour mutant p53 (Section 3.2.1). Further, using ACHN cells with down-regulated p53, we have shown that this inhibition of proliferation is indeed a p53-dependent effect (Section 3.2.2). To ensure that the inhibition of proliferation observed was taking place via a conserved cell death pathway and not simply non-specific cell death, we determined the nature of this inhibition of proliferation. Using live cell phase contrast microscopy and AV/PI staining, it has been demonstrated that this combination of drugs was promoting cell death via apoptosis (Section 3.2.3). Interestingly, the behaviour of 117 cells, RCC cells that have very low levels of wild type p53, is very similar to that observed in the p53 mutant RCC cell lines, suggesting a relatively higher level of wild type p53 is required for this combination to be effective. Taking this into account, and the fact that data presented herein (Section 3.2.2) suggest that the effectiveness of this combination treatment in inducing apoptosis in RCC cells is p53-depenent, the pharmacological restoration of p53-mediated apoptosis in a biomarker-specific subset of RCC cell lines has been demonstrated in this chapter. We have further demonstrated that it is inhibition of the MDM2-p53 interaction in combination with ABT-737 is synergistic in RCC cells that harbour wild type p53 rather than inhibition of the ubiquitin ligase activity of MDM2. This observation raises an

interesting point regarding the nature of MDM2-mediated regulation of p53 in RCC cells as whether binding of MDM2 is of greater relevance to regulation of p53 than ubiquitination followed by degradation. Or it may be the case that p53-independent effects of HLI373 mask a synergistic interaction between both HLI373 and ABT-737. In the following chapter, data are presented that further explore the mechanism underlying the induction of apoptosis in response to the combination of Nutlin-3 and ABT-737.

Chapter 4: A study into the mechanism underlying the p53-dependent apoptosis observed in response to the combination of Nutlin-3 and ABT-737 in renal carcinoma cells harbouring wild type p53

4.1 Introduction

In Chapter 3, it was demonstrated that RCC cells harbouring wild type p53 underwent apoptosis in response to the combination of Nutlin-3 and ABT-737. It was apparent that ABT-737 alone was promoting apoptosis in these cells and that the addition of Nutlin-3 to ABT-737 enhanced this pro-apoptotic effect (section 3.2.3). Nutlin-3 alone did not promote a detectable increase in apoptosis. In this chapter, understanding the mechanism of action of the apoptosis observed in response to the combination treatment was the focus.

ABT-737 has been described as being primarily a mimetic of the BH3-only protein Bad (Certo et al., 2006) based on the differential binding affinity of ABT-737 for the different members of the anti-apoptotic Bcl-2 family of proteins. ABT-737 is thought to promote apoptosis by displacing 'activator' BH3-only proteins such as tBid and Bim from anti-apoptotic members of the Bcl-2 family members, resulting in activation of Bak or Bax which activates the signalling cascade leading to apoptosis (Van Delft et al., 2006; Certo et al., 2006; Ren et al., 2010; Garrison et al., 2012).

As discussed in Section 1.2.7.5 of the Introduction, one of the determinants of resistance to ABT-737 is the relative expression levels of the different members of the anti-apoptotic Bcl-2 family members. ABT-737 has a high affinity for Bcl-2, Bcl-xL and Bcl-w but has a low affinity for Mcl-1 and Bfl-1. Indeed, over-expression of Mcl-1 in a variety of models has been demonstrated to confer resistance to ABT-

737-mediated apoptosis (van Delft et al., 2006). A further refinement to this model suggests that sensitivity to ABT-737 is primarily determined by levels of Bcl-2, rather than Bcl-xL or Bcl-w (Rooswinkel et al., 2012), despite there being a high binding affinity of ABT-737 for both Bcl-xL and Bcl-w. Thus, we sought to determine whether the protein levels of Bcl-2 family member could be implicated in resistance or sensitivity to ABT-737.

4.2.1 Relative protein levels of Bcl-2 family members in RCC cells

To determine whether protein levels of Bcl-2 family members might mediate resistance to the combination of Nutlin-3 and ABT-737, western blot analyses on cell lysates from the panel of cell lines used in the drug combination studies was performed. We sought to observe whether there was a correlation between steady-state protein levels of members of the Bcl-2 family members and resistance or sensitivity to ABT-737. Also included in this analysis, for comparison were H1299 non-small cell lung cancer cells and HL-60 promyelocytic leukaemia cells. H1299 cells have been documented to be relatively resistant to ABT-737 (IC_{50} > 50μM) and express relatively high levels of Mcl-1 and relatively low levels Bcl-2 (Wesarg et al., 2007). HL-60 have been documented to be relatively sensitive to ABT-737 (IC_{50} of 190nM) and as having relatively low levels of Mcl-1 (Chen et al., 2007). Sub-confluent cells from each cell line were harvested and subsequently lysed and analysed by western blot as described in Section 2.4. The western blots are shown in figure 4.2.1.1. Table 4.2.1.1 summarizes the relative levels of protein of Bcl-2, Bcl-xL, Bcl-w and Mcl-1 in these cell lines. There was no obvious correlation between levels of the different Bcl-2 family members and sensitivity to ABT-737 (Table

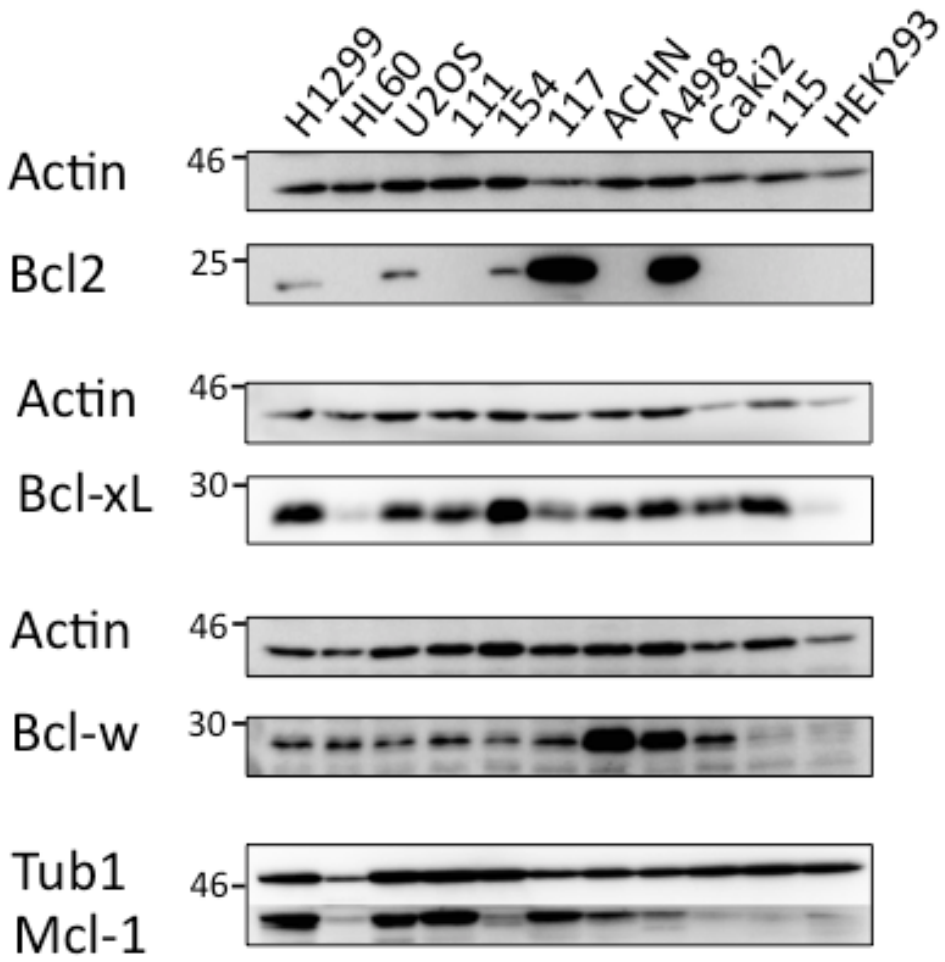

Figure 4.2.1.1 Analysis of relative levels of Bcl-2 family proteins. Subconfluent cells from each cell line were harvested and lysed as described in section 2.4.2. 20 µg of protein was analysed in each lane and antibodies used for detection are described in table 2.1. The migration of protein standards of the indicated approximate molecular weights are shown in kDa.

Table 4.2.1.1 Summary of relative protein level of Bcl-2 family members in renal cell lines used in this study. WT – wild type, MT – mutant, N/D – not detected. N/A – data not available. Protein level refers to relative level of protein shown in western blot from figure 4.2.1.1.

Cell line	p53 Status	Bcl-2 level	Bcl-xL level	Bcl-w level	Mcl-1 level	ABT-737 IC_{50} (μM)	ABT-737 IC_{70} (μM)
ACHN	WT	N/D	High	High	Intermediate	10	18
A498	WT	High	High	High	Low	14	23
115	WT	N/D	High	Low	Low	17	28
Caki2	WT	N/D	Intermediate	Low	Low	1.3	2.2
117	WT	High	Intermediate	Low	High	10	22
111	MT	N/D	High	Low	High	18	23
154	MT	Low	High	N/D	Intermediate	20	28
HEK293	WT	N/D	Low	N/D	Low	N/A	N/A

4.2.1.1). Bcl-2 protein level was low or undetectable in all cell lines tested with the exceptions of 117 and A498 cell lines, where the protein was present at relatively high levels in comparison to the other cell lines analysed. Both 117 and A498 cell lines exhibited similar sensitivities to ABT-737. Indeed, there was only a two-fold difference in the sensitivity to ABT-737 across the RCC cell lines tested, with the exception of Caki2 cells and yet the relative levels of Bcl-2 protein are very varied. Bcl-xL was expressed at a relatively high or intermediate level in all of the renal cells tested with the exception of HEK293 cells, where it was almost undetectable. Expression of protein was categorised into three groups – relatively high, intermediate and relatively low. Intermediate was a level of protein lower than the proteins that were expressed the highest but present at a level greater than proteins that were present at a relatively low level. Bcl-w protein was present at high levels only in ACHN and A498 cell lines, the remaining cell lines having either low or undetectable levels of Bcl-w. Mcl-1 protein was present at a relatively high level in 111 and 117 cell lines, but this was not associated with increased resistance in these lines when compared to lines with lower levels of Mcl-1 expression as shown in table 4.2.1.1.

Interestingly, the Caki2 cell line, which was the most sensitive cell line to ABT-737 of the cell lines tested (IC_{50} and IC_{70} of 1.3 and 2.2μM respectively) expressed relatively low levels of Mcl-1, Bcl-2 and Bcl-w protein and an intermediate level of Bcl-xL protein. The low levels of Mcl-1 and other Bcl-2 family members in this cell line may be consistent with increased sensitivity to ABT-737 however, cell line 115 which displayed a similar expression pattern to Caki2, exhibited a roughly ten-fold increased resistance to ABT-737 and therefore other factors clearly influence the

sensitivity of Caki2 cells to ABT-737. One simple explanation might be that Caki2 cells may have relatively higher basal levels of pro-apoptotic proteins than 115 cells.

Correlation between ABT-737 sensitivity and increased level of Bcl-2 protein, or resistance to ABT-737 and increased level of Mcl-1 in panels of small cell and non-small cell lung cancer cell lines have been observed in previous studies (Wesarg et al., 2007; Tahir et al., 2007). The cell lines used in the aforementioned studies displayed an approximately binary pattern of expression for Bcl-2 and Mcl-1 and their corresponding sensitivity to ABT-737 reflected this. To elaborate further on this statement, cell lines used in these studies possessed either relatively high levels of Bcl-2 and relatively low levels of Mcl-1 or relatively low levels of Bcl-2 and relatively high levels of Mcl-1. As expected, cell lines that expressed relatively higher levels of Mcl-1 were more resistant to the pro-apoptotic effects of ABT-737 than the cell lines that expressed relatively lower levels of Mcl-1.

The cell lines used in our study did not display such an obviously binary pattern of expression for Bcl-2 and Mcl-1; indeed, Bcl-2 was only expressed at relatively high levels in the 117 and A498 cells. The relatively high expression of Mcl-1 the 117 cell line may have been responsible for the observed resistance to ABT-737 in the presence of high levels of Bcl-2. To summarise, the RCC cell lines tested in this study harbour a varied pattern of levels of anti-apoptotic Bcl family members. These different levels of protein of Bcl-2 family members do not correlate in an obvious manner with sensitivity to ABT-737.

4.2.2 The combination of Nutlin-3 and ABT-737 enhances apoptotic signalling in RCC cell lines harbouring wild type p53

In section 4.2.1, the levels of different members of the anti-apoptotic Bcl-2 family members in the cell lines used in this study were analysed to attempt to discern a relationship between the levels of these proteins and sensitivity or resistance to ABT-737. Since no correlation was observed between the levels of the members of this family of anti-apoptotic proteins with resistance to ABT-737, a different approach as attempted. We sought to directly address what was taking place in response to the combination treatment by attempting to elucidate downstream events taking place in response to single agents and also the combination treatment.

Previous studies using renal cell carcinoma cell lines harbouring wild type p53 showed that in response to Nutlin-3 treatment, up-regulation of Bax does not take place, nor does apoptosis (Tsao and Corn, 2010; Polanski et al., submitted) but p53 is stabilized and this leads to increased transcription of p21, which results in cell cycle arrest or senescence. This phenotype has also been observed in cells from a variety of tumour backgrounds (Tovar et al., 2006). Nutlin-3 treatment in other cell line models can result in apoptosis and this can be accompanied by up-regulation of Bax and other pro-apoptotic proteins (Kojima et al., 2005; Van Maerken et al., 2006). Because p53 is a transcription factor that can promote the transcription of a number of pro-apoptotic genes, such as PUMA and NOXA, we hypothesised that p53 rescued from the MDM2 mediated degradation by Nutlin-3 treatment could promote the transcription of pro-apoptotic genes other than Bax. We hypothesized that the combined effect of inhibition of Bcl-2 family members by ABT-737 and the potential increase in the transcription of pro-apoptotic genes as a result of Nutlin-3-

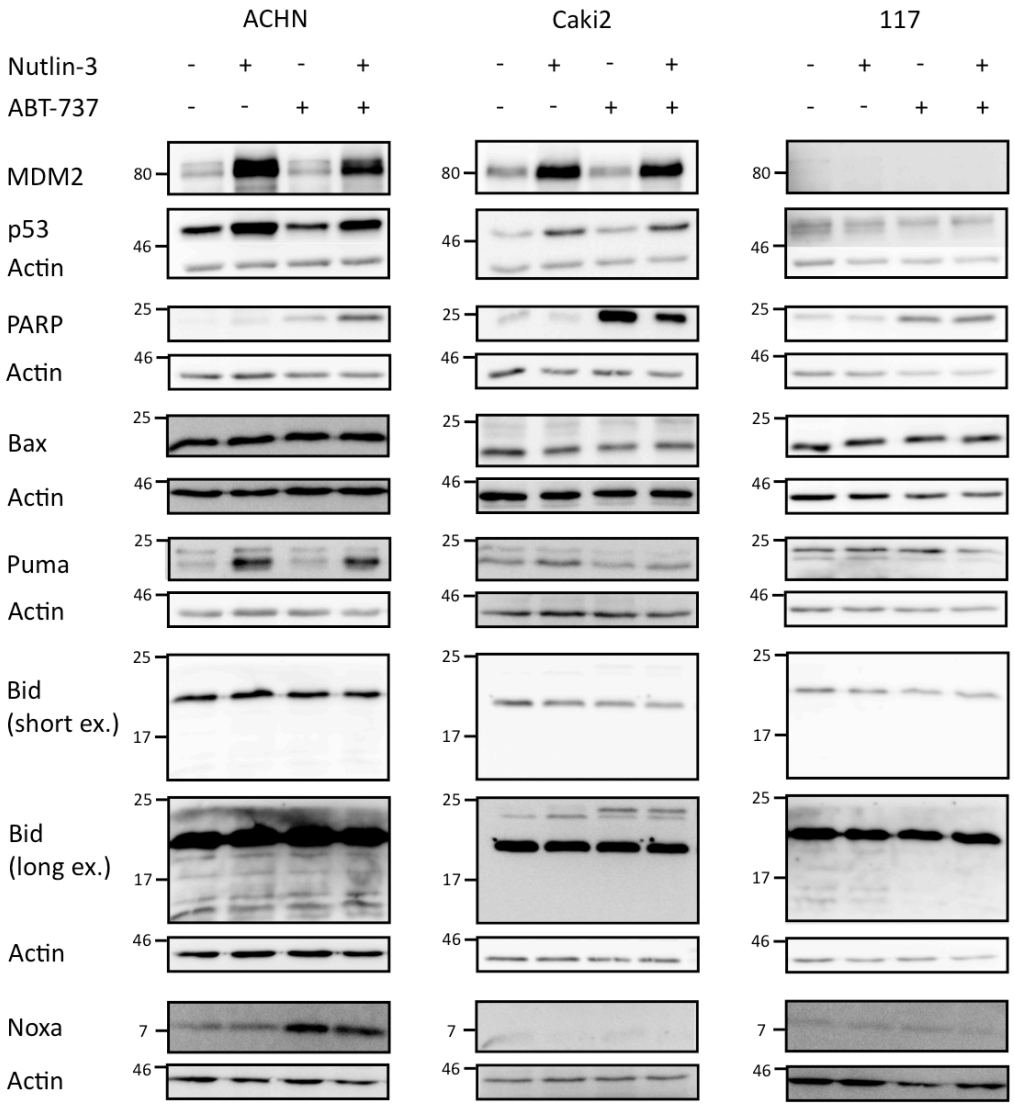

Figure 4.2.2.1 Steady state level of p53, MDM2 and proteins associated with apoptosis in wild type p53-harbouring ACHN, Caki2 and 117 cell lines. Cells were treated for 36 h with 3μM Nutlin-3, 10μM ABT-737 or a combination of both treatments. Caki2 cells were treated with only 1μM ABT-737 because of their increased sensitivity to this compound. Cells were harvested and lysates were prepared as described in section 2.4. 20 μg of protein was analysed in each lane and antibodies used for detection are described in table 2.1. The migration of protein standards of the indicated approximate molecular weights are shown in kDa.

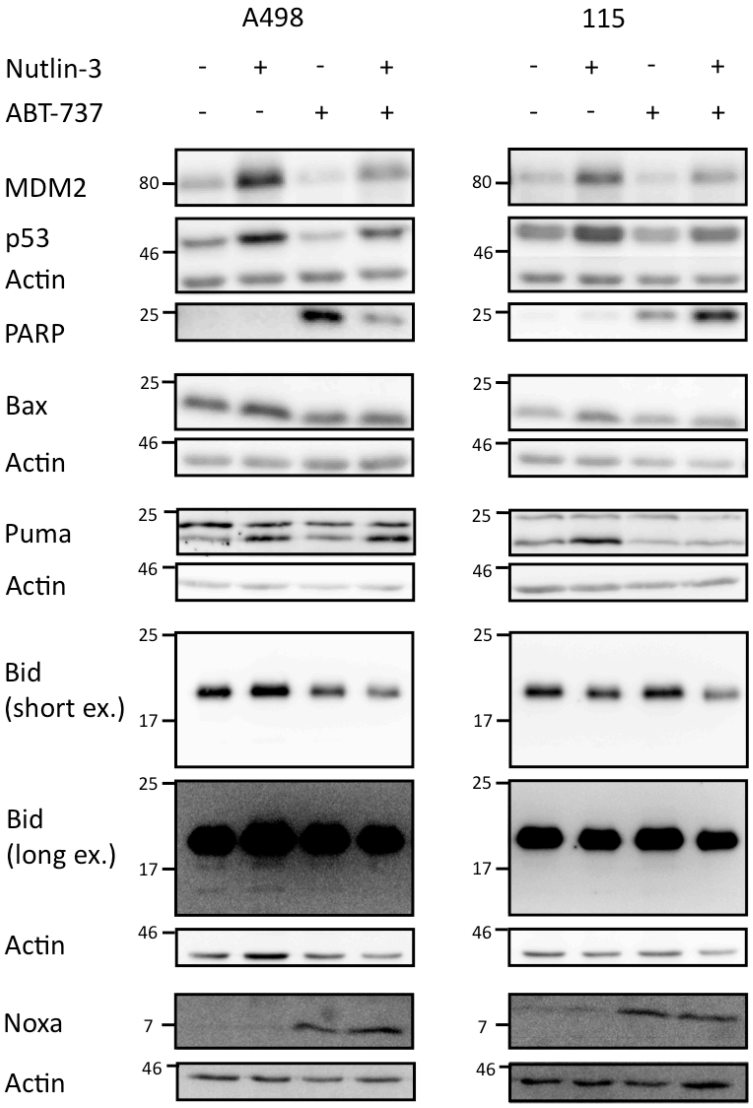

Figure 4.2.2.2 Steady state level of p53, MDM2 and proteins associated with apoptosis in wild type p53-harbouring A498 and 115 cell lines. Cells were treated for 36 h with 3μM Nutlin-3, 10μM ABT-737 or a combination of both treatments. Cells were harvested and lysates were prepared as described in section 2.4. 20 μg of protein was analysed in each lane and antibodies used for detection are described in table 2.1. The migration of protein standards of the indicated approximate molecular weights are shown in kDa.

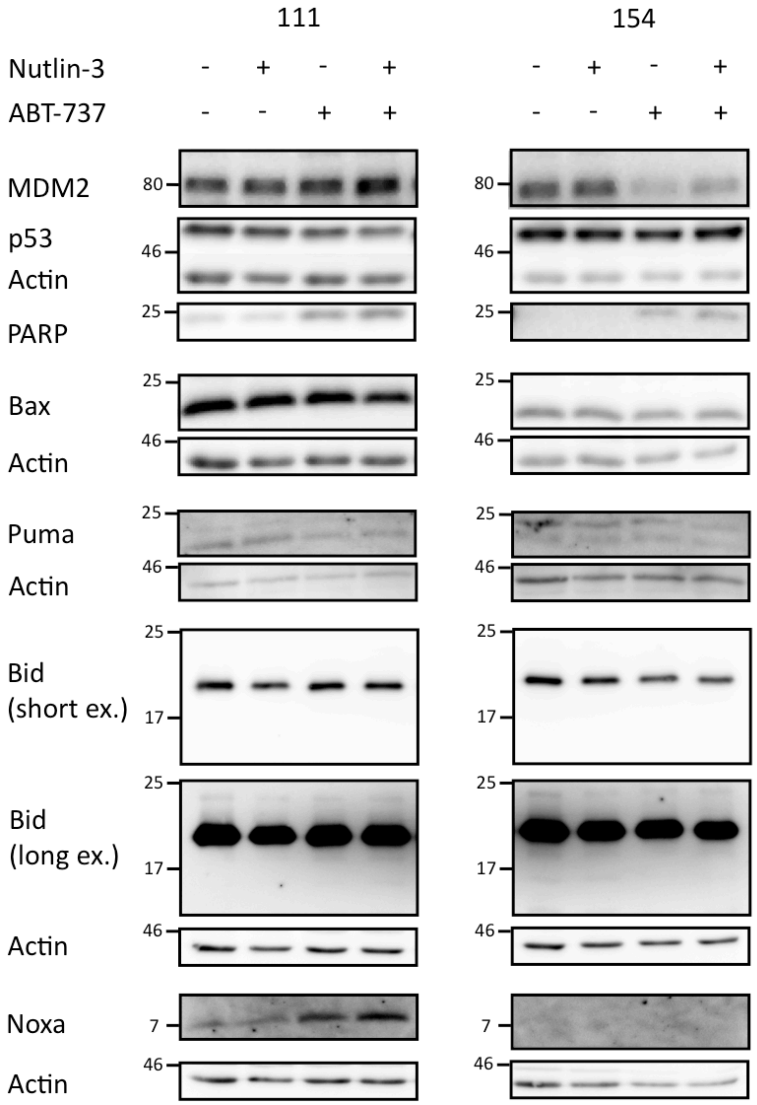

Figure 4.2.2.3 Steady state level of p53, MDM2 and proteins associated with apoptosis in mutant p53-harbouring 111 and 154 cell lines. Cells were treated for 36 h with 3μM Nutlin-3, 10μM ABT-737 or a combination of both treatments. Cells were harvested and lysates were prepared as described in section 2.4. 20 μg of protein was analysed in each lane and antibodies used for detection are described in table 2.1. The migration of protein standards of the indicated approximate molecular weights are shown in kDa.

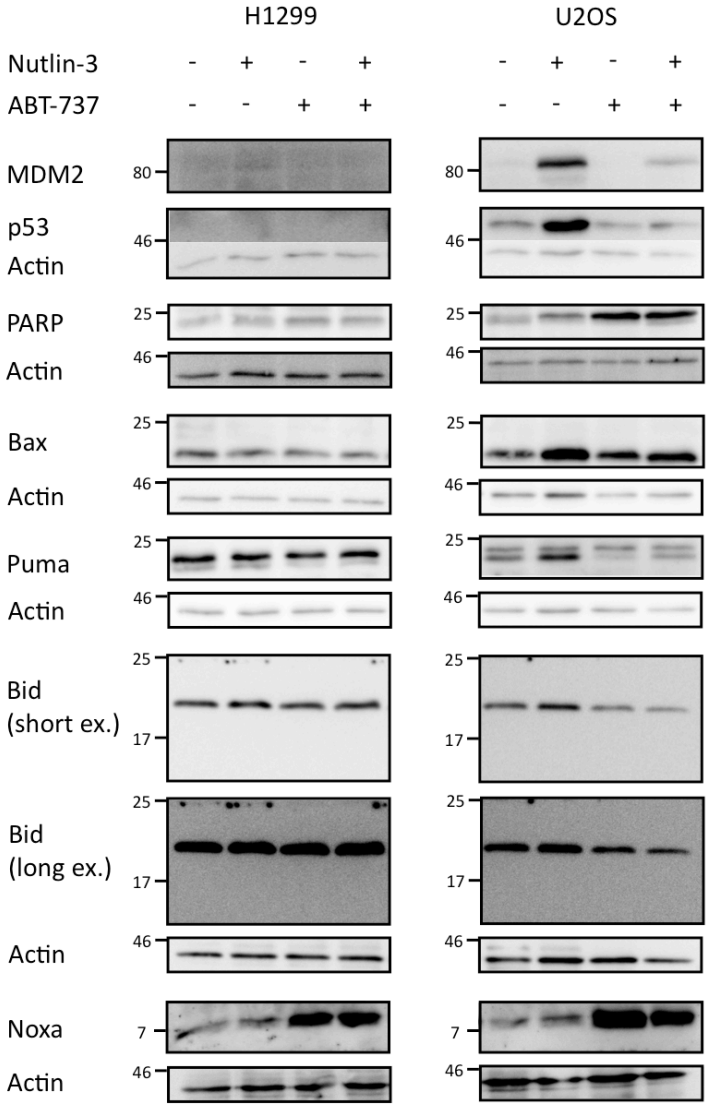

Figure 4.2.2.4 Steady state level of p53, MDM2 and proteins associated with apoptosis in H1299 and U2OS cell lines. p53-null H1299 and p53 wild type U2OS cells were treated for 36 h with 3μM Nutlin-3, 10μM ABT-737 or a combination of both treatments. Cells were harvested and lysates were prepared as described in section 2.4. 20μg of protein was analysed in each lane and antibodies used for detection are described in table 2.1. The migration of protein standards of the indicated approximate molecular weights are shown in kDa.

mediated rescue of p53 may be responsible for the increase in apoptosis observed when comparing the effect of Nutlin-3 and ABT-737 combination treatment with ABT-737 treatment alone.

As a preliminary approach to determine which pro-apoptotic proteins were involved in the apoptotic response to the combination of Nutlin-3 and ABT-737, western blot analysis of lysates from cells that were treated with single agents or a combination was performed. RCC cells were treated with drug vehicle, 3μM Nutlin-3, 10μM ABT-737 or a combination of both agents for 36h. Caki2 cells were treated with only 1μM ABT-737 because these cells were found to be approximately ten times more sensitive to ABT-737 than the other cell lines tested (see section 3.2.1). The cells were subsequently harvested, lysed and subjected to western blot analysis as described in section 2.4. p53 levels were monitored to determine whether the treatments rescued p53 from negative regulation by MDM2. Since MDM2 is regulated at the transcriptional level by p53 in RCC cells that harbour wild type p53 (Warburton et al., 2005), we also monitored MDM2 protein levels as a surrogate indicator of p53 transcriptional activity. Cleavage of PARP is a hallmark of apoptosis (Duriez and Shah, 1997), hence levels of cleaved PARP were monitored to indirectly monitor the occurrence of apoptosis. Levels of Bax, Puma and Noxa were monitored as these proteins are known transcriptional targets of p53 that are involved in mediating an apoptotic response (Miyashita et al., 1995; Nakano and Vousden et al., 2001; Oda et al., 2000).

In addition to RCC cells, p53-null H1299 non-small cell lung cancer cells and U2OS osteosarcoma cells were analysed for comparison to RCC cells to determine the

effects of the combination treatment in p53 null cells and cells harbouring wild type p53 respectively from a non-renal background.

Nutlin-3 treatment alone resulted in an increase in p53 protein levels and a concomitant increase in MDM2 in the ACHN, Caki2, A498 and 115 cell lines (figures 4.2.2.1 and 4.2.2.2) as would be expected in cell lines that harbour wild type p53. The 117 RCC cell line that also harbours wild type p53 showed no apparent rise in p53 level (figure 4.2.2.1). There was also no detectable change in the p53 protein level in either mutant p53 RCC cell line 111 or 154 in response to Nutlin-3 treatment. MDM2 protein levels remained the same in Nutlin-3-treated 111 and 154 cells as would be expected of cell lines harbouring mutant p53 (figure 4.2.2.3). As expected, the p53-null H1299 cell line displayed no discernable phenotype in terms of p53 or MDM2 protein level as a result of treatment with Nutlin-3, consistent with the absence of the p53 gene in these cells (figure 4.2.2.4). p53 was up-regulated in U2OS cells treated with Nutlin-3 (figure 4.2.2.4), with an increase in MDM2 protein in a manner similar to that observed in the RCC cells harbouring high levels of wild type p53. All of these observations are consistent with previous studies that have shown rescue of p53 from the inhibitory effects of MDM2 promote stabilization of p53 and resultant up-regulation of MDM2 in cells that possess wild type p53 (Vassilev et al., 2004; Tovar et al., 2006).

An increase in MDM2 and p53 protein levels was observed in ACHN, Caki2, A498 and 115 cell lines in response to the combination of Nutlin-3 and ABT-737 when compared to drug-vehicle treated cells (figures 4.2.2.1 and 4.2.2.2); with the exception of Caki2 cells (figure 4.2.2.1), this increased level of both proteins was

less than the increase observed in response to Nutlin-3 treatment alone. This maybe an intermediate phenotype between the up-regulation of p53 in response to Nutlin-3 alone and the decrease in p53 in response to ABT-737 alone. The significance of this remains to be elucidated. There was a decrease in the level of p53 in 117 cells in response to the combination of Nutlin-3 and ABT-737 in comparison to drug-vehicle treated cells (figure 4.2.2.1). In combination-treated U2OS cells, there was an increase in MDM2 protein when compared to cells treated with drug-vehicle but this increase was not as great as that observed in response to Nutlin-3 treatment alone (figure 4.2.2.4). There appeared to be no detectable increase in p53 protein in the U2OS cells in response to the combination treatment when compared to drug-vehicle treated cells. No change in p53 protein level was observed in the 111 and 154 cells lines in response to the combination treatment when compared to cells treated with drug-vehicle, which is expected when taking into account the presence of mutant p53 in these cells (figure 4.2.2.3).

Consistent with data presented in section 3.2.3, cleavage of PARP, an event associated with apoptosis, takes place in response to treatment with either ABT-737 alone or the combination of Nutlin-3 and ABT-737 in most of the cell lines tested. In both ACHN and 115 cell lines, there was greater PARP cleavage observed in response to the combination treatment relative to treatment with ABT-737 alone (figures 4.2.2.1 and 4.2.2.2) and this was consistent with observation made in figure 3.2.3.9, whereby ABT-737 alone promoted some apoptosis, but this apoptosis was enhanced by the addition of Nutlin-3. PARP was cleaved in Caki2 and A498 cells in response to ABT-737 alone and the combination treatment however, there appeared

to be increased PARP cleavage in the ABT-737-treated cells when compared to the combination treated cells (figures 4.2.2.1 and 4.2.2.2). Thus, it appeared there was a disconnect between PARP cleavage and apoptosis, since both of these cell lines responded to the combination treatment with increased apoptosis (figure 3.2.3.8). Consistent with observations made in the previous section, the RCC cells harbouring mutant p53 showed no increase in cleaved PARP levels in response to the combination treatment over that observed in response to ABT-737 alone (figure 4.2.2.3). These data show that this combination promotes PARP cleavage in the RCC cells tested, consistent with data presented in section 3.2.3 although PARP cleavage in Caki2 and A498 cells in response to the combination treatment was inconsistent with data presented in section 3.2.3.

As mentioned previously, treatment of RCC cells that harbour wild type p53 with Nutlin-3 results in neither apoptosis (Polanski et al., submitted; Tsao and Corn, 2010) nor in up-regulation of Bax. There was no observable increase in Bax protein level in response to Nutlin-3 in any of the RCC cell lines tested nor in H1299 cells (figures 4.2.2.1, 4.2.2.2, 4.2.2.3 and 4.2.2.4). In contrast, there was an increase in Bax protein level in response to Nutlin-3 in the U2OS cell line (figure 4.2.2.4). Treatment with ABT-737 alone appeared to have no effect on Bax protein levels in any of the cell lines tested. Bax protein levels were similarly unchanged in the panel of RCC cell lines tested in response to the combination of Nutlin-3 and ABT-737. Hence, apoptosis in response to the combination of Nutlin-3 and ABT-737 in RCC cells harbouring wild type p53 is independent of Bax-upregulation must require and alternative mechanism to Bax-up-regulation to commit these cells to apoptosis.

Puma exists as four different isoforms and only two isoforms (α and ß) possess the conserved BH3-only domain that allows the protein to contribute to apoptosis (Nakano and Vousden, 2003). The antibody used in this study allowed the detection of a slower migrating form of Puma, which may have been Puma α and a faster migrating form, which may have been Puma ß. Puma α levels remained unchanged in all of the cell lines tested, under all of the experimental conditions (figures 4.2.2.1, 4.2.2.2, 4.2.2.3 and 4.2.2.4). Puma ß protein, on the other hand, was up-regulated at the protein level in ACHN, Caki2, A498 115 and U2OS in response to Nutlin-3 treatment alone when compared to cells treated with drug-vehicle (figures 4.2.2.1, 4.2.2.2 and 4.2.2.4). In contrast, there was no change in the levels of Puma ß in 117, H1299, 111 and 154 cells in response to Nutlin-3 (figures 4.2.2.1, 4.2.2.3 and 4.2.2.4). Treatment with ABT-737 had no effect on Puma protein levels in any of the cell lines tested when compared to cells treated with drug vehicle, with the exception of U2OS cells, where there was a decrease in Puma in response to the ABT-737 treatment (figure 4.2.2.4). The combination of Nutlin-3 and ABT-737 increased the level of Puma protein in ACHN and A498 cells relative to their respective drug-vehicle treated cells (figures 4.2.2.1 and 4.2.2.2). The combination treatment decreased the level of Puma protein in U2OS cells when compared to drug-vehicle treated cells (figure 4.2.2.4). Level of Puma protein were unaffected by the combination treatment in the 117, 115, 111, 154 and H1299 cell lines when compared to their respective drug-vehicle treated cells (figures 4.2.2.1, 4.2.2.2, 4.2.2.3 and 4.2.2.4). Because of the well documented role of Puma promoting apoptosis through the intrinsic apoptosis pathway (see Section 1.2.7.2), up-regulation of Puma ß in response to Nutlin-3 and in the combination of Nutlin-3 and ABT-737 suggests a possible role for Puma in the apoptosis observed in response to the

combination of these agents. The observation that Puma protein level was decreased in response to the combination treatment relative to Nutlin-3 alone in some of the wild type p53 RCC cell lines does not necessarily preclude the ability Puma to promote apoptosis in these cells. The time point chosen for these experiments was 36h because this was previously shown to be the duration at which synergistic induction of apoptosis in response to the combination was observed (see Section 3.2.3). It is plausible that Puma may have been degraded in the combination-treated cells after a certain time point and to address this question, the same experiment would need to be repeated but at earlier time points to observe fluctuations in Puma levels.

Bid is a p53-inducible protein that, upon cleavage to tBid, is effective in promoting apoptosis via the intrinsic pathway (Wang et al., 1996; Sax et al., 2001). Levels of Bid protein were largely unaffected by Nutlin-3, ABT-737 or combination treatment in any of the cell lines tested. Included in the figures is a longer exposure of the Bid blot to detect the cleaved form of Bid, tBid. Cleavage of Bid into tBid was not observed in response to any of the treatments in any of the cell lines tested. There was a modest increase in Bid protein level in U2OS cells in response to Nutlin-3 alone (figure 4.2.4.4), however this increase was not observed in cells treated with ABT-737 alone or the combination treatment. There was a slight decrease in Bid protein level in A498 cells in response to ABT-737 and combination treatments when compared to the drug-vehicle treated cells (figure 4.2.2.2). This data suggests that it is unlikely that Bid plays any role in the response to the combination of Nutlin-3 and ABT-737, because of the absence of both up-regulation of Bid in

response to the combination treatment and subsequent Bid cleavage to its active form, tBid.

Noxa is a pro-apoptotic BH3-only domain family member that can be up-regulated by p53 in response to various signals (Oda et al., 2000). It was therefore surprising that up-regulation of Noxa was not observed in any of the cell lines tested in response to Nutlin-3 treatment, but rather Noxa protein levels increased in a number of cell lines in response to either ABT-737 treatment alone or in response to the combination treatment. ABT-737 treatment alone increased Noxa protein level relative to drug-vehicle treatment in ACHN, A498, 115, 111, H1299 and U2OS cells (figures 4.2.2.1, 4.2.2.2, 4.2.2.3 and 4.2.2.4). Noxa appeared to be undetectable in 154 cells and only just detectable in Caki2 cells (figures 4.2.2.1 and 4.2.2.3). The combination of Nutlin-3 with ABT-737 did not appear to alter the extent of the Noxa up-regulation that was observed in response to the ABT-737 treatment alone in ACHN, A498, 115, 111 and H1299 cells (figures 4.2.2.1, 4.2.2.2, 4.2.2.3 and 4.2.2.4). There was a modest decrease in the level of Noxa in U2OS cells in response to the combination treatment when compared to cells treated with the ABT-737 single treatment (figure 4.2.2.4). As mentioned in Section 1.2.7.5 of the Introduction, ABT-737 can induce up-regulation of Noxa independently of p53 (Bertin-Ciftci et al., 2013) and this is most likely what is taking place here in the cell lines that respond to ABT-737 or combination treatment with up-regulation of Noxa. Considering that Noxa up-regulation appeared to be p53-independent in the cell lines tested, and synergy between Nutlin-3 and ABT-737 is p53-dependent in RCC cells, it is unlikely that Noxa plays an important role in this synergistic induction of

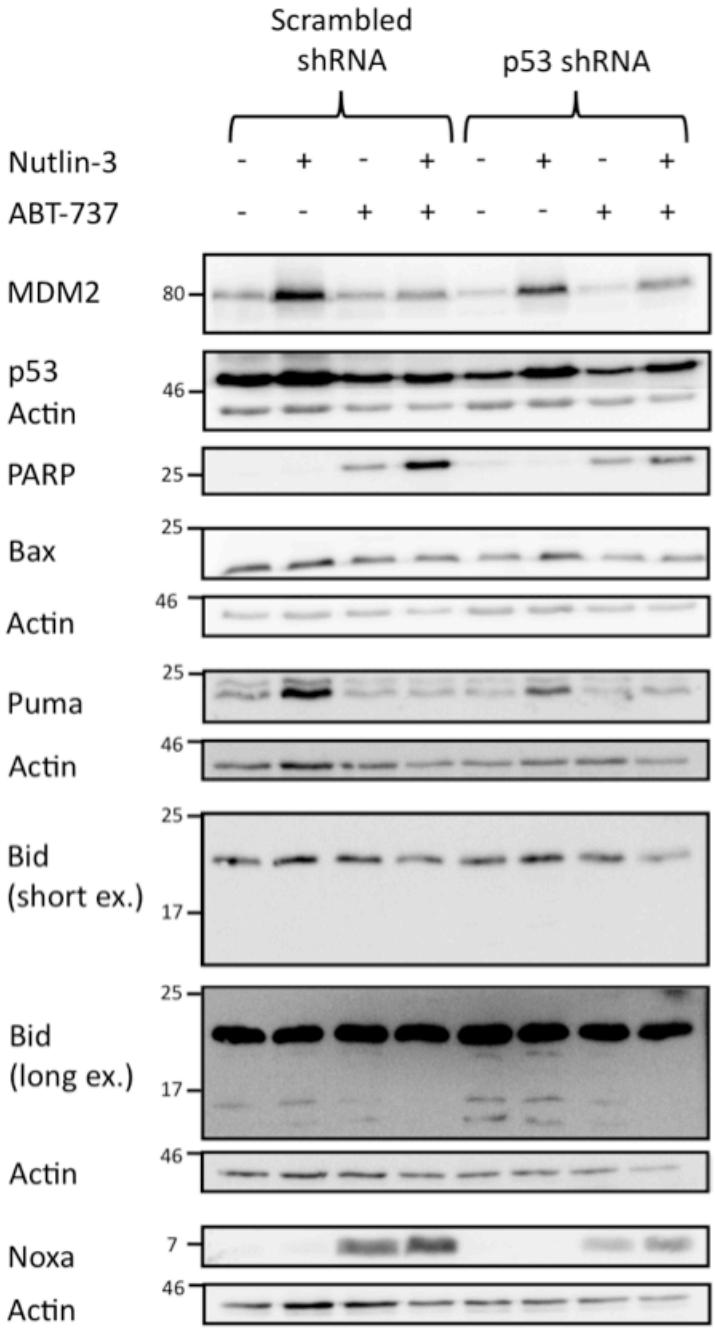

Figure 4.2.2.5 Steady state level of p53, MDM2 and proteins associated with apoptosis in scACHN and sh-p53ACHN cell lines. Cells were treated for 36 h with 3μM Nutlin-3, 10μM ABT-737 or a combination of both treatments. Cells were harvested and lysates were prepared as described in section 2.4. 20 μg of protein was analysed in each lane and antibodies used for detection are described in table 2.1. The migration of protein standards of the indicated approximate molecular weights are shown in kDa.

apoptosis although the possibility cannot be eliminated. Interestingly, up-regulation of Noxa was not detected in Caki2 cells, the most sensitive of the cell lines tested to ABT-737, in response to ABT-737 treatment. How therefore this cell line was so sensitive to ABT-737 remains unclear.

This experiment showed that p53 was important in enhancing apoptotic signalling in the RCC cells harbouring wild type p53 in response to the combination of Nutlin-3 and ABT-737, for example, up-regulation of Puma was only observed in some of the cell lines harbouring wild type p53 but not in the p53 mutant cell lines. To determine the extent to which p53 was involved in promoting this response, we performed the same experiment described above, but with sc-ACHN cells and sh-p53ACHN cells, described in Section 3.2.2 (figure 4.2.2.5). Up-regulation of p53 and MDM2 in response to Nutlin-3 treatment in the scrambled control ACHN cell line appeared to be more modest in comparison to the parental ACHN cell line. The scrambled control ACHN cells did not show increased p53 and MDM2 protein levels in response to the combination treatment relative to drug vehicle, which was another different response when compared to the parental ACHN cells. As expected, down-regulation of p53 by short hairpin RNA resulted in a less up-regulation of p53 and MDM2 protein in response to Nutlin-3 and the combination treatment, when compared to the scrambled control cells. Consistent with the data presented in section 3.2.2, that the apoptotic response of RCC cells harbouring wild type p53 in response to the combination of Nutlin-3 and ABT-737 is p53-dependent, down regulation of p53 by shRNA resulted in reduced PARP cleavage when compared to the scrambled control cells.

In all of the RCC cell lines harbouring wild type p53, there was no increase in Bax protein level in response to treatment with single agents or the combination. It therefore followed that down-regulation of p53 with shRNA would have little effect on Bax levels in response to treatment with either Nutlin-3 or the combination treatment. There was no detectable difference in the level of Bax protein in the ACHN cell line expressing the short hairpin to p53 in response to any of the treatments when compared to the equivalent cell line harbouring scrambled shRNA (figure 4.2.2.5). Similar to the parental ACHN cell line, the clone of the ACHN cell line expressing scrambled shRNA showed increased Puma levels in response to treatment with Nutlin-3. Unlike the parental cell line however, Puma protein level did not increase in response to the combination of Nutlin-3 and ABT-737. Up-regulation of Puma in response to either Nutlin-3 or the combination of Nutlin-3 and ABT-737 was only observed in cell lines that harboured wild type p53, with the exception of the 117 cell line, that had extremely low levels of wild type p53. Because of the responsiveness of Puma to wild type p53 in these RCC cells, it is not surprising that basal levels of Puma, would be lower in the cells that had reduced expression of wild type p53. This was indeed observed in the sh-p53ACHN cells when compared to scACHN cells (figure 4.2.2.5); there was a lower basal level of Puma in the cells that had reduced levels of p53. By extension of this, it followed that there would be a reduced up-regulation of Puma in the ACHN cell line that had down-regulated p53 expression as a result of shRNA to p53 in response to Nutlin-3. Indeed, in response to Nutlin-3, Puma was up-regulated in the ACHN cells harbouring shRNA to p53, however the degree to which Puma was up-regulated was less than that observed in the cells that had scrambled control shRNA. Therefore, Puma up-regulation in response to Nutlin-3 is p53-dependent, as expected.

Similar to Bax protein levels in the RCC cells harbouring wild type p53, there were no fluctuations in Bid protein level in response to either Nutlin-3 or the combination of Nutlin-3 and ABT-737. The level of Bid protein, and the cleaved form of this protein, tBid, was unaltered ACHN cells harbouring scrambled control shRNA in response to single agents and the combination treatment. Down-regulation of p53 with shRNA did not have any affect on the Bid or tBid protein levels in response to single agents or the combination treatment (figure 4.2.2.5). Therefore, it may be implied that transcription of neither Bid, nor Bax can be promoted by p53 in RCC cells harbouring wild type p53 and that basal transcription of genes coding for both of these proteins is regulated by another mechanism.

An increase in Noxa protein level was observed in H1299, U2OS, A498, 115, 111 and ACHN cells in response to ABT-737. A p53-independent mechanism for the induction of Noxa in response to ABT-737 is discussed in the section 1.2.7.5, hence it is unsurprising that Noxa levels increased in cell lines with wild type or mutant p53 status or indeed p53-null cells. The existence of a p53-independent pathway for the induction of Noxa did not preclude the possibility of p53 contributing towards the increased level of Noxa protein in the RCC cells harbouring wild type p53 in response to ABT-737 and the combination treatment. The absence of Noxa induction in any of the cell lines tested in response to Nutlin-3 treatment was a very interesting observation. Noxa has been observed to be induced by Nutlin-3 treatment in other cell lines that harbour wild type p53 (Tabe et al., 2009; Bhattacharya et al., 2011) hence it is likely that the absence of Nutlin-3-mediated Noxa induction is a phenomenon that is particular to RCC cells. Why Puma was induced in RCC cells in

response to Nutlin-3 treatment in RCC cells but Noxa not induced is a topic for further investigation. There was an increase in Noxa protein in response to ABT-737 and the combination of Nutlin-3 and ABT-737 in the ACHN cell line harbouring scrambled shRNA, as previously observed in the parental ACHN cell line (figure 4.2.2.5). There was also an increase in the level of Noxa protein in response to ABT-737 and the combination treatment in the ACHN cell line that harboured shRNA to p53, however this was to a lesser degree than that observed in the scrambled control cell line. This result suggested that the Noxa up-regulation in response to ABT-737 and the combination treatment in the RCC cells harbouring wild type p53 is at least partially dependent upon the presence of wild type p53. The observation that Noxa levels can be modulated by p53 in these cells suggests that Noxa induced by ABT-737 may contribute to the synergy observed between Nutlin-3 and ABT-737.

As expected, the combination of Nutlin-3 and ABT-737 promotes an up-regulation of pro-apoptotic proteins in the cell lines tested, particularly in the RCC cells harbouring wild type p53. In response to treatment with Nutlin-3 p53 was up-regulated in all of the cell lines harbouring wild type p53 with the exception of 117 cells. This is inconsistent with the observations of Polanski et al., wherein stabilization of p53 was observed in 117 cells in response to Nutlin-3 treatment. This inconsistency may be explained by the differences in experimental conditions used. Cells in our experiment were treated with 3μM Nutlin-3 for 36h whereas 117 cells in Polanski et al., were treated for 48h at a minimum concentration of 5μM Nutlin-3.

Up-regulation of Puma as a result of p53 stabilization may be important in the pro-apoptotic response to the combination treatment in the RCC cells harbouring wild

type p53 because of the established role of Puma in apoptosis. The absence of Puma up-regulation in RCC cell lines harbouring mutant p53 and the decreased level of Puma induction in the ACHN cells with down-regulated p53 would support this reasoning. The up-regulation of Noxa in response to the combination treatment observed in four p53 wild type cell lines, one of the mutant p53 cell lines and a p53 null cell line implies a more modest role for Noxa in the pro-apoptotic response to this combination treatment. The balance between Noxa and Mcl-1 protein levels are important in response to ABT-737 if apoptosis is to be achieved (Van Delft et al., 2006; Tromp et al., 2012). Intriguingly, Caki2 cells were the most sensitive to treatment with ABT-737 alone, of all of the cell lines tested in this study yet up-regulation of Noxa was not observed neither in response to ABT-737 nor combination treatment. This may be accounted for by the very low levels of Mcl-1 in Caki2 cells (section 4.2.1). The 115 cell line had an identical pattern of levels of Bcl-2 family member proteins, with the exception of higher Bcl-xL protein level than Caki2 yet was ten-fold more resistant to ABT-737 than the Caki2 cells. It is unlikely this difference in sensitivity between both Caki2 and 115 cell lines can be explained by differences in levels of Bcl-xL protein alone, because Bcl-xL is not the most important target for inhibition by ABT-737 (Rooswinkel et al., 2012). In the following section, the issue of Bax and Bak activation in response to the combination of Nutlin-3 and ABT-737 RCC cells is addressed.

4.2.3 The combination of Nutlin-3 and ABT-737 promotes Bax oligomerization at mitochondria

It was shown in section 3.2.1 that the combination of Nutlin-3 and ABT-737 synergistically inhibits the proliferation of RCC cells harbouring wild type p53. Furthermore, it was shown in sections 3.2.2 and 3.2.3 that this inhibition of proliferation was due to cell death in the form of apoptosis and that this cell death was p53-dependent. Data presented in section 4.2.2 showed that this combination of Nutlin-3 and ABT-737 did not result in an increase in level of pro-apoptotic Bax protein, an effector of apoptosis that is a transcriptional target of p53 (see in Section 1.2.8).

As discussed in the 1.2.7 and 1.2.7.4, an essential requirement for the intrinsic pathway of apoptosis to take place is the homo-multimerization of Bak, Bax, or both proteins at the mitochondrial outer membrane (MOM). Multimerization of Bak and/or Bax at the MOM results in formation of pores at the MOM, leading to an efflux of apoptogenic factors from the inter-mitochondrial space in a process termed mitochondrial outer membrane permeabilization (MOMP). Caspase activation results from this release of apoptogenic factors and cellular destruction ensues.

Bax and Bak activation are complex, multi-step processes involving allosteric interactions with other proteins and conformational changes that lead to an activated state; this results in oligomerization of Bax and/or Bak at the MOM. The absence of an increase in the level of Bax protein as a result of either Nutlin-3 or the combination of Nutlin-3 and ABT-737 does not preclude the possibility that Bax activation can occur without an increase in Bax protein level (Kojima et al., 2006;

Henry et al., 2012). Indeed, as shown in section 4.2.2, changes in the levels of Puma and Noxa are observed in response to treatment of RCC cells harbouring wild type p53 with the combination of Nutlin-3 and ABT-737. We therefore hypothesised that this increase in the levels of Puma and Noxa may be involved in the activation of Bax, Bak or both proteins to form oligomers at the MOM.

Individual Bak or Bax molecules possess non-reduced cysteine residues that are brought into close proximity with each other when Bak or Bax oligomerize. Homo-bifunctional cross-linkers, such as bismaleimidohexane (BMH) can be used to irreversibly bind individual Bak or Bax molecules within an oligomer to one another (figure 4.2.3.1) (Wei et al., 2000; reviewed in Renault et al., 2013). Using chemical cross-linking and isolation of mitochondria it can be demonstrated that Bax and/or Bak oligomers co-purify with mitochondria. Oligomerized Bak/Bax that has been can subsequently be detected on a SDS-PAGE gel, with slower migrating bands representing the oligomerized form of Bak/Bax.

To determine whether Bax, Bak or both proteins were forming oligomers at the MOM in response to treatment of RCC cell with the combination of Nutlin-3 and ABT-737, chemical cross-linking in combination with subcellular fractionation by differential centrifugation were used to identify oligomers of these proteins on SDS-PAGE gels.

A protocol to lyse cells, leaving most mitochondria intact, followed by differential centrifugation to enrich for mitochondria and finally, cross-linking of mitochondrial proteins, was optimized. The following is a description of the optimization of the

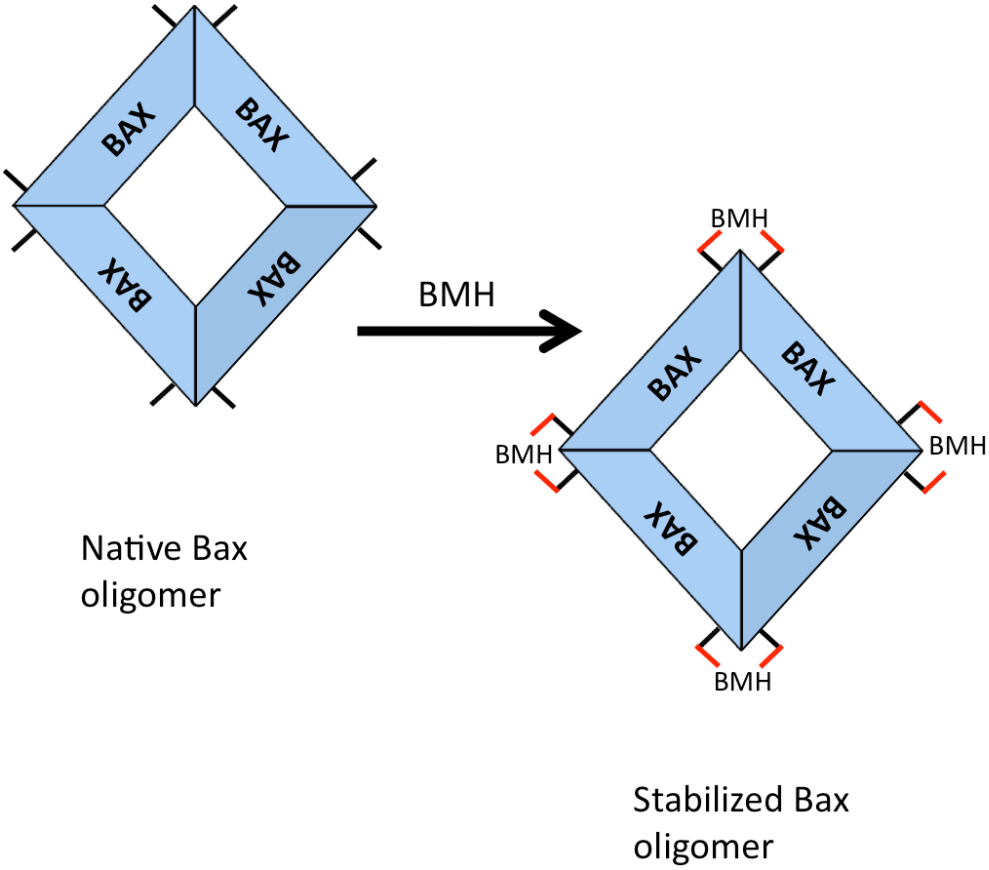

Figure 4.2.3.1 Schematic illustrating stabilization of Bax oligomer with BMH. Addition of BMH irreversibly stabilizes the oligomerized form of Bax or Bak (not shown). Each reactive groups of BMH forms a covalent bond with a sulphydryl-group from a different Bax molecule.

lysis stage of the protocol. Hypotonic shock followed by homogenization with a Potter-Elvehjem homogenizer was used to lyse cell membranes but leave organellar membranes unperturbed. Cells were harvested and washed twice in PBS then re-suspended in 1 X RSB buffer, a hypotonic, detergent-free buffer used for lysis of cell membrane (a detailed description of the composition of the buffer is presented in Section 2.5). Swelling of the cells was then monitored using a phase contrast microscope. Figure 4.2.3.2a shows cells suspended in isotonic PBS, which did not appear to cause swelling. Figure 4.2.3.2b shows cells suspended in RSB for 2 minutes, which resulted in some swelling. As time progressed, an increase in the cell swelling took place. Figure 4.2.3.2c shows cells suspended in RSB after 15 minutes. After 15 minutes, the cells were transferred to the homogenizer and homogenized initially with 30 strokes (figure 4.2.3.2d). This did not result in sufficient breakage of the cells, hence the cells were subjected to a further 30 strokes in the homogenizer (figure 4.2.3.2.e). Some intact cells were present after the accumulated 50 strokes, which are indicated by white triangles on figure 4.2.3.2e, and the cells were subjected to another 20 strokes (figure 4.2.3.2f). Figure 4.2.3.2f shows almost 100% cell breakage, with intact nuclei marked by white arrows. To protect membrane bound organelles in the homogenate from the low tonicity of the RSB buffer, 2 X MS buffer was added to raise the tonicity of the suspension. It was thus determined that 15 minutes of swelling in RSB followed by 70 strokes with the homogenizer were necessary to disrupt the cell membrane.

Following disruption of the cell membrane, the homogenate was centrifuged at 1,300 x g for 5 minutes to pellet nuclei, unbroken cells, large membrane fragments and other debris. The pellet from this centrifugation step was kept and designated the '1st

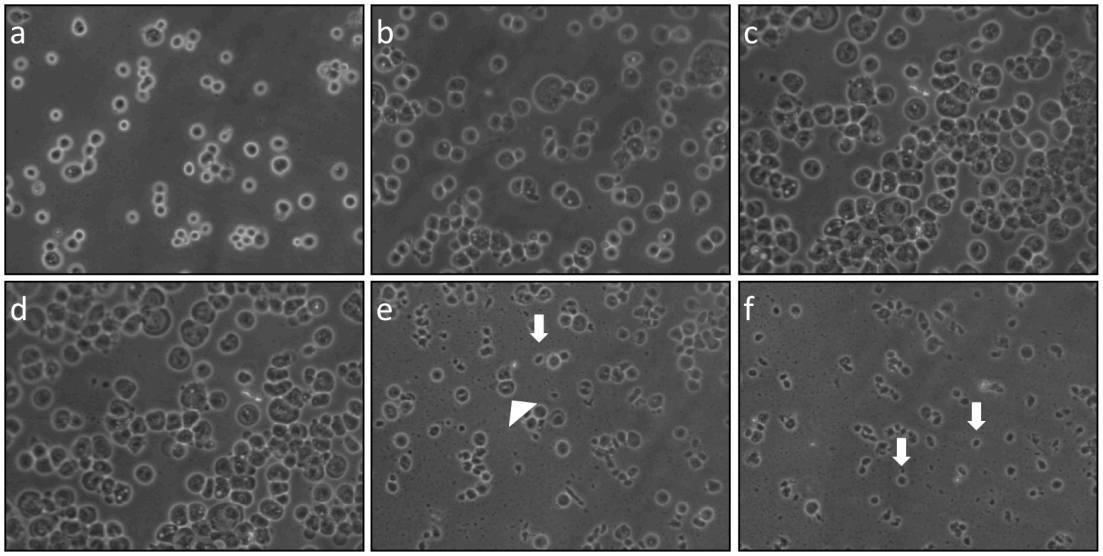

Figure 4.2.3.2 Optimization of homogenization of ACHN cells. ACHN cells were suspended in hypotonic RSB buffer and swelling was monitored using a phase contrast microscope as described in Sections 2.5 and 4.2.3. Panels a – f do not represent the same field of cells. White triangles indicate undisrupted cells. White arrows indicate intact nuclei of disrupted cells.
a - cells suspended in isotonic PBS.
b - cells after 2 minutes suspension in hypotonic RSB.
c - cells after 15 minutes suspension in RSB.
d - cells after 30 strokes in the Potter-Elvehjem homogenizer.
e - cells after 50 strokes in the Potter-Elvehjem homogenizer.
f - cells after 70 strokes in the Potter-Elvehjem homogenizer.

pellet'. The supernatant was transferred to a new tube and centrifuged again. This centrifugation step was repeated until no pellet could be observed at the end of the centrifugation. The supernatant was then centrifuged at 17,000 x g for 30 minutes to pellet mitochondria. The supernatant was kept as the cytosolic fraction.

For the first attempt of this experiment, the mitochondrial pellet was lysed in SLIP buffer and insoluble material cleared by centrifugation. This mitochondrial protein that remained in the SLIP buffer was quantified then treated with either 10mM BMH-DMSO or DMSO for 30 minutes. The cross-linking reaction was quenched by diluting 0.5M DTT to a 1:20 final concentration in the cross-linking reaction mixture. To monitor the quality of the fractionation procedure, the presence of different proteins as markers for the enrichment of different organellar fractions were observed on a western blot. Histone H3 was used as a marker for the nuclear protein, cytochrome C oxidase IV (COX4) was used as a marker for mitochondrial protein and Tubulin was used as a marker for cytosolic protein. Figure 4.2.3.3 shows an enrichment of mitochondria compared to whole cell lysate, suggesting that the differential centrifugation protocol was capable of isolating mitochondria from a crude homogenate of cells. There was an increase in the presence of histone H3 in the mitochondrial fractions from cells treated with ABT-737 and cells treated with the combination of both Nutlin-3 and ABT-737. There appeared to be a smaller band that was cross-reactive for a smaller Histone H3 fragment below the major band of Histone H3, in the all of the fractions from cells that were treated with the combination but not the other treatments. As described in Section 3.2.3, cells treated with ABT-737 or the combination of Nutlin-3 and ABT-737 more readily underwent

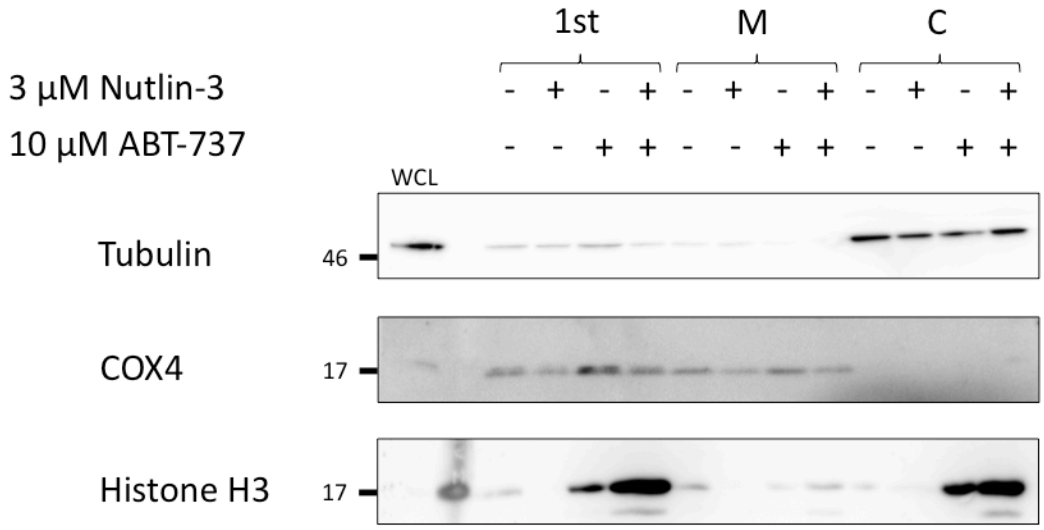

Figure 4.2.3.3 Subcellular fractionation of ACHN cells. Cells were homogenized and then fractionated as described in section 4.2.3 and mitochondria were lysed and clarified lysate was subsequently treated with 10mM BMH. "1st" indicates first pellet following first centrifugation of homogenate. "M" indicates mitochondrial fraction. "C" indicates cytoplasmic fraction. 5µg of protein was analyzed in each lane and antibodies used for detection are described in table 2.1. The migration of protein standards of the indicated approximate molecular weights are shown in kDa.

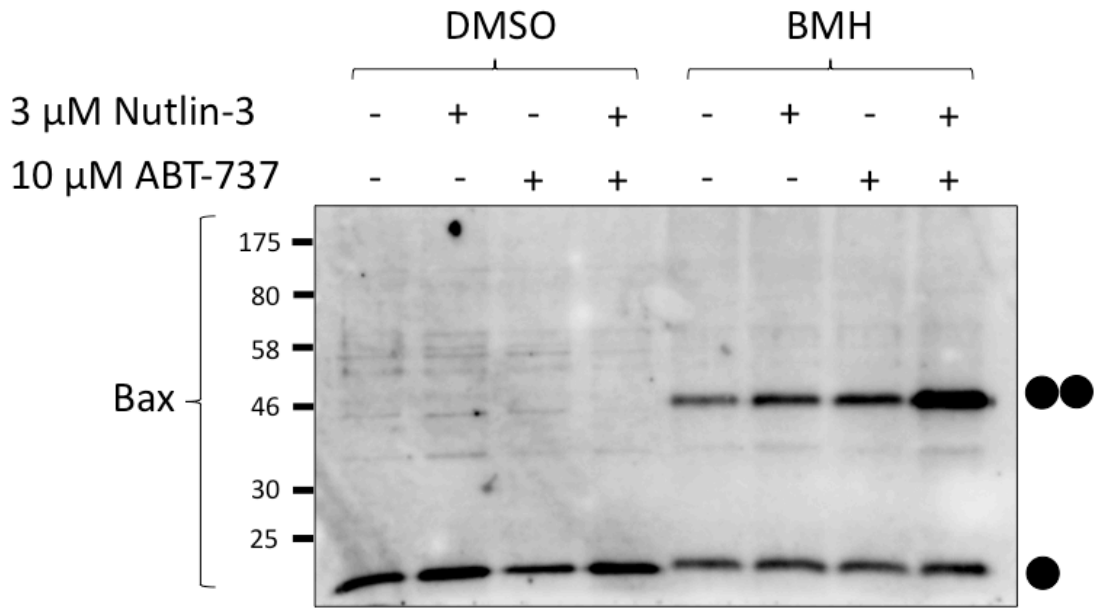

Figure 4.2.3.4 Western blot of mitochondrial lysates treated with BMH or DMSO. Lysate of mitochondria from ACHN cells treated with either drug vehicle, Nutlin-3, ABT-737 or a combination of drugs was treated with either DMSO or BMH and analysed by western. The whole membrane was probed with antibody to Bax. Black circles indicate the position of putative monomers and oligomers of Bax (table 2.1). 5µg of protein was analyzed in each lane. The migration of protein standards of the indicated approximate molecular weights are shown in kDa.

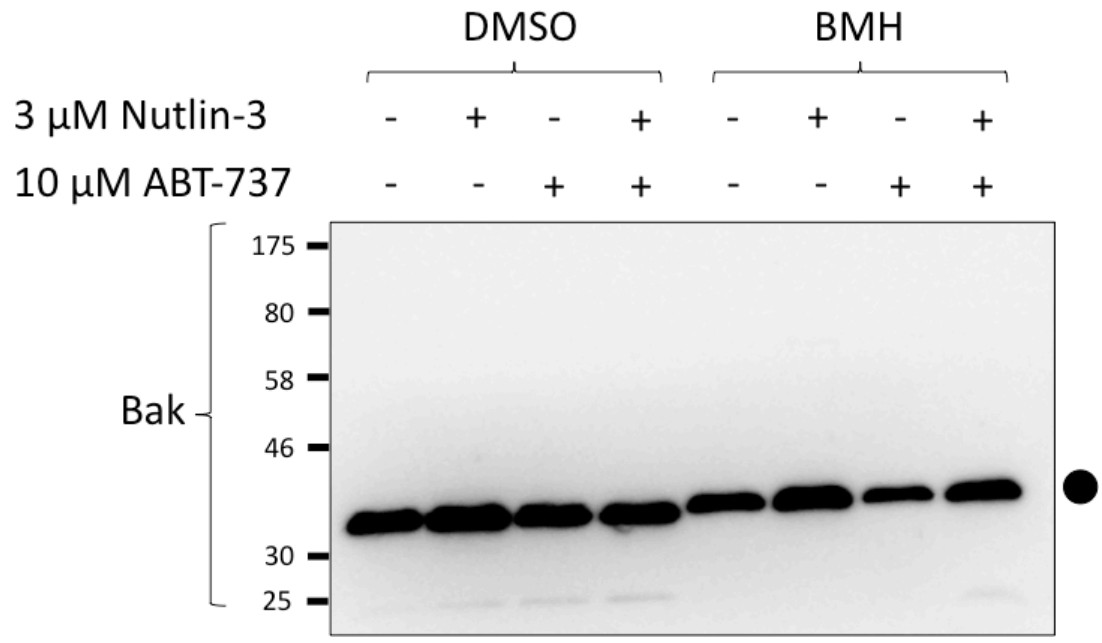

Figure 4.2.3.5 Western blot of mitochondrial lysates treated with BMH or DMSO. Lysate of mitochondria from ACHN cells treated with either drug vehicle, Nutlin-3, ABT-737 or a combination of drugs was treated with either DMSO or BMH and analysed by western. The whole membrane was probed with antibody to Bak. Black circles indicate the position of monomeric Bak. 5µg of protein was analysed in each lane and antibody used for detection is described in table 2.1. The migration of protein standards of the indicated approximate molecular weights are shown in kDa.

apoptosis in comparison to cells treated with vehicle control or Nutlin-3 only. Thus, the increase in Histone H3 in the mitochondrial fractions in cells treated with ABT-737 and the combination treatment may be attributed to micro-nucleation that takes place during apoptosis. Figure 4.2.3.4 shows the mitochondrial fractions from the cells treated with vehicle, Nutlin-3, ABT-737 or a combination of both treatments resolved on an SDS-PAGE gel. Bax is detected on a SDS-PAGE at ~23 kDa. The presence of slower migrating Bax at ~46 kDa suggested that treatment with BMH resulted what appeared to be stabilisation of Bax dimers. There appeared to be a slight increase in Bax dimer formation in the mitochondria of cells treated with Nutlin-3 or the combination treatment, relative to vehicle and ABT-737 alone. Figure 4.2.3.5 shows the same lysates in the previous figure but the membrane from the western blot was probed with an antibody against Bak. There was no evidence for any oligomerization of Bak in response to the combination of Nutlin-3 and ABT-737 upon cross-linking of mitochondrial protein. Slower migrating forms of Bax, such as trimers and tetramers were not present on the SDS-PAGE gel. One possibility that could explain the absence of slower migrating forms of Bax from figure 4.2.3.4 was that Bax oligomers required stabilisation with BMH as soon as possible after disruption of the cell membrane, rather than stabilizing with BMH after the long process of differential centrifugation, lysis of mitochondria and quantification of protein. The protocol was modified to reflect this possibility.

The cells were treated with drug vehicle, Nutlin-3, ABT-737 and the combination treatment as described previously. The homogenization was performed as described previously and the homogenate was centrifuged once at 1,300 x g to remove most of the debris. The supernatant from this centrifugation was immediately treated with

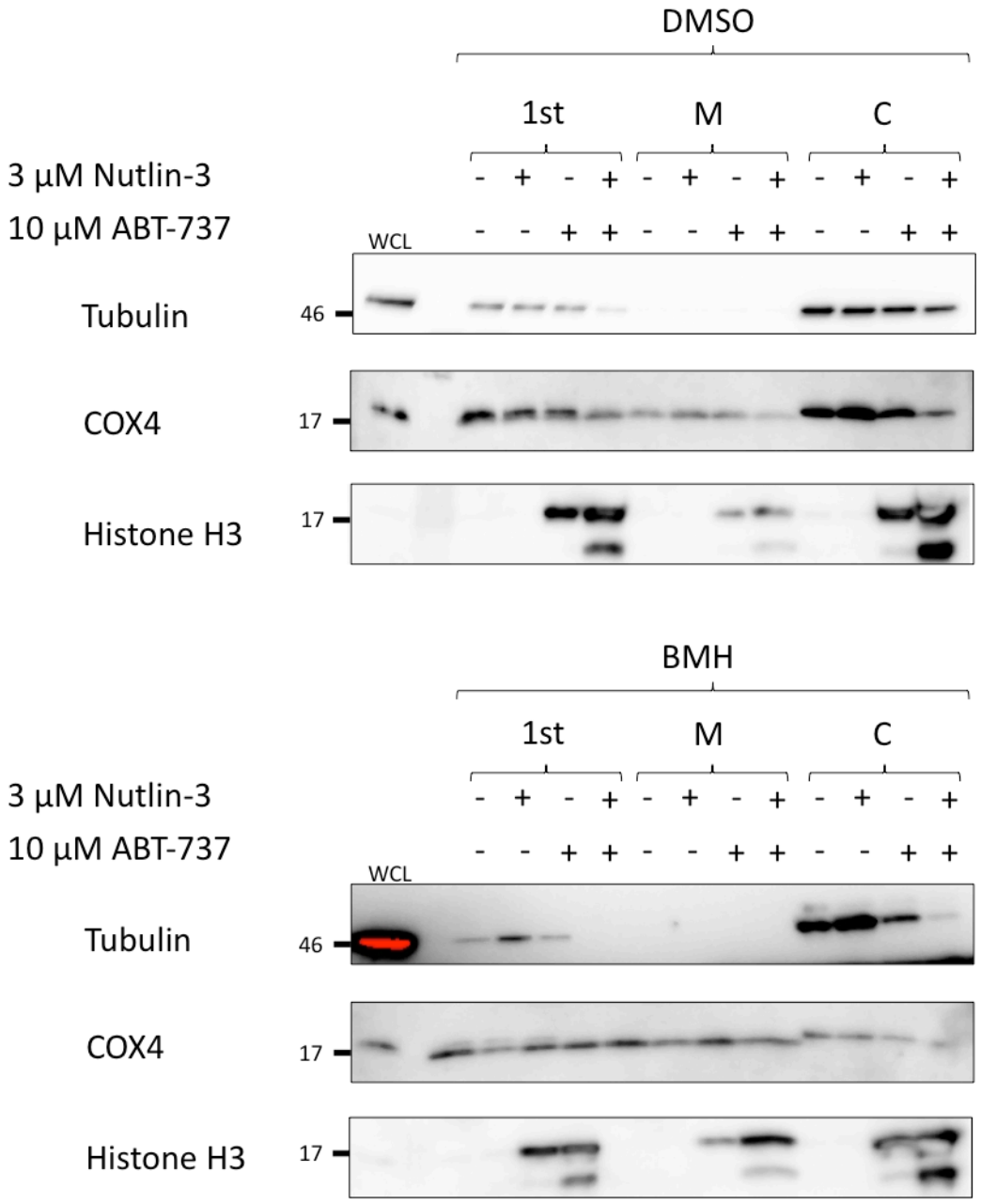

Figure 4.2.3.6 Subcellular fractionation of ACHN cells following treatment of homogenate with BMH or DMSO. ACHN cells were homogenized as described in section 4.2.3 and the homogenates were treated with either DMSO or 10mM BMH to a final concentration of 10% DMSO. Following cross-linking and quenching with 0.5M DTT, homogenates were fractionated by differential centrifugation. "1st" indicates first pellet following first centrifugation of homogenate. "M" indicates mitochondrial fraction. "C" indicates cytoplasmic fraction. 5µg of protein was analysed in each lane and antibodies used for detection are described in table 2.1. The migration of protein standards of the indicated approximate molecular weights are shown in kDa.

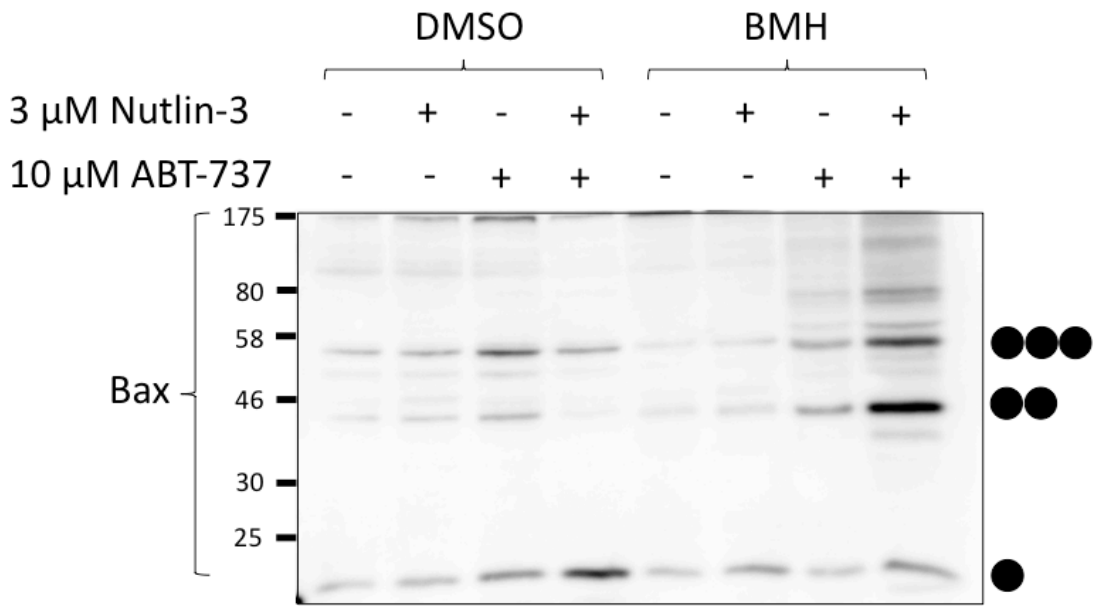

Figure 4.2.3.7 Western blot of mitochondria from ACHN cells treated with DMSO or BMH in homogenate. ACHN cells were treated with drugs and homogenized as described previously. Following one centrifugation step, DMSO or BMH was added to the homogenate to a final concentration of 10%. Quenching and fractionation was carried out as described in section 4.2.3. The whole membrane was probed with antibody to Bax (table 2.1). 5µg of protein was analysed in each lane. The migration of protein standards of the indicated approximate molecular weights are shown in kDa. Black circles indicate the position of monomeric Bax and putative Bax oligomers.

either DMSO or BMH dissolved in DMSO for 30 minutes, to a final concentration of 10% DMSO. The reaction was quenched using DTT as described previously. This was followed by several centrifugation steps at 1,300 x g to remove the remaining debris from homogenization and isolation of mitochondria, followed by lysis and quantification of protein as described above. As observed previously, histone H3 signal was observed in the mitochondrial and cytosolic fractions in the ABT-737 and combination treated cells (figure 4.2.3.6). COX4 signal was observed in 1st pellet, mitochondrial and cytosolic fractions, suggesting this fractionation was not as effective as the previous attempt. Figure 4.2.3.7 shows the mitochondrial fractions from this experiment on membrane transferred from an SDS-PAGE gel treated with antibody to Bax. Slower migrating forms of Bax are apparent in both the cross-linked ABT-737 and combination treated cells and these slower migrating forms are less abundant in the vehicle and Nutlin-3 treated cells. Taken together, these figures suggest that addition of BMH directly to the homogenate before isolation of mitochondria stabilised Bax sufficiently for the detection of slower migrating forms of the protein; however, this may have had an affect on the integrity of the mitochondria in the homogenate. Because DMSO is a potent solvent, there was a possibility that mitochondrial membranes were dissolved by the high concentration of DMSO added to the homogenate. Thus, the protocol was modified so that a lower concentration of DMSO was added to the homogenate.

The experiment was performed exactly as described previously, with the exception of the final concentration of DMSO or BMH dissolved in DMSO added to the homogenate. DMSO or BMH dissolved in DMSO was added to a final

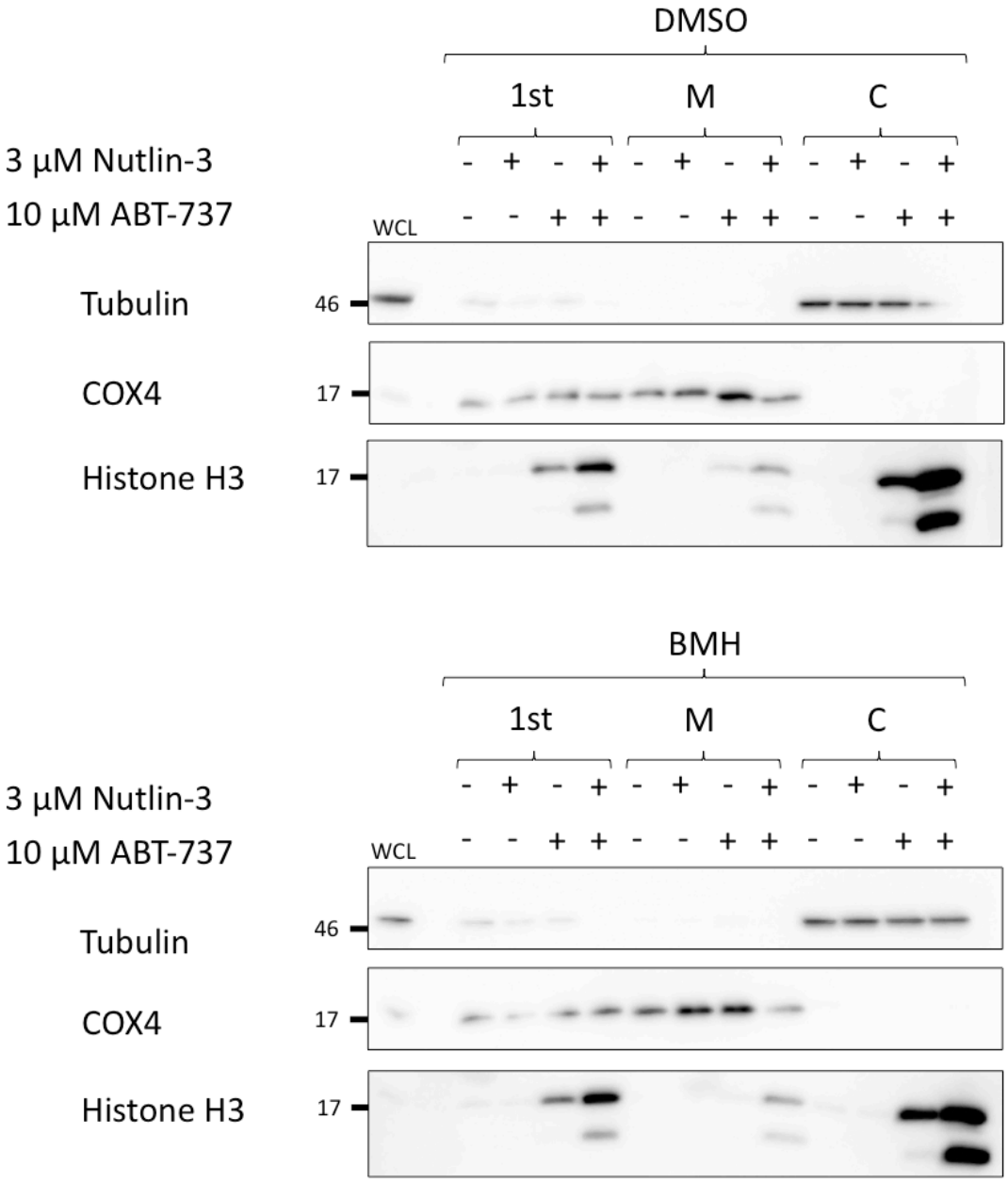

Figure 4.2.3.8 Subcellular fractionation of ACHN cells following treatment of homogenate with BMH or DMSO. ACHN cells were homogenized as described in section 4.2.3 and the homogenates were treated with either DMSO or 10mM BMH to a final concentration of 1% DMSO. Following cross-linking and quenching with 0.5M DTT, homogenates were fractionated by differential centrifugation. "1st" indicates first pellet following first centrifugation of homogenate. "M" indicates mitochondrial fraction. "C" indicates cytoplasmic fraction. 5µg of protein was analysed in each lane and antibodies used for detection are described in table 2.1. The migration of protein standards of the indicated approximate molecular weights are shown in kDa.

concentration of 1% of the total volume of homogenate for 30 minutes. Subsequent isolation of mitochondria was as described above. Histone H3 was again observed in the mitochondrial fractions of ABT-737 and combination treated cells, consistent with the previous two experiments. The COX4 signal was enriched in the mitochondrial fraction and absent from the cytosolic fraction, mimicking the first experiment (figures 4.2.3.8 and 4.2.3.3 respectively), suggesting that the higher concentration of DMSO in the previous experiment may have been responsible for the COX4 signal observed in the cytosolic fraction. Figure 4.2.3.9 shows the mitochondrial fractions from this experiment on membrane transferred from an SDS-PAGE gel treated with antibody to Bax. Slower migrating forms of Bax were only present on this figure where the cells had been treated with the combination of Nutlin-3 and ABT-737 followed by cross-linking. These slower migrating forms appeared to run predominantly at slightly over 30 kDa, ~45 kDa and roughly 58 kDa. A longer exposure of the same western blot, shows that fainter bands are present that migrate at approximately 50 kDa and 80 kDa. Monomeric Bax ran at ~23kDa. The slower migrating form of Bax present at 30 kDa may have represented monomeric Bax cross-linked to another protein. The slower migrating forms of Bax at ~45 and 58 kDa respectively may have represented both dimers and trimers of Bax. The same samples were run on an SDS-PAGE gel and transferred onto a membrane that was treated with an antibody towards Bak (figure 4.2.3.10). Slower migrating forms of Bak were observed at ~60 kDa. A very high exposure of the western blot was required to observe this slower migrating from, suggesting this form of Bak was in low abundance in comparison to the monomeric form of Bak. Because monomeric Bak runs at 29 kDa, the slower migrating form of Bak running at ~60 kDa may have represented dimeric Bak. There appeared to be a higher level of this putative dimeric

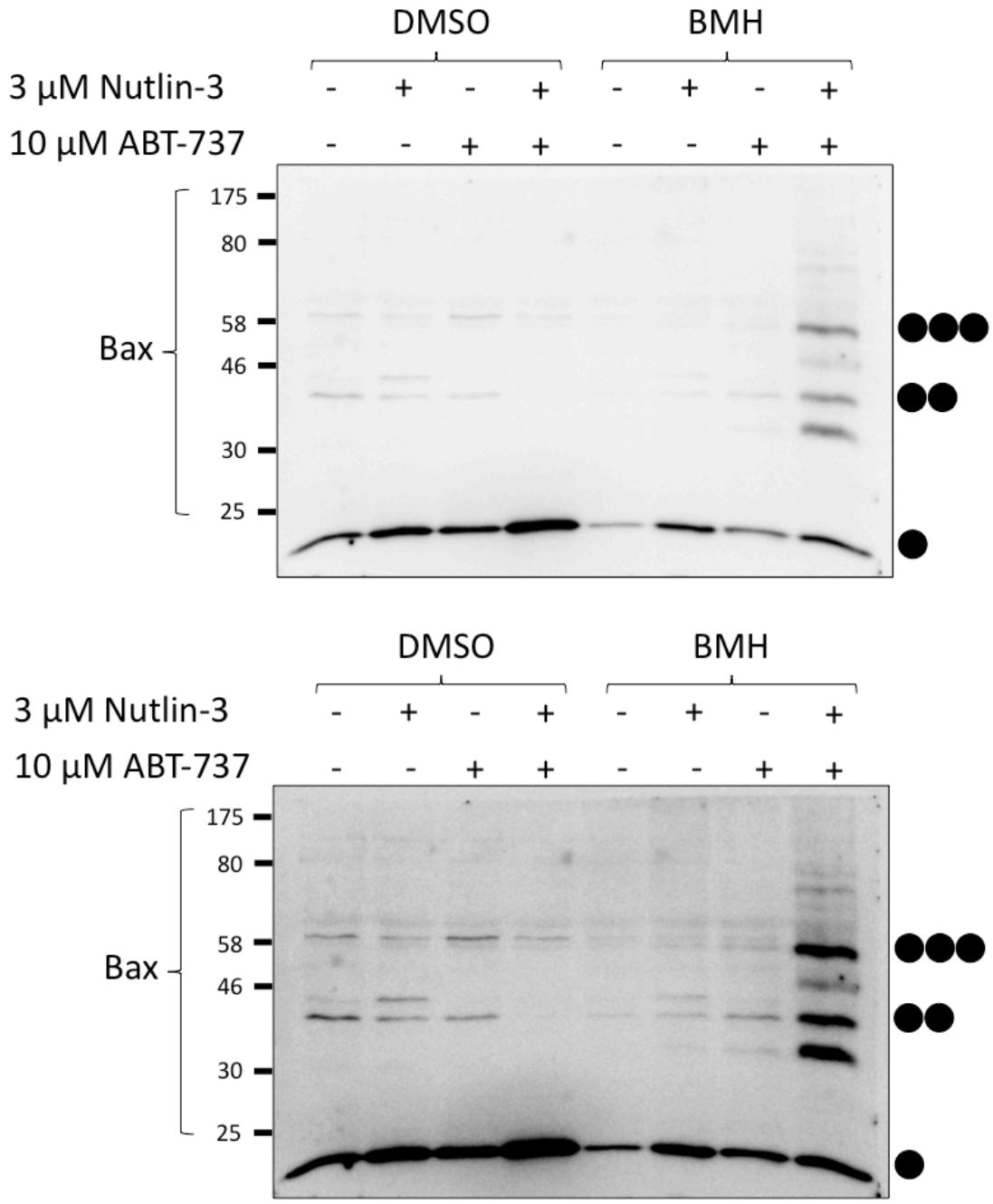

Figure 4.2.3.9 Western blot of mitochondria from ACHN cells treated with DMSO or BMH in homogenate. ACHN cells were treated with drugs and homogenized as described previously. Following one centrifugation step, DMSO or BMH was added to the homogenate to a final concentration of 1 %. Quenching and fractionation was carried out as described in section 4.2.3. The whole membrane was probed with antibody to Bax (table 2.1). 5µg of protein was analysed in each lane. The migration of protein standards of the indicated approximate molecular weights are shown in kDa. Black circles indicate the position of monomeric Bax and putative Bax oligomers. Short exposure top, long exposure bottom.

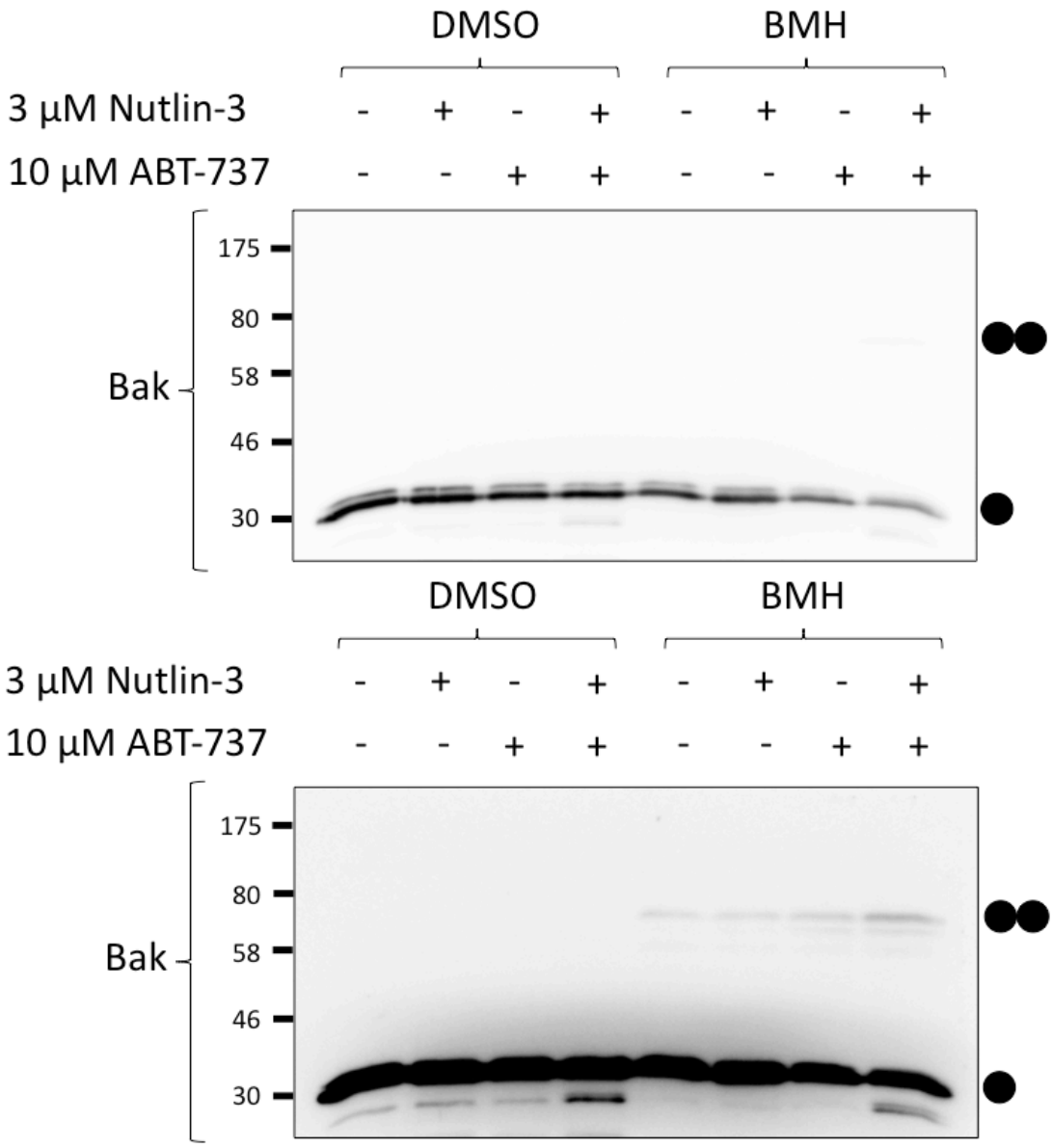

Figure 4.2.3.10 Western blot of mitochondria from ACHN cells treated with DMSO or BMH in homogenate. ACHN cells were treated with drugs and homogenized as described previously. Following one centrifugation step, DMSO or BMH was added to the homogenate to a final concentration of 1 %. Quenching and fractionation was carried out as described in section 4.2.3. The whole membrane was probed with antibody to Bak (table 2.1). 5µg of protein was analysed in each lane. The migration of protein standards of the indicated approximate molecular weights are shown in kDa. Black circles indicate the position of monomeric Bak and putative Bak oligomers. Short exposure top, long exposure bottom.

Bak in cells treated with both Nutlin-3 and ABT-737 followed by cross-linking. Hence, it appeared that it was Bax that is implicated in mediating the apoptotic response to the combination of Nutlin-3 and ABT-737 rather than Bak, because of the increased presence of slower migrating forms of Bax in comparison to Bak.

Previously, we showed that there was a slight increase in apoptotic cells in the mutant p53 111 cell line in response to the combination of Nutlin-3 and ABT-737 in comparison to the control. Because 111 cells are mutated for p53, and it had previously been shown that cell death in response to the combination of Nutlin-3 and ABT-737 was dependent on wild type p53 (Section 3.2.2), we hypothesised that involvement of Bax or Bak in the response of 111 cells to the combination treatment we be to a lesser degree than observed in ACHN cells. Figure 4.2.3.11 shows the western blots for the different fractions probed with antibodies to histone H3, COX4 and tubulin. This figure showed that a similar distribution of histone H3 was observed in this cell line as was observed in the ACHN cells, although there was an absence of the cleaved Histone H3 fragment observed previously. Because some apoptosis took place in the 111 cell line in response to ABT-737 alone and the combination treatment (see figure 3.2.3.9), it was unsurprising that histone H3 was present in both the mitochondrial fraction and the cytosolic fraction in response to these treatments. There was a clear depletion of the tubulin signal from the mitochondrial fraction and a depletion of COX4 from the cytosolic fraction, suggesting the fractionation was effective. Figure 4.2.3.12 shows a western blot showing the mitochondrial fractions of 111 cells treated for 36h with vehicle, Nutlin-3, ABT-737 or combination treatment, with or without cross-linking. Some bands of what appeared to be higher migrating Bax forms were visible at ~58 kDa. A longer

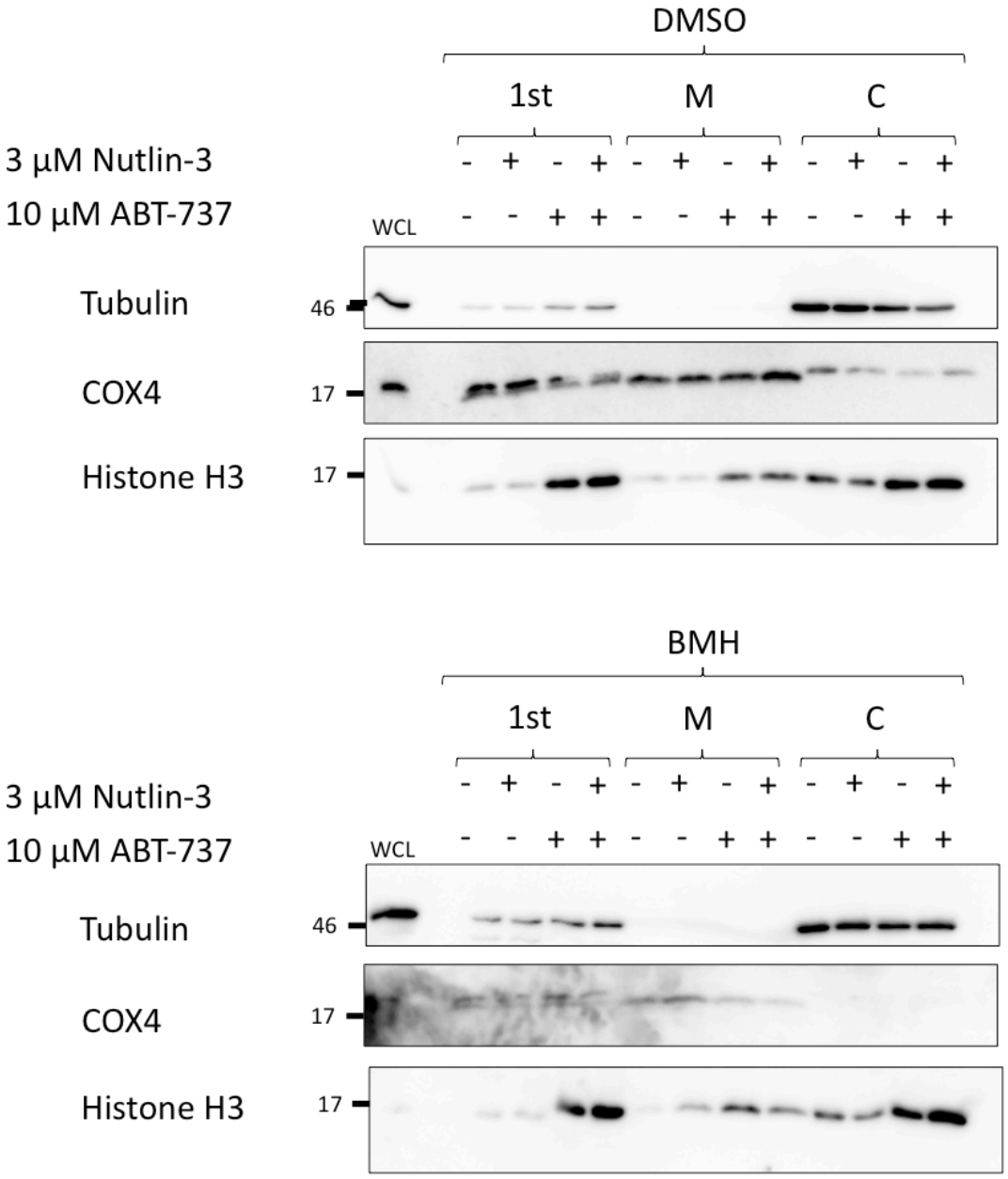

Figure 4.2.3.11 Subcellular fractionation of 111 cells following treatment of homogenate with BMH or DMSO. 111 cells were homogenized as described in section 4.2.3 and the homogenates were treated with either DMSO or 10mM BMH to a final concentration of 1% DMSO. Following cross-linking and quenching with 0.5M DTT, homogenates were fractionated by differential centrifugation. "1st" indicates first pellet following first centrifugation of homogenate. "M" indicates mitochondrial fraction. "C" indicates cytoplasmic fraction. 5µg of protein was analysed in each lane and antibodies used for detection are described in table 2.1. The migration of protein standards of the indicated approximate molecular weights are shown in kDa.

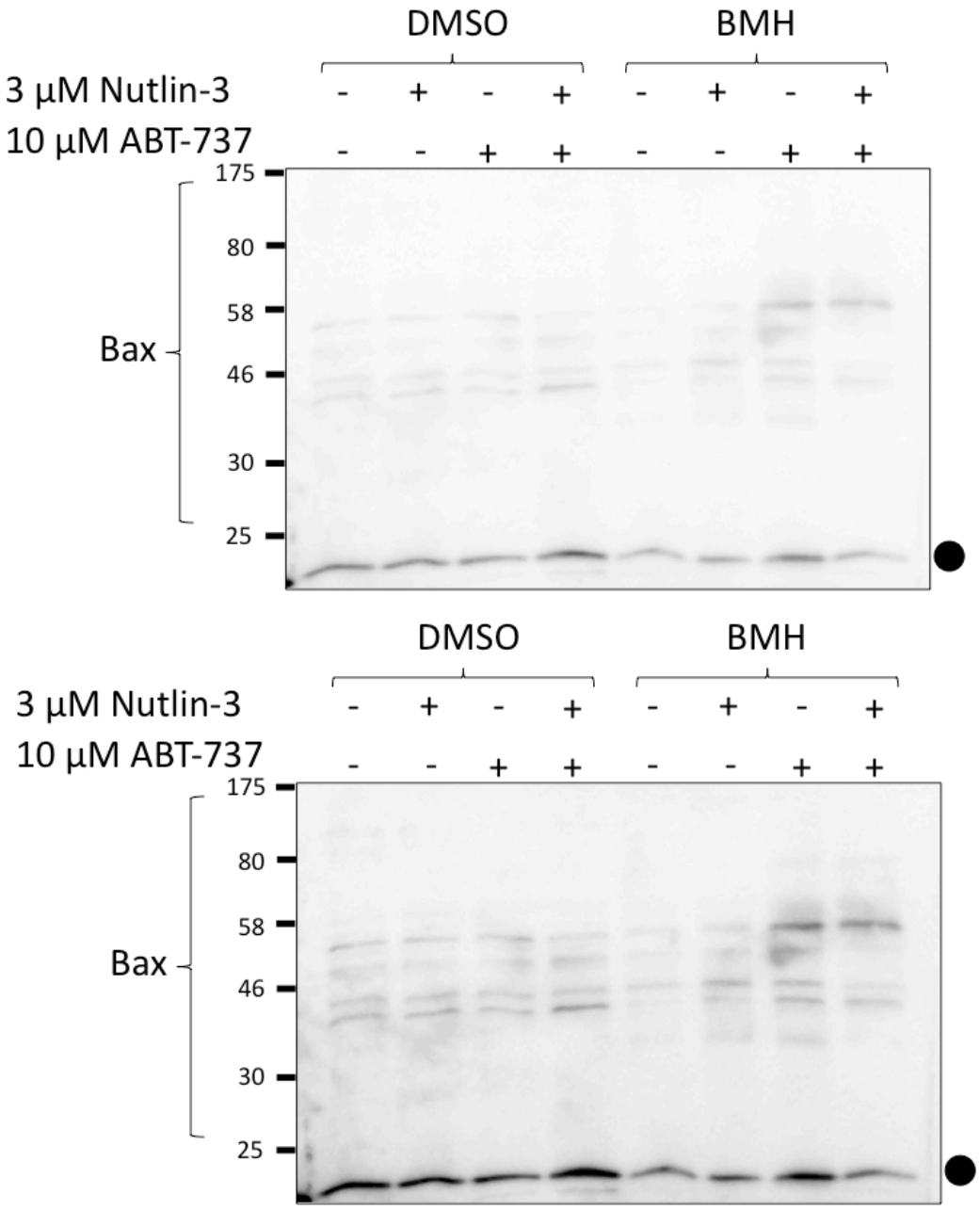

Figure 4.2.3.12 Western blot of mitochondria from 111 cells treated with DMSO or BMH in homogenate. 111 cells were treated with drugs and homogenized as described previously. Following one centrifugation step, DMSO or BMH was added to the homogenate to a final concentration of 1 %. Quenching and fractionation was carried out as described in section 4.2.3. The whole membrane was probed with antibody to Bax (table 2.1). 5µg of protein was analysed in each lane. The migration of protein standards of the indicated approximate molecular weights are shown in kDa. Black circles indicate the position of monomeric Bax and putative Bax oligomers. Short exposure top, long exposure bottom.

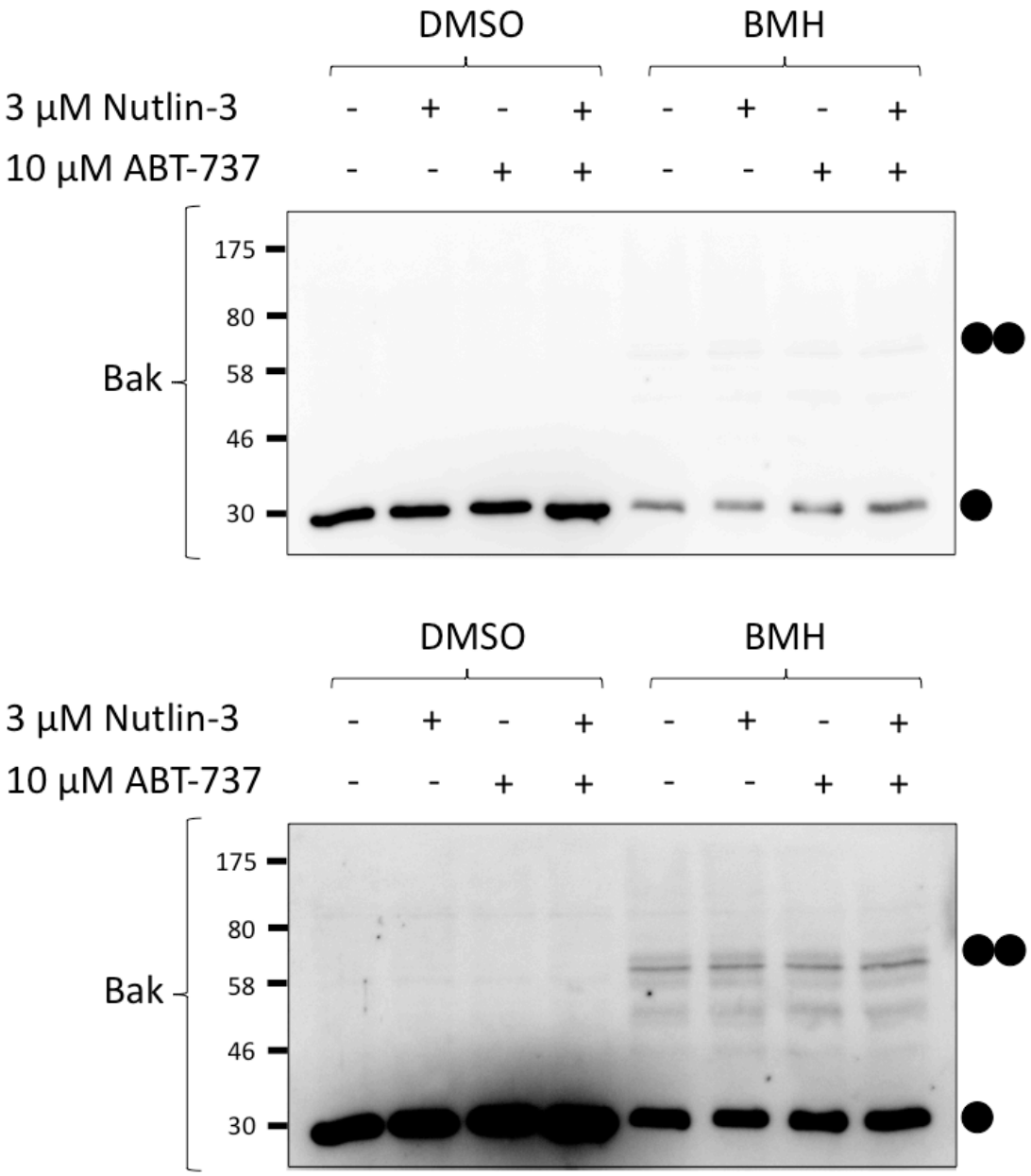

Figure 4.2.3.13 Western blot of mitochondria from 111 cells treated with DMSO or BMH in homogenate. 111 cells were treated with drugs and homogenized as described previously. Following one centrifugation step, DMSO or BMH was added to the homogenate to a final concentration of 1%. Quenching and fractionation was carried out as described in section 4.2.3. The whole membrane was probed with antibody to Bak (table 2.1). 5µg of protein was analysed in each lane. The migration of protein standards of the indicated approximate molecular weights are shown in kDa. Black circles indicate the position of monomeric Bak and putative Bak oligomers. Short exposure top, long exposure bottom.

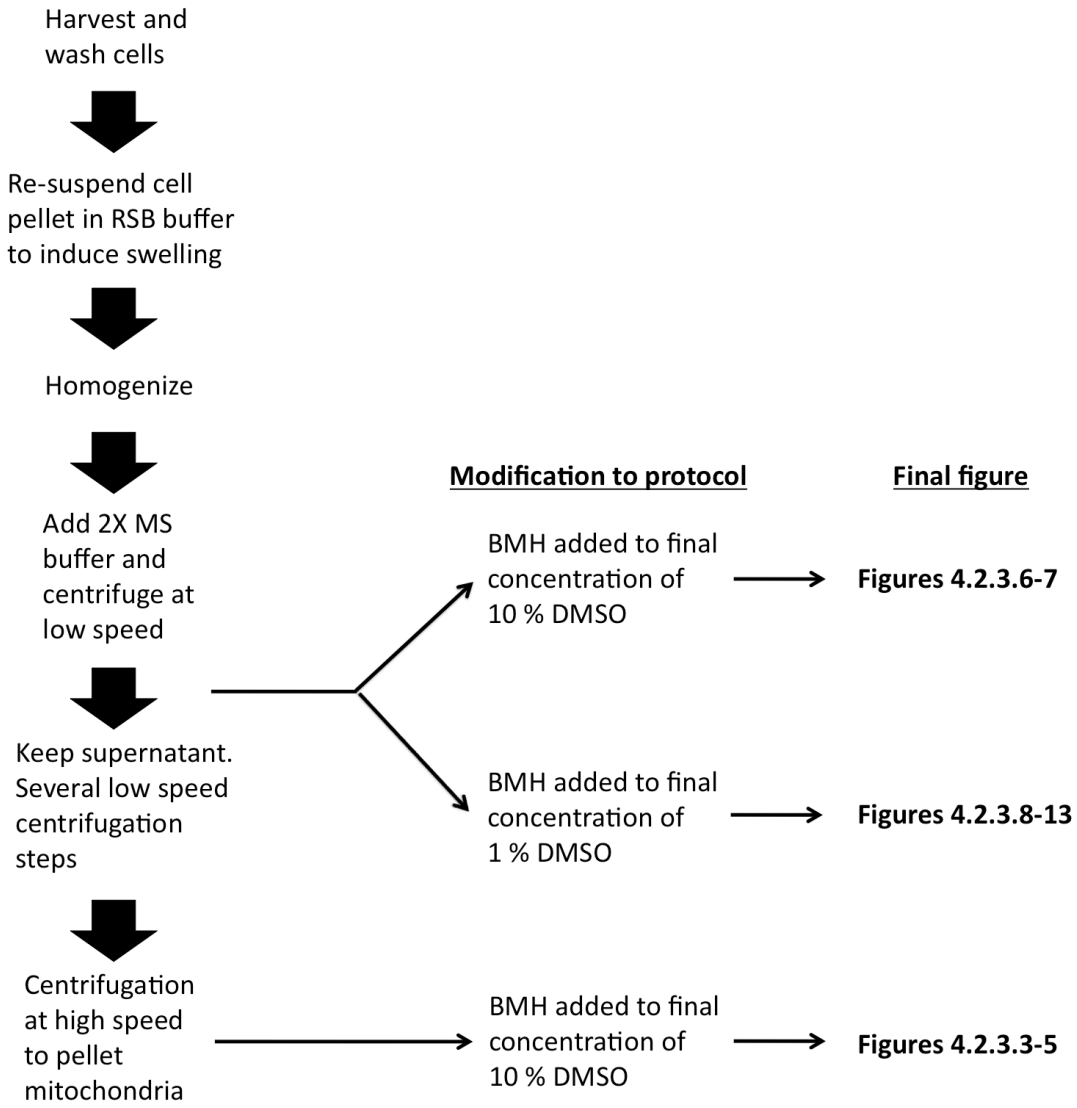

Figure 4.2.3.14 Summary of approaches taken to co-purify Bax and/or Bak oligomers with mitochondria. "Modification to protocol" represents the different approaches described in the main text. "Final figure" represents the figures in this section that were a result of the different modifications made.

exposure of this western blot shown in figure 4.2.3.12 shows that this higher migrating form of Bax was present in all of the treatment conditions, with and without cross-linking. Hence, these slower migrating forms of Bax were more likely to be an artefact on the western blot. Figure 4.2.3.13 shows the mitochondrial fractions from the treated 111 cells but detected with an antibody towards Bak. On initial inspection, it appeared that the BMH-treated mitochondria contained less Bak protein than DMSO-treated mitochondria from this experiment (figure 4.2.3.13). The longer exposure of this western blot however showed that BMH-treatment of these mitochondria results in the apparent dimerization of Bak, independent of the drug-treatment used on the cells. Why BMH induced dimerization of Bak at the mitochondria 111 cells regardless of drug-treatment used remains to be elucidated.

The absence of slower migrating Bax and Bak in the cross-linker-treated mitochondrial fractions from 111 cells treated with the combination of Nutlin-3 and ABT-737 suggested that the recruitment of the machinery involved in the intrinsic apoptosis pathway in response to this treatment is peculiar to RCC cells harbouring wild type p53. In conclusion, the slower migrating forms of Bax present in the cross-linker-treated mitochondrial fractions from ACHN cells implicated Bax oligomerization in the apoptotic response to the combination of Nutlin-3 and ABT-737. The absence of these slower migrating forms in the analogously treated 111 cells suggests a role for p53 in this Bax oligomerization. This implies that apoptosis in response to the combination of Nutlin-3 and ABT-737 is Bax-dependent. Figure 4.2.3.14 summarises the different approaches taken in this experiment. Considering that ABT-737 alone induces some apoptosis in both ACHN and 111 cells, and that

oligomerization of Bax and/or Bak is a pre-requisite for intrinsic apoptosis, it is surprising that oligomers of neither protein were detected in response to ABT-737 in either cell line upon crosslinking. It is possible that the presence of oligomerized Bax/Bak was below a certain threshold necessary for cross-linking and subsequent detection using this technique. To summarize, Bax appears to form oligomers at the mitochondria of ACHN cells in response to the combination of Nutlin-3 and ABT-737, suggesting that apoptosis observed in response to this treatment is Bax-dependent. This possibility will be discussed in the next section. Interestingly, whilst the Bax protein level itself was not increased in response to Nutlin-3 (figure 4.2.2.1) or the combination of Nutlin-3 and ABT-737, this data suggests that there is an alternative mechanism through which Bax multimerization at the mitochondria can take place in the absence of up-regulation of Bax.

4.2.4 Apoptosis in response to the combination of Nutlin-3 and ABT-737 is Bax-dependent

In the previous section, isolation of mitochondria and chemical cross-linking were used to show that Bax was a possible mediator of MOMP, resulting in apoptosis in response to treatment with Nutlin-3 and ABT-737. To determine whether it was indeed Bax that was responsible for promoting apoptosis in response to this treatment, it was hypothesised that down-regulation of Bax using siRNA followed by treatment with the combination of Nutlin-3 and ABT-737 would confer some protection to cells from apoptosis. To determine if this was the case, 4 different siRNAs were tested on ACHN cells to determine which siRNA would be the most effective at reducing Bax expression.

ACHN cells were transfected with siRNA to a final concentration of 32nM using Lipofectamine 2000 as described in Section 2.2.5. ACHN cells were mock transfected or transfected with scrambled siRNA or Bax siRNAs 1-4. Cells were harvested at 24, 48 and 72 hours post-transfection and lysates were analysed by western blot as described in Section 2.4.2. Figure 4.2.4.1 shows a western blot of the level of Bax protein in transfected cells at 24, 48 and 72 hours after transfection. At 24 h post-transfection, there was a decrease in the level of Bax protein in cells that were transfected with siRNAs 3 and 4 (figure 4.2.4.1) relative to mock treated cells and cells transfected with scrambled siRNA. At 48 h, there was a decrease in Bax protein level only in cells that were treated with siRNA 4. At 72h post-transfection, there appeared to be a decrease in Bax protein level in cells that were treated with

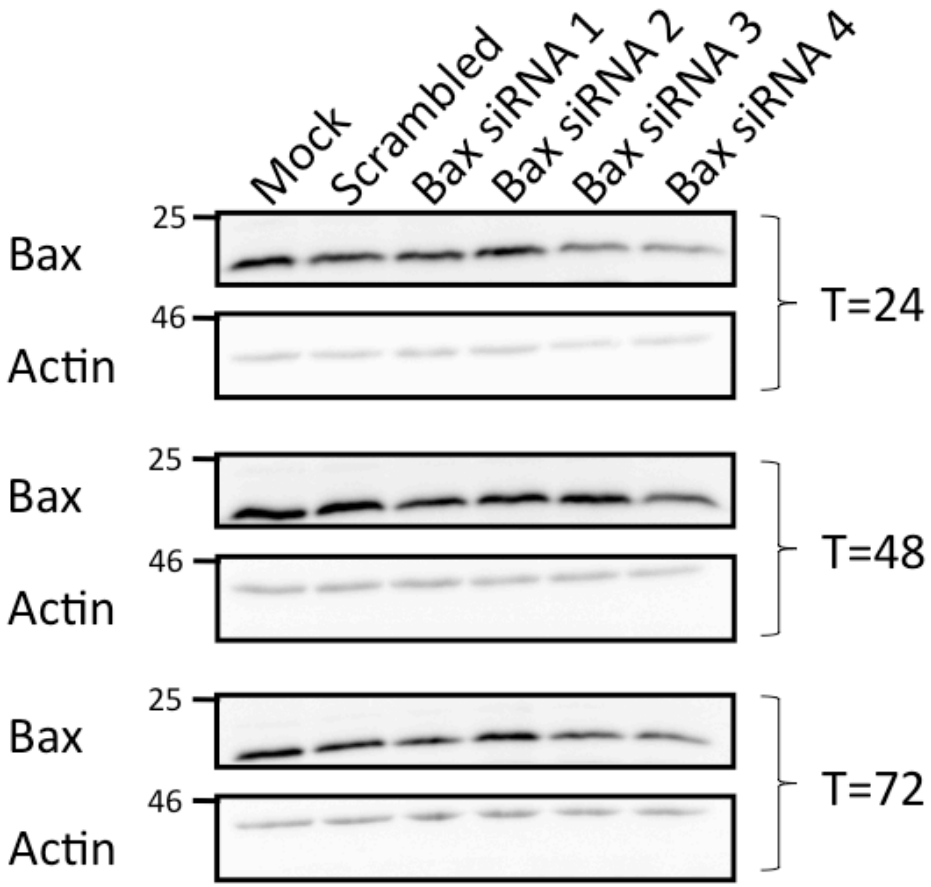

Figure 4.2.4.1 Optimization of Bax knockdown in ACHN cells using siRNA. ACHN cells were transfected with Lipofectamine-2000 according to the manufacturer's instructions. At time (T) 24, 48 and 72 hours post-transfection, cells were harvested, lysates were prepared and analysed by western blot as described in Section 2.4. Proteins were probed as indicated. 20μg of protein was analysed in each lane and the antibody used for detection of Bax is described in table 2.1. The migration of protein standards of the indicated approximate molecular weights are shown in kDa.

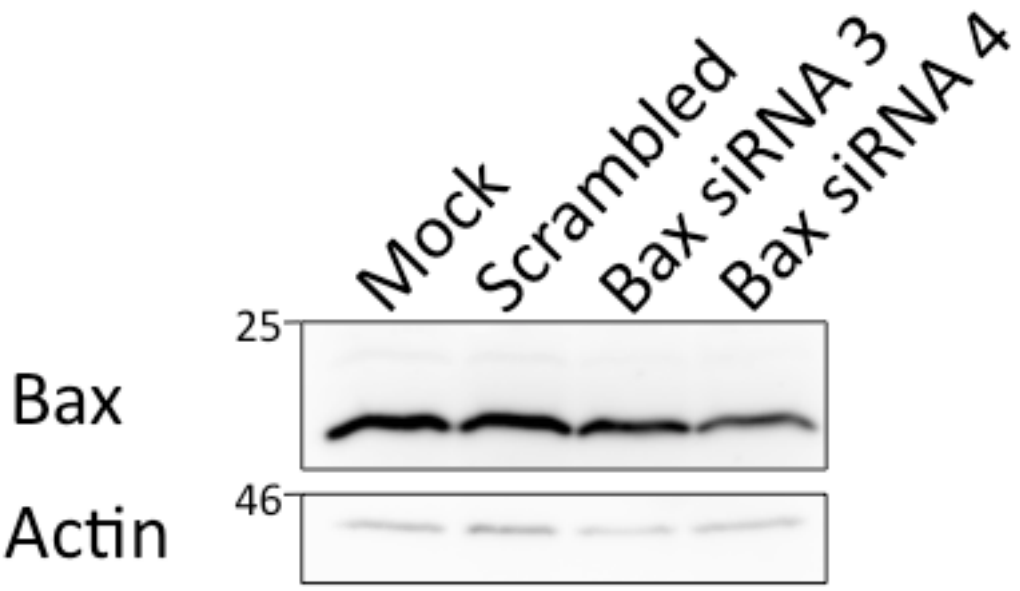

Figure 4.2.4.2 Knockdown of Bax in ACHN cells transfected with siRNAs 3 and 4. ACHN cells were transfected with siRNAs to Bax 3 and 4 using Lipofectamine-2000. Cells were harvested 24h after transfection and lysates were prepared as described in Section 2.4.2 and subjected to analysis by western blot. 20μg of protein was analysed in each lane and the antibody used for detection of Bax is described in table 2.1.

siRNAs 3 and 4. siRNA to Bax numbers 3 and 4 were duly chosen for the experiment.

To determine whether the apoptotic response to the combination of Nutlin-3 and ABT-737 was indeed Bax-dependent, ACHN cells were mock transfected or transfected with either Bax siRNA 3 or 4 or scrambled control siRNA. 24h following transfection, cells from each transfection condition was treated with vehicle, Nutlin-3, ABT-737 or a combination of both Nutlin-3 and ABT-737. After 36h of drug treatment, cells were harvested and subjected to Annexin V and PI staining followed by FACS analysis as described in Section 2.3.2. Figure 4.2.4.2 shows the western blot for the siRNA-mediated knockdown of Bax in ACHN cells prior to treatment with the drugs or drug vehicle. The Bax siRNA 3 lane appeared to be slightly under-loaded relative to the other three lanes in this figure, however there was a reduction in the level of Bax protein in the lane containing protein from cells transfected with siRNA 4 treated relative to the other two treatments. Dot plots from flow cytometry of the treated cells are shown in figure 4.2.4.3 and the overall percentages of Annexin V positive cells in all of the treatments used are summarized in figure 4.2.4.4. See Sections 2.3.2 and 3.2.3 for discussions regarding interpretation of Annexin V and PI positivity. Mock transfected cells and cells transfected with scrambled control siRNA behaved similarly in response to the different treatments used. Treatment with ABT-737 resulted in some apoptosis in cells transfected this way (figure 4.2.4.4, 16.9% and 15.08% apoptotic cells respectively). Treatment with the combination of Nutlin-3 and ABT-737 resulted in greater apoptosis than observed with the single treatments alone. This was consistent with the response of ACHN cells to the combination of Nutlin-3 and ABT-737

described in Section 3.2.3. There appeared to be an increased positivity for Annexin V in the combination-treated cells resulting in what appears to be a migration of the population of live cells in the lower left quadrant of the dot plot into the lower right quadrant (figure 4.2.4.3). In response to the combination of Nutlin-3 and ABT-737, 62.93% of mock-transfected cells and 61.08% of scrambled control transfected cells underwent apoptosis (figure 4.2.4.4). Hence, mock-transfected ACHN cells and ACHN cells transfected with scrambled siRNA responded to the combination of Nutlin-3 and ABT-737 much as un-transfected ACHN cells did (figures 3.2.3.7 and 3.2.3.9).

ACHN cells transfected with either siRNA 3 or 4 to Bax responded to the single drug treatments in a similar fashion to the mock transfected and scramble control transfected cells (figures 4.2.4.3 and 4.2.4.4). In response to the combination of both Nutlin-3 and ABT-737 however, there was decrease in the number of cells undergoing apoptosis in the cells that were treated with siRNA to Bax when compared to the mock-transfected cells and the cells transfected with scrambled siRNA. In response to the combination treatment, 43.39% of cells transfected with Bax siRNA 3 and 33.10% of cells transfected with Bax siRNA 4 underwent apoptosis. This is a decrease from the ~60% apoptosis observed in mock transfected cells and cells transfected with scrambled siRNA when treated with the combination of Nutlin-3 and ABT-737, suggesting that apoptosis in response to the combination of Nutlin-3 and ABT-737 was Bax-dependent. The population of cells that appeared to migrate to the lower right quadrant in response to the combination treatment in the mock and scrambled siRNA treated cells remained in the lower left quadrant when cells were transfected with either siRNA to Bax (figure 4.2.3.3).

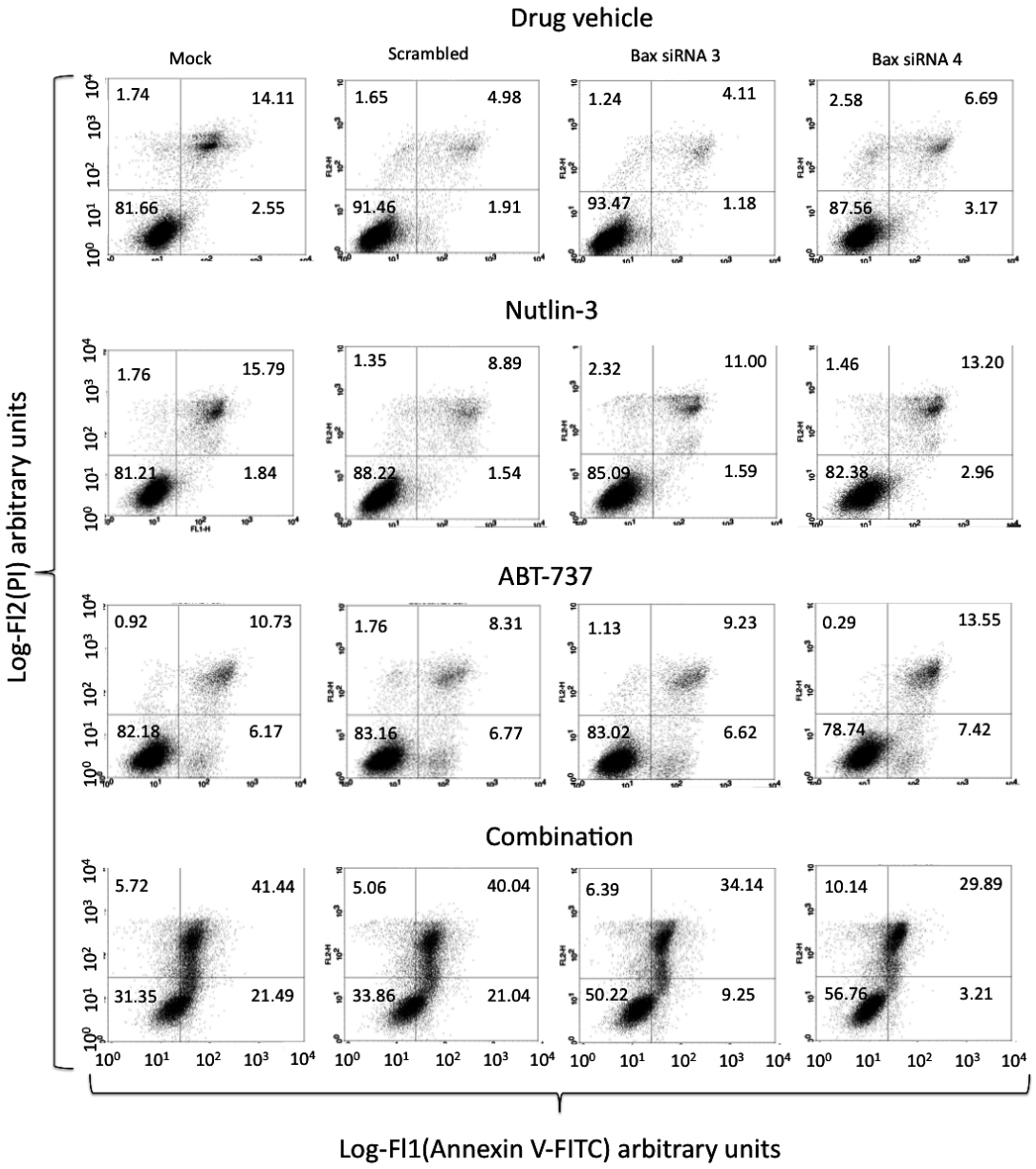

Figure 4.2.4.3 Analysis of apoptosis and cell death in ACHN cells treated with Nutlin-3 and/or ABT-737 upon down-regulation of Bax (I). ACHN cells were transfected using Lipofectamine-2000 with the relevant siRNA to a final concentration of 32nM siRNA. 24 h after transfection, cells were treated with drug vehicle, Nutlin-3, ABT-737 or a combination of both treatments. 36 h after treatment with drug, cells were harvested and stained with Annexin V and PI then subject to analysis by flow cytometry as described in Section 2.3.2. Dot plots represent analysis of 20 000 cells.

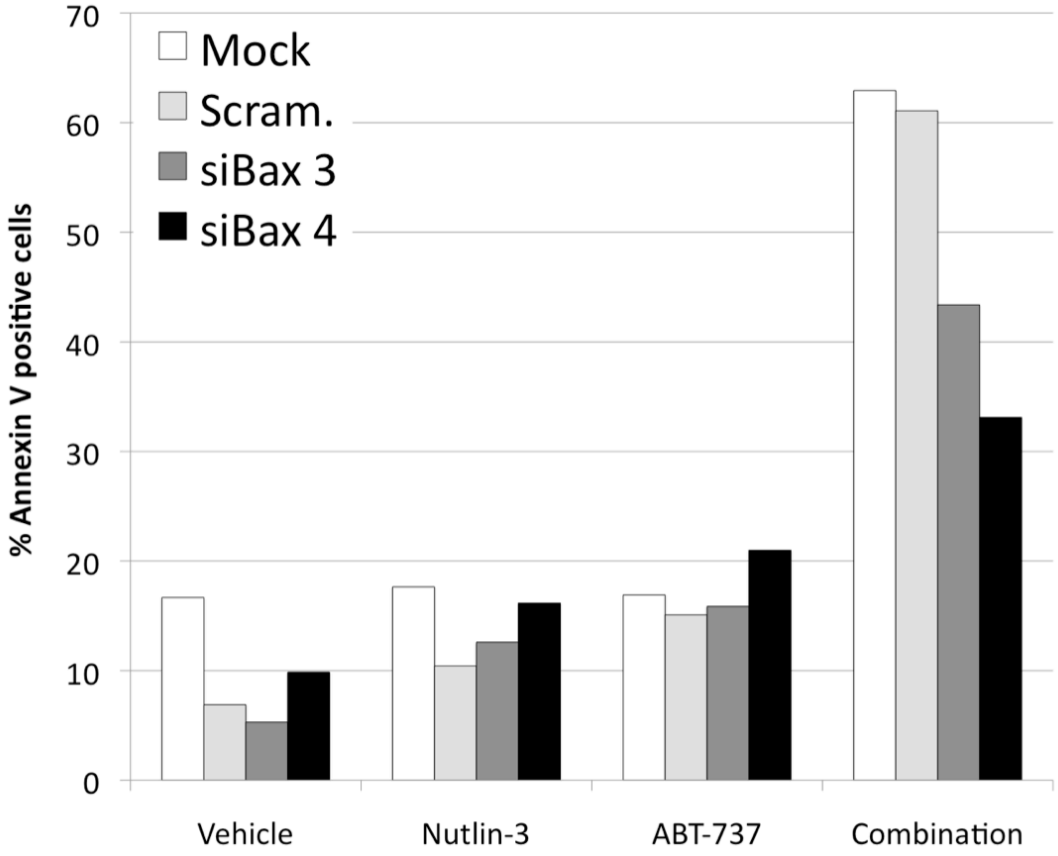

Figure 4.2.4.4 Analysis of apoptosis and cell death in ACHN cells treated with Nutlin-3 and/or ABT-737 upon down-regulation of Bax (II). Summary of flow cytometry analysis of ACHN cells that were mock transfected or transfected with scrambled siRNA or siRNA to Bax. 24h following transfection, cells were treated3μM Nutlin-3, 10μM ABT-737 or a combination of both treatments for 36h. Histogram bars represent the sum of lower right quadrant events (apoptotic cells) and upper right quadrant events (cells that had died as result of apoptosis).

Transfection of ACHN cells with siRNA to Bax appeared to partially rescue the cells from the pro-apoptotic affects of the combination of Nutlin-3 and ABT-737. This was not observed in mock-transfected cells or cells transfected scrambled siRNA. This suggested that apoptosis in response to the combination of Nutlin-3 and ABT-737 in RCC cells was Bax-dependent. Some of the cells that were transfected with siRNA to Bax died (upper right quadrants, figure 4.2.4.3) and this was likely due to the partial nature of the knockdown observed. Most of the reduction of apoptotic cells as a result of Bax knockdown was observed in the lower right quadrant when compared to the mock transfected and scrambled siRNA transfected cells. The lower right quadrant of the dot plot is representative of cells in the early stages of apoptosis and the upper right quadrant represents dead cells that have most likely undergone apoptosis, as discussed in Section 3.2.3. This reduction of cells in the lower right quadrant in the cells treated with Bax siRNA in response to combination treatment is consistent with the observation that recruitment of Bax to the mitochondria and subsequent multimerization is an early apoptotic event (Eskes et al., 2000), since knockdown of Bax resulted in a decrease in the number of cells in the lower right quadrant in response to the combination of Nutlin-3 and ABT-737 when compared ot mock-transfected cells or cells transfected with scrambled siRNA.. In the following section, possible events that take place upstream of Bax activation in response to treatment with Nutlin-3 and ABT-737 are discussed.

4.2.5 A study of pro-apoptotic proteins at the mitochondria in response to the combination of Nutlin-3 and ABT-737

Proteins that mediate the intrinsic apoptosis pathway function at the mitochondrial outer membrane (MOM) and are part of a dynamic interplay of protein-protein interactions that either permit permeablization of the MOM or inhibit it. As discussed in Section 1.2.7.4, there are a number of models that are being validated which are being used to explain the interactions between the proteins that promote apoptosis and proteins that promote survival at the mitochondria. One step towards commitment to the intrinsic apoptosis pathway that is agreed upon in all of the models in the current discourse is the accumulation of pro-apoptotic family members at the mitochondria. Whilst performing western blots on whole cell lysates from cells treated with single or combination drug treatments was useful in elucidating fluctuations of a particular protein on a whole cell level, this method was limited as far as explaining what was taking place at the mitochondrial level. It was hypothesised that an important step that would permit the Bax-dependent apoptosis described in Section 4.2.4 would be the accumulation of pro-apoptotic Puma and Noxa at the mitochondria. This is the site at which anti-apoptotic Bcl-2 family members such as Bcl-2 and Bcl-xL are inhibited by both of these proteins. To study the presence or absence of pro-apoptotic proteins at the mitochondria, the aim was to produce very pure preparations of mitochondria then to study the fluctuations of pro-apoptotic proteins in these mitochondrial preparations.

Hypotonic lysis of cells and Potter-Elvehjem homogenization to disrupt the cell membrane without rupturing mitochondria, was used to lyse cells, exactly as described in Sections 2.5.2 and 4.2.3. This was followed by repeated centrifugations

at 1,300 x g to remove nuclei, unbroken cells and large membrane fragments. The clarified homogenate was then laid onto a two-step discontinuous sucrose gradient and ultra-centrifuged at 85,000 x g at 4 ºC for 1 hour. Mitochondria were recovered from the interphase of the gradient by lateral suction with a syringe and needle and subsequently washed and prepared in loading buffer for western blot analysis. Figure 4.2.5.1 shows a photograph of a centrifuge tube loaded with the two layers of sucrose and the crude homogenate before and after ultra-centrifugation.

ACHN and 111 cells were treated with drug vehicle, Nutlin-3 or ABT-737 alone or a combination of both treatments for 36h. The cells were then harvested and mitochondria were purified as described above. Fractions recovered were designated 1st pellet, mitochondrial and cytosolic. The first pellet was the pellet that formed after the first 5-minute centrifugation at 1,300 x g following homogenization. The mitochondrial fraction was the layer removed from the interphase of the sucrose gradient. The cytosolic fraction was the clarified homogenate above the layers of sucrose that remained after ultracentrifugation. Tubulin, COX4 and Histone H3 were again used as markers to monitor the quality of the fractionation procedure. Figures 4.2.5.2 and 4.2.5.3 show controls for fractionation for both ACHN and 111 cells respectively. Figures 4.2.5.4 and 4.2.5.5 are western blots from both treated ACHN and 111 cells that take a closer look at the levels of COX4 and tubulin in comparison to whole cell lysate. In a similar fashion to what had been observed previously, the Histone H3 signal from the ACHN cells treated with the combination of Nutlin-3 and ABT-737 was distributed amongst the mitochondrial fraction and the cytosolic fraction (figure 4.2.5.2) and it appeared in the form of a doublet. Some

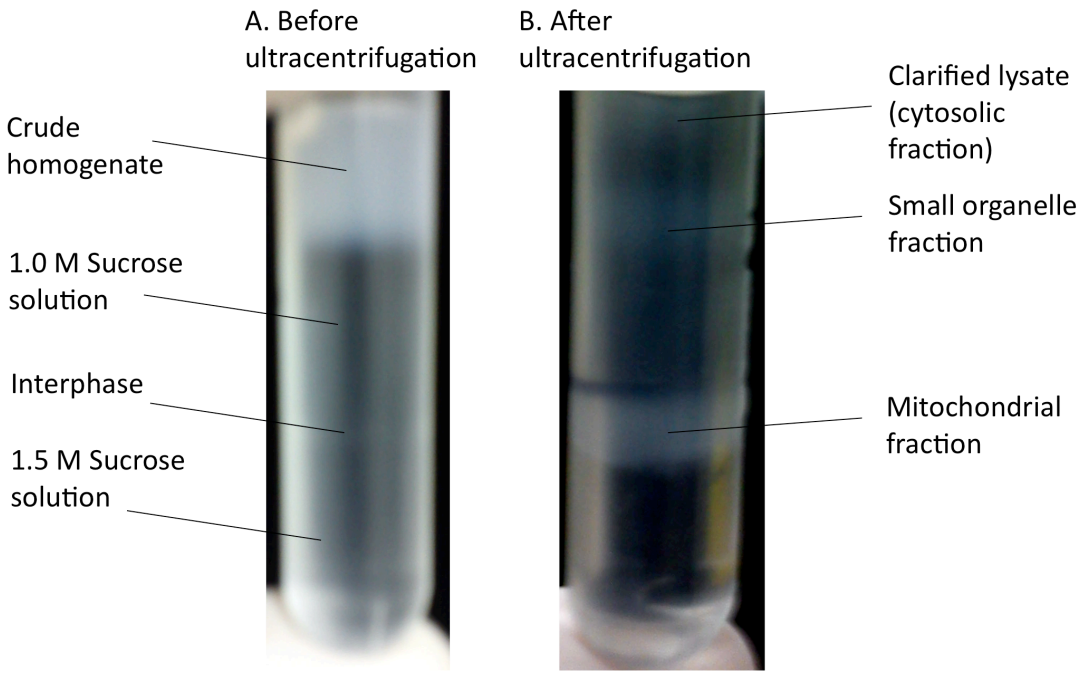

Figure 4.2.5.1 Centrifuge tube prepared for purification of mitochondria from crude homogenate before and after ultra-centrifugation. Cells were homogenized as described in section 4.2.5 and the crude homogenate was laid over two layers of Sucrose/Tris-HCl/EDTA solution (A). Ultra-centrifugation separated mitochondria from soluble cytosolic proteins and smaller organelles (B).

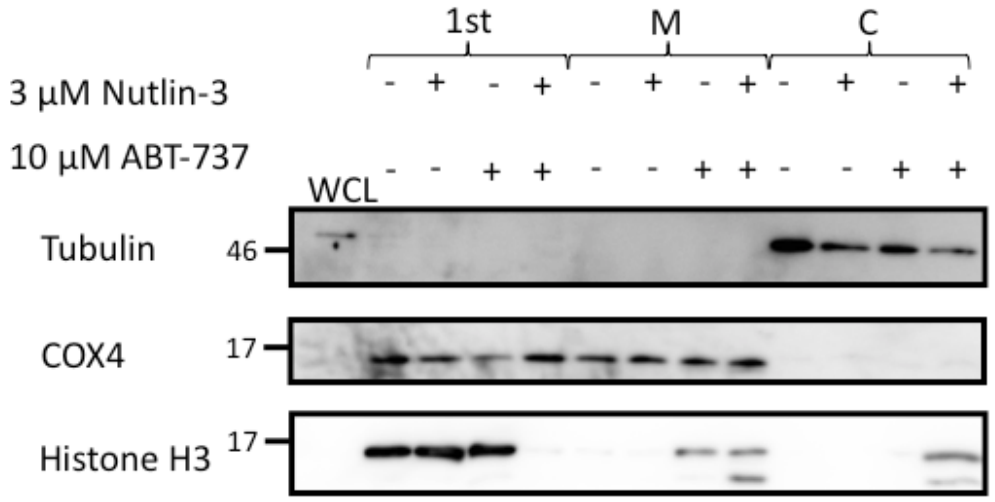

Figure 4.2.5.2 Analysis of subcellular fractions following fractionation of wild type p53 ACHN cells by sucrose density gradient centrifugation. ACHN cells were treated with drug vehicle, Nutlin-3, ABT-737 or a combination of both for 36h. Cells were then harvested and fractionated as described in section 4.2.5 and samples for western blot analysis were prepared as described in Section 2.4.2 and subjected to analysis by western blot. 5µg of protein was analysed in each lane and the antibodies used for detection of protein are described in table 2.1. "1st" indicates first pellet following first centrifugation of homogenate. WCL indicates whole cell lysate. "M" indicates mitochondrial fraction. "C" indicates cytoplasmic fraction. The migration of protein standards of the indicated approximate molecular weights are shown in kDa.

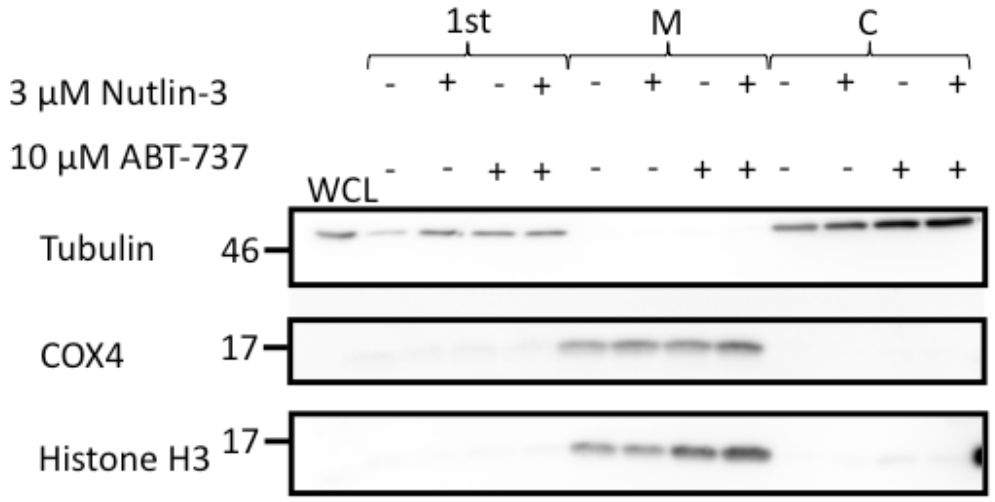

Figure 4.2.5.3 Analysis of subcellular fractions following fractionation of mutant p53 111 cells by sucrose density gradient centrifugation. 111 cells were treated with drug vehicle, Nutlin-3, ABT-737 or a combination of both. Cells were then fractionated as described in section 4.2.5 and samples for western blot analysis were prepared as described in Section 2.4.2 and subjected to analysis by western blot. 5µg of protein was analysed in each lane and the antibodies used for detection of protein are described in table 2.1. "1st" indicates first pellet following first centrifugation of homogenate. WCL indicates whole cell lysate. "M" indicates mitochondrial fraction. "C" indicates cytoplasmic fraction. The migration of protein standards of the indicated approximate molecular weights are shown in kDa.

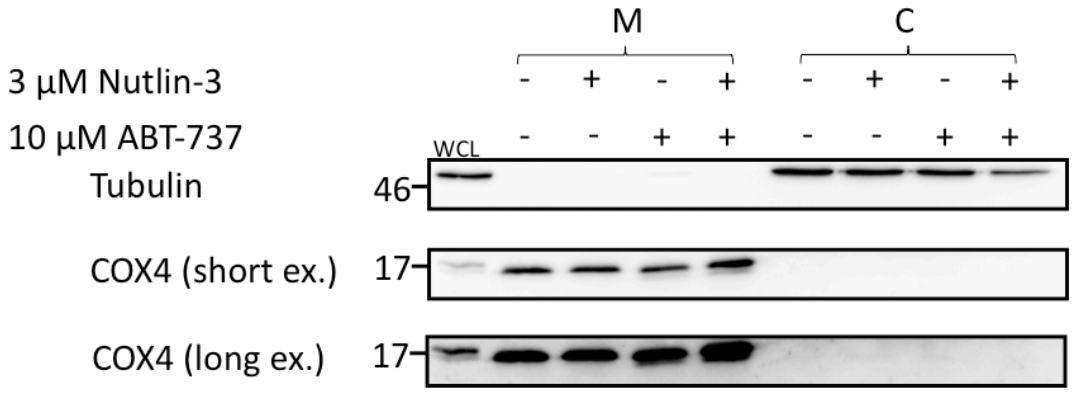

Figure 4.2.5.4 Enrichment of mitochondria from wild type p53 ACHN cells. Western blot showing enrichment of mitochondria relative to whole cell lysate from mitochondrial fraction of treated ACHN cells. Lysates were prepared as described in the legend of figure 4.2.5.2. 5µg of protein was analysed in each lane and the antibodies used for detection of protein are described in table 2.1. WCL indicates whole cell lysate. "1st" indicates first pellet following first centrifugation of homogenate. "M" indicates mitochondrial fraction. "C" indicates cytoplasmic fraction. The migration of protein standards of the indicated approximate molecular weights are shown in kDa.

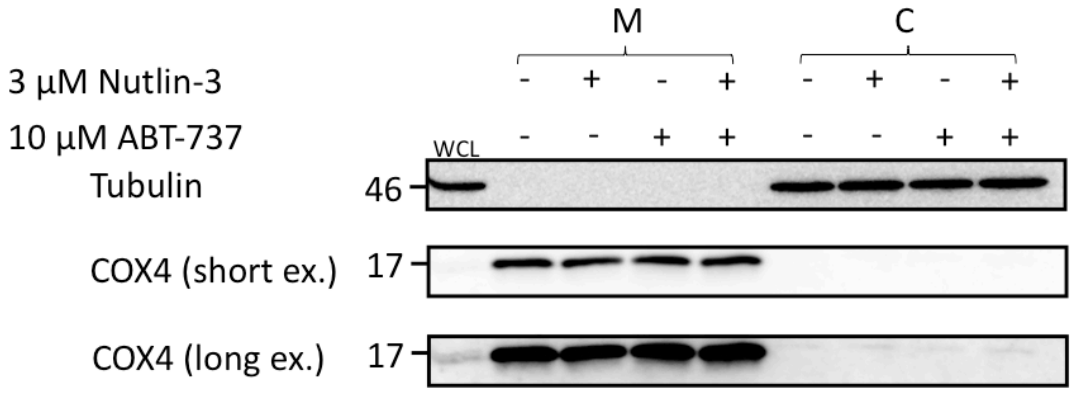

Figure 4.2.5.5 Enrichment of mitochondria from mutant p53 111 cells. Western blot showing enrichment of mitochondria relative to whole cell lysate from mitochondrial fraction of treated 111 cells. Lysates were prepared as described in the legend of figure 4.2.5.3. 5µg of protein was analysed in each lane and the antibodies used for detection of protein are described in table 2.1. WCL indicates whole cell lysate. "1st" indicates first pellet following first centrifugation of homogenate. "M" indicates mitochondrial fraction. "C" indicates cytoplasmic fraction. The migration of protein standards of the indicated approximate molecular weights are shown in kDa.

Histone H3 signal could be observed in the mitochondrial fraction of the ABT-737-treated ACHN cells (figure 4.2.5.2). Again, micronucleation due to apoptosis seemed to be the most likely explanation for this observation. This method was however, successful in depleting cytosolic Tubulin from the mitochondrial fraction and mitochondrial COX4 from the cytosolic fraction. Figure 4.2.5.4 shows an increase in the COX4 signal in the mitochondrial fraction when compared to that observed in the whole cell lysate, which suggest that this method was suitable for the enrichment of mitochondria.

In the treated 111 cells, Histone H3 signal was primarily observed at the mitochondrial fraction (figure 4.2.5.3) and was not observed as a doublet. A higher level of this protein observed was in the ABT-737 and combination-treated mitochondria than that observed in the mitochondria from drug-vehicle and Nutlin-3 treatments, consistent with the slight increase in apoptosis taking place in these cells in response to the drug treatments used (figure 3.2.3.9). COX4 signal was only observed at the mitochondrial fraction and tubulin was only observed at the cytosolic fraction (figures 4.2.5.4 and 4.2.5.5). The COX4 signal was enhanced in the mitochondrial fraction over that observed in the whole cell lysate, suggesting this method had enriched for mitochondria at the mitochondrial fraction (figure 4.2.5.5).

Figure 4.2.5.6 are the western blots for the different pro-apoptotic proteins studied in mitochondrial preparations of ACHN and 111 cells treated with drug vehicle, Nutlin-3, ABT-737 and the combination of both treatments. p53 has been attributed a role in promoting the intrinsic apoptosis pathway at the mitochondria (reviewed in Speidel, 2010). Because of the obviously compromised nature of the nuclei from

cells undergoing apoptosis in these experiments, we elected not to study p53 levels in these mitochondrial lysates. Bax levels remained unchanged at the mitochondria of ACHN cells in response to all of the drug treatments used (figure 4.2.5.6). This implications of this finding will be discussed shortly. There was a slight but detectable increase in Bax at the mitochondria of 111 cells in response to the combination of Nutlin-3 and ABT-737 when compared to the other treatments. In Nutlin-3-treated ACHN cells, there was an accumulation of Puma at the mitochondria when compared to drug vehicle-treated cells. Unlike the western blot for Puma in whole cell lysates of ACHN cells shown in figure 4.2.2.1, there appeared to be an absence of the putative α isoform of the protein at the mitochondria (figure 4.2.5.6). To confirm this, we compared Puma protein from whole cell lysates on the same western blot as Puma protein from mitochondria (figure 4.2.5.7). There was indeed an absence of putative Puma α band at the mitochondria. ABT-737-treated ACHN cells showed a decrease in Puma protein level when compared to drug-vehicle cells and Puma appeared to be completely absent from the mitochondria of cells treated with the drug combination (figure 4.2.5.6). Puma levels at the mitochondria appeared unchanged in response to the single drug or combination treatment in 111 cells. Full-length Bid protein levels at the mitochondria of ACHN cells did not change in response to either Nutlin-3 or ABT-737 alone. In response to the combination treatment, however, there was a decrease in the level of full-length Bid at the mitochondria. This was not accompanied by an increase in tBid. Bid protein levels at the mitochondria of 111 cells increased in response to Nutlin-3, ABT-737 and the combination treatment. A very faint band running below 17 kDa

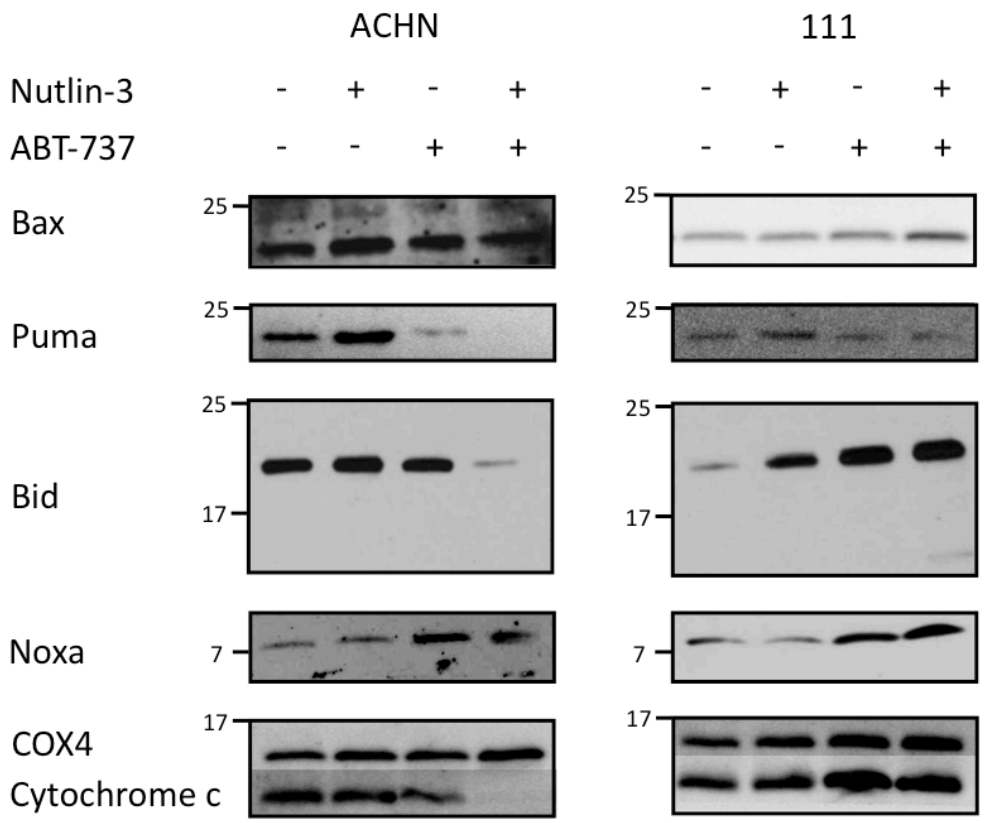

Figure 4.2.5.6 Pro-apoptotic proteins at the mitochondrial fractions from fractionated ACHN and 111 cells. Western blots of mitochondrial fractions from wild type p53 ACHN cells and mutant p53 111 cells treated as described in section 4.2.5.6. Proteins were probed as indicated.

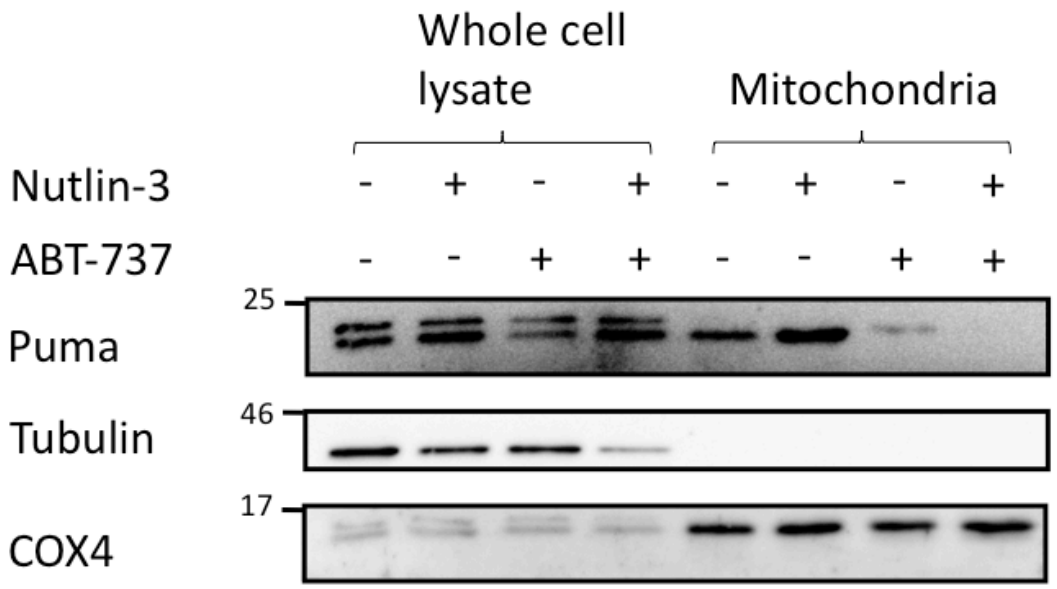

Figure 4.2.5.7 Comparison of Puma protein in whole cell lysates and mitochondrial fractions of wild type p53 ACHN cells. Whole cell lysates were prepared by lysing treated cells with CHAPS-modified SLIP buffer. Mitochondria were isolated by sucrose density gradient centrifugation. Proteins were probed as indicated.

was observed at the mitochondria of 111 cells treated with the combination of Nutlin-3 and ABT-737, which may have represented tBid. The Noxa protein level at the mitochondria of ACHN cells increased only in response to ABT-737 and the combination treatment. A similar observation regarding elevation of Noxa at the mitochondria of 111 cells was made: Noxa protein increased in response to ABT-737 and the combination treatment, but not in response to drug vehicle. This observation implied that the localization of Noxa to the mitochondria may have been involved in promoting apoptosis in response to ABT-737 and the combination of Nutlin-3 and ABT-737. The level of cytochrome c at the isolated mitochondria from these cell lines was also examined. As expected, there was a decrease in cytochrome c protein level at the mitochondria of ACHN cells in response to ABT-737 alone and a complete loss of cytochrome c from the mitochondria in response to the combination treatment. The level of cytochrome c protein at the mitochondria of 111 cells did not alter in response to Nutlin-3, ABT-737 or the combination of both treatments. This observation is consistent with data presented in Section 3.2.3, which shows that cell death in response to the combination of Nutlin-3 and ABT-737 in RCC cells harbouring wild type p53 is a result of apoptosis.

As predicted, there was a fluctuation of pro-apoptotic proteins at the mitochondria of ACHN and 111 cells treated with Nutlin-3, ABT-737 and a combination of both agents. There was no increase in Bax at the mitochondria of ACHN cells in response to the combination treatment (figure 4.2.5.6). This is in apparent contradiction with figure 4.2.3.9, where an increase in Bax protein level can be observed at the mitochondria of ACHN cells treated with the combination. Mitochondria were treated differently in both experiments: in the former, mitochondria were treated with

DMSO for 30 min whilst suspended in crude homogenate, then the mitochondria were isolated by differential centrifugation before lysis with CHAPS-modified SLIP buffer and subsequent elimination of detergent-insoluble proteins and membranes. In the latter case, mitochondria were isolated by sucrose density gradient centrifugation and whole mitochondrial suspension in MS buffer was used to make samples for western blot. Because of the superior enrichment of mitochondria from the latter described protocol (compare figures 4.2.5.4 and 4.2.5.5 to figures 4.2.3.8 and 4.2.3.11) we would be more inclined to accept figure 4.2.5.6 as the more accurate representation of Bax levels at the mitochondria. Further, an increase in mitochondrial Bax is not a mandatory pre-requisite for Bax-dependent apoptosis (Desagher et al., 1999). It has recently been shown that only an increase of mitochondrial Bax by 1.8 ± 1.5% at the onset of MOMP is sufficient to induce pore formation at the outer mitochondrial memebrane (Düssmann et al., 2010) which is not high enough to be detected by western blot, as has been attempted in this study. A recent refinement in the model of Bax translocation and activation during apoptosis suggests that Bax translocation from the cytosol to the mitochondria and vice versa is in a state of dynamic equilibrium and that it is activation of Bax that is already accumulated at the mitochondria that can promote apoptosis. The traditional view was that cytosolic Bax required activation upstream of mitochondrial accumulation, recent data suggests that this may not be the case (Schellenberg et al., 2013).

Noxa protein level increased at the mitochondria in response to ABT-737 alone and the combination of Nutlin-3 and ABT-737 in both ACHN and 111 cell lines (figure 4.2.5.6). Noxa binds anti-apopototic Mcl-1 with high affinity (Certo et al., 2006;

Van Delft et al., 2006) and therefore may play a role in promoting the apoptosis observed in response to the combination treatment. As this elevation of mitochondrial Noxa was observed in both p53 wild type and mutant cell line, it is likely that Noxa does not play a central role in this process.

Increased mitochondrial Puma in ACHN cells treated with Nutlin-3, and the lack of apoptosis observed in these cells (Section 3.2.3) in response to this treatment suggested that Puma elevation at the mitochondria alone was insufficient to promote apoptosis in these cells. One model of the pro-apoptotic role of Puma states that Puma can transiently interact with Bax and Bak to promote the oligomerization of these proteins (Kim et al., 2006, 2009). The decrease in Puma at the mitochondria of ABT-737-treated ACHN cells may be attributed to the possible displacement of this protein from Bcl-xL and Bcl-w (ACHN cells are virtually Bcl-2 null, figure 4.2.1.1) at the mitochondria of these cells. Indeed the observation that mitochondrial Puma was lower in the ABT-737 treated ACHN cells when compared to the Nutlin-3 treated cells suggested that Bcl-xL, Bcl-w and possibly Mcl-1 may have been acting as a "sink" for Puma (Kim et al, 2006), binding the protein and inhibiting the Puma-Bax interaction. Puma was up-regulated in the whole cell lysates of ACHN cells treated with the combination of Nutlin-3 and ABT-737 (figure 4.2.2.1) and yet was absent from the mitochondria of cells that had undergone the same treatment. This suggests that Puma may have been dissociated from the mitochondrial outer membrane at this stage of events and had become present in the cytosol. A model of ligand-induced Bax and Bak activation, termed the "hit and run" model proposes that activator BH3-only family members, tBid, Bim and Puma, transiently interact with Bax or Bak at membranes, inducing a conformational change that results in the

activation and subsequent oligomerization of each protein (Wei et al., 2000; Eskes et al., 2000; Walensky et al., 2006; Lovell et al., 2008). Treatment of ACHN cells with the combination of Nutlin-3 and ABT-737 at 36h resulted in such a dramatic apoptotic response (Section 3.2.3) that it is likely that the Puma-mediated Bax activation was no longer taking place nor required. Indeed, no cytochrome c could be observed at the mitochondrial fraction after this treatment (figure 4.2.5.6), suggesting that almost all of the cells in this treatment were undergoing apoptosis. It may be interesting to look at the Puma localization at the mitochondria in combination treated cells over a time course. The issue of Puma-mediated Bax activation will be addressed in greater detail in the following section.

4.2.6 A study into the possible role of Puma in promoting Bax activation in response to the combination of Nutlin-3 and ABT-737

Section 4.2.4 showed that apoptosis in response to the combination of Nutlin-3 and ABT-737 was substantially Bax-dependent. The next question to be addressed was what event was taking place upstream of Bax activation in response to the combination of Nutlin-3 and ABT-737? One of the models suggested for the oligomerization of Bak and/or Bax at the MOM is the direct activation of either of these proteins by "activator" BH3-only family members tBid, Bim or Puma, discussed in Section 1.2.7.4, whereupon "sensitizer" BH3-only family members displace "activator" BH3-only family members from the anti-apoptotic Bcl-2 family members, permitting a transient interaction between the "activator" BH3-only family member with Bak or Bax, resulting in oligomerization of either of the two proteins at the MOM and subsequent apoptosis. BH3-only family members that are thought to be "activators" are tBid, Bim and Puma. Of these three proteins, only Bid, the full-length precursor of tBid, and Puma are p53-inducible. Noxa is currently the only known putative "sensitizer" that is induced by p53. Section 4.2.2 presented a study of the steady state levels of Puma, Noxa and Bid/tBid in response to Nutlin-3, ABT-737 or the combination of both treatments after 36h in the cell lines used in this study. Puma was induced in response to Nutlin-3 and the combination of Nutlin-3 and ABT-737 in the majority of the RCC cell lines tested that harboured wild type p53 (figures 4.2.2.1 and 4.2.2.2). Noxa was induced by ABT-737 and the combination treatment in the majority of the RCC cell lines tested that harbour wild type p53 but also in the p53 mutant 111 cell line and the p53-null H1299 cell line (figures 4.2.2.1, 4.2.2.2, 4.2.2.3 and 4.2.2.4). Data presented in Section 3.2.2 demonstrated that the pro-apoptotic effect of the combination of Nutlin-3 and ABT-

737 was p53-dependent, and a p53-independent pathway describing the up-regulation of Noxa in response to ABT-737 had already been delineated (Bertin-Ciftci et al., 2013), it was hypothesized that Puma was more important than Noxa in contributing to the apoptosis in response to the combination of Nutlin-3 and ABT-737.

As discussed in Section 1.2.7.2 of the Introduction, Puma is a potent inducer of apoptosis and is believed to be essential to the promotion of apoptosis in the absence of both tBid and Bim (Ren et al., 2010; Kim et al., 2006). Puma is also believed to directly activate Bax to commit cells to apoptosis, via a transient protein-protein interaction (Cartron et al., 2004; Gallenne et al., 2009). Major conformational changes in Bax preclude formation of Bax oligomers at the MOM in response to a pro-apoptotic stimulus. One of these conformational changes is exposure of the N-terminal of Bax (Reviewed in Westphal et al., 2013). The monoclonal antibody 6A7 to amino acids 13-19 of Bax has proven to be useful in the detection of the exposure of N-terminal of Bax during the activation of the protein (Hsu and Youle, 1997; Peyerl et al., 2007). When Bax is in a native, non-activated state, residues 13-19 are buried deep within the globular Bax polypeptide. In response to a pro-apoptotic stimulus, changes in pH or treatment with non-ionic surfactants, the N-terminal of Bax is exposed, permitting cross reactivity with the 6A7 antibody (Lalier et al., 2007). To address the question as to whether Puma was involved in Bax activation in response to the combination of Nutlin-3 and ABT-737, cells that had Puma down-regulated by siRNA would be treated with both drugs, followed by immunoprecipitation of activated Bax using the 6A7 antibody. A decrease in the

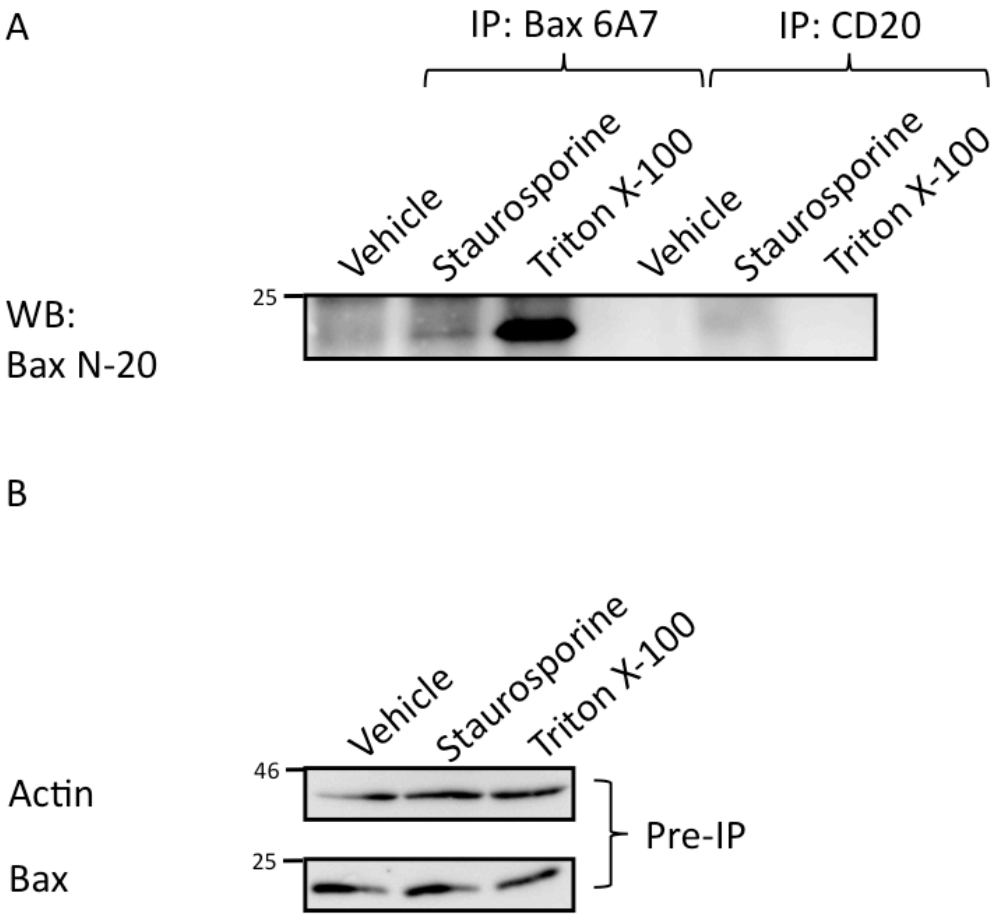

Figure 4.2.6.1 Optimization of Bax 6A7 immunoprecipitation. ACHN cells were treated with 5 mM Staurosporine for 24h and cells were harvested and Bax 6A7 antibody was used in the immunoprecipitation of 500µg protein as described in Section 2.8. Untreated cells were treated with Triton X-100 as a positive control for Bax activation. A. Western blot analysis of lysates that had undergone IP. B. Western blot analysis of 20µg protein before IP. IP – immunoprecipitation. Antibodies used for detection are summarized in table 2.1.

immunoprecipitated Bax upon Puma knockdown would have suggested a role for Puma in Bax activation. This process required optimization of a number of steps, which will be discussed below.

Whilst Bax 6A7 is a commonly used antibody for the detection of N-terminal-exposed Bax, it was important to validate the specificity of this antibody in the experimental system described in this thesis. ACHN cells were treated for 24h with 5mM Staurosporine, a known inducer of apoptosis (Chae et al., 2000) or vehicle control. Cells were harvested as described in section 2.4 and lysed with Bax N-terminal capture buffer (BNTC buffer). An untreated pellet of cells was lysed with BNTC buffer containing 0.1% Triton X-100 for reasons that will be discussed below. Protein was quantified by Bradford assay and 500 μg of protein was pre-cleared with Protein G sepharose beads before overnight incubation with either Bax 6A7 antibody or an isotype matched CD20 mouse monoclonal antibody. The remainder of the immunoprecipitation is described in section 2.8. A western blot showing protein from the immunoprecipitation is shown in figure 4.2.6.1A and a western blot showing the protein from the lysates before immunoprecipitation is shown in figure 4.2.6.1B. There was no visible increase in Bax protein in response to treatment with Staurosporine (figure 4.2.6.1B). Upon detection of Bax protein from the immunoprecipitates with Bax N-20 antibody, no bands are visible in the first lane, which is represents protein from vehicle treated cells immunoprecipitated with Bax 6A7 antibody (figure 4.2.6.1A). A faint band can be observed in the second lane, suggesting Staurosporine induced some Bax N-terminal exposure. Non-ionic detergents such as Triton X-100 induce Bax N-terminal exposure and cross-reactivity for the 6A7 monoclonal antibody whereas zwitterionic detergents such as CHAPS do

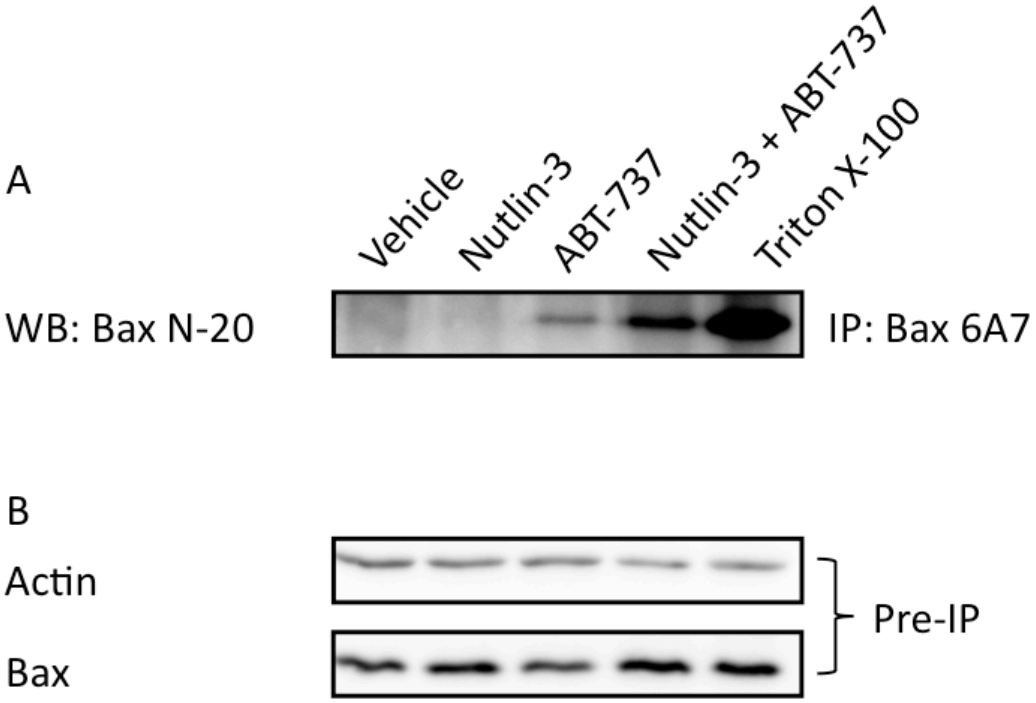

Figure 4.2.6.2 N-terminal exposure of Bax. ACHN cells were for 36 h with 3μM Nutlin-3, 10μM ABT-737 or a combination of both treatments. 500μg of protein was subjected to IP as described in section 2.8.1 using Bax 6A7 antibody. A. Western blot analysis of immunoprecipitates. B. Western blot analysis of 20μg protein before immunoprecipitation.

not (Hsu and Youle, 1997). Indeed, recombinant Bax treated with Triton X-100 or another non-ionic detergent, such as octyl glucoside, has been shown to induce pore formation in both liposomes and purified mitochondria (Antonsson et al., 2000). A very strong band for Bax can be observed in the lane containing protein from cells lysed with buffer containing Triton X-100. This is consistent with observations that non-ionic detergents artificially promote N-terminal exposure of Bax (Lalier et al., 2007). No bands representing Bax can be observed in lysates immunoprecipitated with isotype control antibody to CD20, even upon lysis of cells with Triton X-100 (figure 4.2.6.1A). The absence of detectable Bax in the samples immunoprecipitated with anti-CD20 and the presence of detectable Bax from cells treated with Staurosporine and Triton X-100 suggested that Bax 6A7 is capable of immunoprecipitating N-terminal-exposed Bax from ACHN cells.

The same immunoprecipitation was performed on lysates from ACHN cells treated with drug-vehicle, 3μM Nutlin-3, 10μM ABT-737 or a combination of both treatments for 36h. Immunoprecipitated protein from cells lysed with SLIP buffer containing Triton X-100 was included as a positive control for Bax N-terminal exposure. The western blots showing the immunoprecipitates and the protein before immunoprecipitation (Pre-IP) are shown in figures 4.2.6.2A and B. Consistent with the data in figure 4.2.2.1, there was no increase in Bax protein level in response to any of the treatments (figure 4.2.6.2B). A band representing Bax on the western blot of the Bax 6A7 immunoprecipitates was observed in response to ABT-737 treatment (figure 4.2.6.2A) and a stronger band is observed in response to the combination treatment. This is consistent with the observation that some apoptosis takes place in response to ABT-737 in ACHN cells but even greater apoptosis results

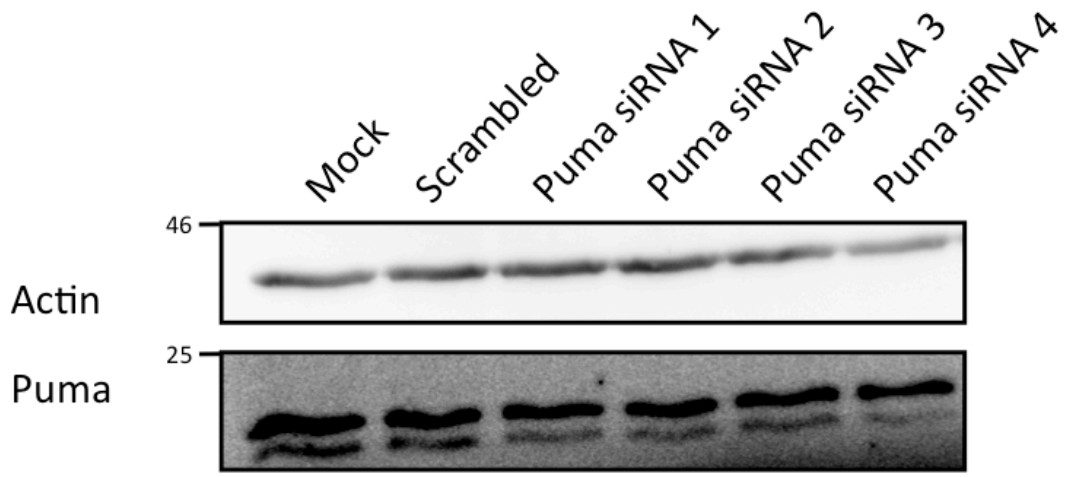

Figure 4.2.6.3 Optimization of Puma knockdown using siRNA. ACHN cells were transfected with siRNA to Puma using Lipofectamine-2000 as described in section 2.2.5 of Materials and Methods. 24 h after transfection, cells were harvested and protein was subjected to western blot analysis as described in section 2.4. 20µg of protein was analysed by western blot and antibodies used for detection are summarized on table 2.1.

in response to the combination (figure 3.2.3.7). As observed previously, treatment of ACHN cells with buffer containing Triton X-100 promoted N-terminal exposure of Bax (figure 4.2.6.2A). As expected, treatment with the combination of Nutlin-3 and ABT-737 resulted in the greatest Bax activation of all of the treatments used. Taking into account figure 4.2.3.9, where Bax oligomers were detected in response to the combination of Nutlin-3 and ABT-737 but not in response to ABT-737 alone, the data presented in figure 4.2.6.2A appeared to contradict this. However, N-terminal exposure of Bax is believed to precede the formation of oligomers at MOM in stepwise models for Bax activation (Kim et al., 2009; Westphal et al., 2013). Hence, it is possible that ABT-737 alone can promote the N-terminal exposure of Bax without subsequent oligomerisation taking place. Alternatively, as discussed in section 4.2.3, Bax oligomerisation may well have taken place in response to ABT-737 alone but this may be below a certain threshold that was detectable by the method used in that section.

Four different siRNAs were tested for their ability to reduce the level of Puma protein in ACHN cells. ACHN cells were transfected with siRNA to a final concentration of 32nM using Lipofectamine 2000 as described in section 2.2.5. ACHN cells were mock transfected or transfected with scrambled siRNA or siRNA to Puma 1-4. Cells were harvested at 24 hours post-transfection and lysates were analysed by western blotting. Figure 4.2.6.3 shows a western blot of the level of Puma protein in transfected cells 24 hours after transfection. There appeared to be subtle decrease in Puma protein in response to siRNAs 1 and 4 (lower bands) hence both of these siRNAs were selected to perform the experiment in conjunction with immunoprecipitation of activated Bax.

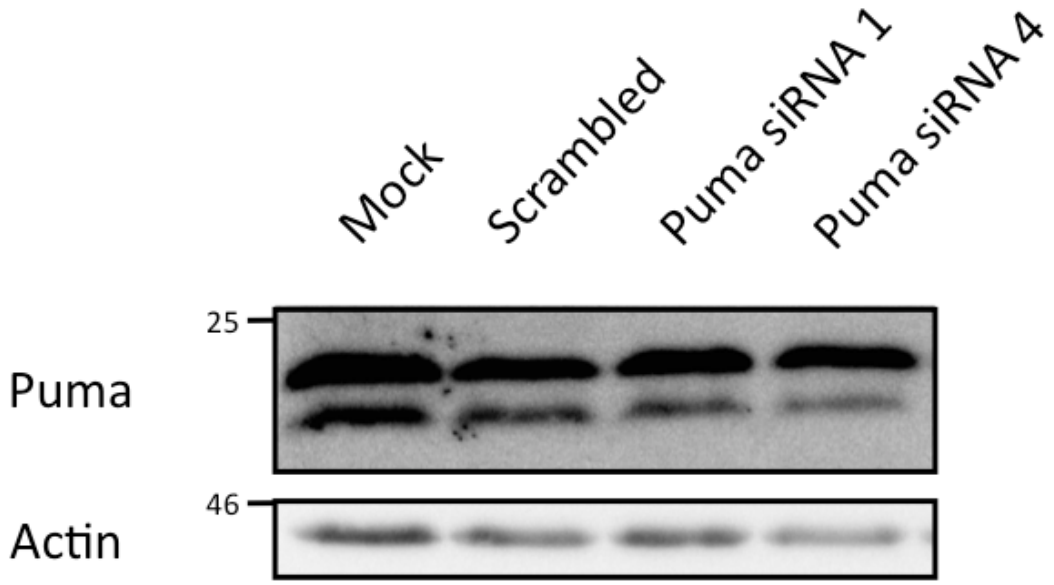

Figure 4.2.6.4 Steady state level of Puma upon transfection with siRNAs to Puma 1 and 4. ACHN cells were transfected with siRNA to Puma using Lipofectamine-2000 as described in section 2.2.5 of Materials and Methods. 24h after transfection, cells were harvested and protein was subjected to western blot analysis as described in section 2.4. 20μg of protein was analysed by western blot and antibodies used for detection are summarized on table 2.1.

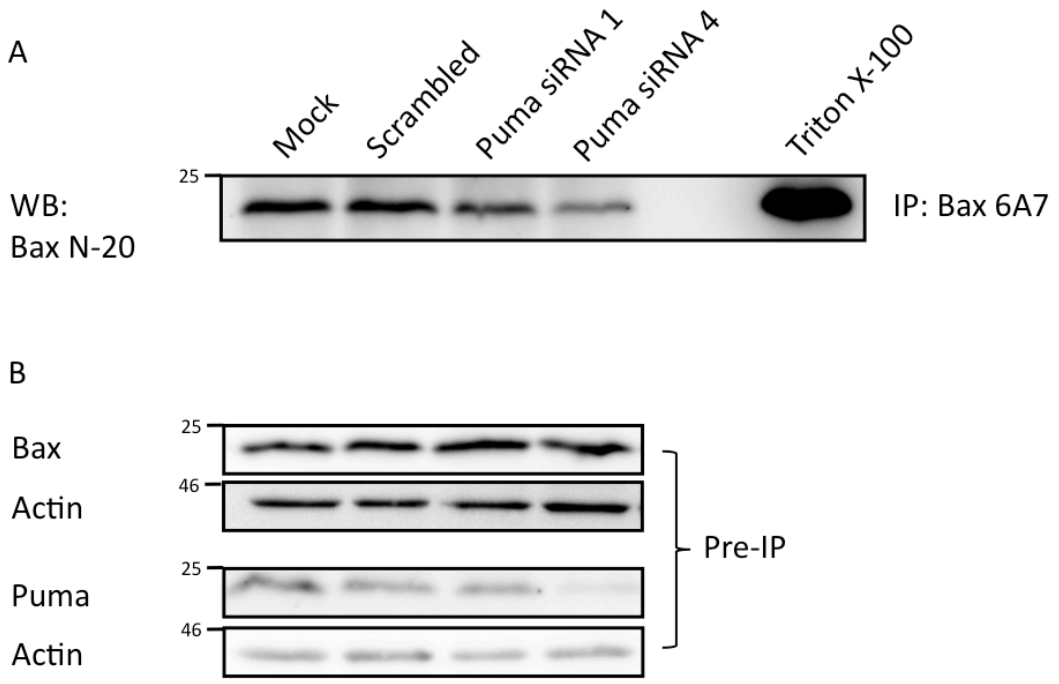

Figure 4.2.6.5 Bax N-terminal exposure of ACHN cells upon down-regulation of Puma and treatment with Nutlin-3 and ABT-737. ACHN cells were transfected with siRNA to Puma using Lipofectamine-2000 as described in section 2.2.5 of Materials and Methods. Cells were for 36 h with 3μM Nutlin-3, 10μM ABT-737 or a combination of both treatments after transfection. 500μg of protein were subjected to IP as described in section 2.8.1 using Bax 6A7 antibody. A. Western blot analysis of immunoprecipitates. B. Western blot analysis of 20μg protein before immunoprecipitation.

ACHN cells were either mock transfected, transfected with scrambled siRNA, or siRNAs to Puma 1 or 4. 24 hours later, the cells were treated with a combination of both 3μM Nutlin-3 and 10μM ABT-737 for a further 36h. Because the possible dependence of Bax activation on Puma in response to the combination of Nutlin-3 and ABT-737 was being studied and because Bax N-terminal exposure was observed in response to the combination treatment (figure 4.2.6.2A), it was reasoned that treatment of transfected cells with only the combination of Nutlin-3 and ABT-737 would have been sufficient to address this question and treatment with the single agents was excluded in this experiment. Figure 4.2.6.4 is a western blot showing the steady state level of Puma protein after transfection, immediately before treatment with Nutlin-3 and ABT-737. Puma appeared to be slightly down-regulated in cells transfected with siRNA 4 to Puma, however the actin band from this treatment appeared slightly under-loaded when compared to the remaining actin bands, suggesting this decrease in Puma may have been an artefact of this under-loading. Figure 4.2.6.5A shows the western blot for the Bax 6A7 immunoprecipitates detected with Bax N-20 polyclonal antibody and figure 4.2.6.5B is a summary of Bax and Puma protein levels before the immunoprecipitation. There was no increase or decrease in Bax protein when all of the transfection conditions are compared (figure 4.2.6.5B). Puma protein level appeared to have decreased in the cells transfected with Puma siRNA 4, when compared to the other treatments. Less activated Bax was immunoprecipitated from the cells transfected with siRNA to Puma 1 and 4 when compared to mock and scrambled transfection. Because of the difference of the knockdown of Puma with siRNA 4 at the start of the experiment (figure 4.2.6.4) and the level of Puma protein from the lysates after 36 h of treatment with the combination of agents, it is difficult to definitively state whether this apparent

decrease in Puma was responsible for the slight decrease in the immunoprecipitated activated Bax (figure 4.2.6.5A).

4.3 Summary

In this chapter, it has been demonstrated that the combination of Nutlin-3 and ABT-737 promoted the up-regulation of p53 in the RCC cells that harboured wild type p53. Not surprisingly, this resulted in an increase in pro-apoptotic Puma. ABT-737 treatment alone and the combination was shown to induce Noxa in a p53-independent manner however, using cells that expressed shRNA to p53, it was shown that p53 was at least partially responsible for the up-regulation of Noxa in response to this treatment. In a study of the oligomerization of pro-apoptotic Bax and Bak at the MOM, it was shown that only Bax was oligomerized at the MOM. Bak oligomerization was almost undetectable by the method used in this study. Further, this Bax oligomerization was only observed in wild type p53 RCC cells and not in RCC cells that possessed mutant p53. Using siRNA to Bax, it was demonstrated that apoptosis in response to the combination of Nutlin-3 and ABT-737 was Bax-dependent. In an attempt to elucidate the role of pro-apoptotic proteins at the mitochondria, levels of these proteins were examined in purified mitochondrial preparations. Noxa protein was elevated at the mitochondria in both p53 wild type and mutant RCC cells in response to ABT-737 alone and the combination of Nutlin-3 and ABT-737. Puma was only elevated at the mitochondria of p53 wild type RCC cells in response to Nutlin-3 alone. Because Puma up-regulation was p53-dependent and the synergy observed between Nutlin-3 and ABT-737 was p53-dependent, Puma was selected as a possible direct activator of Bax downstream of the combination treatment. A protocol for the immunoprecipitation of N-terminal exposed Bax (an

activated conformation of Bax) was optimized and it was shown that the combination of Nutlin-3 and ABT-737 promoted the most Bax N-terminal exposure of the drug treatments used. To determine whether Puma was involved in this process, knockdown of Puma using siRNA was optimised. It was not apparent whether Puma was involved in Bax activation downstream of treatment with the combination of Nutlin-3 and ABT-737 because of a poor knockdown of Puma in the experiment. Puma is the most likely mediator of Bax activation in response to this combination for the following reasons: Bax activation is an essential pre-requisite for the intrinsic pathway of apoptosis to take place and considering that Bid/tBid, the only other p53-inducible Bax activator was not up-regulated/cleaved in response to the combination treatment, only Puma remained as a likely candidate. The implications of these findings and possible ways to address remaining questions about the mechanism underlying the apoptosis induced by this combination of drugs are discussed in the next chapter.

Chapter 5: Discussion

The incidence of RCC is increasing and the inadequacy of current treatment regimens for the metastatic disease has necessitated the development of novel therapeutic strategies. Multiple observations have shown that mutation of p53 is rare in RCC and the function of wild type p53 in cultured RCC cells has been shown to be partially intact (Noon et al., 2010; Warburton et al., 2005). This observation has highlighted wild type p53 as a novel therapeutic target for pharmacological rescue in RCC. Attempts to rescue wild type p53 from inhibition by MDM2 using inhibitors of the p53-MDM2 interaction in RCC cells have resulted in cell cycle arrest or senescence but not apoptosis (Tsao and Corn et al., 2010; Polanski et al., submitted). Because of the potentially harmful properties of senescent cells (reviewed in Davalos et al., 2010, discussed in Section 1.2.5), the focus of this study has been to restore wild type p53 function in RCC cells to commit RCC cells to apoptosis as opposed to cell cycle arrest or senescence. One of the hallmarks of cancer is the evasion of apoptosis (Hanahan and Weinberg, 2000). RCC cells in both patients and cell culture are resistant to the pro-apoptotic effects of radiation and chemotherapy (Rini et al., 2009; Yagoda et al., 1995). In this study, the novel, pro-apoptotic inhibitor of the Bcl-2 family of anti-apoptotic proteins ABT-737 was combined with an MDM2-p53 interaction antagonist Nutlin-3 and this induced p53-dependent apoptosis in a panel of RCC cells harbouring wild type p53.

This combination treatment has been examined previously. For example Kojima et al., combined both Nutlin-3 and ABT-737 to induce apoptosis in acute myeloid leukaemia cells harbouring wild type p53 (Kojima et al., 2006). However, unlike the

cells used in our study, Nutlin-3 alone promotes apoptosis in AML cells (Kojima et al., 2005) and both Nutlin-3 alone and the combination of Nutlin-3 and ABT-737 in AML cells resulted in up-regulation of Bax, one of the important effectors of the intrinsic apoptosis pathway. Similar observations were made of Burkitt's lymphoma cell lines that were treated with either Nutlin-3 or the combination of Nutlin-3 and ABT-737: Bax-dependent apoptosis took place in response to Nutlin-3 alone or in combination with ABT-737 (Renouf et al., 2009; Pujals et al., 2011). Our study has shown that RCC cells harbouring wild type p53 do not respond to Nutlin-3 by undergoing apoptosis and treatment with Nutlin-3 or the combination of Nutlin-3 and ABT-737 does not result in the up-regulation of Bax. These studies emphasize that different cell fates can be determined, or enhanced by the action of p53 rescued from inhibition by Nutlin-3. Further, work presented in this study has shown that liberation of p53 from MDM2 is insufficient to push cell fate towards apoptosis and further "assistance" from ABT-737 was required to achieve this. It is likely that apoptosis observed in response to the combination of Nutlin-3 and ABT-737 in RCC cell harbouring wild type p53 is consistent with the apoptotic threshold model of p53 determination of cell fate as proposed by Kracikova and colleagues: commitment to apoptosis is ultimately determined by the balance of anti-apoptotic proteins to pro-apoptotic proteins. Changing the equilibrium of both of these types of proteins results in apoptosis (Kracikova et al., 2013). It was demonstrated in this thesis that up-regulation of p53 alone by Nutlin-3 treatment was insufficient to promote apoptosis but lowering the apoptotic threshold by combining a BH3-only protein mimetic with Nutlin-3 allowed apoptosis to take place. One interesting issue raised by this is the contribution of Noxa to the synergistic effect of this combination treatment on RCC cells that were sensitive to the combination treatment. Which was

more important to the promotion of apoptosis, ABT-737-mediated inhibition of anti-apoptotic proteins or induction of Noxa by ABT-737? The observations that Caki2 cells were the most sensitive cell line to ABT-737 alone and the level of Noxa protein in this cell line did not increase in response to ABT-737 (figure 4.2.2.1) may suggest that it is the ability of ABT-737 to inhibit anti-apoptotic proteins that is more important to mediating this pro-apoptotic effect. Conversely, the observation that Noxa up-regulation in response to ABT-737 was at least partially dependent on wild type p53 (figure 4.2.2.5) suggests that transcriptional up-regulation of Noxa by ABT-737 may have contributed to the synergistic induction of apoptosis in response to this combination. One way to address this question would be to down-regulate Noxa using siRNA then treat cells with the combination of Nutlin-3 and ABT-737. If knockdown of Noxa conferred some protection of the cells from the pro-apoptotic effects of the combination, then it could be implied that Noxa up-regulation in response to the combination treatment is important towards promoting apoptosis. On the other hand, if knockdown of Noxa did not promote resistance to the combination treatment, then it could be implied that inhibition of Bcl-2 family members by ABT-737 is more important to promotion of apoptosis in response to the combination. This experiment had been considered and designed however time limitations did not permit the author to perform this experiment.

It was demonstrated that apoptosis in response to the combination of Nutlin-3 and ABT-737 was substantially Bax-dependent (Section 4.2.4). Because others have observed that Puma can directly activate Bax in a number of model systems (Cartron et al., 2004; Ren et al., 2010), an attempt was made in this thesis to determine whether Puma played a critical role in the activation of Bax in response to the

combination of Nutlin-3 and ABT-737 by down-regulating Puma using siRNA and then performing immunoprecipitation of activated Bax (section 4.2.6). This may have been too simplistic an approach to address what was taking place upstream of Bax activation in response to the combination treatment. One of the proposed models for Bax activation is a direct, allosteric interaction with Puma (Gallenne et al., 2009). If Puma up-regulation alone were responsible for Bax activation, Puma induced by Nutlin-3 alone would have promoted Bax N-terminal exposure, especially when considering the increase in Puma protein at the mitochondria in response to Nutlin-3 alone (figure 4.2.5.6). The absence of Bax N-terminal exposure (figure 4.2.6.2) in response to Nutlin-3 alone showed that this was evidently not the case. Bax activation is more likely a result of the combined effect of Puma up-regulation, the possible liberation of Bax from anti-apoptotic proteins at the mitochondria by ABT-737 and Noxa-dependent inhibition of anti-apoptotic Mcl-1. We speculate that one of these events may be necessary before allosteric activation of Bax by Puma. It would be interesting to observe sensitivity of RCC cells that harbour wild type p53 to the combination treatment upon simultaneous down-regulation of both Puma and Noxa using siRNA to the genes encoding both proteins. One prediction that this knockdown of both proteins would reduce the sensitivity to the combination treatment. Again, this experiment was considered but time limitations did allow it to be performed. One issue that remains to be elucidated is why Puma induction in response to Nutlin-3 alone does not result in any observable apoptosis. This may be related to the threshold model of p53-mediated apoptosis described above; Puma up-regulation alone in RCC cells that have wild type p53 is not sufficient to commit these cells to apoptosis. A recently developed small molecule inhibitor of Puma mediated apoptosis could be a useful tool in dissecting

the role of Puma in relation to this drug combination (Mustata et al., 2011). Lead compounds tested in Mustata et al., perturbed the interaction between the BH3 domain of Puma and the anti-apoptotic Bcl-2 family members, such that these compounds partially protected NCCIT cells from the pro-apoptotic effects of ionizing radiation (Mustata et al., 2011). It would be interesting to see whether this inhibitor could protect RCC cells from the pro-apoptotic effect of the Nutlin-3/ABT-737 combination.

One question that has not been addressed in this study, which may be worth pursuing, is the role of p53 in directly inducing apoptosis at the mitochondria. This has been a controversial issue amongst researchers in the p53 field (Speidel, 2010) and the exact role of p53 at the mitochondria is still subject to debate. Methodology described in this study permitted the preparation of enriched mitochondrial fractions (figures 4.2.5.4 and 4.2.5.5) however contamination of nuclear protein in the form of Histone H3 was present (figures 4.2.5.3 and 4.2.5.2). This would have cast doubt on any potential observations regarding p53 at the mitochondrial because the function of p53 as a transcription factor means p53 is predominantly a nuclear protein and it would be impossible to distinguish p53 that had leaked from the nucleus due to apoptosis (or the homogenization technique) and mitochondrial p53. Because the combination of Nutlin-3 and ABT-737 was such a potent inducer of apoptosis, it was almost impossible to isolate mitochondria from cells without contamination from proteins from the nucleus. One possibility to address the possible role of mitochondrial p53 in response to the combination of Nutlin-3 and ABT-737 is the use of a small molecule inhibitor of mitochondrial p53-mediated apoptosis (Strom et al., 2006). This compound, pifithrin-μ has been shown to inhibit transcription-

independent-p53-dependent mitochondrial apoptosis (Vaseva et al., 2009) by interfering with the interaction between p53 and anti-apoptotic protein Bcl-xL (Hagn et al., 2010). If treatment, or pre-treatment of RCC cells harbouring wild type p53 with pifithrin-μ rescued these cells from the pro-apoptotic effects of the combination of Nutlin-3 and ABT-737, it could be speculated that p53 acting at the mitochondria was contributing towards that apoptosis taking place in response to the combination. This is unlikely to be the case however, as studies examining p53 localization to mitochondria in the kidney epithelium of healthy mice treated with whole body ionizing radiation showed that p53 did not localize to the mitochondria in response to this stressor (Erster et al., 2004) and as expected, apoptosis did not take place.

The basis p53-dependent cell death in renal epithelial cells has been well characterised in response to certain stimuli but remains elusive in response to others. For example, apoptosis in renal epithelial cells is believed to involve p53 in response to ischemia-reperfusion injury, cisplatin treatment and chronic obstructive uropathy (Jiang et al., 2004; Kelly et al., 2003; Choi et al., 2001). However, as discussed in Section 1.1.6.2, p53-dependent apoptosis does not take place in the renal epithelium in response to ionizing radiation (MacCallum et al., 1996). Of the stressors that can promote apoptosis in renal epithelium cells, the role of p53 is best characterized in the response to the chemotherapeutic drug, cisplatin. Cisplatin treatment can promote both p53-dependent and p53-independent apoptosis in renal epithelial cells (Jiang et al., 2009; Dos Santos et al., 2012). Puma is up-regulated by p53 in renal epithelial cells in response to cisplatin treatment and this results in Bax activation and apoptosis (Jiang et al., 2006). To the author's knowledge, there has been no study of Puma levels at the renal epithelium in response to ionizing radiation,

however, regardless of whether ionizing radiation can promote the up-regulation of Puma at the renal epithelium, the fact remains that cells derived from the renal epithelium are incapable of undergoing p53-dependent apoptosis in response to ionizing radiation (MacCallum et al., 1996). Thus, the pro-apoptotic response of p53 in renal tubular cells appears to be stimulus-specific. This issue is confounded further by the observation that RCC cells are resistant to cisplatin and other chemotherapeutic agents. Whilst the phenotype of RCC cells in response to ionizing radiation is consistent with the response of renal epithelium cells to the same stimulus, it is plausible that mutations acquired during the transformation process that result in aberrant death/survival signalling render RCC cells insensitive to the pro-apoptotic effects of cisplatin. Why p53 in RCC cells is incapable of inducing apoptosis, even upon inhibition of MDM2 remains elusive. Data presented herein showed that p53 was capable of up-regulating Puma in RCC cells upon inhibition of MDM2, but up-regulation of Puma alone was insufficient to commit RCC cells to apoptosis (Sections 3.2.3 and 4.2.2). The role of Noxa in promoting apoptosis in renal epithelial cells is less well characterized. One possible to mechanism that RCC cells depend upon to resist pro-apoptotic signals is an increase in the expression of the anti-apoptotic Bcl-2 family members. The observation that RCC cells possess higher levels of anti-apoptotic proteins when compared to non-tumour derived HEK293 cells (Section 4.2.1) is consistent with this possibility. Additional evidence in support of this hypothesis comes from the use of BH3 profiling, a functional assay that measures "priming" of the mitochondria by pro-apoptotic BH3-only proteins, using peptides derived from the alpha helices of BH3-only proteins (Certo et al., 2006). Mitochondrial "priming" describes proximity to the apoptotic threshold governed by the balance between pro-apoptotic and anti-apoptotic proteins. In

samples derived from patients presenting with different cancers, higher mitochondrial priming by pro-apoptotic BH3-only proteins was correlated with increased sensitivity to chemotherapy and lower mitochondrial priming was correlated with chemo-resistance (Ni Chongaille et al., 2011). Renal cancer samples exhibited low mitochondrial priming, consistent with other tumour types that are traditionally chemo-resistant. Hence, one mechanism RCC cells may use to resist pro-apoptotic signals is the up-regulation of anti-apoptotic proteins. One way to determine whether members of the anti-apoptotic Bcl-2 family are involved in resistance to the combination of Nutlin-3 and ABT-737 would be to perform siRNA knockdown of individual members of the Bcl-2 family in RCC cells and treat with the combination drugs. Increased sensitivity upon knockdown of Bcl-w, for example, would suggest that Bcl-w is involved in mediating resistance to the combination treatment.

Most of the experiments in this study used 10μM ABT-737, which is considered to be a high concentration of ABT-737 (Rooswinkel et al., 2012). As ABT-737 functions most effectively as an inhibitor of Bcl-2, and less so for Bcl-xL and Bcl-w, this is may be due to the relatively low or undetectable level of Bcl-2 protein in most of the cells lines tested (figure 4.2.1.1). On the other hand, relatively high levels of Bcl-xL were present in most of the cell lines tested. It may therefore prove useful to test Nutlin-3 in combination with commercially available inhibitors of Bcl-xL (Shoemaker et al., 2006; Park et al., 2013) to observe whether the synergistic effect is greater than that observed in response to Nutlin-3 and ABT-737. Using a compound that has increased specificity to the relevant member of the anti-apoptotic

Bcl-2 family member may result in a greater pro-apoptotic effect when combined with Nutlin-3.

Data presented in Section 3.2.4 showed that combining an inhibitor of the ubiquitin ligase activity of MDM2 rather than an inhibitor of the p53-MDM2 interaction with ABT-737 did not result in a synergistic drug interaction in the cell lines tested, which all possessed wild type p53. This raised some interesting questions regarding the nature of the regulation of p53 by MDM2 in RCC cells that harbour wild type p53. What is more important to the regulation of p53 by MDM2 in RCC cells, binding of MDM2 to p53 or ubiquitination of p53 by MDM2? The HLI series of compound have not been studied to the degree that the Nutlins have been but the HLI compounds have been shown to be inhibitors of ubiquitin ligases with some specificity towards MDM2. The HLI series of compounds, and their derivatives, the MPD family (Roxburgh et al., 2012) have been shown to promote stabilization of p53 via the inhibition of the ubiquitin ligase activity of MDM2 (Yang et al., 2005; Kitagaki et al., 2008). This has resulted either p53-dependent cell cycle arrest or apoptosis. One issue regarding the HLI compounds that has not been addressed is the degree to which MDM2 can bind to p53 following treatment with HLI compounds. This could be addressed by immunoprecipitating p53 from cells that had been treated with HLI373 and then using an antibody towards MDM2 to detect binding between p53 and MDM2 in the immunoprecipitates. This experiment would ideally be performed in cells that lack both p53 and MDM2 or at least cells that did not possess the p53-inducible MDM2 promoter, to account for increased p53-MDM2 interaction as a result of p53-mediated MDM2 up-regulation that would result from treatment of cells with HLI373. This way the effect of HLI373 treatment on the p53-

MDM2 interaction could be addressed. To determine the downstream effects of HLI373 treatment on MDM2 functions that are independent of the ubiquitin ligase function of MDM2, p53-null cells such as H1299 or SAOS2 cells could be co-transfected with expression vectors for p53 and MDM2 that has the Cys464Ala mutation in the ring-finger domain of MDM2. This would begin to address how MDM2 that is inhibited by HLI373 could affect p53 function.

Noon et al., showed that up-regulation of both p53 and MDM2 could serve as a biomarker for the identification of patients with poor prognosis (Noon et al., 2012). Data presented in this thesis showed that the combination of Nutlin-3 and ABT-737 was most effective in cell lines that harboured relatively high levels of wild type p53 and MDM2. The 117 cell line, which has relatively low levels of wild type p53 and MDM2 behaved very similarly to RCC cells that possessed mutant p53 with respect to sensitivity of this cell line to the combination of Nutlin-3 and ABT-737 (figure 3.2.3.9). Further, down-regulation of p53 by shRNA in ACHN cells also abrogated the pro-apoptotic effect of the combination (figure 3.2.2.3). Hence, we have identified a combination of drugs that hypothetically would appear to be most effective in a biomarker-defined subset of patients. Preliminary *in vitro* testing of this combination of Nutlin-3 and ABT-737 in combination with the tyrosine kinase inhibitors used to treat patients suffering from RCC, Sorafenib and Sunitinib, suggest that the inhibitory effect of the combination of Nutlin-3 and ABT-737 is unaffected by tyrosine kinase inhibitors (data not shown). A clinical trial using the combination of Nutlin-3 and ABT-737 would be conducted in combination with the current standard of care, which would be a tyrosine kinase inhibitor or a mTOR inhibitor, hence the importance of testing Nutlin-3 and ABT-737 in combination with

Sorafenib and Sunitinib. Further pre-clinical research into the combination of Nutlin-3 and ABT-737 would be required before any testing on patients and this would take the form of xenograft models in nude mice. Studies determining dose limiting toxicity of the combination of compounds would be required initially, followed by optimization of the dosing schedule. Factors to be optimized would the dose of compounds, timing and frequency of administration of the drugs and possibly staggering each drug as a way of limiting toxicity. Should this combination of compounds ever proceed to phase I trials, it would interesting to test the combination on patients that have tumours with high levels of wild type p53, which could be established from IHC analysis of resected tumours, if the patient had a relapse following nephrectomy.

To summarize, the combination of Nutlin-3 and ABT-737 synergistically promotes p53-dependent apoptosis in RCC cells harbouring wild type p53. The apoptosis is substantially Bax-dependent and further work is required to elucidate the exact mechanism underlying the induction of apoptosis however we believe that this combination offers potential for pre-clinical development.

References

Acosta JC, Gil J. Senescence: a new weapon for cancer therapy. Trends Cell Biol. 2012; 22(4): 211-9.

Andree HA, Willems GM, Hauptmann R, Maurer-Fogy I, Stuart MC, Hermens WT, Frederik PM, Reutelingsperger CP. Aggregation of phospholipid vesicles by a chimeric protein with the N-terminus of annexin I and the core of annexin V. Biochemistry. 1993; 32(17): 4634-40.

Azam F, Mehta S, Harris AL. Mechanisms of resistance to antiangiogenesis therapy. Eur J Cancer. 2010; 46(8):1323

Baba M, Hong SB, Sharma N, Warren MB, Nickerson ML, Iwamatsu A, Esposito D, Gillette WK, Hopkins RF 3rd, Hartley JL, Furihata M, Oishi S, Zhen W, Burke TR Jr, Linehan WM, Schmidt LS, Zbar B. Folliculin encoded by the BHD gene interacts with a binding protein, FNIP1, and AMPK, and is involved in AMPK and mTOR signaling. Proc Natl Acad Sci U S A. 2006;103(42):15552-7

Baker SJ, Fearon ER, Nigro JM, Hamilton SR, Preisinger AC, Jessup JM, vanTuinen P, Ledbetter DH, Barker DF, Nakamura Y, White R, Vogelstein B. Chromosome 17 deletions and p53 gene mutations in colorectal carcinomas. Science. 1989; 244(4901):217-21.

Baldewijns MM, van Vlodrop IJ, Vermeulen PB, Soetekouw PM, van Engeland M, de Bruïne AP. VHL and HIF signalling in renal cell carcinogenesis. J Pathol. 2010; 221(2):125-38.

Banin S, Moyal L, Shieh S, Taya Y, Anderson CW, Chessa L, Smorodinsky NI, Prives C, Reiss Y, Shiloh Y, Ziv Y. Enhanced phosphorylation of p53 by ATM in response to DNA damage. Science. 1998; 281(5383):1674-7.

Bender T, Martinou JC. Where killers meet-permeabilization of the outer mitochondrial membrane during apoptosis. Cold Spring Harb Perspect Biol. 2013; 5(1):a011106.

Bertin-Ciftci J, Barré B, Le Pen J, Maillet L, Couriaud C, Juin P, Braun F. pRb/E2F-1-mediated caspase-dependent induction of Noxa amplifies the apoptotic effects of the Bcl-2/Bcl-xL inhibitor ABT-737. Cell Death Differ. 2013; 20(5):755-64.

Bhattacharya S1, Ray RM, Chaum E, Johnson DA, Johnson LR. Inhibition of Mdm2 sensitizes human retinal pigment epithelial cells to apoptosis. Invest Ophthalmol Vis Sci. 1;52(6):3368-80

Biswas S, Eisen T. Immunotherapeutic strategies in kidney cancer--when TKIs are not enough. Nat Rev Clin Oncol. 2009; 6(8):478-87.

Bliss, C.I., 1939. The toxicity of poisons applied jointly. Annals of Applied Biology 26, 585–615.

Bouvard V, Zaitchouk T, Vacher M, Duthu A, Canivet M, Choisy-Rossi C, Nieruchalski M, May E. Tissue and cell-specific expression of the p53-target genes: bax, fas, mdm2 and waf1/p21, before and following ionising irradiation in mice. Oncogene. 2000; 19(5):649-60.

Bradford, MM. "A rapid and sensitive method for the quantitation of microgram quantities of protein utilizing the principle of protein-dye binding." Anal. Biochem 1976; 72: 248-54.

Bratton SB, Salvesen GS. Regulation of the Apaf-1-caspase-9 apoptosome. J Cell Sci. 2010; 123(Pt 19):3209-14.

Bretheau D, Lechevallier E, de Fromont M, Sault MC, Rampal M, Coulange C. Prognostic value of nuclear grade of renal cell carcinoma. Cancer. 1995; 76(12):2543-9.

Brown JP, Wei W, Sedivy JM. Bypass of senescence after disruption of p21CIP1/WAF1 gene in normal diploid human fibroblasts. Science. 1997; 277(5327):831-4.

Bykov VJ, Issaeva N, Shilov A, Hultcrantz M, Pugacheva E, Chumakov P, Bergman J, Wiman KG, Selivanova G. Restoration of the tumor suppressor function to mutant p53 by a low-molecular-weight compound. Nat Med. 2002; 8(3):282-8.

Bykov VJ, Lambert JM, Hainaut P, Wiman KG. Mutant p53 rescue and modulation of p53 redox state. Cell Cycle. 2009; 8(16):2509-17.

Cartron PF, Gallenne T, Bougras G, Gautier F, Manero F, Vusio P, Meflah K, Vallette FM, Juin P. The first alpha helix of Bax plays a necessary role in its ligand-induced activation by the BH3-only proteins Bid and PUMA. Mol Cell. 2004 Dec 3;16(5):807-18.

Canman CE, Lim DS, Cimprich KA, Taya Y, Tamai K, Sakaguchi K, Appella E, Kastan MB, Siliciano JD. Activation of the ATM kinase by ionizing radiation and phosphorylation of p53. Science. 1998; 281(5383):1677-9.

Certo M, Del Gaizo Moore V, Nishino M, Wei G, Korsmeyer S, Armstrong SA, Letai A. Mitochondria primed by death signals determine cellular addiction to antiapoptotic BCL-2 family members. Cancer Cell. 2006; 9(5):351-65.

Chae HJ, Kang JS, Byun JO, Han KS, Kim DU, Oh SM, Kim HM, Chae SW, Kim HR. Molecular mechanism of staurosporine-induced apoptosis in osteoblasts. Pharmacol Res. 2000; 42(4):373-81.

Chan DA, Giaccia AJ. Harnessing synthetic lethal interactions in anticancer drug discovery. Nat Rev Drug Discov. 2011 May;10(5):351-64.

Chang J, Kim DH, Lee SW, Choi KY, Sung YC. Transactivation ability of p53 transcriptional activation domain is directly related to the binding affinity to TATA-binding protein. J Biol Chem. 1995; 270(42):25014-9.

Chemeris G, Loktinov A, Rempel A, Schwarz M, Bannasch P. Elevated content of p53 protein in the absence of p53 gene mutations as a possible prognostic marker for human renal cell tumors. Virchows Arch. 1995; 426(6):563-9.

Chen J, Marechal V, Levine AJ. Mapping of the p53 and mdm-2 interaction domains. Mol Cell Biol. 1993; 13(7):4107-14.

Chen L, Willis SN, Wei A, Smith BJ, Fletcher JI, Hinds MG, Colman PM, Day CL, Adams JM, Huang DC. Differential targeting of prosurvival Bcl-2 proteins by their BH3-only ligands allows complementary apoptotic function. Mol Cell. 2005; 17(3):393-403.

Chipuk JE, Maurer U, Green DR, Schuler M. Pharmacologic activation of p53 elicits Bax-dependent apoptosis in the absence of transcription. Cancer Cell. 2003; 4(5):371-81.

Chipuk JE, Bouchier-Hayes L, Kuwana T, Newmeyer DD, Green DR. PUMA couples the nuclear and cytoplasmic proapoptotic function of p53. Science. 2005; 309(5741):1732-5.

Chipuk JE, Moldoveanu T, Llambi F, Parsons MJ, Green DR. The BCL-2 family reunion. Mol Cell. 2010; 37(3):299-310.

Cho Y, Gorina S, Jeffrey PD, Pavletich NP. Crystal structure of a p53 tumor suppressor-DNA complex: understanding tumorigenic mutations. Science. 1994; 265(5170):346-55.

Choi YJ, Mendoza L, Rha SJ, Sheikh-Hamad D, Baranowska-Daca E, Nguyen V, Smith CW, Nassar G, Suki WN, Truong LD. Role of p53-dependent activation of caspases in chronic obstructive uropathy: evidence from p53 null mutant mice. J Am Soc Nephrol. 2001; 12(5):983-92.

Chou TC. Theoretical basis, experimental design, and computerized simulation of synergism and antagonism in drug combination studies. Pharmacol Rev. 2006 Sep;58(3):621-81.

Chow WH, Dong LM, Devesa SS. Epidemiology and risk factors for kidney cancer. Nat Rev Urol. 2010; 7(5):245-57.

Cockman ME, Masson N, Mole DR, Jaakkola P, Chang GW, Clifford SC, Maher ER, Pugh CW, Ratcliffe PJ, Maxwell PH. Hypoxia inducible factor-alpha binding

and ubiquitylation by the von Hippel-Lindau tumor suppressor protein. J Biol Chem. 2000; 275(33):25733-41.

Clore GM, Omichinski JG, Sakaguchi K, Zambrano N, Sakamoto H, Appella E, Gronenborn AM. High-resolution structure of the oligomerization domain of p53 by multidimensional NMR. Science. 1994; 265(5170):386-91

Cory S, Adams JM. The Bcl2 family: regulators of the cellular life-or-death switch. Nat Rev Cancer. 2002; 2(9):647-56.

Coppé JP, Desprez PY, Krtolica A, Campisi J. The senescence-associated secretory phenotype: the dark side of tumor suppression. Annu Rev Pathol. 2010; 5:99-118.

Danial NN, Korsmeyer SJ. Cell death: critical control points. Cell. 2004; 116(2):205-19.

Davalos AR, Coppe JP, Campisi J, Desprez PY. Senescent cells as a source of inflammatory factors for tumor progression. Cancer Metastasis Rev. 2010; 29(2):273-83.

Deng J, Carlson N, Takeyama K, Dal Cin P, Shipp M, Letai A. BH3 profiling identifies three distinct classes of apoptotic blocks to predict response to ABT-737 and conventional chemotherapeutic agents. Cancer Cell. 2007; 12(2):171-85.

de Riese W, Goldenberg K, Allhoff E, Stief C, Schlick R, Liedke S, Jonas U. Metastatic renal cell carcinoma (RCC): spontaneous regression, long-term survival and late recurrence. Int Urol Nephrol. 1991; 23(1):13-25.

Desagher S, Osen-Sand A, Nichols A, Eskes R, Montessuit S, Lauper S, Maundrell K, Antonsson B, Martinou JC. Bid-induced conformational change of Bax is responsible for mitochondrial cytochrome c release during apoptosis. J Cell Biol. 1999; 144(5):891-901.

DeVita VT Jr, Young RC, Canellos GP. Combination versus single agent chemotherapy: a review of the basis for selection of drug treatment of cancer. Cancer. 1975 Jan;35(1):98-110.

Diaz-Moralli S, Tarrado-Castellarnau M, Miranda A, Cascante M. Targeting cell cycle regulation in cancer therapy. Pharmacol Ther. 2013; 138(2):255-71.

Ding K, Lu Y, Nikolovska-Coleska Z, Qiu S, Ding Y, Gao W, Stuckey J, Krajewski K, Roller PP, Tomita Y, Parrish DA, Deschamps JR, Wang S. Structure-based design of potent non-peptide MDM2 inhibitors. J Am Chem Soc. 2005; 127(29):10130-1.

dos Santos NA, Carvalho Rodrigues MA, Martins NM, dos Santos AC. Cisplatin-induced nephrotoxicity and targets of nephroprotection: an update. Arch Toxicol.

2012; 86(8):1233-50

Druker BJ, Guilhot F, O'Brien SG, Gathmann I, Kantarjian H, Gattermann N, Deininger MW, Silver RT, Goldman JM, Stone RM, Cervantes F, Hochhaus A, Powell BL, Gabrilove JL, Rousselot P, Reiffers J, Cornelissen JJ, Hughes T, Agis H, Fischer T, Verhoef G, Shepherd J, Saglio G, Gratwohl A, Nielsen JL, Radich JP, Simonsson B, Taylor K, Baccarani M, So C, Letvak L, Larson RA; IRIS Investigators. Five-year follow-up of patients receiving imatinib for chronic myeloid leukemia. N Engl J Med. 2006 Dec 7;355(23):2408-17.

Duriez PJ, Shah GM. Cleavage of poly(ADP-ribose) polymerase: a sensitive parameter to study cell death. Biochem Cell Biol. 1997;75(4):337-49.

Düssmann H, Rehm M, Concannon CG, Anguissola S, Würstle M, Kacmar S, Völler P, Huber HJ, Prehn JH. Single-cell quantification of Bax activation and mathematical modelling suggest pore formation on minimal mitochondrial Bax accumulation. Cell Death Differ. 2010;17(2):278-90.

Ebos JM, Lee CR, Cruz-Munoz W, Bjarnason GA, Christensen JG, Kerbel RS. Accelerated metastasis after short-term treatment with a potent inhibitor of tumor angiogenesis. Cancer Cell. 2009 Mar 3;15(3):232-9

Elmore JM, Kadesky KT, Koeneman KS, Sagalowsky AI. Reassessment of the 1997 TNM classification system for renal cell carcinoma. Cancer. 2003; 98(11):2329-34.

Elmore S. Apoptosis: a review of programmed cell death. Toxicol Pathol. 2007; 35(4):495-516.

El-Deiry WS, Kern SE, Pietenpol JA, Kinzler KW, Vogelstein B. Definition of a consensus binding site for p53. Nat Genet. 1992; 1(1):45-9.

El-Deiry WS, Tokino T, Velculescu VE, Levy DB, Parsons R, Trent JM, Lin D, Mercer WE, Kinzler KW, Vogelstein B. WAF1, a potential mediator of p53 tumor suppression. Cell. 1993; 75(4):817-25.

El-Deiry WS, Harper JW, O'Connor PM, Velculescu VE, Canman CE, Jackman J, Pietenpol JA, Burrell M, Hill DE, Wang Y, et al. WAF1/CIP1 is induced in p53-mediated G1 arrest and apoptosis. Cancer Res. 1994; 54(5):1169-74.

Eliyahu D, Raz A, Gruss P, Givol D, Oren M. Participation of p53 cellular tumour antigen in transformation of normal embryonic cells. Nature. 1984; 312(5995):646-9.

Eliyahu D, Michalovitz D, Eliyahu S, Pinhasi-Kimhi O, Oren M. Wild-type p53 can inhibit oncogene-mediated focus formation. Proc Natl Acad Sci U S A. 1989; 86(22):8763-7.

Erster S, Mihara M, Kim RH, Petrenko O, Moll UM. In vivo mitochondrial p53

translocation triggers a rapid first wave of cell death in response to DNA damage that can precede p53 target gene activation. Mol Cell Biol. 2004 Aug;24(15):6728-41.

Eskes R, Desagher S, Antonsson B, Martinou JC. Bid induces the oligomerization and insertion of Bax into the outer mitochondrial membrane. Mol Cell Biol. 2000; 20(3):929-35.

Fang S, Jensen JP, Ludwig RL, Vousden KH, Weissman AM. Mdm2 is a RING finger-dependent ubiquitin protein ligase for itself and p53. J Biol Chem. 2000; 275(12):8945-51.

Ficarra V, Righetti R, Martignoni G, D'Amico A, Pilloni S, Rubilotta E, Malossini G, Mobilio G. Prognostic value of renal cell carcinoma nuclear grading: multivariate analysis of 333 cases. Urol Int. 2001; 67(2):130-4.

Fridman JS, Lowe SW. Control of apoptosis by p53. Oncogene. 2003; 22(56): 9030-40.

Fuhrman SA, Lasky LC, Limas C. Prognostic significance of morphologic parameters in renal cell carcinoma. Am J Surg Pathol. 1982; 6(7):655-63.

Fyfe G, Fisher RI, Rosenberg SA, Sznol M, Parkinson DR, Louie AC. Results of treatment of 255 patients with metastatic renal cell carcinoma who received high-dose recombinant interleukin-2 therapy. J Clin Oncol. 1995; 13(3):688-96.

Gallenne T, Gautier F, Oliver L, Hervouet E, Noël B, Hickman JA, Geneste O, Cartron PF, Vallette FM, Manon S, Juin P. Bax activation by the BH3-only protein Puma promotes cell dependence on antiapoptotic Bcl-2 family members. J Cell Biol. 2009; 185(2):279-90.

Garrison SP, Phillips DC, Jeffers JR, Chipuk JE, Parsons MJ, Rehg JE, Opferman JT, Green DR, Zambetti GP. Genetically defining the mechanism of Puma- and Bim-induced apoptosis. Cell Death Differ. 2012;19(4):642-9.

Gire V, Roux P, Wynford-Thomas D, Brondello JM, Dulic V. DNA damage checkpoint kinase Chk2 triggers replicative senescence. EMBO J. 2004; 23(13):2554-63.

Goldoni M, Johansson C. A mathematical approach to study combined effects of toxicants in vitro: evaluation of the Bliss independence criterion and the Loewe additivity model. Toxicol In Vitro. 2007; 21(5):759-69.

Gnarra JR, Tory K, Weng Y, Schmidt L, Wei MH, Li H, Latif F, Liu S, Chen F, Duh FM, et al. Mutations of the VHL tumour suppressor gene in renal carcinoma. Nat Genet. 1994; 7(1):85-90.

Gu W, Roeder RG. Activation of p53 sequence-specific DNA binding by acetylation

of the p53 C-terminal domain. Cell. 1997; 90(4):595-606.

Gupta K, Miller JD, Li JZ, Russell MW, Charbonneau C. Epidemiologic and socioeconomic burden of metastatic renal cell carcinoma (mRCC): a literature review. Cancer Treat Rev. 2008; 34(3):193-205.

Hagn F, Klein C, Demmer O, Marchenko N, Vaseva A, Moll UM, Kessler H. BclxL changes conformation upon binding to wild-type but not mutant p53 DNA binding domain. J Biol Chem. 2010 Jan 29;285(5):3439-50.

Hainaut P, Soussi T, Shomer B, Hollstein M, Greenblatt M, Hovig E, Harris CC, Montesano R. Database of p53 gene somatic mutations in human tumors and cell lines: updated compilation and future prospects. Nucleic Acids Res. 1997; 25(1):151-7.

Haitel A, Wiener HG, Baethge U, Marberger M, Susani M. mdm2 expression as a prognostic indicator in clear cell renal cell carcinoma: comparison with p53 overexpression and clinicopathological parameters. Clin Cancer Res. 2000; 6(5):1840-4.

Han J, Flemington C, Houghton AB, Gu Z, Zambetti GP, Lutz RJ, Zhu L, Chittenden T. Expression of bbc3, a pro-apoptotic BH3-only gene, is regulated by diverse cell death and survival signals. Proc Natl Acad Sci U S A. 2001; 98(20):11318-23.

Hanahan D, Weinberg RA. The hallmarks of cancer. Cell. 2000; 100(1):57-70.

Happo L, Strasser A, Cory S. BH3-only proteins in apoptosis at a glance. J Cell Sci. 2012; 125(5):1081-7.

Hardcastle IR, Ahmed SU, Atkins H, Calvert AH, Curtin NJ, Farnie G, Golding BT, Griffin RJ, Guyenne S, Hutton C, Källblad P, Kemp SJ, Kitching MS, Newell DR, Norbedo S, Northen JS, Reid RJ, Saravanan K, Willems HM, Lunec J. Isoindolinone-based inhibitors of the MDM2-p53 protein-protein interaction. Bioorg Med Chem Lett. 2005; 15(5):1515-20.

Hasumi H, Baba M, Hong SB, Hasumi Y, Huang Y, Yao M, Valera VA, Linehan WM, Schmidt LS. Identification and characterization of a novel folliculin-interacting protein FNIP2.
Gene. 2008; 415(1-2):60-7.

Hauck P, Chao BH, Litz J, Krystal GW. Alterations in the Noxa/Mcl-1 axis determine sensitivity of small cell lung cancer to the BH3 mimetic ABT-737. Mol Cancer Ther. 2009; 8(4):883-92

Henry RE, Andrysik Z, París R, Galbraith MD, Espinosa JM. A DR4:tBID axis drives the p53 apoptotic response by promoting oligomerization of poised BAX.

EMBO J. 2012 Mar 7;31(5):1266-78.

Herman JG, Latif F, Weng Y, Lerman MI, Zbar B, Liu S, Samid D, Duan DS, Gnarra JR, Linehan WM, et al. Silencing of the VHL tumor-suppressor gene by DNA methylation in renal carcinoma. Proc Natl Acad Sci U S A. 1994; 91(21):9700-4.

Hermeking H, Lengauer C, Polyak K, He TC, Zhang L, Thiagalingam S, Kinzler KW, Vogelstein B. 14-3-3 sigma is a p53-regulated inhibitor of G2/M progression. Mol Cell. 1997 Dec;1(1):3-11.

Hinds P, Finlay C, Levine AJ. Mutation is required to activate the p53 gene for cooperation with the ras oncogene and transformation. J Virol. 1989; 63(2):739-46.

Hikisz P, Kiliańska ZM. PUMA, a critical mediator of cell death--one decade on from its discovery. Cell Mol Biol Lett. 2012; 17(4):646-69.

Hollstein M, Sidransky D, Vogelstein B, Harris CC. p53 mutations in human cancers. Science. 1991; 253(5015):49-53

Honda R, Tanaka H, Yasuda H. Oncoprotein MDM2 is a ubiquitin ligase E3 for tumor suppressor p53. FEBS Lett. 1997; 420(1):25-7.

Hudson CC, Liu M, Chiang GG, Otterness DM, Loomis DC, Kaper F, Giaccia AJ, Abraham RT. Regulation of hypoxia-inducible factor 1alpha expression and function by the mammalian target of rapamycin. Mol Cell Biol. 2002;22(20):7004-14.

Hunt JD, van der Hel OL, McMillan GP, Boffetta P, Brennan P. Renal cell carcinoma in relation to cigarette smoking: meta-analysis of 24 studies. Int J Cancer. 2005; 114(1):101-8.

Hutson TE. Targeted therapies for the treatment of metastatic renal cell carcinoma: clinical evidence. Oncologist. 2011; 16 Suppl 2:14-22.

Iliopoulos O, Kibel A, Gray S, Kaelin WG Jr. Tumour suppression by the human von Hippel-Lindau gene product. Nat Med. 1995; 1(8):822-6.

Iwakuma T, Lozano G. MDM2, an introduction. Mol Cancer Res. 2003; 1(14):993-1000.

Jeffers M, Schmidt L, Nakaigawa N, Webb CP, Weirich G, Kishida T, Zbar B, Vande Woude GF. Activating mutations for the met tyrosine kinase receptor in human cancer. Proc Natl Acad Sci U S A. 1997; 94(21):11445-50.

Jiang M, Yi X, Hsu S, Wang CY, Dong Z. Role of p53 in cisplatin-induced tubular

cell apoptosis: dependence on p53 transcriptional activity. Am J Physiol Renal Physiol. 2004; 287(6):F1140-7.

Jiang M, Wei Q, Wang J, Du Q, Yu J, Zhang L, Dong Z. Regulation of PUMA-alpha by p53 in cisplatin-induced renal cell apoptosis. Oncogene. 2006; 25(29):4056-66.

Jiang M, Wang CY, Huang S, Yang T, Dong Z. Cisplatin-induced apoptosis in p53-deficient renal cells via the intrinsic mitochondrial pathway. Am J Physiol Renal Physiol. 2009; 296(5):F983-93

Nicholson J., Neelagandan K, Huart AS, Ball K, Molloy MP and Hupp T. An iTRAQ Proteomics Screen Reveals the Effects of the MDM2 Binding Ligand Nutlin-3 on Cellular Proteostasis. J. Proteome Res., 2012, 11(11):5464–5478

Jonasch E, Haluska FG. Interferon in oncological practice: review of interferon biology, clinical applications, and toxicities. Oncologist. 2001;6(1):34-55

Jones SN, Roe AE, Donehower LA, Bradley A. Rescue of embryonic lethality in Mdm2-deficient mice by absence of p53. Nature. 1995; 378(6553):206-8.

Kamura T, Koepp DM, Conrad MN, Skowyra D, Moreland RJ, Iliopoulos O, Lane WS, Kaelin WG Jr, Elledge SJ, Conaway RC, Harper JW, Conaway JW. Rbx1, a component of the VHL tumor suppressor complex and SCF ubiquitin ligase. Science. 1999; 284(5414):657-61.

Kastan MB, Zhan Q, el-Deiry WS, Carrier F, Jacks T, Walsh WV, Plunkett BS, Vogelstein B, Fornace AJ Jr. A mammalian cell cycle checkpoint pathway utilizing p53 and GADD45 is defective in ataxia-telangiectasia. Cell. 1992 Nov;71(4):587-97.

Katayama K, Fujita N, Tsuruo T. Akt/protein kinase B-dependent phosphorylation and inactivation of WEE1Hu promote cell cycle progression at G2/M transition. Mol Cell Biol. 2005; 25(13):5725-37.

Kelly KJ, Plotkin Z, Vulgamott SL, Dagher PC. P53 mediates the apoptotic response to GTP depletion after renal ischemia-reperfusion: protective role of a p53 inhibitor. J Am Soc Nephrol. 2003; 14(1):128-38.

Kerr JF, Wyllie AH, Currie AR. Apoptosis: a basic biological phenomenon with wide-ranging implications in tissue kinetics. Br J Cancer. 1972; 26(4):239-57.

Khoo SK, Kahnoski K, Sugimura J, Petillo D, Chen J, Shockley K, Ludlow J, Knapp R, Giraud S, Richard S, Nordenskjöld M, Teh BT. Inactivation of BHD in sporadic renal tumors. Cancer Res. 2003; 63(15): 4583-7.

Khosravi R, Maya R, Gottlieb T, Oren M, Shiloh Y, Shkedy D. Rapid ATM-

dependent phosphorylation of MDM2 precedes p53 accumulation in response to DNA damage. Proc Natl Acad Sci U S A. 1999; 96(26):14973-7.

Kim H, Rafiuddin-Shah M, Tu HC, Jeffers JR, Zambetti GP, Hsieh JJ, Cheng EH. Hierarchical regulation of mitochondrion-dependent apoptosis by BCL-2 subfamilies. Nat Cell Biol. 2006;8(12):1348-58.

Kim H, Tu HC, Ren D, Takeuchi O, Jeffers JR, Zambetti GP, Hsieh JJ, Cheng EH. Stepwise activation of BAX and BAK by tBID, BIM, and PUMA initiates mitochondrial apoptosis. Mol Cell. 2009;36(3):487-99.

Kitagaki J, Agama KK, Pommier Y, Yang Y, Weissman AM. Targeting tumor cells expressing p53 with a water-soluble inhibitor of Hdm2. Mol Cancer Ther. 2008; 7(8):2445-54.

Knudson AG Jr. Mutation and cancer: statistical study of retinoblastoma. Proc Natl Acad Sci U S A. 1971; 68(4):820-3.

Kojima K, Konopleva M, Samudio IJ, Shikami M, Cabreira-Hansen M, McQueen T, Ruvolo V, Tsao T, Zeng Z, Vassilev LT, Andreeff M. MDM2 antagonists induce p53-dependent apoptosis in AML: implications for leukemia therapy. Blood. 2005; 106(9):3150-9.

Kojima K, Konopleva M, McQueen T, O'Brien S, Plunkett W, Andreeff M. Mdm2 inhibitor Nutlin-3a induces p53-mediated apoptosis by transcription-dependent and transcription-independent mechanisms and may overcome Atm-mediated resistance to fludarabine in chronic lymphocytic leukemia. Blood. 2006; 108(3):993-1000.

Koopman G, Reutelingsperger CP, Kuijten GA, Keehnen RM, Pals ST, van Oers MH. Annexin V for flow cytometric detection of phosphatidylserine expression on B cells undergoing apoptosis. Blood. 1994 Sep 1;84(5):1415-20.

Kopp RP, Mehrazin R, Palazzi KL, Liss MA, Jabaji R, Mirheydar HS, Lee HJ, Patel N, Elkhoury F, Patterson AL, Derweesh IH. Survival Outcomes after Radical and Partial Nephrectomy for Clinical T2 Renal Tumors Categorized by RENAL Nephrometry Score. BJU Int. 2013 Nov 26.

Kracikova M, Akiri G, George A, Sachidanandam R, Aaronson SA. A threshold mechanism mediates p53 cell fate decision between growth arrest and apoptosis. Cell Death Differ. 2013; 20(4):576-88.

Kress M, May E, Cassingena R, May P. Simian virus 40-transformed cells express new species of proteins precipitable by anti-simian virus 40 tumor serum. J Virol. 1979 Aug;31(2):472-83.

Krtolica A, Parrinello S, Lockett S, Desprez PY, Campisi J. Senescent fibroblasts promote epithelial cell growth and tumorigenesis: a link between cancer and aging. Proc Natl Acad Sci U S A. 2001; 98(21):12072-7.

Kruse JP, Gu W. Modes of p53 regulation. Cell. 2009 May; 137(4):609-22.

Kubbutat MH, Jones SN, Vousden KH. Regulation of p53 stability by Mdm2. Nature. 1997 May 15;387(6630):299-303.

Kummar S, Chen HX, Wright J, Holbeck S, Millin MD, Tomaszewski J, Zweibel J, Collins J, Doroshow JH. Utilizing targeted cancer therapeutic agents in combination: novel approaches and urgent requirements. Nat Rev Drug Discov. 2010 Nov;9(11):843-56

Kussie PH, Gorina S, Marechal V, Elenbaas B, Moreau J, Levine AJ, Pavletich NP. Structure of the MDM2 oncoprotein bound to the p53 tumor suppressor transactivation domain. Science. 1996; 274(5289):948-53.

Lane DP, Crawford LV. T antigen is bound to a host protein in SV40-transformed cells. Nature. 1979; 278(5701):261-3.

Lane DP. Cancer. p53, guardian of the genome. Nature. 1992; 358(6381):15-6

Laplante M, Sabatini DM. mTOR signaling in growth control and disease. Cell. 2012; 149(2):274-93.

Larsson LG. Oncogene- and tumor suppressor gene-mediated suppression of cellular senescence. Semin Cancer Biol. 2011; 21(6):367-76.

Latif F, Tory K, Gnarra J, Yao M, Duh FM, Orcutt ML, Stackhouse T, Kuzmin I, Modi W, Geil L, et al. Identification of the von Hippel-Lindau disease tumor suppressor gene. Science. 1993; 260(5112):1317-20.

Lavrik IN, Krammer PH. Regulation of CD95/Fas signaling at the DISC. Cell Death Differ. 2012; 19(1):36-41.

Lekanidi K, Vlachou PA, Morgan B, Vasanthan S. Spontaneous regression of metastatic renal cell carcinoma: case report. J Med Case Rep. 2007; 1:89.

Letai A. BH3 domains as BCL-2 inhibitors: prototype cancer therapeutics. Expert Opin Biol Ther. 2003; 3(2):293-304.

Lin Y, Ma W, Benchimol S. Pidd, a new death-domain-containing protein, is induced by p53 and promotes apoptosis. Nat Genet. 2000; 26(1):122-7.

Linares LK, Hengstermann A, Ciechanover A, Müller S, Scheffner M. HdmX stimulates Hdm2-mediated ubiquitination and degradation of p53. Proc Natl Acad Sci U S A. 2003; 100(21):12009-14.

Linehan WM, Grubb RL, Coleman JA, Zbar B, Walther MM. The genetic basis of cancer of kidney cancer: implications for gene-specific clinical management. BJU Int. 2005; 95 Suppl 2:2-7.

Linzer DI, Levine AJ. Cell. Characterization of a 54K dalton cellular SV40 tumor antigen present in SV40-transformed cells and uninfected embryonal carcinoma cells. 1979; 17(1):43-52.

Liu X, Miller CW, Koeffler PH, Berk AJ. The p53 activation domain binds the TATA box-binding polypeptide in Holo-TFIID, and a neighboring p53 domain inhibits transcription. Mol Cell Biol. 1993;13(6):3291-300.

Lodish H, Berk A, Zipursky SL, Matsudaira P, Baltimore D, Darnell J. Molecular Cell Biology, 4th edition. New York: W. H. Freeman; 2000.

Lopez-Beltran A, Scarpelli M, Montironi R, Kirkali Z. 2004 WHO classification of the renal tumors of the adults. Eur Urol. 2006; 49(5):798-805

Lohrum MA, Woods DB, Ludwig RL, Bálint E, Vousden KH. C-terminal ubiquitination of p53 contributes to nuclear export. Mol Cell Biol. 2001; 21(24):8521-32.

Lovell JF, Billen LP, Bindner S, Shamas-Din A, Fradin C, Leber B, Andrews DW. Membrane binding by tBid initiates an ordered series of events culminating in membrane permeabilization by Bax. Cell. 2008; 135(6):1074-84.

Loewe S (1953) The problem of synergism and antagonism of combined drugs. Arzneim-Forsch 3:285–290.

Lowe SW, Sherr CJ. Tumor suppression by Ink4a-Arf: progress and puzzles. Curr Opin Genet Dev. 2003; 13(1):77-83.

Lu H, Levine AJ. Human TAFII31 protein is a transcriptional coactivator of the p53 protein. Proc Natl Acad Sci U S A. 1995; 92(11):5154-8.

Lubensky IA, Gnarra JR, Bertheau P, Walther MM, Linehan WM, Zhuang Z. Allelic deletions of the VHL gene detected in multiple microscopic clear cell renal lesions in von Hippel-Lindau disease patients. Am J Pathol. 1996; 149(6):2089-94.

Luo J, Su F, Chen D, Shiloh A, Gu W. Deacetylation of p53 modulates its effect on cell growth and apoptosis. Nature. 2000; 408(6810):377-81.

MacCallum DE, Hupp TR, Midgley CA, Stuart D, Campbell SJ, Harper A, Walsh FS, Wright EG, Balmain A, Lane DP, Hall PA. The p53 response to ionising radiation in adult and developing murine tissues. Oncogene. 1996; 13(12):2575-87.

Marine JC, Dyer MA, Jochemsen AG. MDMX: from bench to bedside. J Cell Sci. 2007 Feb 1;120(Pt 3):371-8.

Maxwell PH, Wiesener MS, Chang GW, Clifford SC, Vaux EC, Cockman ME, Wykoff CC, Pugh CW, Maher ER, Ratcliffe PJ. The tumour suppressor protein VHL targets hypoxia-inducible factors for oxygen-dependent proteolysis. Nature. 1999; 399(6733):271-5.

McDermott DF, Regan MM, Clark JI, Flaherty LE, Weiss GR, Logan TF, Kirkwood JM, Gordon MS, Sosman JA, Ernstoff MS, Tretter CP, Urba WJ, Smith JW, Margolin KA, Mier JW, Gollob JA, Dutcher JP, Atkins MB. Randomized phase III trial of high-dose interleukin-2 versus subcutaneous interleukin-2 and interferon in patients with metastatic renal cell carcinoma. J Clin Oncol. 2005; 23(1):133-41

Medcalf AS1, Klein-Szanto AJ, Cristofalo VJ. Expression of p21 is not required for senescence of human fibroblasts. Cancer Res. 1996 Oct 15;56(20):4582-5.

Medeiros LJ, Gelb AB, Weiss LM. Renal cell carcinoma. Prognostic significance of morphologic parameters in 121 cases. Cancer. 1988 Apr 15;61(8):1639-51.

Mendrysa SM, Perry ME. The p53 tumor suppressor protein does not regulate expression of its own inhibitor, MDM2, except under conditions of stress. Mol Cell Biol. 2000 Mar;20(6):2023-30.

Menko FH, van Steensel MA, Giraud S, Friis-Hansen L, Richard S, Ungari S, Nordenskjöld M, Hansen TV, Solly J, Maher ER; European BHD Consortium. Birt-Hogg-Dubé syndrome: diagnosis and management. Lancet Oncol. 2009 Dec;10(12):1199-206.

Mercer WE, Avignolo C, Baserga R. Role of the p53 protein in cell proliferation as studied by microinjection of monoclonal antibodies. Mol Cell Biol. 1984; 4(2):276-81.

Milner J, McCormick F. Lymphocyte stimulation: concanavalin A induces the expression of a 53K protein. Cell Biol Int Rep. 1980; 4(7):663-7.

Miyashita T, Krajewski S, Krajewska M, Wang HG, Lin HK, Liebermann DA, Hoffman B, Reed JC. Tumor suppressor p53 is a regulator of bcl-2 and bax gene expression in vitro and in vivo. Oncogene. 1994; 9(6):1799-805.

Miyashita T, Reed JC. Tumor suppressor p53 is a direct transcriptional activator of the human bax gene. Cell. 1995; 80(2):293-9.

Moch H, Sauter G, Gasser TC, Buchholz N, Bubendorf L, Richter J, Jiang F, Dellas A, Mihatsch MJ. p53 protein expression but not mdm-2 protein expression is associated with rapid tumor cell proliferation and prognosis in renal cell carcinoma. Urol Res. 1997;25 Suppl 1:S25-30.

Mosmann T. Rapid colorimetric assay for cellular growth and survival: application

to proliferation and cytotoxicity assays. J Immunol Methods. 1983; 65(1-2):55-63.

Mustata G, Li M, Zevola N, Bakan A, Zhang L, Epperly M, Greenberger JS, Yu J, Bahar I. Development of small-molecule PUMA inhibitors for mitigating radiation-induced cell death. Curr Top Med Chem. 2011;11(3):281-90.

Nakano K, Vousden KH. PUMA, a novel proapoptotic gene, is induced by p53. Mol Cell. 2001; 7(3):683-94.

Ni Chonghaile T, Sarosiek KA, Vo TT, Ryan JA, Tammareddi A, Moore Vdel G, Deng J, Anderson KC, Richardson P, Tai YT, Mitsiades CS, Matulonis UA, Drapkin R, Stone R, Deangelo DJ, McConkey DJ, Sallan SE, Silverman L, Hirsch MS, Carrasco DR, Letai A. Pretreatment mitochondrial priming correlates with clinical response to cytotoxic chemotherapy. Science. 2011; 334(6059):1129-33.

Nickerson ML, Warren MB, Toro JR, Matrosova V, Glenn G, Turner ML, Duray P, Merino M, Choyke P, Pavlovich CP, Sharma N, Walther M, Munroe D, Hill R, Maher E, Greenberg C, Lerman MI, Linehan WM, Zbar B, Schmidt LS. Mutations in a novel gene lead to kidney tumors, lung wall defects, and benign tumors of the hair follicle in patients with the Birt-Hogg-Dubé syndrome. Cancer Cell. 2002; (2):157-64.

Noon AP, Polański R, El-Fert AY, Kalirai H, Shawki H, Campbell F, Dodson A, Eccles RM, Lloyd BH, Sibson DR, Coupland SE, Lake SL, Parsons K, Vlatković N, Boyd MT. Combined p53 and MDM2 biomarker analysis shows a unique pattern of expression associated with poor prognosis in patients with renal cell carcinoma undergoing radical nephrectomy. BJU Int.;109(8):1250-7.

Noon AP, Vlatković N, Polański R, Maguire M, Shawki H, Parsons K, Boyd MT. p53 and MDM2 in renal cell carcinoma: biomarkers for disease progression and future therapeutic targets? Cancer. 2010; 116(4):780-90.

Norbury C, Nurse P. Animal cell cycles and their control. Annu Rev Biochem. 1992; 61:441-70.

Oda E, Ohki R, Murasawa H, Nemoto J, Shibue T, Yamashita T, Tokino T, Taniguchi T, Tanaka N. Noxa, a BH3-only member of the Bcl-2 family and candidate mediator of p53-induced apoptosis. Science. 2000; 288(5468):1053-8.

Ohh M, Park CW, Ivan M, Hoffman MA, Kim TY, Huang LE, Pavletich N, Chau V, Kaelin WG. Ubiquitination of hypoxia-inducible factor requires direct binding to the beta-domain of the von Hippel-Lindau protein. Nat Cell Biol. 2000; 2(7):423-7.

Ohki R, Nemoto J, Murasawa H, Oda E, Inazawa J, Tanaka N, Taniguchi T. Reprimo, a new candidate mediator of the p53-mediated cell cycle arrest at the G2 phase. J Biol Chem. 2000; 275(30):22627-30.

O'Keefe K, Li H, Zhang Y. Nucleocytoplasmic shuttling of p53 is essential for

MDM2-mediated cytoplasmic degradation but not ubiquitination. Mol Cell Biol. 2003; 23(18):6396-405.

Okorokov AL, Orlova EV. Structural biology of the p53 tumour suppressor. Curr Opin Struct Biol. 2009; 19(2):197-202.

Oliner JD, Pietenpol JA, Thiagalingam S, Gyuris J, Kinzler KW, Vogelstein B. Oncoprotein MDM2 conceals the activation domain of tumour suppressor p53. Nature. 1993; 362(6423):857-60.

Oltersdorf T, Elmore SW, Shoemaker AR, Armstrong RC, Augeri DJ, Belli BA, Bruncko M, Deckwerth TL, Dinges J, Hajduk PJ, Joseph MK, Kitada S, Korsmeyer SJ, Kunzer AR, Letai A, Li C, Mitten MJ, Nettesheim DG, Ng S, Nimmer PM, O'Connor JM, Oleksijew A, Petros AM, Reed JC, Shen W, Tahir SK, Thompson CB, Tomaselli KJ, Wang B, Wendt MD, Zhang H, Fesik SW, Rosenberg SH. An inhibitor of Bcl-2 family proteins induces regression of solid tumours. Nature. 2005; 435(7042):677-81.

Owen-Schaub LB, Zhang W, Cusack JC, Angelo LS, Santee SM, Fujiwara T, Roth JA, Deisseroth AB, Zhang WW, Kruzel E, et al. Wild-type human p53 and a temperature-sensitive mutant induce Fas/APO-1 expression. Mol Cell Biol. 1995; 15(6):3032-40.

Park D, Magis AT, Li R, Owonikoko TK, Sica GL, Sun SY, Ramalingam SS, Khuri FR, Curran WJ, Deng X. Novel small-molecule inhibitors of Bcl-XL to treat lung cancer. Cancer Res. 2013 Sep 1;73(17):5485-96.

Pavlovich CP, Schmidt LS. Searching for the hereditary causes of renal-cell carcinoma. Nat Rev Cancer. 2004; 4(5):381-93.

Perry, M. E., Piette, J., Zawadzki, J. A., Harvey, D., and Levine, A. J. The mdm-2 gene is induced in response to UV light in a p53-dependent manner. Proc. Natl. Acad. Sci. USA, 90: 11623–11627, 1993.

Peruzzi B, Bottaro DP. Targeting the c-Met signaling pathway in cancer. Clin Cancer Res. 2006; 12(12):3657-60.

Petitjean A, Mathe E, Kato S, Ishioka C, Tavtigian SV, Hainaut P, Olivier M. Impact of mutant p53 functional properties on TP53 mutation patterns and tumor phenotype: lessons from recent developments in the IARC TP53 database. Hum Mutat. 2007; 28(6):622-9.

Polański R, Warburton HE, Ray-Sinha A, Devling T, Pakula H, Rubbi CP, Vlatković N, Boyd MT. MDM2 promotes cell motility and invasiveness through a RING-finger independent mechanism. FEBS Lett. 2010 19; 584(22):4695-702.

Radosław Polański, Aidan P. Noon, Jeremy Blaydes, Anna Philips, Carlos P. Rubbi, Keith Parsons, Nikolina Vlatković and Mark T. Boyd. Senescence induction in renal carcinoma cells by Nutlin-3: a potential therapeutic strategy based on MDM2 antagonism (Manuscript submitted)

Prives C, Hall PA. The p53 pathway. J Pathol. 1999; 187(1):112-26.

Quelle DE, Zindy F, Ashmun RA, Sherr CJ. Alternative reading frames of the INK4a tumor suppressor gene encode two unrelated proteins capable of inducing cell cycle arrest. Cell. 1995; 83(6):993-1000.

Reich NC, Levine AJ. Growth regulation of a cellular tumour antigen, p53, in nontransformed cells. Nature. 1984; 308(5955):199-201.

Reiter RE, Anglard P, Liu S, Gnarra JR, Linehan WM. Chromosome 17p deletions and p53 mutations in renal cell carcinoma. Cancer Res. 1993; 53(13):3092-7.

Ren D, Tu HC, Kim H, Wang GX, Bean GR, Takeuchi O, Jeffers JR, Zambetti GP, Hsieh JJ, Cheng EH. BID, BIM, and PUMA are essential for activation of the BAX- and BAK-dependent cell death program. Science. 2010; 330(6009):1390-3.

Renault TT, Floros KV, Chipuk JE. BAK/BAX activation and cytochrome c release assays using isolated mitochondria. Methods. 2013;61(2):146-55.

Renehan AG, Tyson M, Egger M, Heller RF, Zwahlen M. Body-mass index and incidence of cancer: a systematic review and meta-analysis of prospective observational studies. Lancet. 2008; 371(9612):569-78.

Rew Y, Sun D, Gonzalez-Lopez De Turiso F, Bartberger MD, Beck HP, Canon J, Chen A, Chow D, Deignan J, Fox BM, Gustin D, Huang X, Jiang M, Jiao X, Jin L, Kayser F, Kopecky DJ, Li Y, Lo MC, Long AM, Michelsen K, Oliner JD, Osgood T, Ragains M, Saiki AY, Schneider S, Toteva M, Yakowec P, Yan X, Ye Q, Yu D, Zhao X, Zhou J, Medina JC, Olson SH. Structure-based design of novel inhibitors of the MDM2-p53 interaction. J Med Chem. 2012; 55(11):4936-54.

Ren D, Tu HC, Kim H, Wang GX, Bean GR, Takeuchi O, Jeffers JR, Zambetti GP, Hsieh JJ, Cheng EH. BID, BIM, and PUMA are essential for activation of the BAX- and BAK-dependent cell death program. Science. 2010 Dec 3;330(6009):1390-3

Rini BI, Campbell SC, Escudier B. Renal cell carcinoma. Lancet. 2009; 373(9669):1119-32.

Rini BI, Escudier B, Tomczak P, Kaprin A, Szczylik C, Hutson TE, Michaelson MD, Gorbunova VA, Gore ME, Rusakov IG, Negrier S, Ou YC, Castellano D, Lim HY, Uemura H, Tarazi J, Cella D, Chen C, Rosbrook B, Kim S, Motzer RJ. Comparative effectiveness of axitinib versus sorafenib in advanced renal cell carcinoma (AXIS): a randomised phase 3 trial. Lancet. 2011; 378(9807):1931-9.

Rooswinkel RW, van de Kooij B, Verheij M, Borst J. Bcl-2 is a better ABT-737 target than Bcl-xL or Bcl-w and only Noxa overcomes resistance mediated by Mcl-1, Bfl-1, or Bcl-B. Cell Death Dis. 2012; 3:e366

Roth J, Dobbelstein M, Freedman DA, Shenk T, Levine AJ. Nucleo-cytoplasmic shuttling of the hdm2 oncoprotein regulates the levels of the p53 protein via a pathway used by the human immunodeficiency virus rev protein. EMBO J. 1998; 17(2):554-64.

Roxburgh P, Hock AK, Dickens MP, Mezna M, Fischer PM, Vousden KH. Small molecules that bind the Mdm2 RING stabilize and activate p53. Carcinogenesis. 2012; 33(4):791-8

Rousalova I, Krepela E. Granzyme B-induced apoptosis in cancer cells and its regulation. Int J Oncol. 2010; 37(6):1361-78.

Sale MJ, Cook SJ. The BH3 mimetic ABT-263 synergizes with the MEK1/2 inhibitor selumetinib/AZD6244 to promote BIM-dependent tumour cell death and inhibit acquired resistance. Biochem J. 2013; 450(2):285-94.

Sakaguchi K, Herrera JE, Saito S, Miki T, Bustin M, Vassilev A, Anderson CW, Appella E. DNA damage activates p53 through a phosphorylation-acetylation cascade. Genes Dev. 1998; 12(18):2831-41.

Sattler M, Liang H, Nettesheim D, Meadows RP, Harlan JE, Eberstadt M, Yoon HS, Shuker SB, Chang BS, Minn AJ, Thompson CB, Fesik SW. Structure of Bcl-xL-Bak peptide complex: recognition between regulators of apoptosis. Science. 1997; 275(5302):983-6.

Sasiela CA, Stewart DH, Kitagaki J, Safiran YJ, Yang Y, Weissman AM, Oberoi P, Davydov IV, Goncharova E, Beutler JA, McMahon JB, O'Keefe BR. Identification of inhibitors for MDM2 ubiquitin ligase activity from natural product extracts by a novel high-throughput electrochemiluminescent screen. J Biomol Screen. 2008; 13(3):229-37

Saucedo LJ, Myers CD, Perry ME. Multiple murine double minute gene 2 (MDM2) proteins are induced by ultraviolet light. J Biol Chem. 1999; 274(12):8161-8.

Schellenberg B, Wang P, Keeble JA, Rodriguez-Enriquez R, Walker S, Owens TW, Foster F, Tanianis-Hughes J, Brennan K, Streuli CH, Gilmore AP. Bax exists in a dynamic equilibrium between the cytosol and mitochondria to control apoptotic priming. Mol Cell. 2013; 49(5):959-71.

Seizinger BR, Rouleau GA, Ozelius LJ, Lane AH, Farmer GE, Lamiell JM, Haines J, Yuen JW, Collins D, Majoor-Krakauer D, et al. Von Hippel-Lindau disease maps to the region of chromosome 3 associated with renal cell carcinoma. Nature. 1988 17;332(6161):268-9

Schlegel RA, Williamson P. Phosphatidylserine, a death knell. Cell Death Differ. 2001;8(6):551-63.

Schmidt L, Duh FM, Chen F, Kishida T, Glenn G, Choyke P, Scherer SW, Zhuang Z, Lubensky I, Dean M, Allikmets R, Chidambaram A, Bergerheim UR, Feltis JT, Casadevall C, Zamarron A, Bernues M, Richard S, Lips CJ, Walther MM, Tsui LC, Geil L, Orcutt ML, Stackhouse T, Lipan J, Slife L, Brauch H, Decker J, Niehans G, Hughson MD, Moch H, Storkel S, Lerman MI, Linehan WM, Zbar B. Germline and somatic mutations in the tyrosine kinase domain of the MET proto-oncogene in papillary renal carcinomas. Nat Genet. 1997; 16(1):68-73.

Schmidt L1, Junker K, Nakaigawa N, Kinjerski T, Weirich G, Miller M, Lubensky I, Neumann HP, Brauch H, Decker J, Vocke C, Brown JA, Jenkins R, Richard S, Bergerheim U, Gerrard B, Dean M, Linehan WM, Zbar B. Novel mutations of the MET proto-oncogene in papillary renal carcinomas. Oncogene. 1999; 18(14):2343-50.

Schmitt CA, Fridman JS, Yang M, Lee S, Baranov E, Hoffman RM, Lowe SW. A senescence program controlled by p53 and p16INK4a contributes to the outcome of cancer therapy. Cell. 2002; 109(3):335-46.

Semenza GL. Regulation of oxygen homeostasis by hypoxia-inducible factor 1. Physiology (Bethesda). 2009; 24:97-106.

Semenza GL. Defining the role of hypoxia-inducible factor 1 in cancer biology and therapeutics. Oncogene. 2010a;29(5):625-34.

Semenza GL. HIF-1: upstream and downstream of cancer metabolism. Curr Opin Genet Dev. 2010b; 20(1):51-6.

Serrano M, Lin AW, McCurrach ME, Beach D, Lowe SW. Oncogenic ras provokes premature cell senescence associated with accumulation of p53 and p16INK4a. Cell. 1997; 88(5):593-602.

Shen C, Kaelin WG Jr. The VHL/HIF axis in clear cell renal carcinoma. Semin Cancer Biol. 2013; 23(1):18-25

Shoemaker AR, Oleksijew A, Bauch J, Belli BA, Borre T, Bruncko M, Deckwirth T, Frost DJ, Jarvis K, Joseph MK, Marsh K, McClellan W, Nellans H, Ng S, Nimmer P, O'Connor JM, Oltersdorf T, Qing W, Shen W, Stavropoulos J, Tahir SK, Wang B, Warner R, Zhang H, Fesik SW, Rosenberg SH, Elmore SW. A small-molecule inhibitor of Bcl-XL potentiates the activity of cytotoxic drugs in vitro and in vivo. Cancer Res. 2006 Sep 1;66(17):8731-9.

Snow RM, Schellhammer PF. Spontaneous regression of metastatic renal cell carcinoma. Urology. 1982; 20(2):177-81.

Song JH, Kandasamy K, Kraft AS. ABT-737 induces expression of the death receptor 5 and sensitizes human cancer cells to TRAIL-induced apoptosis. J Biol Chem. 2008; 283: 25003-13

Soussi T, Béroud C. Assessing TP53 status in human tumours to evaluate clinical outcome. Nat Rev Cancer. 2001; 1(3):233-40.

Speidel D. Transcription-independent p53 apoptosis: an alternative route to death. Trends Cell Biol. 2010; 20(1):14-24.

Stebbins CE, Kaelin WG Jr, Pavletich NP. Structure of the VHL-ElonginC-ElonginB complex: implications for VHL tumor suppressor function. Science. 1999; 284(5413):455-61.

Steensma DP, Timm M, Witzig TE. Flow cytometric methods for detection and quantification of apoptosis. Methods Mol Med. 2003; 85:323-32.

Stommel JM, Marchenko ND, Jimenez GS, Moll UM, Hope TJ, Wahl GM. A leucine-rich nuclear export signal in the p53 tetramerization domain: regulation of subcellular localization and p53 activity by NES masking. EMBO J. 1999; 18(6):1660-72.

Strom E, Sathe S, Komarov PG, Chernova OB, Pavlovska I, Shyshynova I, Bosykh DA, Burdelya LG, Macklis RM, Skaliter R, Komarova EA, Gudkov AV. Small-molecule inhibitor of p53 binding to mitochondria protects mice from gamma radiation. Nat Chem Biol. 2006 Sep;2(9):474-9

Sykes SM, Mellert HS, Holbert MA, Li K, Marmorstein R, Lane WS, McMahon SB. Acetylation of the p53 DNA-binding domain regulates apoptosis induction. Mol Cell. 2006; 24(6):841-51.

Tabe Y, Sebasigari D, Jin L, Rudelius M, Davies-Hill T, Miyake K, Miida T, Pittaluga S, Raffeld M. MDM2 antagonist nutlin-3 displays antiproliferative and proapoptotic activity in mantle cell lymphoma. Clin Cancer Res. 2009 Feb 1;15(3):933-42

Tahir SK, Yang X, Anderson MG, Morgan-Lappe SE, Sarthy AV, Chen J, Warner RB, Ng SC, Fesik SW, Elmore SW, Rosenberg SH, Tse C. Influence of Bcl-2 family members on the cellular response of small-cell lung cancer cell lines to ABT-737. Cancer Res. 2007; 67(3):1176-83.

Tang Y, Luo J, Zhang W, Gu W. Tip60-dependent acetylation of p53 modulates the decision between cell-cycle arrest and apoptosis. Mol Cell. 2006; 24(6):827-39.

Tanimura S, Ohtsuka S, Mitsui K, Shirouzu K, Yoshimura A, Ohtsubo M. MDM2

interacts with MDMX through their RING finger domains. FEBS Lett.; 447(1):5-9.

Tao W, Levine AJ. P19(ARF) stabilizes p53 by blocking nucleo-cytoplasmic shuttling of Mdm2. Proc Natl Acad Sci U S A. 1999; 96(12):6937-41.

Tartaglia LA, Ayres TM, Wong GH, Goeddel DV. A novel domain within the 55 kd TNF receptor signals cell death. Cell. 1993; 74(5):845-53.

Tazawa H1, Kagawa S, Fujiwara T. Advances in adenovirus-mediated p53 cancer gene therapy. Expert Opin Biol Ther. 2013;13(11):1569-83

Theis RP, Dolwick Grieb SM, Burr D, Siddiqui T, Asal NR. Smoking, environmental tobacco smoke, and risk of renal cell cancer: a population-based case-control study. BMC Cancer. 2008; 8:387.

Thomas MC, Chiang CM. The general transcription machinery and general cofactors. Crit Rev Biochem Mol Biol. 2006; 41(3):105-78.

Thomas GV, Tran C, Mellinghoff IK, Welsbie DS, Chan E, Fueger B, Czernin J, Sawyers CL. Hypoxia-inducible factor determines sensitivity to inhibitors of mTOR in kidney cancer. Nat Med. 2006; 12(1):122-7.

Tibbetts RS, Brumbaugh KM, Williams JM, Sarkaria JN, Cliby WA, Shieh SY, Taya Y, Prives C, Abraham RT. A role for ATR in the DNA damage-induced phosphorylation of p53. Genes Dev. 1999; 13(2):152-7.

Tomita Y, Bilim V, Kawasaki T, Takahashi K, Okan I, Magnusson KP, Wiman KG. Frequent expression of Bcl-2 in renal-cell carcinomas carrying wild-type p53. Int J Cancer. 1996; 66(3):322-5.

Tovar C, Rosinski J, Filipovic Z, Higgins B, Kolinsky K, Hilton H, Zhao X, Vu BT, Qing W, Packman K, Myklebost O, Heimbrook DC, Vassilev LT. Small-molecule MDM2 antagonists reveal aberrant p53 signaling in cancer: implications for therapy. Proc Natl Acad Sci U S A. 2006; 103(6):1888-93.

Tromp JM, Geest CR, Breij EC, Elias JA, van Laar J, Luijks DM, Kater AP, Beaumont T, van Oers MH, Eldering E. Tipping the Noxa/Mcl-1 balance overcomes ABT-737 resistance in chronic lymphocytic leukemia. Clin Cancer Res. 15;18(2):487-98.

Tse C, Shoemaker AR, Adickes J, Anderson MG, Chen J, Jin S, Johnson EF, Marsh KC, Mitten MJ, Nimmer P, Roberts L, Tahir SK, Xiao Y, Yang X, Zhang H, Fesik S, Rosenberg SH, Elmore SW. ABT-263: a potent and orally bioavailable Bcl-2 family inhibitor. Cancer Res. 2008; 68(9):3421-8.

Uren RT, Dewson G, Chen L, Coyne SC, Huang DC, Adams JM, Kluck RM. Mitochondrial permeabilization relies on BH3 ligands engaging multiple prosurvival Bcl-2 relatives, not Bak. J Cell Biol. 2007; 177(2):277-87.

Uzzo RG, Novick AC. Nephron sparing surgery for renal tumors: indications, techniques and outcomes. J Urol. 2001; 166(1):6-18.

Van Delft MF, Wei AH, Mason KD, Vandenberg CJ, Chen L, Czabotar PE, Willis SN, Scott CL, Day CL, Cory S, Adams JM, Roberts AW, Huang DC. The BH3 mimetic ABT-737 targets selective Bcl-2 proteins and efficiently induces apoptosis via Bak/Bax if Mcl-1 is neutralized. Cancer Cell 2006; 10(5):389-99.

Van Maerken T, Speleman F, Vermeulen J, Lambertz I, De Clercq S, De Smet E, Yigit N, Coppens V, Philippé J, De Paepe A, Marine JC, Vandesompele J. Small-molecule MDM2 antagonists as a new therapy concept for neuroblastoma. Cancer Res. 2006; 66(19):9646-55.

Vaseva AV, Marchenko ND, Moll UM. The transcription-independent mitochondrial p53 program is a major contributor to nutlin-induced apoptosis in tumor cells. Cell Cycle. 2009 Jun 1;8(11):1711-9.

Vassilev LT, Vu BT, Graves B, Carvajal D, Podlaski F, Filipovic Z, Kong N, Kammlott U, Lukacs C, Klein C, Fotouhi N, Liu EA. In vivo activation of the p53 pathway by small-molecule antagonists of MDM2. Science. 2004; 303(5659):844-8.

Vlatković N, Crawford K, Rubbi CP, Boyd MT. Tissue-specific therapeutic targeting of p53 in cancer: one size does not fit all. Curr Pharm Des. 2011;17(6):618-30.

Vousden KH, Lu X. Live or let die: the cell's response to p53. Nat Rev Cancer. 2002; 2(8):594-604.

Waga S, Hannon GJ, Beach D, Stillman B. The p21 inhibitor of cyclin-dependent kinases controls DNA replication by interaction with PCNA. Nature. 1994; 369(6481):574-8.

Warburton HE, Brady M, Vlatković N, Linehan WM, Parsons K, Boyd MT. p53 regulation and function in renal cell carcinoma. Cancer Res. 2005; 65(15):6498-503.

Weber JD, Kuo ML, Bothner B, DiGiammarino EL, Kriwacki RW, Roussel MF, Sherr CJ. Cooperative signals governing ARF-mdm2 interaction and nucleolar localization of the complex. Mol Cell Biol. 2000; 20(7):2517-28.

Wei MC, Lindsten T, Mootha VK, Weiler S, Gross A, Ashiya M, Thompson CB, Korsmeyer SJ. tBID, a membrane-targeted death ligand, oligomerizes BAK to release cytochrome c. Genes Dev. 2000; 14(16):2060-71.

Wei MC, Zong WX, Cheng EH, Lindsten T, Panoutsakopoulou V, Ross AJ, Roth KA, MacGregor GR, Thompson CB, Korsmeyer SJ. Proapoptotic BAX and BAK: a

requisite gateway to mitochondrial dysfunction and death. Science. 2001; 292(5517):727-30.

Wesarg E, Hoffarth S, Wiewrodt R, Kröll M, Biesterfeld S, Huber C, Schuler M. Targeting BCL-2 family proteins to overcome drug resistance in non-small cell lung cancer. Int J Cancer. 2007; 121(11):2387-94.

Westphal D, Kluck RM, Dewson G. Building blocks of the apoptotic pore: how Bax and Bak are activated and oligomerize during apoptosis. Cell Death Differ. 2013 Oct 25.

Willis SN, Fletcher JI, Kaufmann T, van Delft MF, Chen L, Czabotar PE, Ierino H, Lee EF, Fairlie WD, Bouillet P, Strasser A, Kluck RM, Adams JM, Huang DC. Apoptosis initiated when BH3 ligands engage multiple Bcl-2 homologs, not Bax or Bak. Science. 2007; 315(5813):856-9.

Wu X, Bayle JH, Olson D, Levine AJ. The p53-mdm-2 autoregulatory feedback loop. Genes Dev. 1993; 7(7A):1126-32.

Wu GS, Burns TF, McDonald ER 3rd, Jiang W, Meng R, Krantz ID, Kao G, Gan DD, Zhou JY, Muschel R, Hamilton SR, Spinner NB, Markowitz S, Wu G, el-Deiry WS. KILLER/DR5 is a DNA damage-inducible p53-regulated death receptor gene. Nat Genet. 1997; 17(2):141-3.

Xiong Y, Hannon GJ, Zhang H, Casso D, Kobayashi R, Beach D. p21 is a universal inhibitor of cyclin kinases. Nature. 1993; 366(6456):701-4.

Xue W, Zender L, Miething C, Dickins RA, Hernando E, Krizhanovsky V, Cordon-Cardo C, Lowe SW. Senescence and tumour clearance is triggered by p53 restoration in murine liver carcinomas. Nature. 2007; 445(7128):656-60.

Yagoda A, Abi-Rached B, Petrylak D. Chemotherapy for advanced renal-cell carcinoma: 1983-1993. Semin Oncol. 1995 Feb;22(1):42-60.

Yeh P, Kishony R. Networks from drug-drug surfaces. Mol Syst Biol. 2007;3:85.

You H, Pellegrini M, Tsuchihara K, Yamamoto K, Hacker G, Erlacher M, Villunger A, Mak TW. FOXO3a-dependent regulation of Puma in response to cytokine/growth factor withdrawal. J Exp Med. 2006; 203(7):1657-63.

Yu J, Zhang L, Hwang PM, Kinzler KW, Vogelstein B. PUMA induces the rapid apoptosis of colorectal cancer cells. Mol Cell. 2001; 7(3):673-82.

Zall H, Weber A, Besch R, Zantl N, Häcker G. Chemotherapeutic drugs sensitize human renal cell carcinoma cells to ABT-737 by a mechanism involving the Noxa-dependent inactivation of Mcl-1 or A1. Mol Cancer. 2010; 9:164

Zbar B, Tory K, Merino M, Schmidt L, Glenn G, Choyke P, Walther MM, Lerman M, Linehan WM. Hereditary papillary renal cell carcinoma. J Urol. 1994;151(3):561-6.

Zbar B, Klausner R, Linehan WM. Studying cancer families to identify kidney cancer genes. Annu Rev Med. 2003; 54:217-33

Zhan Q, Antinore MJ, Wang XW, Carrier F, Smith ML, Harris CC, Fornace AJ Jr. Association with Cdc2 and inhibition of Cdc2/Cyclin B1 kinase activity by the p53-regulated protein Gadd45. Oncogene. 1999; 18(18):2892-900.

Zhang C, Li X, Hao H, Yu W, He Z, Zhou L. The correlation between size of renal cell carcinoma and its histopathological characteristics: a single center study of 1867 renal cell carcinoma cases. BJU Int. 2012; 110(11 Pt B):E481-5.

Zhong H, Chiles K, Feldser D, Laughner E, Hanrahan C, Georgescu MM, Simons JW, Semenza GL. Modulation of hypoxia-inducible factor 1alpha expression by the epidermal growth factor/phosphatidylinositol 3-kinase/PTEN/AKT/FRAP pathway in human prostate cancer cells: implications for tumor angiogenesis and therapeutics. Cancer Res. 2000 Mar; 60(6):1541-5.

Zhu S, Cohen MB, Bjorge JD, Mier JW, Cho DC. PI3K inhibition potentiates Bcl-2-dependent apoptosis in renal carcinoma cells. J Cell Mol Med. 2013; 17:377-85.

Appendices

Appendix 1

Movies of ACHN and 111 cells treated with Nutlin-3 and/or ABT-737 (see section 3.2.3) are on the attached CD.